University of Glasgow

Campbell, Fay M.A. (2007) *The role of supraglacial snowpack hydrology in mediating meltwater delivery to glacier systems.*
PhD thesis.

http://theses.gla.ac.uk/2871/

UNIVERSITY
of
GLASGOW

DEPARTMENT *of* **GEOGRAPHICAL**
and **EARTH SCIENCES**

The role of supraglacial snowpack hydrology in mediating meltwater delivery to glacier systems

Fay M. A. Campbell

Submitted to the Faculty of Physical Sciences
for the degree of Doctor of Philosophy

January 2007

Abstract

This thesis investigates the role that supraglacial snowpack hydrology plays in mediating meltwater delivery to glacier systems. The movement of water through glaciers is of fundamental importance as a control on proglacial hydrograph amplitude and timing, subglacial and proglacial geomorphic processes, the hydrochemistry of glacial runoff, and glacier dynamics, and as such has been the subject of considerable research effort. Although studies in non-glacial environments have shown that meltwater waves are both dampened and delayed by passage through snow, the role of supraglacial snowcover in mediating water inputs to the rest of the glacier system has received limited attention in studies of glacier hydrology to date. It has been suggested, however, that the varying thickness, and ultimately removal, of the supraglacial snowpack may play a role in controlling the timing and magnitude of ice velocity events. Despite this suggested importance there have been few field observations of the hydrological behaviour of supraglacial snowpacks or of the way in which this behaviour evolves during the melt season. A thorough assessment of the linkages between supraglacial snowpack conditions and glacier dynamic events has therefore not been possible. This study helps fill this gap in our knowledge by explicitly investigating the hydrological behaviour of the supraglacial snowpack at an alpine glacier and its evolution during the summer melt season.

Field data was collected during two summer field seasons (2003 and 2004) at Haut Glacier d'Arolla, Valais, Switzerland. Dye tracing experiments were used as the primary method of obtaining information about water flow through the snowpack. Dye was used both qualitatively, to give a visual impression of flow patterns through the snowpack, and quantitatively, with return curves detected by a fluorometer providing detailed information about rates of dye movement and dispersion through the snowpack. Physically-based modelling representations of water flow through snow also informed consideration of the characteristics of snowpack runoff. Experiments were designed to determine: i) the nature of water flow through the supraglacial snowpack; ii) if, and in what way, this evolves over the course of the melt season; and iii) what factors control water movement, and the importance of their roles. In order that links between supraglacial snowpack hydrology and other parts of the glacier system could be considered, season-long records of glacier dynamics, proglacial meltwater discharge, and water quality parameters indicating subglacial conditions were also collected.

Observations of the movement of dye-stained water demonstrated the complexity of percolation patterns in snow and the influence of ice layers and preferential flow zones on flow rates. Fluorometric techniques measured percolation velocities of between 0.08 and 0.49 m hr^{-1}, showing the delay that passage through snow will impart on runoff. Corresponding net snowpack permeability values (ranging from 2.02×10^{-13} to 1.05×10^{-9} m^2)

are significantly lower than those used in previous modelling studies, thereby indicating a need for future work to be better informed by field-derived measurements of snow permeability. Velocities for water flow in the basal saturated layer were found to be one to two orders of magnitude greater than for percolation (ranging from 1.35 to 18.48 m hr^{-1}), and this part of snowpack runoff therefore plays a lesser role than percolation in altering runoff timing. The velocity and dispersion of flow through *both* snowpack flow regimes, however, indicate the marked difference in runoff that will occur across a snow-covered as opposed to bare-ice glacier surface. Records of runoff through the saturated layer at the base of the snowpack confirm the net delaying and attenuating effect of the snowpack, revealing lag times of up to 20 hours between peak surface melt input and peak runoff and almost total dampening of diurnal runoff cycles in the early melt season. The hydrological influence of the supraglacial snowpack must therefore be accounted for in order for runoff through the supraglacial environment and meltwater delivery to the subglacial drainage system to be correctly predicted.

In addition, the hydrological behaviour of the snowpack was observed to evolve through time. In particular, it is shown here that increasing net snowpack permeability can reduce the delay and attenuation of runoff, and permeability values measured in the field were observed to increase through the 2004 melt season. The influence of this increase in permeability on runoff can be equivalent to that of decreasing snow depth, but has not been considered in previous studies. Changes in preferential flow organisation and in particular ice layer permeability and number are suggested as factors leading to increased snowpack permeability. Information about hydrological processes operating within the snowpack, and the way in which they evolve through time, is therefore required in order to understand changing runoff patterns.

Ice velocity events began around 3rd June 2003 and 10th and 24th June 2004. The glacier remained extensively and thickly snow-covered on these dates, showing that runoff through a supraglacial snowpack can be sufficiently high as to trigger an ice dynamic response despite the delaying and attenuating effects noted above. High surface melt fluxes are the first-order control on the occurrence of such speed-up events, but it is suggested that the hydrological behaviour of the supraglacial snowpack can mediate the magnitude of the glacier's dynamic response to high melt inputs. An improved understanding of the supraglacial snowpack's hydrological effect is therefore important not only for our ability to predict runoff timing and magnitude (with implications for the management and use of water resources from glaciated catchments), but also for our understanding of ice dynamic response to melt inputs.

Contents

List of Tables

List of Figures

Chapter 6

Acknowledgements

I am grateful to my supervisors, Pete Nienow (University of Edinburgh) and Ross Purves (University of Zurich), for valuable guidance during my PhD. Pete's supervision has kept me right on the theoretical and methodological approaches appropriate to my topic, particularly as it relates to wider issues of glacier hydrology and dynamics. Ross, despite his physical distance from Glasgow, provided major input to both the modelling and field-based parts of the work as well as much-appreciated field visits and, on more than one occasion, bits of field equipment that I had forgotten to take with me when I headed into the field…

The highlight of my PhD experience, undoubtedly, was fieldwork at Haut Glacier d'Arolla. In both 2003 and 2004 I was incredibly lucky to be joined by a number of outstanding undergraduate field assistants from the Universities of Bristol, Aberystwyth, Cambridge and Edinburgh, who not only provided excellent assistance with my work but contributed to the fun, friendly, and frequently ridiculous atmosphere that will be my lasting impression of my field seasons. For 2003, huge thanks to the "glaciology girlies" - Harriet Astbury, Liz Bagshaw, Charlotte Colls, Marion McMillan, Louise Davidson, Sally Earthrowl, Jenny Bush, and Josie Fowler. Thanks also to Ebby Ritchie, David Boyd (honorary glaciology girlie) and Lizzy Seal for excellent field assistance. In 2004, Nia Erain Roberts, Katy Gell, Jo Usborne (twice! – thank you!), Andrew Sole, Ian Greenwood, Alexa Clarke, Cameron Rye, Sam Parry and Marion McMillan (again! – thanks!) got stuck with worse weather but did excellent work and helped me have a lot of fun. Kirsty Stronach provided driving companionship and loads of help setting up the second field season (during the few days that we weren't snowed-in…). Also for help in the field, I'm very grateful to Russell Salisbury and Dave Chandler. Finally, thanks to Ralf Schmall not only for help in the field, but for completing the alpine experience with some lovely alphorn music.

My immediate predecessors in the Glasgow glaciology PhD world – Karin Grust and Rob Bingham – have been a source of considerable advice and glaciological friendship over the last few years, and I'm very grateful for their help and encouragement.

The prolonged desk-based parts of the PhD have been made infinitely more fun by the company of my lunch-pal Allan Lafferty and office-mate Heather McFerran. Big thanks also to Elizabeth MacKay for all the thermistor calibration, and to Susan Tulley for field help and driving company.

Geography departments at the Universities of Bristol, Cambridge and Edinburgh are thanked for lending equipment for use in the field, without which I would simply have been unable to collect a significant part of the data that contributed to this thesis. The Department of Geography and Earth Sciences at the University of Glasgow provided all other equipment, and Peter Chung was a huge technical help while preparing both field seasons. Thank you also to Brian Black for much computer support.

I am very grateful to M. Victor Anzevui for permission to camp and work at Haut Glacier d'Arolla, Hydro Exploitation SA for providing discharge data for the Haut Arolla catchment, Andrew Sole for providing a DEM of the glacier, and ETH Zurich (in particular Javier Corripio and Francesca Pellicciotti) for providing met data from their automatic weather stations and photographs showing changing snowcover conditions through time. Andy Fox very kindly provided the version of the SNTHERM model used in this thesis, and the adaptations made to the model during his own PhD work made it much easier for me to work with. The US Army Cold Regions Research and Engineering Laboratory is acknowledged for its work developing SNTHERM over the last ~15 years; in making the model freely available, they have provided a valuable resource for much snow research.

Last but not least, the family get a mention. Huge thanks to my mum and dad for their support, financial and otherwise, throughout my PhD and life in general, and for their (quite impressive!) glaciological efforts during visits to the field. Thanks also to my sister Cath for encouragement and support.

Declaration

This thesis embodies the results of original research carried out by the author between October 2002 and September 2006. References to existing works are made as appropriate. Any remaining errors or omissions are the responsibility of the author.

Fay M. A. Campbell
January 2007

Chapter 1. Introduction to the research

1.1 INTRODUCTION AND RATIONALE

This thesis seeks to advance our understanding of the role that a supraglacial snowpack plays in controlling meltwater discharge into the glacier hydrological system. The movement of water through glaciers is of fundamental importance as a control on proglacial hydrograph amplitude and timing, subglacial and proglacial geomorphic processes, the hydrochemistry of glacial runoff, and glacier dynamics, and as such has been the subject of considerable research effort. Research has focussed largely on the subglacial drainage system, with significant advances made in our understanding of subglacial drainage configurations, their associated hydraulics, and their evolution through time. In contrast, there has been little work addressing the movement of water above the glacier surface, even though processes in the supraglacial environment will control runoff into the rest of the glacier hydrological system. In particular, the presence of a supraglacial snowpack will play a key role in mediating the delivery of meltwater produced at the snowpack surface to the rest of the glacier system, but has been inadequately dealt with in the majority of glacier hydrology studies to date.

Studies of snow hydrology in non-glacial environments show that meltwater flow through snow acts to dampen and delay the passage of the diurnal meltwater wave (Colbeck, 1972; Colbeck and Davidson, 1973; Jordan, 1983a; Fountain, 1996), and analyses of seasonal changes in the shape and timing of diurnal runoff hydrographs from glaciers show that such effects also apply in the glacial environment (Elliston, 1973; Fountain, 1992, 1996; Hannah et al., 1999). It has been suggested that the varying thickness of the snowpack may play a critical role in controlling the timing and magnitude of the 'spring event' observed at several glaciers (Nienow, 1997), a period of enhanced glacier flow thought to be caused by increased surface meltwater input to a hydraulically inefficient subglacial drainage system (Röthlisberger and Lang, 1987, p.262; Nienow, 1997). However, despite its suggested importance there have been few field observations of the hydrological behaviour of supraglacial snowpacks or of the way in which this behaviour evolves during the melt season. Such investigations are necessary to assess the validity of assumptions made when modelling meltwater inputs to the glacio-hydrological system and should ultimately enable better understanding of the linkages between supraglacial snowpack conditions and changes in glacier dynamics.

This study aims to help fill this gap in our knowledge by explicitly investigating the hydrological behaviour of the supraglacial snowpack at an alpine glacier and its evolution during the summer melt season. Fieldwork carried out during two summer field seasons (2003 and 2004) at Haut Glacier d'Arolla, Valais, Switzerland, used dye tracer techniques as the primary method of obtaining both qualitative and quantitative information about water flow through the snowpack. A particularly valuable technique, developed in this study, is the use of a down-borehole fluorometer installed at the snow-ice interface to accurately detect dye concentrations and recover quantitative information about rates of dye, and therefore water, movement and dispersion through the snowpack. Although this study is primarily field-based, techniques for modelling water movement through snow are also considered, as our understanding of the physical processes controlling water flow can shed light on the way in which runoff from the snowpack will evolve through time in response to changes in snowpack properties and input melt flux. Data collected in the field is also valuable in enabling assessment of the reliability of modelling techniques used to represent supraglacial snowpack hydrology and the choice and required accuracy of controlling parameters.

1.2 OBJECTIVES

The principal aim of this thesis is therefore to discover what role the movement of water through the supraglacial snowpack of one alpine glacier plays in controlling meltwater runoff, and to understand which mechanisms are important in this respect. The achievement of this aim depends primarily on the observation of the hydrological behaviour of a natural snowpack in a field setting. Field investigation of snowpack hydrology aims to:

i)   determine the nature of water flow through the supraglacial snowpack of the studied glacier;

ii)   explore and develop the use of dye tracing techniques to obtain quantitative information about water flow through snow;

iii)   determine if, and in what way, the nature of water flow through the snowpack evolves over the course of the melt season; and

iv)   establish what are the factors controlling water movement through the snowpack, and the importance of their roles.

As outlined above, it has been suggested that the movement of water through the supraglacial snowpack has important implications for patterns of proglacial meltwater discharge, conditions in the subglacial environment, and potentially the timing and magnitude of glacier velocity events. This project therefore also aimed to:

v)   obtain season-long records of glacier dynamics, proglacial meltwater discharge, and water quality parameters indicating subglacial conditions; and

vi)   assess the possible links between the changing hydrological behaviour of the snowpack and the factors listed in v).

Investigations using modelling representations of snow hydrology also add to our assessment of the factors controlling runoff from the snowpack, with model runs undertaken to address aims iii) and iv) using our understanding of the physical factors controlling water movement. By drawing together field observations and model runs, a final research aim is to:

vii)   identify any weaknesses in, and suggest possible improvements to, existing approaches to modelling supraglacial snow hydrology.

1.3 THESIS STRUCTURE

The thesis consists of eight chapters. Chapter 2 reviews previous studies of snow hydrology in both glacial and non-glacial settings and summarises existing knowledge in the field. Shortcomings in this knowledge and areas in which progress is needed are identified. An overview of glacial hydrology and its links to conditions in the subglacial environment and ice dynamics is also provided in order to show the wider context within which snowpack hydrology is important.

Chapter 3 introduces the field site and describes and justifies the techniques used in the field. A wider discussion of the role which field data and modelling work play in the project is also included.

Results from field investigations are presented in Chapters 4 and 5. Chapter 4 presents observations and measurements of snowpack properties and dye flow patterns, while Chapter 5 presents results and analyses of quantitative investigations of water flow through the snowpack, obtained by dye-tracing and other techniques. Data is analysed with the aim of determining the nature of water flow through the snowpack and the factors controlling water movement, and to establish if, and in what way, the snowpack's influence on water runoff changes over the course of the melt season.

Modelling approaches to snowpack hydrology are considered in Chapter 6. Established physical representations of water movement through snow are used to further investigate the importance of various factors in controlling runoff and to consider the extent to which snowpack changes observed in the field might play a role in influencing runoff. Knowledge

gained from fieldwork is also used to assess modelling techniques and suggest improvements.

Chapter 7 presents and analyses field data concerning hydrological conditions in the wider glacier system and the rate of glacier movement. Data is analysed to determine conditions in the subglacial drainage system and identify any glacier velocity events. When viewed alongside the knowledge of supraglacial snowpack hydrological behaviour presented in Chapters 4 to 6, this data enables consideration of the possible linkages between conditions in the supraglacial and subglacial hydrological systems, and ultimately the role which the snowpack may play in influencing glacier velocity events.

Finally, Chapter 8 summarises the main findings of the thesis and outlines the contribution which it has made to our understanding of supraglacial snow hydrology and its links to ice dynamics. The implications of this research for work in glacier hydrology and ice dynamics are then discussed, and areas in which further work is required are identified.

Chapter 2. Snow and glacier hydrology: a review

2.1 INTRODUCTION

Although the hydrology of the supraglacial snowpack has been largely neglected within the glaciological literature, the extensive body of snow science knowledge developed from research in non-glacial environments has much relevance for snow hydrology in the glacial setting and informs our consideration of supraglacial snowpack hydrology here. This chapter therefore first reviews the knowledge gained from previous studies of snow hydrology in non-glacial environments, focussing on our understanding of how water moves through the snowpack and the factors that control this (section 2.2).

An overview of glacier hydrology is then provided, in order to demonstrate the context within which supraglacial snowpack hydrology operates (section 2.3). The established links between glacier hydrology and ice dynamics are summarized and suggestions of the possible role of the snowpack outlined. Ways in which flow through a snow-covered supraglacial catchment influences runoff are summarised and previous work on supraglacial snow hydrology is reviewed, with issues requiring attention identified.

2.2 SNOW HYDROLOGY: CURRENT KNOWLEDGE AND UNRESOLVED ISSUES

The term 'snow hydrology' as it is often used refers to all aspects of water occurrence in snow, from meltwater production at the snowpack surface to runoff at the snowpack base. Significant research has investigated the physical processes controlling snowmelt (summarized by Male and Gray (1981) and Hock (2005)) and its spatial variation (Luce et al., 1998; Brock et al., 2000b; Daly et al., 2000; Greuell and Smeets, 2001; Motoya et al., 2001), such that snowpack depletion can be satisfactorily reproduced by a number of models (Brun et al., 1989; Greuell and Konzelmann, 1994; Arnold et al., 1996; Brock and Arnold, 2000; Lehning et al., 2002a; Etchevers et al., 2004). In comparison, the subsequent movement of liquid water through the snowpack remains much less well understood. As the timing and magnitude of runoff from a snowpack depends not only on the pattern of water production at the snowpack surface but also crucially on the way in which water flows through the snow itself, this lack of understanding poses a significant barrier to our ability to better understand and predict snowpack runoff. It is with the movement of water through the snowpack that this thesis is primarily concerned, and the term 'snow hydrology' will hereafter be used to refer to just this aspect of water occurrence in snow.

In order to improve our understanding of and ability to predict snowpack runoff, research has sought to uncover the physical processes that control the movement of water through snow. Both field and laboratory studies have revealed a complex series of processes that influence the organisation and rate of water flow, including the input of water to the snowpack surface and the flow of water, both vertically and horizontally, through a porous medium with properties that vary in both space and time. It is these processes which must be taken into account in any attempt to understand snowpack outflow, and which will be reviewed in this section. Other useful reviews of research in snow hydrology are provided by Colbeck (1978a), Wankiewicz (1979), Male and Gray (1981), Bales and Harrington (1995) and Marsh (1991, 1999, 2005).

2.2.1 Physical properties of the seasonal snowcover

The physical properties of the seasonal snowcover are controlled by processes operating on the snow during its formation in the atmosphere and time on the ground. In turn, it is these physical properties which to a large degree control the hydrological behaviour of the snowpack. A thorough understanding of the processes of snowcover formation and the resulting character of the snowpack therefore forms an important basis for further work in snow hydrology. More comprehensive discussions of snowcover development and properties, from deposition to melt, are provided by Male (1980), Male and Gray (1981), Marsh (1991), and Lehning et al. (2002a, b); a summary of those aspects most relevant to hydrology is given here.

2.2.1.1 Snowcover formation and evolution: dry snow processes
Snow crystals forming in the atmosphere take on a range of sizes and a diverse variety of intricate forms depending on the temperature and humidity of the atmosphere at the time of their formation and as they fall to the ground (Male, 1980; Figure 2.1). Crystal size and shape may be altered by wind action both as snowflakes fall to the ground and once deposited, with grains broken and abraded into more equidimensional particles (Male, 1980; Figure 2.1h).

As the seasonal snowpack is typically deposited by a series of winter storms, a characteristic layered structure develops, with varying layer properties depending initially on the conditions under which the snow was deposited. Between storms, the snowpack surface may be modified by freezing rain, packing by wind action, or surface melting and refreezing, resulting in the formation of thin, high density layers which subsequently separate snow strata (Male, 1980). These "ice" layers, though rarely of solid ice, are relatively impermeable compared to the lower density and more permeable snow strata, and may play an important role in snow hydrology, as discussed later.

Once on the ground, snowflakes undergo a rapid metamorphism driven by water vapour gradients between convex and concave surfaces, allowing the snowpack to assume a lower energy state by reducing its total surface area relative to mass. In this process, known as equilibrium growth or equi-temperature metamorphism due to the small temperature gradients under which it takes place (Bader et al., 1939; Sommerfeld and LaChappelle, 1970; Lehning et al., 2002b), snowflakes and broken particles can be reduced to more spherical snow grains in a matter of days, and smaller grains melt and disappear as larger grains grow. In this way, grains may attain a diameter of up to 1 mm even while still below 0°C, and the rounding of grains can allow an increase in snow density to between 580 and 600 kg m^{-3} (Sommerfeld and LaChappelle, 1970), compared to only 50 – 70 kg m^{-3} for new snow deposited under calm conditions (Paterson, 1994).

If the snowpack is subject to a temperature gradient, the resulting movement of water vapour between grains that are at different temperatures drives kinetic growth metamorphism, producing characteristic faceted grains known as surface and depth hoar. More detailed information about the processes of equilibrium growth and kinetic growth metamorphism can be found in Sommerfeld and LaChappelle (1970), Male (1980), and Lehning et al. (2002b).

As metamorphism proceeds, the breaking-up and rounding of dendritic particles is accompanied by the formation of bonds at points of contact between grains. This process, known as sintering, leads to an increase in snow density and strength. The snowpack, previously a matrix of single crystal or polycrystalline ice grains, becomes a complex three-dimensional network of connected particles (Male, 1980).

2.2.1.2 The metamorphism of wet snow
When liquid water is first introduced into the snowcover it initiates a rapid metamorphism, with important implications for subsequent hydrology. As observed by Wakahama (1968), small ice grains are eliminated while larger grains grow rapidly until they reach diameters of 1 to 2 mm. A thermodynamic analysis of the relationship between grain size and phase equilibrium temperature (Colbeck, 1975b) shows that this process can be understood as the result of differences in the melting temperature of small and large grains caused by the difference in their radii of curvature. Due to their smaller radius of curvature, melting temperature is higher for large grains than for small, and larger grains therefore exist at a higher temperature than smaller grains. This temperature difference drives heat flow by conduction towards the smaller grains. As a result, smaller grains decrease in size and eventually disappear, while larger grains increase in size, conserving the total mass.
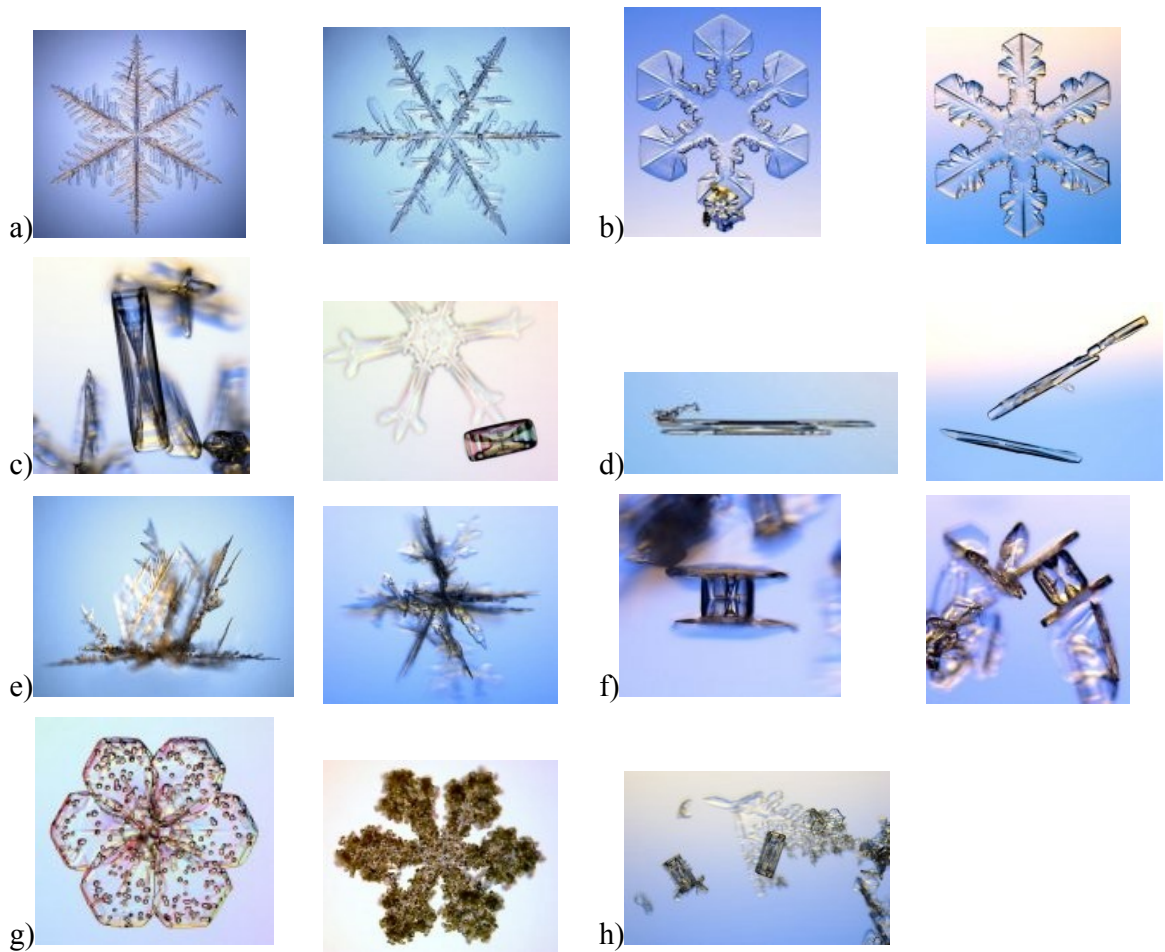
Figure 2.1: Snow crystal forms. Although no two snow crystals are exactly alike, a number of general forms can be identified: a) *stellar dendrites* have six symmetrical main branches and a large number of randomly placed side branches, and can be large, up to 5mm in diameter. Although they have complex shapes, each stellar dendrite is a single crystal of ice; b) *sectored plates* have plate-like arms divided into sectors by tiny ice ridges; c) *hollow columns* make up the majority of most snowfalls (although classic 'snowflake' forms (types a) and b)) get more attention) and are hexagonal in cross-section and often with conical hollow features in their ends; d) *needles* are elongated columnar crystals, which may split into multiple branches at the ends; e) *spatial dendrites* are made from many individual ice crystals tangled together, with multiple, randomly-orientated branches each like one arm of a stellar (type a) or b)) crystal; f) *capped crystals* start to grow as columns, but switch to plate-like growth under changing temperature conditions; g) *rimed crystals* form when small water droplets freeze onto a snow crystal; h) in a turbulent atmosphere most snow crystals are broken and experience different growth conditions, and an *irregular* mixture of forms arrives at the ground.

(adapted from Professor K.G. Libbrecht's Field Guide to Falling Snow, found at SnowCrystals.com (http://www.its.caltech.edu/~atomic/snowcrystals/)).

The diverse grain forms found in both dry and wet snow at various stages of development were brought together by Colbeck et al. (1990) in the International Classification for Seasonal Snow on the Ground (Appendix A). While primarily based on grain morphology, the scheme includes valuable information about the physical processes that lead to different grain types.

2.2.2 Hydrological behaviour of wet snow

The flow of water through snow has parallels with that through other porous media such as coarse sand, and theory developed from work on other media can accordingly be used to address problems in snow hydrology. However, the seasonal snowpack has additional unique qualities that must be taken into consideration (Jordan, 1983a). Most importantly, the fluid and the porous medium are different phases of the same material, and phase changes between liquid water and ice can complicate flow. Secondly, as described above, the physical properties of the snowpack are subject to change through time as metamorphism takes place. Finally, ablation of the snowpack means that the changing thickness of the porous medium, and ultimately its disappearance, must also be taken into account. The resulting hydrological behaviour of wet snow, as it has been established to date, is reviewed in this section.

2.2.2.1 The occurrence and movement of liquid water in snow

When liquid water first percolates into a cold snowpack, it freezes on contact with subfreezing snow and the latent heat released plays an important role in raising the temperature of the snowpack to 0°C (Colbeck, 1976; Illangasekare et al., 1990; Tseng et al., 1994). Likewise, if refreezing takes place in a wet snowpack overnight, its temperature must be raised to 0°C before water is free to move the next morning. Before water is free to move through the snowpack, the irreducible water saturation S_{wi} (the amount of water held immobile at grain boundaries by capillary forces and not available for flow; expressed as a percentage of the total pore volume) must also be satisfied. A range of values between 2 and 20 % have been found for S_{wi} (Gerdel, 1954; Colbeck, 1973; Ebaugh and DeWalle, 1997; Coléou and Lesaffre, 1998; Waldner et al., 2004), with the natural heterogeneity of snowpacks both within and between sites and the difficulty of measuring water saturation accurately in the field making agreement on a representative value particularly hard to achieve. Colbeck et al. (1990) suggest 3% as a general value. The value of S_{wi} is generally believed to decrease with increasing grain size as a result of reduced capillary effect at large-angle grain intersections, and S_{wi} is therefore expected to decrease through time as metamorphic processes cause grain growth (Marsh, 1991).

The subsequent downward propagation of water has been said to proceed as a sharp, uniform wetting front separating the snowpack horizontally into dry sub-freezing snow at the base and wet isothermal (0°C) snow above (Yosida, 1973; Tseng et al., 1994). As the wetting front encounters cold snow, refreezing may be sufficient to form ice layers, particularly where the wetting front is slowed by an impeding stratigraphic horizon (Marsh, 1991). The wetting front must reach the snowpack base before runoff can take place, and its

rate of downward propagation will be controlled by the need to a) raise the snowpack temperature to 0°C and b) satisfy S_{wi} (Colbeck, 1976; Marsh, 1991). However, field observations have shown percolation to take place in a much more uneven manner, such that water may move through zones of preferential flow and be released from the snowpack while other regions remain below freezing (e.g. Kattelman and Dozier, 1999). Heterogeneous patterns of water movement are therefore an important control on the timing of runoff and will be discussed at length in section 2.2.2.3.

The rate of water evacuation through the snowpack compared to the rate of meltwater production at the surface is generally such that the snowpack is unsaturated by liquid water (Marsh, 1991). When free-water content is around 2 to 10% of the pore volume, as is generally the case in freely draining, mature snow, air is present in continuous paths throughout the snow matrix and free to move in response to the movement of liquid water, a situation known as the pendular regime (Colbeck, 1978a; Figure 2.2). When saturation exceeds about 14% of the pore volume, air is present only as isolated bubbles while water exists in continuous flow paths completely surrounding the snow grains (Colbeck, 1973; Denoth, 1980, 1982). This saturation condition is known as the funicular regime, and exists in natural snowpacks when the downward movement of water is inhibited by some relatively impermeable boundary (Denoth, 1982).
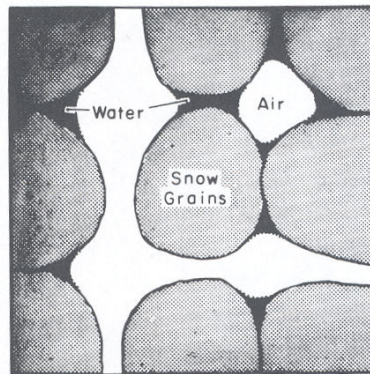
Figure 2.2: An idealised thin-section of snow in the pendular regime of saturation, showing snow grains, water held at grain boundaries, and continuous pore spaces filled with air (from Colbeck (1972)).

Water flow in the unsaturated regime is believed to take place primarily through thin films of water that cover the surface of snow grains (Wakahama, 1968; de Quervain, 1973). If snow is fine-grained or flow rates unusually large, droplet movement may also take place (Colbeck, 1978a). Percolation takes place in this manner until arrested by some less permeable layer, which may be the substrate at the base of the snowpack or an ice layer

within the snowpack depth. Thereafter, saturated flow will take place in a lateral direction, guided by the slope of the impermeable layer, until water reaches the margin of the snowpack or, in the case of flow over an ice layer, is able to find a permeable pathway to continue its downward movement.

Vertical water drainage through the snowpack is predominantly driven by gravity (Colbeck, 1972), although water pressure gradients at boundaries between snow layers and across wetting fronts have been argued to be locally significant (Wankiewicz, 1979). Wankiewicz's (1979) FINA (Flow Impeding, Neutral or Accelerating) model proposes that a horizon between snow layers will impede, accelerate, or have no effect on percolation depending on a number of factors, including the difference in permeability of the two adjacent layers, the slope and curvature of the horizon, heterogeneities in the lower layer, and the value of flux and its rate of increase. If these factors combine such that the gravity flow pressure in the lower layer would be greater than that in the upper layer, flow will be impeded and water will accumulate above the horizon until pressure there is equal to that in the layer below and it can continue its downward movement. If pressure would be lower in the lower layer, flow will be accelerated; if there is no difference in pressure, there is no effect on flow.

The difficulty of reliably measuring the liquid water content of snow is a major limitation to research in snow hydrology. Available techniques such as melting or freezing calorimetry (Kawashima et al., 1998) and the use of centrifuges are frequently difficult to apply in the field and yield large errors (Colbeck, 1978b; Marsh, 1991; Stein et al., 1997). Moreover, being destructive in nature such techniques rule out the possibility of tracking changing snow water content through time without spatial heterogeneity influencing results. Techniques that make use of the dielectric and capacitance properties of wet snow to infer water content (Sihvola and Tiuri, 1986; Bergman, 1987; Denoth, 1994, 1997; Lundberg, 1997; Stein et al., 1997; Schneebeli et al., 1998) offer improved accuracy and can be non-destructive, but equipment is expensive and the techniques are still not widely used.

2.2.2.2 Snowpack permeability to water flow
The ability of water to move through the snowpack is governed by the permeability of the snow. Permeability is controlled by snow properties at the microscopic scale, including the size, structure, and interconnectivity of pore spaces and the thickness of water films covering grains (Conway and Abrahamson, 1984; Hardy and Albert, 1993). However, microscopic properties such as these are in general difficult to determine in the field, and permeability is therefore most commonly considered as a macroscopic property

representing the aggregate behaviour of these smaller-scale factors (Jordan et al., 1999b). Various relationships between permeability and snow properties have been developed (Kozeny, 1927; Carman, 1937; Dullien, 1992). Shimizu (1970) provides a formula for the intrinsic (saturated) permeability of snow that has been widely used (Bear, 1972; Colbeck, 1978a), relating the intrinsic permeability k of the pore space to dry snow density ρ_s and mean grain diameter d according to the expression

$$k = 0.077d^2 \exp\left[-7.8\left(\rho_s / \rho_w\right)\right] \qquad (2.1)$$

where ρ_w is the density of water. Although Shimizu put forward this equation for use with fine-grained, compacted snow ($d \leq 1$ mm), Colbeck (1978a) suggests that it can be reasonably extended to cover mature snowpacks with grain sizes of 1 - 2 mm. As a result of the metamorphism induced by liquid water, the grains in a mature snowpack are generally large enough to provide a high intrinsic permeability to water flow and reduced capillary retention (Colbeck, 1978a). These two factors, as will be shown later (section 2.2.3), greatly simplify modelling of water flow through snow.

While the intrinsic permeability k applies to saturated snow and is dependent only upon the pore geometry, the permeability of unsaturated snow k_w depends both on the pore geometry and the volume of water present (Colbeck, 1972). Specifically, for a given pore geometry k_w will increase as the area available for water flow (that is, the pore space occupied by liquid water, or the liquid water content) increases. When the liquid water content decreases such that the only water present is held in place at the intersections of grain boundaries and other small-angle corners by capillary forces (the irreducible water saturation S_{wi} has been reached), k_w is zero and no water flow can occur. Water saturation S_w (liquid water volume expressed as a percentage of pore volume) is therefore a crucial factor affecting the transmission of water through the snowpack, and introduces an important positive feedback mechanism between the amount of water present and the hydrological behaviour of the snowpack.

2.2.2.3 Vertical movement of water in snow

The way in which water is transferred vertically through the snowpack is a key control on the timing of meltwater discharge and the form of the runoff hydrograph, and various studies have investigated the patterns and rates of water movement in this zone. However, the great natural variability of snowpack properties together with the difficulties of investigating water movement without disturbing the physical equilibrium of the system (and thereby invalidating results) continue to frustrate efforts to draw general conclusions

that can be applied to wider studies. This section reviews existing understanding of water percolation in snow, emphasizing established principles and areas of continued uncertainty.

Rates of water percolation

A variety of techniques have been used to investigate the rate of water movement as it percolates through snow, and the findings of major studies are presented in Table 2.1. There is notable variability in the flow rates reported. Some observations, such as those of Gerdel (1954), Bengtsson (1981), Conway and Raymond (1993), Singh et al. (1997) and Waldner et al. (2004), have suggested that water drains rapidly through the snowcover, at rates of up to 36 m hr^{-1} (Waldner et al., 2004). Conway and Raymond (1993) report water drainage through a maritime snowpack more than 2m deep in a matter of minutes. It is likely that such observations are part of the reason for the omission of the snowpack in studies of glacier hydrology, as its role would be assumed to be minor.

In contrast, many other observations suggest much slower flow rates (Table 2.1). The vast range in observed flow rates can no doubt be attributed to the great variation in snowpack characteristics that is expected in both space and time, in particular in snow density, grain size, liquid water saturation, and the presence of impermeable strata.

Table 2.1: Rates of water percolation through snow, as found by previous studies.

Study location	Rate of water percolation/m hr^{-1}	Method of calculation	Reference
Sierra Nevada, California, USA	(0.9-24 inches per minute =) 1.38-36.6	Dielectric measurement of wetting front passage	Gerdel (1954)
-	0.36 – 3.6	-	De Quervain (1972) (cited in Langham, 1974c)
Seward Glacier, Canada (firn)	0.225	Lysimeter data	Colbeck (1972) based on data by Sharp (1952)
Laboratory	0.288-0.576	Drainage experiments in homogeneous laboratory snow	Colbeck and Davidson (1973)
California and Vermont	0.685-0.755	Lysimeter data	Colbeck (1977)
British Columbia Rockies	0.25-0.3	Potentiometer	Jordan (1983a)
Sierra Nevada, USA	0.18-0.54	Lysimeter data	McGurk and Kattelman (1986)
Austrian Alps	6.0	Gauging of runoff from snow plot exposed to artificial rainfall	Singh et al. (1997)
Colorado Front Range, USA	0.061-0.176	Lysimeter data	Fox et al. (1999)
Swiss Alps	0.08-0.54	Analysis of dye return curves	Grust (2004)
Laboratory	(0.1 – 1 cm s^{-1} =) 3.6 – 36.00	Photo analysis of tracer propagation in artificial snow	Waldner et al. (2004)

Patterns of water flow through snow

In stark contrast to the idea of water percolation as a uniform wetting front (see section 2.2.2.1), the vast majority of experimental observations have shown that percolation occurs in a highly uneven manner. In particular, water has been observed to percolate both arctic and temperate snowpacks via a number of isolated channels or fingers which occupy only a fraction of total snowpack volume but transmit a large proportion of flow (Marsh and Woo, 1984a; Sturm and Holmgren, 1993; Conway and Benedict, 1994; McGurk and Marsh, 1995; Schneebeli, 1995; Albert et al, 1999; Waldner et al, 2004). As liquid water saturation S_w is increased within flow channels, so too is permeability (section 2.2.2.2), and as a result flow rates are locally increased, with water observed to drain rapidly through the snowpack via these channels (Gerdel, 1954; Wakahama, 1975; Colbeck, 1979; Marsh and Woo, 1984a, 1985; Kattelman, 1985, 1989). These features, called preferential flow fingers or zones, carry water to the base of the snowpack long before the background wetting front propagates that far (Gerdel, 1954; Schneebeli, 1995).

Wankiewicz (1979) states that flux within flow fingers will be amplified relative to the flux if flow was uniform by a factor *f*, the inverse of the specific area occupied by the flow fingers:

$$f = \frac{1}{m_s A_s} \qquad\qquad (2.2)$$

where m_s is the number of flow fingers per unit area of the snowpack and
A_s is the average cross-sectional area of a flow finger.

The formation of preferential flow fingers may be due to horizontal variations in snowpack properties at the grain scale, horizontal variability of or depressions in horizons separating snow layers (including variable permeability of ice layers), or the instability of a wetting front as it crosses either an impeding (Waldner et al., 2004) or accelerating (Wankiewicz, 1979; Kattelman and Dozier, 1999) horizon. Their occurrence even in laterally homogeneous soils has demonstrated the importance of stratigraphic boundaries in triggering flow instability and the contribution of inherent wetting front instability (Hill and Parlange, 1972; Glass et al., 1989a, b). Other possible causal factors are variability of surface flux and spatial concentration of flow by the topography of the snowpack surface (discussed below).

Two positive feedback mechanisms have been described which further increase the effect of these preferential flow channels on water flow. Firstly, water flows preferentially along a path that is already wet, such that channels, once established, are expected to persist. The largest channels, through which flow can most easily take place, have been observed to grow at the expense of smaller, less efficient, channels (Conway and Benedict, 1994). Secondly, the permeability of drainage channels is expected to be further enhanced by grain growth occurring within them due to their increased saturation (Colbeck, 1979), further increasing their permeability compared to the rest of the snowpack.

Although preferential flow fingers have been widely observed and their importance in increasing rates of vertical water movement recognised, the huge variety of flow patterns observed in the field has made their effect difficult to quantify. In recent years, a significant amount of effort has attempted to discover the size and spacing of, and amount of water carried by, such channels. Conway and Raymond (1993) report flow fingers of 20 to 30 cm in diameter and spaced 0.5 to 2 metres apart, often penetrating the full depth of the snowpack. In work by Marsh and Woo (1985), an average of 22% of a snowpack section was occupied by flow fingers, in which flux was locally around twice that generated at the surface. This agrees well with the observations of McGurk and Kattelman (1988), in which ~25% of the snowpack was transmitting water; McGurk and Marsh (1995), in comparison, found flow taking place through only 4 to 6% of the snowpack volume. Albert et al. (1999), using high frequency radar to detect flow channels, obtained measurements of 3 channels per m^2. By examining ice columns in a Colorado snowpack, believed to provide a snapshot of major flowpaths during melting, Williams et al. (2000) found 2 to 3 columns per m^2, each of 10 to 30 cm width. Most recently, image analysis of dye flowpaths has been shown to be a valuable technique for quantifying flow patterns in both snow and other media at high spatial resolution (Stadler et al., 2000; Waldner et al., 2004); Waldner et al. (2004) observed preferential flow paths occupying just 10% of the snow cross-sectional area, and enlarging and changing location through time. Field studies have therefore produced a range of estimates of flow finger size, spacing, and amount of water carried, and choosing representative generalised values suitable for use in runoff modelling remains a problem. However, as Kattelman and Dozier (1999) have commented, although quantification of these phenomena may continue to be difficult, recent work has at least taught us that we must avoid the temptation to assume homogeneity of flow, something existing modelling studies have often not managed.

It is likely that the size and spacing of preferential flow pathways is highly dependent on surface melt conditions, with flow paths observed to change completely between melt

events (Schneebeli, 1995). Through time, Conway and Raymond (1994) observed flow fingers to grow from around 1 cm to over 20 cm as a result of several days of rain, while Marsh (1991) states that flow fingers will disappear and flow become more even as a result of sustained melt. Much therefore remains to be clarified about the temporal evolution of these features.

Surface indications of heterogeneous flow

It has been suggested by several workers that the spatial variability in flow through the snowpack will be expressed at the snowpack surface, with numerous studies noting surface depressions that can be related to subsurface flow patterns. Both Gerdel (1954) and Albert et al. (1999) report a pock-marked snow surface indicating the probable location of flow fingers, while McGurk and Kattelman (1988) describe "bowl-shaped melt depressions". This relationship between flow channels and surface lowering can be easily understood, with increased grain growth and densification in zones of higher water content expected to allow greater settling of the snowpack above flow fingers and therefore the formation of surface depressions (Conway and Raymond, 1993).

It has also been suggested that surface depressions, in turn, play a role in concentrating flux within flow fingers. The topography of the snow surface may both enhance melt production in depressions due to radiation reflection and cause convergence of near-surface flow in depressions, resulting in the concentration of flow within selected regions of the snowpack (Kattelman and Dozier, 1999; Williams et al., 1999).

This link between surface topography, surface wetness, and subsurface flow pathways means that surface observations can perhaps be used as an indicator of subsurface flow. Williams et al. (1999) used near infrared aerial photographs to study the variability of snowpack surface wetness in an attempt to characterize the spatial distribution of flowpaths within a Colorado snowpack. They found correlation lengths between zones of increased wetness of between 5 and 7 metres, becoming stronger as the melt season progressed. Measurements of surface wetness using a dielectric sensor confirmed that this remotely obtained data was a reflection of surface conditions. For different images of the same site, Erickson et al. (2000) found correlation lengths of 3 to 3.5 m. Similarly, for a Wyoming snowpack Sommerfeld et al. (1994) found a correlation length for surface wetness of 6m from aerial photographs, confirmed by lysimeter data. These results not only show the potential of using remotely sensed data in studies of snow hydrology, but also indicate an organisation of subsurface flow at a scale far greater than most studies of flow fingers have suggested. Williams et al. (1999) suggest that their result represents a distance over which

smaller meltwater flowpaths are 'bunched'. As the authors note, their results are not universal, and there are likely to be different patterns of water flux at sites that differ from the gently sloping (generally ~4°) continental alpine site where this data was gathered. These patterns remain to be further investigated at individual sites.

Spatial variability of runoff

In accordance with the observations of spatial flow variability detailed above, many lysimeter studies have shown runoff from the base of the snowpack to be hugely spatially variable. Harrington and Bales (1998), using eight $1m^2$ lysimeters located in close proximity to each other, found discharge through them to range from 20 to 205 % of the mean flow. Marsh and Woo (1985) found that although daily runoff through a $1m^2$ lysimeter and two $0.25m^2$ lysimeters agreed to within 10%, flow rates from the 16 individual partitions into which one of the smaller lysimeters was divided varied from 0 to 240 % of the mean flow. Kattelman (1989) found that while runoff through three lysimeters agreed to within 15%, discharge to a fourth was much higher, and attributed this to uneven surface melting and ground microtopography. Results such as these confirm the huge spatial variability of flow rates within the snowpack, and indicate that there is a minimum area over which lysimeter measurements must be made in order to represent mean snowpack runoff (Kattelman (1987) has suggested that lysimeter area should be as large as 6 m^2; Marsh and Woo's (1985) findings, in contrast, suggest that a lysimeter size of 0.25 m^2 can yield results representative of a wider area).

As Harrington and Bales (1998) note, quantitative intercomparison of the spatial variability observed in these various studies is made very difficult by the different experimental set ups used and the different scales at which measurements have been made. However, the widespread observation of heterogeneous flow rates in lysimeter studies has made it clear that such features must be taken into account if runoff from the snowpack is to be reliably modelled.

Ice layer effect on percolation

As mentioned in section 2.2.2.1, horizontal layers of ice are commonly present within the body of the snowpack. Kattelman and Dozier (1999) use the term *ice layer* to refer to ice bodies which are horizontally continuous, and *ice lens* to refer to those which are discontinuous. In this thesis, the term *ice layer* will be used more generally to refer to both, although the important role that any gaps in ice layers will play in controlling patterns of water flow is noted. The presence of ice layers within the snowpack has been identified as a

further important factor disrupting water percolation and causing heterogeneous flow, though there remains much disagreement about their precise role.

Many observations have shown that ice layers, as relatively impermeable horizons within the snowpack, delay the movement of water and increase the storage capacity of the snow (Langham, 1974c; Conway and Benedict, 1994; Singh et al., 1997, 1999; Fortin, 2002). Singh et al. (1999) found that the liquid water content above ice layers in an isothermal snowpack was increased to 14.4% compared to 6.6% where flow was unobstructed. In other cases, retention of flow is sufficient to lead to saturated conditions above ice layers, with trapped water observed to spill down the exposed pit wall when vertical excavations are made into the snowpack (Langham, 1974c). Ice layers can hinder water movement in three ways, namely the formation of static internal ponds above dips in ice layers, dynamic retention of flowing water, and diversion of flow along sloping ice layers (Langham, 1974a, c). Meltwater percolating relatively homogeneously above an ice layer is observed to pass through it at isolated points (Langham, 1971), indicating permeability of otherwise solid ice layers via vein systems between ice grains (Langham, 1974a). When flow fingers are present, their arrangement is likely to be completely altered after negotiating an ice layer (McGurk and Marsh, 1995). Fortin (2002) observed that artificial dyed ice layers became permeable once exposed to melt, with the overall dimensions of the layers remaining the same but their texture becoming rougher and more granular. The delay to runoff caused by ice layers may be great: Conway and Benedict (1994) report vertical flow impeded and diverted laterally for several hours by each ice layer in the studied snowpack. Fountain (1996) concludes that the rate of flow through the snowpack is largely determined by ice layers.

In stark contrast, other studies have suggested that ice layers not only have little effect in delaying meltwater runoff, but may even increase flow rates. Gerdel (1954) observed ice layers to disintegrate rapidly when the snowpack was wetted, such that their effect on water flow was only temporary. More recently, Conway and Raymond (1993) found that water penetrated ice layers quickly in a previously wetted maritime snowpack, having little effect on downward percolation. Both Gerdel (1954) and Jordan (1983b) have suggested that ice layers can become high conductivity layers as the ice bonds between the coarse-grained crystals break down, promoting rapid lateral flow. Moreover, the concentration of vertical flow in channels due to spatial variability in the permeability of ice layers can be argued to increase flow rates by increasing local water saturation within these channels (Jordan, 1983b; Furbish, 1988) in a similar manner to preferential flow fingers, and these flow channels may remain dominant even after other areas of the ice layer become permeable.

The net effect of ice layers on water flow would then depend on the balance between water retention above them and increased flux and percolation rates in flow channels.

These contradictory observations can perhaps be better understood in the light of Langham's (1974a) consideration of the relationship between ice layer permeability and temperature. Langham showed theoretically that the size of veins between ice crystals, and therefore ice layer permeability, would respond continuously to changing temperature, pressure, and dissolved air concentration around the layer. In particular, permeability would be highly sensitive to changes in temperature as the snowpack approached 0°C, with a rapid increase in vein size at temperatures above –0.1°C. The permeability of an ice layer may therefore be continuously variable as these controlling parameters vary, quite possibly following a diurnal cycle during the melt season. Specific conditions at the time and location of observations are therefore likely to give widely varying impressions of ice layer effect on water percolation.

A major obstacle to an improved understanding of ice layer effect on water flow, and to the incorporation of ice layers in models of snow hydrology, is the lack of quantitative information available about their role, in particular measurements of ice layer permeability. This lack of information may be attributed to the difficulty of measuring ice layer properties in the field and their rapid evolution during the melt season (Fortin, 2003). Very few values for ice layer permeability in temperate snowpacks have been published. Albert and Perron (2000) obtained permeability values of between 1 and 9 x 10^{-10} m^2 for distinct, fairly solid ice layers between 1 and 3 mm thick, significantly lower than values measured in the surrounding snow (51 to 105 x 10^{-10} m^2). These low values, however, might be due at least in part to the cold weather at the time of measurements, with the snowpack frozen. Fortin (2003) measured ice layer permeability values varying between 0.014 and 35.3 x 10^{-10} m^2 in temperate Canadian snowpacks, but despite a sizable data set (including thickness, density, porosity and pore tortuosity of the ice layers) was unable to identify the controls on permeability or describe in detail the variation of permeability in time and space. However, a slight general increase in permeability through time was found. Multiple sampling of the same ice layer yielded significantly varying results, which, if measurement precision is believed reliable, indicate the spatial variability of ice layer properties. Again, the magnitude of values found is likely to have been affected by the timing of study, which was early in the melt season and in general before significant melt had taken place.

There remains, therefore, much still to be determined about the influence of ice layers on water flow through snow. In particular, there is a need for more field observations of ice

layer effect on flow pattern, and measurements of ice layer permeability, the factors controlling it, and its evolution over time.

Measurements of snowpack permeability

As for ice layers, there are few published values for the permeability of temperate snowpacks during the melt season. In earlier work, the only method available for determining snowpack permeability was the use of lysimeter discharge data and known input surface flux to calculate velocities of water movement through the snowpack, and back-calculation of corresponding permeability values using theory (Marsh, 1991). Values calculated in this manner give the equivalent permeability k_e of the whole snowpack depth, averaging over the different permeability values of snow and ice layers (McGurk and Kattelmann, 1986; Fox et al., 1999). Fox et al. (1999) obtained values of k_e ranging between 3.2×10^{-12} and 6.6×10^{-10} m^2 from lysimeter data collected in a continental alpine snowpack in the Colorado Front Range, USA, stating that their results were in general over an order of magnitude smaller than minimum values reported elsewhere. Colbeck (1972) reported values of 3.3×10^{-10} m^2 for homogeneous snow and 1.5×10^{-10} m^2 for snow containing ice lenses, based on earlier measurements by Kuroiwa (1968) and Sharp (1952). Colbeck and Davidson (1973) found values between 1 and 3×10^{-10} m^2 in homogeneous laboratory snow. Colbeck and Anderson (1982), working with lysimeter data collected in California and Vermont, found values between 1 and 4×10^{-9} m^2, and attributed the lower values found in Vermont to the greater number of ice layers in the snow cover there. Jordan's (1983a) measurements of hydraulic conductivity correspond to an average permeability value of 3.29×10^{-10} m^2. McGurk and Marsh (1986) reported k_e values ranging between 3×10^{-10} and 1.8×10^{-8} m^2 over a two year study period. Denoth et al. (1979) report some of the highest values in the literature, ranging between 1×10^{-9} and 2.5×10^{-8} m^2 (cited by Fox et al. (1999)), although this may be explained by the homogeneity of the glacier firn used in their study.

More recently, permeameters have been used to directly measure the permeability of snow samples. Jordan et al. (1999b) measured the air permeability of samples of natural and sieved snow and found results to vary widely with snow type, ranging across two orders of magnitude between fine-grained, packed snow (permeability around 6×10^{-10} m^2) and large-grained depth hoar (permeability around 5.24×10^{-8} m^2). Their results also confirmed the reliability of using Shimizu's (1970) formula to calculate permeability from snow grain diameter and density. For faceted snow, permeability of around 7×10^{-9} m^2 has also been found (Hardy and Albert, 1993; Albert and Hardy, 1995). For an Antarctic snowpack, Albert et al. (2000) found permeability ranging between approximately 5 and 80×10^{-10} m^2, with snow characteristics at the grain-scale believed to be the principal controlling factor.

Even fewer studies have collected information about the temporal evolution of snowpack permeability, despite the important changes that would be expected as snow density, grain size, preferential flow patterns and ice layer properties evolve over the course of the melt season. Granger et al. (1978) reported a temporal increase in k during the melt season of a Prairie snowcover. Grain growth, ice layer decay and flow channel development have been suggested as the cause of increasing k (Fox et al., 1999). In contrast, McGurk and Kattelmann (1986) found that k_e decreased over time in a Sierra Nevada snowpack. Fox et al. (1999) suggest that this decrease is due to the break down of ice layers, as flow is no longer concentrated in preferential flowpaths below permeable points in layers. As discussed above, this suggestion represents one of the two opposing opinions about the role of ice layers in controlling water movement through snow, and other mechanisms for changing permeability through time can be proposed. There remain very few observations of snowpack permeability over time periods longer than a few days.

2.2.2.4 Saturated flow at the snowpack base

If percolating water meets an impermeable layer at the base of the snowpack, for example glacier ice, saturation will build up to form a shallow water table (Fountain, 1996). Water then moves laterally downslope within this saturated layer, with the rate of water flow in this zone another important control on the timing and magnitude of runoff from the snowpack. Due to the high saturation within this zone, grain growth is expected to lead to permeability values significantly higher than that in the unsaturated zone (Colbeck, 1974). Colbeck (1978a) predicts a difference of more than six orders of magnitude between permeability to water flow in the saturated and unsaturated zones, a result of differing grain size, levels of saturation, and presence of ice layers. In field observations by Fujino (1971), the rate of meltwater percolation in the unsaturated zone was only about one-eightieth of flow rate in the basal saturated zone. As a result of these fast wave speeds, the saturated layer is expected to play little role in dampening diurnal meltwater waves, in contrast to the marked dampening caused by percolation through just a few metres of unsaturated snow (Colbeck, 1974).

2.2.3 Modelling water flow through snow

Empirical observations and investigations of snow hydrology in the field have been complemented, from the 1970s onwards, by work which attempts to bring together our understanding of the physical processes at work in wet snow in order to develop mathematical models of snow hydrology. A variety of approaches have been presented, from finite element modelling of water flux in one-dimension (Jordan, 1983b) to complete snow process models (Jordan, 1991; Brun et al., 1992, Lehning et al., 1999). A key development was the physically-based gravity drainage (or 'kinetic wave') theory for water

percolation through snow developed by Colbeck in a series of papers beginning in 1972 (Colbeck, 1972, 1975a, 1978a), which has been shown to provide a useful tool for modelling investigations of snow hydrology. An expression for flow rate in the basal saturated layer was also developed (Colbeck, 1974). Subsequent work has attempted to incorporate heterogeneous flow features in models. Modelling approaches to both unsaturated and saturated flow will be reviewed in this section, with particular attention to the strengths of existing methods and areas in which further progress is needed.

2.2.3.1 Vertical, unsaturated flow

The gravity flow ('kinetic wave') theory

This section outlines the fundamental principles upon which Colbeck's gravity flow theory is based. These principles remain widely used; more recent work using the gravity flow theory can be found in Sellers (2000), Singh et al. (2000a), and Willis et al. (2002). The first step in Colbeck's (1972, 1978a) consideration of water flow through snow is the treatment of the snowpack as a homogeneous, porous medium. In reality, the natural snowpack will very rarely, if ever, provide such ideal conditions to work with, but a theory of water flow through homogeneous snow provides a useful point at which to begin understanding snow hydrology. Later work can then build on the established theory of homogeneous flow to include complications such as ice layers, preferential flow channels, and the variation of snowpack properties through space and time.

For further simplification, the gravity flow theory assumes the snowpack to be isothermal, such that the complicating effects of refreezing can be neglected. Separate models exist for the refreezing and heat transfer processes involved when liquid water flows into cold snow (Colbeck, 1976; Dunne et al., 1976; Illangasekare et al., 1990; Pfeffer et al., 1990; Tseng et al., 1994).

Colbeck demonstrated that water percolation through homogeneous, unsaturated snow can be described by the straightforward application of Darcian flow (Colbeck, 1972; Colbeck and Davidson, 1973). Darcy's law, originally developed to describe the characteristics of water flow through sand during investigations of aquifer hydrology, expresses Darcy's observation that the rate of flow of water through a saturated porous medium is proportional to the hydraulic gradient to which it is subjected (Darcy, 1856; cited in Davie, 2003). Assuming that air is free to move in response to water flow, as will be the case in a natural snowpack in which saturation values are in the pendular regime, the flux of water u_w (volume of water flowing per unit area per unit time, $m^3 \, m^{-2} \, s^{-1}$ or $m \, s^{-1}$) is

$$u_w = \frac{k_w}{\mu_w}\left[\frac{\delta p_c}{\delta z} + \rho_w g\right] \tag{2.3}$$

where k_w is the permeability of the snow to the water phase (m^2),

μ_w is the viscosity of water (P),

and the terms $\delta p_c/\delta z$ and $\rho_w g$ describe the forces acting to either impede or promote water flow, respectively the capillary pressure gradient (which may act to drive or delay water flow depending on its direction) and the force of gravity acting upon the water (a function of the density of water ρ_w and the acceleration due to gravity g) (Colbeck, 1972, p.373).

Colbeck further showed that, under normal conditions of water drainage in snow, flow occurs under the influence of gravity with little capillary influence (Colbeck, 1972). As a result, the percolation of water through snow can be regarded as being driven by gravity alone, and the pressure gradient term in Equation 2.3 disregarded. Accordingly, a simplified form of Darcy's law can be used to describe water flow in snow:

$$u_w = \frac{\rho_w k_w g}{\mu_w} \tag{2.4}$$

As ρ_w, g, and μ_w will be constant and are easily known, the remaining unknown parameter is k_w, the permeability of the snow to the water phase. It is k_w that determines what water flux u_w will occur. As discussed in section 2.2.2.2, while the total permeability of the snowpack is dependant only upon the pore size and geometry, k_w will in general depend on both the pore characteristics and the volume of water present (Colbeck, 1972). For a given pore geometry, k_w will increase with increasing liquid water content, as the greater amount of water present provides a greater area through which flux can occur. Colbeck uses established relationships for other porous materials to relate k_w to pore space properties and water saturation. Shimizu's (1970) formula (Equation 2.1) is used to calculate the intrinsic (saturated) permeability k of the snow based on snow grain diameter and density. Thereafter, k_w can be found as a fraction of k if the effective water saturation S^* is known, using the relation (Colbeck, 1978a)

$$k_w = k S^{*\varepsilon} \tag{2.5}$$

S^* is the percentage of the pore volume occupied by mobile liquid, defined as

$$S^* = \frac{S_w - S_{wi}}{1 - S_{wi}} \tag{2.6}$$

Colbeck (1972) first suggested a value of 2 for the exponent ε in Equation 2.5, but later revised this to 3.3 based on results from laboratory drainage experiments (Colbeck and Davidson, 1973). Other studies have suggested values for ε between 1.5 and 4.8 (Marsh, 1991; Table 2.2), based on drainage experiments in a variety of natural and laboratory snow types. It is expected that ε will vary depending on snow properties such as grain size, density, and stage of metamorphism, but no clear relationship has been found (Denoth et al., 1979). In the absence of more widespread field evidence from snowpacks of varying characteristics, most studies (including Colbeck (1978a), Jordan (1983a) and Marsh and Woo (1985)) have assumed a value of 3 for ε. Using this exponent, Equation 2.5 predicts that permeability to the liquid phase k_w will increase quickly as S* increases.

Table 2.2: Proposed values for ε (taken from Marsh (1991), with Fox et al. (1999) added).

Reference	ε	Method
Colbeck (1972)	2	Estimate from flux data of Sharp (1952)
Colbeck and Davidson (1972)	3.3	Drainage in homogeneous snow
Wankiewicz (1976) (in Jordan (1983a))	3.3-3.5	Drainage of natural snow
Denoth et al. (1979b)	1.5	Drainage of freshly wetted snow
Denoth et al. (1979b)	3.7	Drainage of metamorphosed snow
Denoth et al. (1979a)	2.2-4.6	Drainage of various snow types
Ambach et al. (1981)	2.8	Drainage from glacial firn
Jordan (1983a)	>3.5	Drainage in natural snow
McGurk and Kattelman (1986)	4.8	Drainage of metamorphosed snow
Fox et al. (1999)	2.93	Drainage in natural snow

Equation 2.5 can now be supplemented into Equation 2.4 to express u_w as a function of snowpack saturation:

$$u_w = \alpha k S *^3 \tag{2.7}$$

where α is a constant encompassing the readily-known terms, given by

$$\alpha \equiv \rho_w g \mu_w^{-1} \tag{2.8}$$

The continuity equation states that liquid water is conserved in wet snow, that is

$$\delta u / \delta z + \phi_e (\delta S * / \delta t) = 0 \tag{2.9}$$

where z is a vertical coordinate through the snowpack and t is time.

The effective porosity ϕ_e is the fraction of total porosity ϕ not already occupied by the irreducible water content S_{wi}, defined as

$$\phi_e \equiv \phi(1 - S_{wi}) \tag{2.10}$$

Equations 2.7 and 2.9 can then be combined to produce a differential equation describing the vertical flux of water:

$$3\alpha^{1/3}k^{1/3}u^{2/3}(\delta u/\delta z)+\phi_e(\delta u/\delta t)=0 \qquad (2.11)$$

Colbeck then solved Equation 2.11 by the method of characteristics to produce a relationship between the flux of liquid u and the rate of vertical descent of that value of flux ($dz/dt|_u$) (Colbeck, 1978):

$$\left.\frac{dz}{dt}\right|_u = 3\alpha^{1/3}k^{1/3}\phi_e^{-1}u^{2/3} \qquad (2.12)$$

This solution shows that the rate of downward movement of a value of flux ($dz/dt|_u$) increases as that value of flux (u) to the two-thirds power. In other words, the speed at which any value of flux is propagated through the snowpack depends on the magnitude of the flux itself, with larger values of flux moving faster than smaller values of flux (Colbeck, 1978a). As a result, larger fluxes produced around midday will tend to 'override' (Colbeck, 1972) the more slowly moving smaller values of flux produced on the rising limb of the hydrograph, resulting in a rapid build-up of flux known as a shock front. Smaller values of flux generated on the falling limb will move at increasingly slower rates, resulting in a gradual decline in runoff after the wave crest has passed. This flux-induced distortion of the wave form (shown in Figure 2.3), a consequence of the physical controls on water flow at the grain scale, has important implications for the form of any runoff hydrograph modelled using Colbeck's theory, and the accuracy of its representation of real-world snow runoff must be considered.

In comparisons with field data, runoff hydrographs modelled using Colbeck's gravity flow theory have been found to reproduce the main features of meltwater waves well (Colbeck, 1972; Colbeck and Anderson, 1982). In particular, the observed asymmetry of the wave form and its increase with depth, the increasing value of the minimum volume flux with depth, and the decreasing maximum value of volume flux with depth are seen to support the physical concepts used in the theory (Figure 2.4). However, runoff hydrographs observed in the field frequently do not show the sudden rise in flux that would indicate the formation of a shock front. This has been attributed to the heterogeneity of flow described earlier, with preferential flow channels carrying water to the base of the snowpack ahead of the background wetting front and accounting for the more gradual rise in flux (Colbeck, 1972). Thus, while the gravity flow theory seems in general to provide a good representation of

waveforms as they percolate through unsaturated snow, there remain more complex features of flow that are unaccounted for.
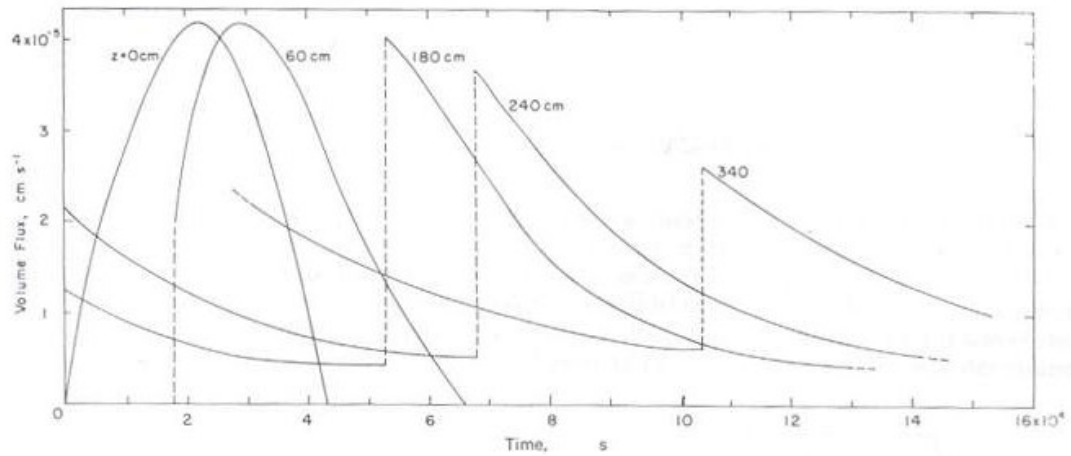
Figure 2.3: Flux at different depths within the snowpack as modelled by the gravity flow theory (Colbeck, 1972). With increasing depth the formation of the shock front (dashed line) and an extended trailing limb can be seen.
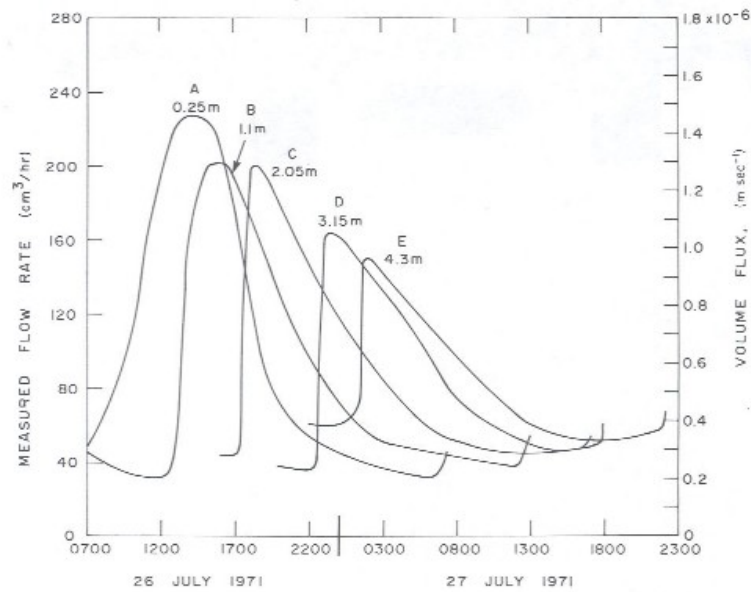
Figure 2.4: Characteristics of a diurnal meltwater wave measured at various depths below the snow surface in a homogeneous snowpack (Colbeck and Davidson, 1973), showing asymmetry of the wave form increasing with depth, decreasing maximum value of volume flux with depth, and increasing value of the minimum volume flux with depth.

The gravity flow theory was further tested in a laboratory setting using isolated columns of repacked, homogeneous snow (Colbeck and Davidson, 1973). After inducing intense surface melting, the values of u arriving at the base of the columns were monitored and converted to speeds ($dz/dt|_u$). The measured speeds are plotted against values of flux u in Figure 2.5. The straight line, which represents Equation 2.12, fits the experimental data well, and its slope supports the use of the exponent 3 in Equation 2.5.
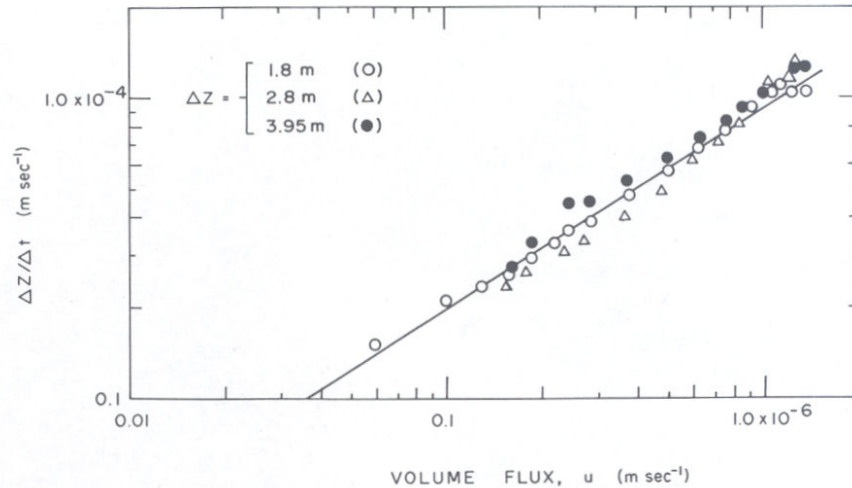
Figure 2.5: The measured relationship between the speed of descent (dz/dt) of values of u for 3 repacked columns of snow (lengths dz indicated). The solid line through the points represents Equation 2.12 and fits the data well, supporting the use of Equation 2.12 to represent percolation through unsaturated snow and the exponent 3 in Equation 2.5. From Colbeck and Davidson (1973).

The intercept of the line in Figure 2.5 is determined by the parameter $k^{1/3}\phi_e^{-1}$, which represents snow properties. $k^{1/3}\phi_e^{-1}$, as Colbeck (1978a) notes, can therefore be determined directly from information about surface and basal fluxes without the need for measurements of grain size or density, which are difficult to measure accurately in the field. If the value of ϕ_e is also known, then a value for k can be calculated. When determined in this way, the permeability value is an integrated average over the entire depth of snow, including the effect of any inhomogeneous features (preferential flow channels, ice layers) that may be present, and is termed the 'snowpack equivalent permeability' k_e. Lysimeter data of meltwater flow at depth, together with information about meltwater inputs at the snow surface, can therefore be used to describe the hydrological behaviour of the snowpack and its change through time. k_e values calculated by this method were reviewed in section 2.2.2.3. It has been suggested (Colbeck, 1978a) that representative values of $k^{1/3}\phi_e^{-1}$ may be found for different types of snow and/or for different stages in snowpack hydrological behaviour, enabling more informed modelling of changing snow runoff through time, but more season-long field investigations are required before this is possible. As Marsh (1991)

points out, a common assumption in modelling studies in the past has been that the evolution of snowpack structure is sufficiently slow that it can be ignored, but a key aim for future work must be clarification of the way in which changes in snowpack material properties affect runoff through the snowpack.

Colbeck's (1972, 1978a) gravity flow solution has gone on to be used in numerous studies of snowpack runoff, including Dunne et al. (1976), Bengtsson (1981), Jordan (1983b), Marsh and Woo (1985), and Willis et al. (2002), and in complete snow process models including the SNTHERM model (Jordan, 1991). Due to the complexity of typical melt conditions, numerical solutions are required, but these are simple and efficient.

2.2.3.2 Modelling inhomogeneous flow

Although the heterogeneity of water flow through snow has been extensively reported from field and laboratory studies, the incorporation of heterogeneous flow features into mathematical modelling continues to pose significant challenges. A quantitative understanding of flow variability, of the sort which could be incorporated in modelling of heterogeneous flow, has not yet been sufficiently attained (section 2.2.2.3). It has been suggested that it is these small-scale variations of flow pattern that are responsible for the inaccuracies which arise when applying water flux models based on the assumption of homogeneous snow properties to natural snow covers (Marsh and Woo, 1985). Several studies have therefore sought to develop flow models which incorporate heterogeneous flow features in order to better represent observed snowpack runoff, and their success will be reviewed here.

Dealing with multiple flow channels

Based on multi-compartment lysimeter measurements of lateral flow variability in an Arctic snow cover, a multiple flow-path model was developed by Marsh and Woo (1985). In this model, meltwater is routed from the snow surface to the snow base along a number of independent flow paths, with each flow path carrying a different proportion of the total flow based on the flow variability measured by lysimeters in the field. Within each flow path, percolation proceeds according to Colbeck's gravity flow theory (Colbeck, 1972). Hydrographs produced with the multiple flow-path model were found to improve the representation of runoff in comparison with observed hydrographs in several ways. Because water carried by more dominant flow paths (meaning those which carry a higher fraction of the total runoff) arrives at the snowpack base earlier than that carried by lower-flow channels, with the rest of the water being delivered at variable rates in between, flow begins to rise earlier, the rising limb is not as steep, and the value of peak flow is reduced (Marsh

and Woo, 1985; Figure 2.6). With these improvements, modelled runoff was shown to agree closely with measured results in terms of time of hydrograph rise, rate of rise to the peak, value of peak flux, and form of recession limb (Figure 2.6). Furthermore, the performance of the model when applied to a different site led Marsh and Woo to suggest that it could be successfully applied to other environments using the flow variability measured in the initial study – that is, without the need for fieldwork at each site. This suggestion is yet to be fully tested using a range of field sites and snowpack types, but the huge range of preferential flow patterns observed in the field seems to suggest that it is unlikely to be true.

The importance of correctly modelling preferential flow patterns was further emphasized by Gustafsson et al. (2004) during verification of the SNTHERM model (Jordan, 1991). While bulk properties of the snowpack were found to be well reproduced, the authors suggested that the lack of representation of preferential flow patterns was important in causing errors in snow grain properties at the small-scale, as liquid water content and distribution, and resulting grain growth, were not correctly modelled.
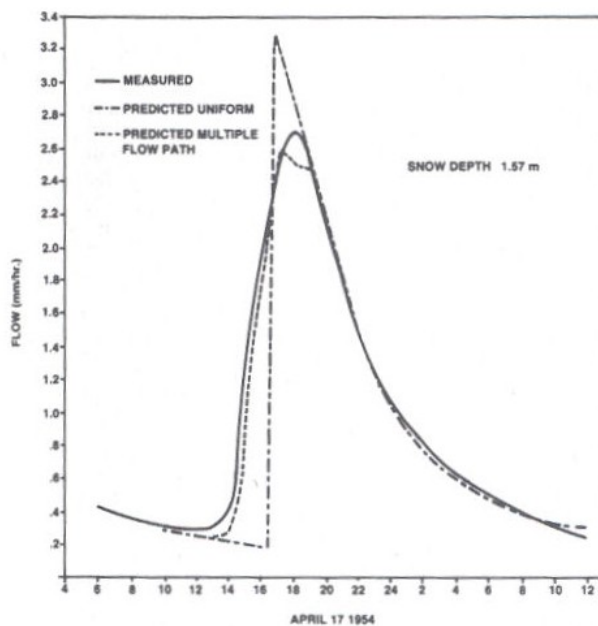
Figure 2.6: Comparison of a measured meltwater wave (lysimeter data from Central Sierra Snow Laboratory, California) with those predicted by either a uniform percolation model or the multiple flow path model (Marsh and Woo, 1985), showing improved modelling of the rising limb when multiple flow paths are taken into account.

Incorporating ice layer effects

The theory of gravity drainage through unsaturated snow was extended by Colbeck (1975a) to consider the role of ice layers in delaying water flow from the snowpack surface to base. By viewing a natural layered snowpack as an equivalent anisotropic porous medium, with known values for the permeability of each snow or ice layer and for the snowpack slope, Colbeck demonstrated how the concepts of one-directional flow can be used to determine flow path, volume flux, and wave speed for stepwise, two-dimensional flow past layers of varying properties. The effect of ice layers in this theory is to increase the transit time for water movement by a factor equal to the ratio of snow permeability to ice layer permeability.

Although a useful way of conceptualising flow around ice layers, the lack of quantitative knowledge about ice layers properties is a serious limitation to the application of such a theory. Although some recent studies have yielded values for ice layer permeability (Albert and Perron, 2000; Fortin, 2003; section 2.2.2.3), these remain spatially isolated and temporally limited. The interplay between the low permeability of most of an ice layer area and the high permeability of gaps in them also remains to be clarified. The question of how to properly incorporate the influence of such features into physical models of snow hydrology remains an important issue to be resolved.

2.2.3.3 Basal, saturated flow

Colbeck further extended his theory of water flow in snow to provide an account of saturated water flow through snow overlying an impermeable boundary (Colbeck, 1974; Colbeck, 1978a; Singh et al. 2000b). As in the gravity flow theory for vertical, unsaturated flow, the theory aims to incorporate sound physical principles yet remain sufficiently simple that it can be reasonably applied (Colbeck, 1974).

Flow in the saturated layer, as in the unsaturated regime, is described by Darcy's law:

$$u_w = -k_s / \mu_w \left(\partial P_w / \partial x - \rho_w g \theta \right) \tag{2.13}$$

In this case, the forces driving water flow are θ, the slope of the impermeable layer, and $\delta p_w / \delta x$, the change in thickness h of the saturated layer along the flowline. h can be expected to vary only slightly downslope, leaving slope θ as the primary force driving the flow of water in the saturated layer (Colbeck, 1974). Colbeck solved the resulting simplified equation to produce an equation for wave speed in the basal layer:

$$c_s = \alpha k_s \theta \phi^{-1}$$
(2.14)

Again, the permeability of the snow to the water phase k plays a key role in controlling the flow rate. Due to the role of liquid water saturation in encouraging wet snow metamorphism and therefore preferential grain growth, it is expected that grain sizes in the saturated layer will be large. The intrinsic permeability of the basal layer will therefore tend to be significantly greater than that of the unsaturated, upper layers, following the grain size-permeability relationship developed by Shimizu (1970) (Equation 2.1). Ice lenses inhibiting percolation in the unsaturated regime may further enhance this difference. It is the effect of saturation, however, which is likely to have the greatest effect on permeability, potentially causing a difference of more than four orders of magnitude between permeability to the liquid phase in the saturated and unsaturated zones; grain growth and ice layer effects can increase this difference to six orders of magnitude (Colbeck, 1978a).

2.2.3.4 Comprehensive snow process models

The physical processes governing snow temperature evolution, grain metamorphism, densification, surface melt and water transport have been brought together to produce comprehensive snow process models to simulate the energy and mass evolution of a snowcover through time given surface meteorological conditions. Well-established models include CROCUS, developed by the French national meteorological service (Brun et al., 1989; 1992), SNTHERM, from the US Army Corps of Engineers Cold Regions Research and Engineering Laboratory (CRREL) (Jordan, 1991), and the Swiss Federal Institute for Snow and Avalanche Research's SNOWPACK (Lehning et al., 1999; 2002a; 2002b; Bartelt and Lehning, 2002). In the case of both CROCUS and SNOWPACK, the need for accurate snow stability information for avalanche warning purposes has provided the impetus for detailed snowpack modelling, with SNOWPACK in particular including detailed information about snow microstructure and resulting mechanical stability (Lehning et al., 2002a). Both CROCUS and SNTHERM base their treatment of water percolation on Colbeck's gravity flow theory (1972, 1978a). The energy budget components of 23 snow models have been validated as part of the SnowMIP project (Etchevers et al., 2004), but the success of models in simulating water flow through the snowpack has received less attention.

2.3 GLACIER HYDROLOGY: PRINCIPLES, IMPORTANCE, AND ROLE OF THE SUPRAGLACIAL SNOWPACK

The drainage of water through glaciers is of both practical and scientific interest, and as such has been the subject of extensive research. On a practical level, an understanding of the factors controlling glacier runoff informs planning for water supply, irrigation and hydroelectric power generation and can enable management of glacier-induced flooding, limiting damage to both infrastructure and human life. Understanding glacier hydrology is also critically important to some major scientific questions. Water movement through glaciers influences subglacial and proglacial geomorphic processes and also influences runoff hydrochemistry. As a factor controlling the dynamics of ice masses, glacier hydrology is of fundamental importance in mediating the way in which glaciers and ice sheets respond to climate change, and in determining the ways in which ice masses shape the landscape (Sharp et al., 1998). What's more, changing meltwater runoff from ice masses under a warming climate will not only contribute to global sea level rise, but has been hypothesized as a mechanism which could disrupt the ocean currents that redistribute heat around the globe (Rahmstorf, 2002; Ottera et al., 2003), changing world temperatures.

This section will review the principles of glacier hydrology and the role that the supraglacial snowpack has been suggested to play in the glacier hydrological system as a whole. Previous work on supraglacial snow hydrology is reviewed, the particularities of snow hydrology in the glacial setting are outlined, and areas in which further research is needed are identified. Comprehensive accounts of the en- and sub-glacial hydrology of temperate glaciers can be found in Röthlisberger and Lang (1987), Hooke (1989), Paterson (1994) and Fountain and Walder (1998); only those points required for an understanding of the supraglacial snowpack's role in glacier hydrology are summarized here.

2.3.1 The glacier hydrological system

2.3.1.1 Water sources

Surface melt of snow and ice is by far the most important source of water in temperate glaciers (Röthlisberger and Lang, 1987; Paterson, 1994), with smaller contributions made by melting within the body and at the base of the glacier, and by rainfall and groundwater flow. Surface melt is driven by the energy balance components, with the amount of energy available for melting, Q_M, calculated as

$$Q_M = Q_{NR} + Q_S + Q_L + Q_P + Q_G \qquad (2.15)$$

where

Q_{NR} =   net short-wave and long-wave radiation

Q_S =   convective or sensible heat flux

Q_L =   latent heat flux

Q_P =   heat provided from precipitation

Q_G =   heat from conduction in the snowpack (Röthlisberger and Lang, 1987).

In mountain areas, shading of the glacier surface by the surrounding peaks may be important in controlling radiation receipt and therefore causing variable patterns of melt across the glacier (Arnold et al, 1996). By far the majority of melt takes place during the summer months, giving rise to a marked seasonal variation in discharge into the glacial drainage system. The change in surface albedo as the winter snowpack ablates and lower albedo glacier ice is exposed also commonly plays an important role in changing meltwater production (Fountain, 1996; Willis et al., 2002).

2.3.1.2 Supraglacial drainage paths

An idealised diagram of drainage pathways in a temperate glacier is shown in Figure 2.7. Following production at the surface, glacial meltwater will first encounter either the glacier ice surface or a supraglacial snowpack. This is a point that has been frequently overlooked, with supraglacial flow in the ablation area assumed in many studies to take place via efficient subaerial channels on the ice surface. The movement of water through glacial snow and firn, as it has been studied to date, will be considered in detail later.
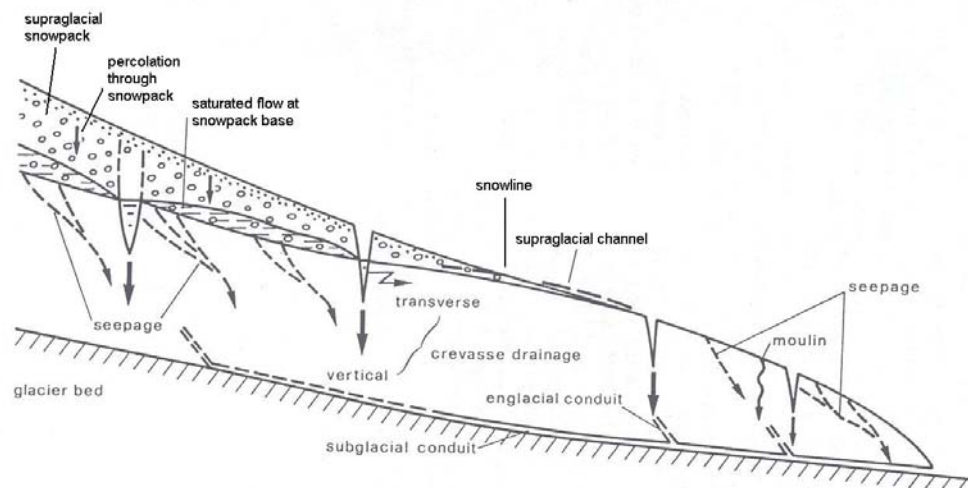
Figure 2.7: Supraglacial, englacial and subglacial drainage pathways in a temperate glacier (adapted from Röthlisberger and Lang (1987)).

On contact with the glacier ice surface, a small amount of meltwater may percolate into the body of the glacier via veins and capillaries in the ice structure (Nye and Frank, 1973). The majority, however, will flow downslope across the ice surface until either joining streams at the glacier margin or entering the englacial drainage system via crevasses or moulins (Stenborg, 1973). Both crevasses (tensional fractures in the ice) and moulins (vertical shafts in the ice body formed by persistent flow of a large supraglacial stream in the same location) are believed to carry water quickly to depth within the glacier, where it joins the subglacial drainage system.

2.3.1.3 Subglacial drainage configurations

The flow of water at the base of glaciers can take place via two main types of system, termed 'distributed' (or non-arborescent/slow) and 'channelised' (or arborescent/fast) (Fountain and Walder, 1998). In reality the distinction between these two types of system will not be clear-cut, with a mix of the two possible beneath any particular glacier, and temporal switching between drainage configurations. These two drainage system types have very different hydraulic properties and therefore pressure responses to input water volumes, with important implications for basal motion (Kamb, 1987).

The structure of the subglacial drainage system is controlled by the nature and variability of meltwater inputs, the physical properties of the overlying ice (especially ice thickness), and the nature of the underlying substrate (Bingham, 2003). Water flowing through a distributed system is generally derived from low-volume, temporally-invariant englacial and subglacial sources, and may flow as a thin film (Weertman, 1969, 1972), through a network of 'linked cavities' (Lliboutry, 1968; Walder, 1986; Kamb, 1987), or along wide, shallow canals incised into overlying ice and underlying till (Walder and Fowler, 1994). If the glacier is underlain by permeable sediment, distributed drainage may take place as Darcian porewater flow or advection (Shoemaker, 1986; Walder and Fowler, 1994).

Channelised flow, in contrast, is derived mainly from surface meltwater that reaches the glacier bed at isolated points via crevasses and moulins. A number of channel forms have been identified, including semi-circular 'R-channels' incised into the ice above when channels are water-filled (Röthlisberger, 1972) and broader, shallower 'H-channels' formed when channels are often only part-filled and melt is therefore concentrated at the base of channel walls (Hooke, 1984, 1990). If the glacier is underlain by bedrock easily eroded by water action (such as limestone) and subglacial channels persist in the same locations over time, 'N-channels' may be incised downwards into the bedrock (Nye, 1973; Sharp et al., 1989). Finally, 'C-channels' have been identified where mobile underlying sediments can be eroded as well as the overlying ice (Clarke et al., 1984).

2.3.1.4 Water pressure-discharge relationships

Water pressure within distributed and channelised drainage systems exhibits fundamentally different responses to changing water discharge, with major implications for the relationship between glacier hydrology and ice dynamics. As water discharge within a distributed drainage system increases, water pressure increases proportionally (Lliboutry, 1968), and as a result may cause instability of the system at high discharges (Walder, 1986; Kamb, 1987; Hooke, 1989). In contrast, increased discharge through channelised drainage systems causes increased melting of channel walls and therefore a decrease in water pressure (Röthlisberger, 1972).

2.3.1.5 Subglacial drainage system evolution

The increase in meltwater discharge through temperate glaciers in summer gives rise to corresponding seasonal changes in the subglacial drainage system (Hock and Hooke, 1993; Nienow et al., 1998; Fountain and Walder, 1998). During winter, low discharges are transmitted through a distributed system. When the melt season begins and increased meltwater discharges reach the base of the glacier through crevasses and moulins, the inefficient basal drainage system is initially unable to transmit the increased meltwater flux and water pressure increases. Correspondingly, numerous studies have observed uplift of the glacier surface and increased ice velocities when surface melt inputs increase in the early melt season (Iken et al., 1983; Hooke, 1989; Mair et al., 2001, 2002a, 2003; Harper et al., 2002). Under sustained or repeated high input fluxes, basal cavities are enlarged by melting and channels begin to develop. The channelised system is likely to persist throughout the melt season, until decreasing water supplies are no longer able to melt channel walls sufficient to offset closure by ice creep/deformation and a distributed system reforms (Sharp et al., 1993).

The evolution of the subglacial drainage system has been observed to vary spatially, with dye-tracer studies at Haut Glacier d'Arolla indicating an upglacier expansion of the channelised drainage network during the melt season, closely correlated with the seasonal retreat of the supraglacial snowline (Nienow, 1997; Nienow et al., 1998). Altitudinal differences in supraglacial water delivery have therefore been suggested as a key factor influencing conditions in the subglacial environment, with the exposure of the ice surface and onset of rapid supraglacial runoff thought to trigger drainage system evolution.

2.3.2 Glacier dynamics

The net motion of glaciers is the sum of movement by three separate mechanisms: internal deformation of the glacier ice, basal sliding, and deformation of basal sediments (Paterson, 1994). Internal deformation of ice is regarded as both making a comparatively small contribution to overall movements and being relatively constant in time, with the two mechanisms of basal motion being responsible for temporal variations in glacier dynamics. By either reducing friction between the glacier base and the underlying substrate, thus enabling sliding (Iken and Bindschadler, 1986; Hooke et al., 1989), or by reducing the strength and viscosity of subglacial sediments (Boulton and Hindmarsh, 1987), high water pressure in the subglacial environments is believed to be the critical factor facilitating rapid basal motion (Sharp et al., 1998). The character of the subglacial drainage network, and hydraulic geometry of the individual drainage passageways of which it is composed, together with the flux of meltwater through it, are critical factors controlling subglacial water pressure. Uncovering the complex linkages between subglacial hydrology and ice dynamics has therefore been a major research focus within glaciology (e.g. Iken, 1981; Iken and Bindschadler, 1986; Kamb, 1987; Mair, 2002a, b, 2003). This section provides a summary of issues in subglacial hydrology and ice dynamics as they may relate to supraglacial snowpack hydrology; for more detailed reviews, see Willis (1995) and van der Veen (1999).

Numerous observations have shown that glacier motion is highly variable over a range of spatial and temporal scales (Willis, 1995). Many glaciers have been observed to exhibit increased flow velocities during the summer months (Iken et al., 1983; Hooke, 1989; Mair et al., 2001, 2003; Harper et al., 2002), with peak downglacier velocities frequently observed over the course of a few days early in the melt season, a phenomenon commonly termed the 'spring event'. Concurrent observations of subglacial conditions, using dye-tracer tests (Nienow et al., 1998) and down-borehole pressure sensors (Hubbard et al., 1995), have indicated that this speed-up event occurs when high subglacial water pressures are generated by increased summertime melt inputs entering an inefficient distributed drainage system not yet adapted to increased flux.

This speed-up in glacier motion has been observed to propagate upglacier over time (Nienow, 1997). Nienow (1997) suggests that this phenomenon may be caused by the presence of a thickening snowpack in an upglacier direction. Due to the dampening effect of flow through snow on runoff magnitudes (section 2.2), the magnitude of discharge through the subglacial drainage system in response to a given surface melt flux will be lower if there is a significant and inefficient supraglacial snowpack than if the ice surface is snow-free. Correspondingly, if supraglacial snow is having a significant dampening effect

on runoff, higher surface melt fluxes will be needed in order to generate subglacial water pressures sufficient to trigger increased flow velocities. As surface melt increases at the start of the summer, therefore, the occurrence of any spring speed-up event may be delayed by the presence of a supraglacial snowpack. Furthermore, when a speed-up event does occur, attenuation of the hydrograph by flow through the snowpack may result in this event having a lower magnitude than it would were the snowpack absent. As identified by Nienow (1997), the fact that the supraglacial snowpack generally becomes thicker and less hydrologically efficient in the upglacier direction is likely to result in both the delaying and dampening effect of the snowpack on the spring speed-up event becoming progressively greater in the upglacier direction. A good understanding of the way in which the supraglacial snowpack influences runoff into the subglacial system is therefore necessary to enhance our understanding of glacier dynamic events and in particular of the way in which supraglacial snowpack hydrology may influence spring event timing and magnitude.

2.3.3 The supraglacial snowpack as part of the glacial drainage system

Few studies have explicitly considered the hydrological influence of the supraglacial snowpack. Water movement through firn in the accumulation area of a glacier has been considered by several studies (e.g. Fountain and Walder, 1998; Schneider, 2001), but supraglacial drainage in the ablation area is often described as characterised by rapid (channelised) flow over the ice surface (e.g. Paterson, 1994), ignoring the fact that a significant snowpack normally exists in the ablation area during the early melt season. Such assumptions risk greatly underestimating the delay and attenuation that will be imparted on runoff if either all or part of supraglacial flow takes place through snow.

This section reviews research that has considered the hydrological role of the supraglacial snowpack. Ways in which flow through a snow-covered supraglacial catchment influences runoff are summarised, measurements of supraglacial snowpack hydrological properties are reviewed, and areas where further research is needed are identified, particularly with regard to the need for better snowpack representation in models of glacier hydrology.

2.3.3.1 Influence of the supraglacial snowpack on runoff

When a supraglacial snowpack is present, meltwater produced at its surface must first percolate through its depth to the glacier ice surface and then flow laterally downslope in either a basal saturated layer, film or channel until it meets a crevasse or moulin through which it can enter the englacial drainage system. As Fountain (1996) notes, the presence of snow will significantly decrease the speed of supraglacial water flow compared with that over bare ice, imparting a delay which is equal to the vertical transit time through the snowpack plus the lateral transit time through the saturated zone to a crevasse or moulin.

Passage through a supraglacial snowpack also attenuates the discharge hydrograph, a result of dispersive forces during percolation but also due to variation in the snow depth and lateral distance through which water passes (Fountain, 1996). Meltwater draining into any single moulin or crevasse is collected across a catchment area controlled by supraglacial topography and the pattern of drainage channels on the ice surface. Within each catchment, the depth of the snowpack will vary (in general with altitude, though snow drifting and avalanching during deposition and variable ablation due to shading effects may also be important) and water will travel different distances through the basal saturated layer before entering the englacial system. As a result, the flow paths followed by water vary in length and give rise not to a constant but to a variable time lag (Fountain, 1996). Peak discharge fluxes produced at the snowpack surface, for example, will not arrive at the catchment outlet at the same time, but will be spread across a longer period of time: the hydrograph is thus attenuated.

Not only must the delaying and attenuating effects of the supraglacial snowpack on runoff be understood, but also the way in which these effects change through time. There is likely to be a marked temporal change in supraglacial runoff first as the supraglacial snowpack thins, decreasing its delaying and attenuating effect, and then as the snowline retreats. In contrast to flow through snow, water is routed rapidly across bare ice causing less delay and attenuation (Fountain and Walder, 1998). Observations have shown that peak diurnal proglacial stream discharge generally occurs earlier in the day as the melt season progresses, indicating a decrease in the lag time for water transfer through the glacier system (Fountain, 1992; Swift et al., 2005). This change must reflect either increasing efficiency of meltwater routing due to rationalisation of supraglacial, englacial or subglacial flowpaths, or increasing melt rates due to a decrease in glacier albedo. The snowpack may play an important role in altering runoff patterns, not only through the temporal decrease of albedo and resulting increase in melt rates and therefore overall flow velocities, but also through a reduction in its delaying and attenuating effect as it thins and is removed. Fountain (1992) observed that peak water discharge from South Cascade Glacier, USA, occurred around 6 hours earlier as the snowpack ablated (Figure 2.8). The role of the snowpack in delaying runoff was particularly well demonstrated by a late summer snowfall that delayed runoff by 3.75 hours compared with pre-snowfall values, despite adding just 16 cm of snow depth to the glacier surface.
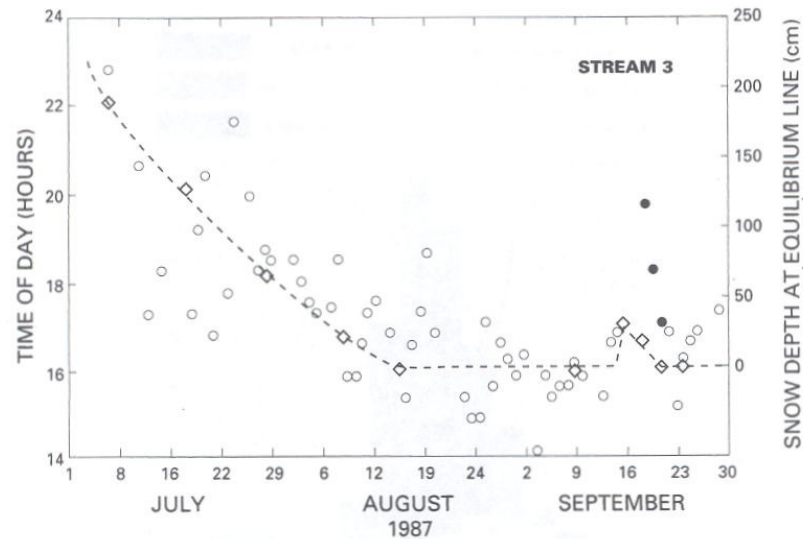
Figure 2.8: Time of daily peak proglacial water discharge (open circles) at South Cascade Glacier, Washington, USA, compared to snow depth at the equilibrium line (open diamonds = measured snow thickness, broken line = interpolated thickness). Closed circles are times of peak daily discharge following a snowfall. From Fountain (1992).

The amplitude of proglacial runoff has also been observed to increase during the melt season. For example, Figure 2.9 shows the diurnal variation in proglacial stream discharge from a glacierized basin in the Swiss Alps (Elliston, 1973). Increasing runoff amplitude has also been observed at Haut Glacier d'Arolla by Swift et al. (2005). It has been suggested that hydrograph evolution is controlled primarily by snowpack conditions (Fountain, 1996; Swift et al., 2005), with the snowpack having less attenuating effect as it thins, although more efficient en- and subglacial water transfer will also play a role in decreasing the attenuation of runoff hydrographs.
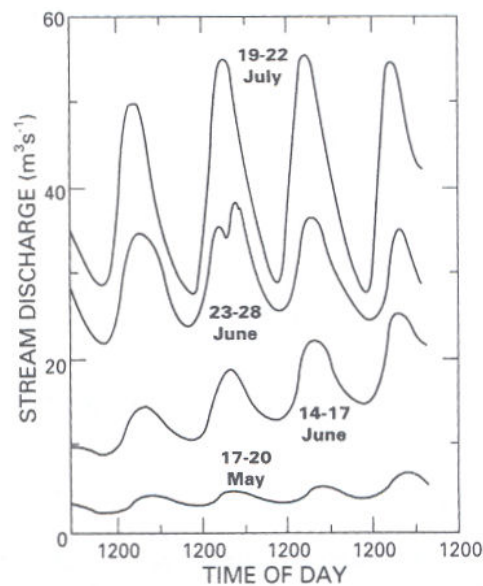
Figure 2.9: Diurnal variation in glacial stream discharge in the Matter-Vispa catchment, Switzerland, at different points in the melt season. From Fountain (1996), modified from Elliston (1973).

2.3.3.2 Hydrological properties of the supraglacial snowpack

Despite such observations of the supraglacial snowpack's likely effect on runoff, there have been few measurements of hydrological parameters, especially flow velocities, which would enable its effect to be more fully considered. Measurements in glacial firn have yielded estimates of around 0.2 m hr^{-1} (0.10 to 0.35 m hr^{-1}) for percolation velocity in the unsaturated regime and hydraulic conductivity of between 4.9x10^{-5} and 1.2x10^{-4} m s^{-1} for the firn aquifer (equivalent to permeability of between 9.0x10^{-12} and 2.2x10^{-11} m^2; Schneider, 2000). However, these values are likely to vary in a seasonally evolving snowpack due to differences in the density and pore structure of the snow. No previous studies have attempted to monitor percolation velocities or snowpack permeability over the course of a melt season.

Several studies have derived storage coefficients for flow in the supraglacial snowpack using theory that treats the snowpack as a linear reservoir. The storage coefficient K for any reservoir is the average delay time imposed on runoff by flow through that reservoir (Raudkivi, 1979). By either analysis of proglacial hydrograph recession limbs, or by optimising a linear reservoir model to produce the best match between measured and modelled discharge, values for K_{snow} of between 4 and 120 hours have been found (Baker et al., 1982; Collins, 1982; Gurnell, 1993; Hock and Noetzli, 1997; Klok et al., 2001; Verbunt et al., 2003; Schaefli et al., 2005). Hannah and Gurnell (2001) present one of the few studies which has considered the evolution of the supraglacial snowpack through time: values for K_{snow} derived from hydrograph recession limb analysis were found to decrease from around 45.0 to 17.75 hours as the melt season progressed. The development of preferential flowpaths was suggested as the cause of this decrease, though no observations of water flow patterns were available to support this.

Although the values for K_{snow} cited above may provide a useful indication of the lag imposed on runoff by flow through the snowpack, they are derived in a way which is remote from the actual processes operating in the snowpack, and may be influenced by other parts of the glacier drainage system besides the snowpack. The validity of linear reservoir modelling for representing snowpack runoff will be further considered in Chapter 5.

2.3.3.3 The supraglacial snowpack in models of glacier hydrology

Several recent models of glacier hydrology have included the possibility of water flow through supraglacial snow, but have differed in the degree of detail considered. Arnold et al. (1998) presented a distributed, physically based model of glacier hydrology in which the routine transferring water across the glacier surface distinguished between snow- and ice-

covered areas. For snow-covered model cells, water percolation and lateral movement in the basal saturated layer were driven by Colbeck's equations for gravity drainage and flow in the basal saturated layer (sections 2.2.3.1 and 2.2.3.3). However, constant values were used for the permeability and porosity of the snow, with the authors (reasonably) stating that the modelling of snowpack evolution at a micro-scale was beyond the scope of that particular project. Model output showed a change in the shape of hydrographs entering moulins as the snowline retreated across supraglacial catchments, and the effect of catchment geometry on the timing and sharpness of that change. Discrepancies between modelled and observed discharge in the early melt season were attributed to errors in estimates of snowpack water storage in the model, and more detailed modelling of water flow through the snowpack was identified as a future aim to resolve this.

Similarly, Willis et al. (2002) used Colbeck's equations in a distributed model of supraglacial hydrology to investigate the way in which the ablation and depletion of the snowpack affect runoff from a supraglacial catchment. A range of values were considered for snowpack water saturation, permeability and porosity, but kept constant during each model run. Results showed the potential importance of the snowpack in controlling catchment runoff, producing very dampened or more 'flashy' diurnal cycles depending on snowpack properties and level of saturation, but no field evidence was available to guide the choice of values for snowpack hydrological properties. In comparison to the field-derived values of snow permeability reviewed in section 2.2.2.3, the permeability values used by Willis et al. (2002) are significantly higher (ranging between $3.52\text{x}10^{-9}$ and $1.12\text{x}10^{-7}$ m^2), and the choice of high permeability values is likely to have had an effect on the outcomes of their study.

Previous modelling of supraglacial snow hydrology has therefore been limited by a lack of field evidence to guide the choice of values for snow hydrological parameters and, in common with work in non-glacial snow hydrology, by a lack of knowledge of how snowpack structural parameters may change through time. It is these gaps that this study aims to fill.

2.4 LIMITATIONS OF EXISTING WORK AND AIMS OF THIS RESEARCH

A review of previous work in snow hydrology (section 2.2) has shown that while many advances have been made, there remain several notable gaps in our understanding of the processes controlling snowpack runoff. These gaps must also be addressed in order to improve the representation of snow hydrology within glacial studies (section 2.3). Important issues requiring further attention are summarised below.

- It has been shown that the physical properties of the snowpack, including grain size, density, and stratigraphy, including the presence of ice layers, are important controls on the passage of water through the snowpack. The volume of water flowing and the way in which it may be distributed through the snowpack in preferential flow zones are further important controls. However, there remains much uncertainty about the exact nature of these controls and little quantitative data to characterize their effect.

- The physical properties of and flow patterns within the snowpack are expected to change through time, particularly during the melt season, but little information is available to assess the nature of these changes or their effect on runoff.

- The supraglacial snowpack has frequently been omitted as an element of the glacier hydrological system, despite having the potential to modify runoff between its production at the snow surface and entry into the englacial and subglacial drainage systems and in doing so, to influence subglacial water pressure and potentially ice dynamics. An improved understanding of supraglacial snowpack hydrology should enable important links between glacier hydrology and ice dynamics to be better understood.

- Very few field measurements have been made of the hydrological behaviour of a supraglacial snowpack. There is therefore little evidence available to guide both the choice of initial values for snow hydrological parameters in modelling, and their evolution through time. As a result, our ability to model runoff from supraglacial snowpacks, and therefore to investigate links to subglacial hydrology and ice dynamics, has been limited.

This study aims to address these issues by seeking to answer the following research questions:

i)   What is the nature of water flow through the supraglacial snowpack of a glacier, do the flow characteristics evolve over the course of the melt season, and if so, in what way?

ii) What are the factors controlling water movement through the snowpack, and how important is each of their roles?

iii) What quantitative information about snowpack hydrological behaviour and hydrological parameters can be collected to inform future modelling studies?

iv) How does the hydrological behaviour of the supraglacial snowpack affect the rest of the glacier system?; in particular, does the presence of a supraglacial snowpack delay the occurrence and reduce the magnitude of the spring dynamic event, and cause spring event timing to be delayed and its magnitude reduced upglacier?

To answer these research questions requires a dedicated field program collecting data to investigate the hydrological behaviour of the supraglacial snowpack throughout the duration of the summer melt season, while also collecting corresponding information about ice dynamics and conditions in the subglacial drainage system. Field campaigns with these aims were carried out at Haut Glacier d'Arolla in the Swiss Alps during summer 2003 and 2004, as described in Chapter 3.

Chapter 3. Field site and methodology

3.1 INTRODUCTION

The review of snow and glacier hydrology literature presented in Chapter 2 has shown that although the movement of water through a supraglacial snowpack is likely to have implications for water delivery to the rest of the glacier system and beyond, and thus potentially for glacier motion, it is yet to be studied in any detail. This thesis presents the results of a study that aimed to advance our understanding of the role that the supraglacial snowpack plays in controlling runoff, explicitly investigating the hydrological behaviour of the supraglacial snowpack at an alpine glacier and its evolution during the summer melt season. The methodology adopted in this project combined empirical data collection and numerical modelling in order to accomplish the research aims stated in section 1.2: section 3.2 expands upon the reasoning behind the methodology selected, considering the interplay between field data and theory and the way in which each contributes to this study.

Fieldwork was undertaken at Haut Glacier d'Arolla, Valais, Switzerland, during the summer melt seasons of 2003 and 2004. In both field seasons, fieldwork was carried out between early May and late July in order to capture the hydrological evolution of the supraglacial snowpack over the course of the melt season. The rest of this chapter introduces the field site (section 3.3) and describes the field methods used to collect useful data about the hydrological behaviour of the snowpack, the factors controlling it, and the possible implications for other parts of the glacier system (sections 3.4 to 3.8).

3.2 METHODOLOGICAL CONSIDERATIONS: THE ROLE OF EMPIRICAL DATA VS. THEORY IN SNOW HYDROLOGY

Recognition of the heterogeneous nature both of natural snowpacks and water flow through them (e.g. Gerdel, 1954; Langham, 1974c; Marsh and Woo, 1985; Harper and Bradford, 2003; Kronholm et al., 2004; Waldner et al., 2004; section 2.2.2.3) has indicated that investigations of snow hydrology must be field-based in order to capture the complexity and variability of the natural snow system. Field data therefore takes a leading role in this project. However, any study of snow hydrology must also maintain a firm base in our theoretical understanding of the physical processes controlling water movement through snow, for several important reasons.

Firstly, the need to study snow hydrology in a field context leads directly to issues of place-specificity, which must be overcome if results are to go beyond the description of the

unique and contribute to scientific understanding that can be more widely applied. It is by maintaining reference to theory that issues of place-specificity can be overcome, and results from one specific location used to aid understanding at a more general level. Furthermore, the difficulties of studying water movement in snow directly without disturbing the natural snow system and therefore invalidating results often necessitate the use of field techniques that are essentially "inverse" in character (Sharp et al., 1998), relying on system outputs together with agreed theoretical understanding of the operation of the physical system in order to infer understanding of the processes taking place. Theory in this case plays a vital role in data interpretation.

Although this study is primarily based on empirical data, theory developed from previous work in snowpack hydrology and existing understanding of the physical processes controlling water flow through snow is important when identifying the factors with which field investigations should be concerned if we wish to relate the changing hydrology of the snowpack to its influencing factors. It is also vital to bear in mind these fundamental controls in order to ensure that the techniques employed in field measurement do not themselves influence the natural operation of the snow hydrological system.

Thus, the goal of objective scientific enquiry demands that there be a strong realist background, informed by established and well-tested theory, even to work that at first glance may seem primarily data-driven. In this study, it is therefore seen as vital that the methods of data collection, the analysis performed, and ultimately the conclusions drawn, maintain a firm base in current theoretical understanding of snow processes.

Theory plays a more explicit role when numerical modelling is used. Existing models that simulate the flow of water through snow according to established understanding of the controlling physical principles are used here to investigate the relative importance of the factors controlling runoff and the way in which their effect would be expected to change through time. The reliability of these existing theoretical models in representing real-world snow processes can be assessed in the light of field observations, and shortcomings identified.

Over the last decade or so, there has been a trend within glaciology towards studies that adopt what has been called an "integrated" approach to fieldwork (Richards et al., 1996). In such studies, inferential power is drawn not from the agreement of multiple case studies, as in a data-driven, functionalist approach, but from the agreement of different but related phenomena observed within one case. Explanation is not based simply on the extrapolation

of empirical results, but relies on the support leant to an explanation by several interrelated measurements and their logical consistency according to a sound theoretical understanding of the processes involved. Although the intensive data requirements of such a study usually necessitate the collection of field data at only one site, reference to the underlying theory allows results to be extended to other locations.

In some ways this project will follow this trend. Fieldwork will investigate various interdependent aspects of meteorology, snow hydrology, glacier hydrology and ice dynamics. Existing theoretical understanding of snow and glacier hydrology and ice dynamics allows some predictions to be made regarding the relationships expected between these elements of the glacial system. When viewed together, these observations should therefore provide a fuller understanding of the linkages operating between several points in the system, thus enabling the influence of snow hydrology on processes in the rest of the glacier system to be understood with greater confidence.

3.3 THE FIELD SITE: HAUT GLACIER D'AROLLA, SWITZERLAND

Haut Glacier d'Arolla is a 4 km-long temperate valley glacier located at the head of the Val d'Hérens in canton Valais, Switzerland (Figures 3.1 and 3.2). The main glacier tongue, approximately 800m wide, flows north, fed by two separate upper basins. The glacier has undergone rapid retreat and thinning in recent years and is in continued poor health, with the snowline observed to retreat as far as the glacier headwall in the course of most recent melt seasons (P. Nienow, pers. comm.). The glacier ranges in altitude from around 2600 m to over 3500 m a.s.l. and has an area of approximately 6.3 km^2 (Willis et al., 2002). Surface slopes are gentle along most of the glacier's length (generally <10°) (Fox, 2003).

The glacier is surrounded by a number of high peaks (including Mont Collon (3637m) and L'Evêque (3716m) to the west, the Bouquetins Ridge (3838m) to the east, and Mont Brulé (3585m) to the south; Figure 3.1), which play an important role in controlling radiation receipt at the glacier surface (Arnold et al., 1996). Observations in boreholes and at the ice margins have shown that the glacier is largely underlain by a layer of unconsolidated sediments (Hubbard et al., 1995). Runoff from the catchment is monitored at a gauging station approximately 1 km downstream from the glacier snout and used for hydroelectric power generation by the Swiss hydroelectric company Hydro Exploitation SA.
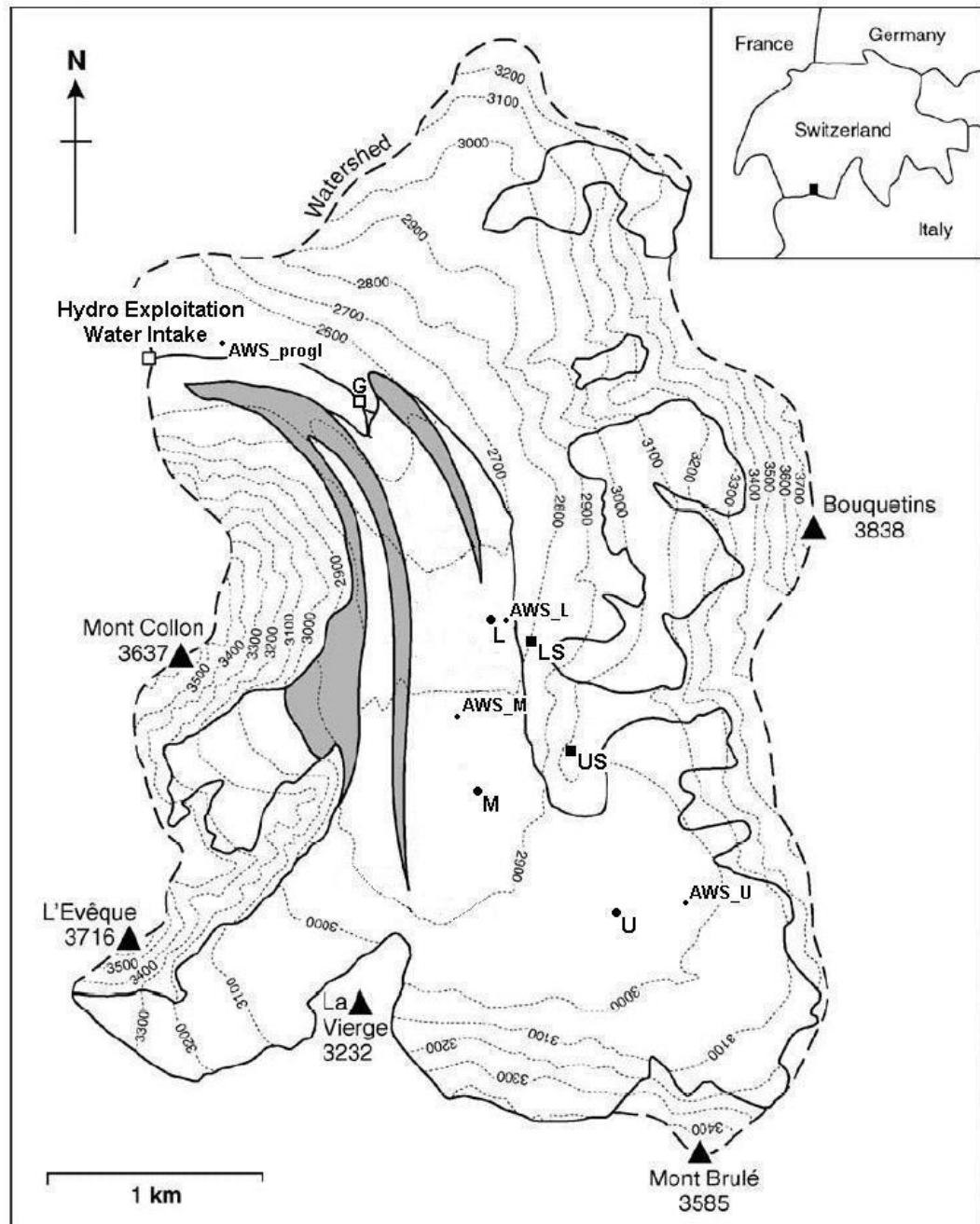
Figure 3.1: Map of Haut Glacier d'Arolla (lat 46°0'N, long 7°30'E) showing the location of studied snow pits L, M and U, automatic weather stations (AWS_progl, _L, _M and _U), survey station (LS) and proglacial gauging sites (Hydro Exploitation Water Intake and EC/turbidity monitoring site G) referred to in this thesis. Base map taken from Figure 1 in Swift et al. (2005).

Figure 3.2: Haut Glacier d'Arolla viewed from the north-west.

Since the late 1980s, Haut Glacier d'Arolla has been the subject of a series of studies that have yielded a detailed understanding of the subglacial hydrological system, its variation both in time and space, and its links to spatial and temporal patterns of glacier surface motion (e.g. Hubbard et al., 1995; Nienow et al., 1998; Mair et al., 2001). Supraglacial hydrology, however, has been less thoroughly investigated (with the exception of Willis et al. (2002) and Fox (2003)), and hydrological processes operating *within* the snowpack have not previously been studied.

The considerable pre-existing knowledge of hydrology and ice dynamics at Haut Glacier d'Arolla provides a valuable context into which information about snow hydrology can be incorporated, allowing the wider role of the snowpack within the glacier system to be considered. Previous work at Arolla (section 2.3) has suggested that the snowpack may be an important controlling factor for runoff patterns, the evolution of the subglacial drainage network, and the timing and magnitude of glacier velocity events (Nienow, 1993, 1997; Nienow et al., 1998; Swift et al., 2005), and information about snowpack hydrology gained during this study will enable more informed consideration of these possible links. Experience and infrastructure developed over the last 15 years, along with the glacier's comparative accessibility, are further benefits of working at this site.

3.4 FIELD METHODS FOR INVESTIGATING SNOW HYDROLOGY

This section discusses the field methods employed at Haut Glacier d'Arolla to investigate the hydrological behaviour of the supraglacial snowpack and its evolution through time. Previous studies of water movement through snow have used a variety of field techniques, often providing different types of information and therefore offering differing possibilities for advancing our knowledge. Hydrological investigations of snow in the supraglacial context require the selection of field methods that are portable and suitable for application in remote locations, and which address not only the percolation of water vertically through the snowpack but also saturated flow above the glacier ice surface and the net result of both these modes of flow in controlling runoff across supraglacial catchments. The combination of methods employed in this study has been carefully chosen such that together they provide information that will enable us to usefully address the cited research aims.

Field investigation of water movement in snow poses significant challenges due to the heterogeneous nature of natural snowpacks and their continuous, and often rapid, evolution in response to a number of factors. Field techniques must take care not to disrupt the delicate thermal equilibrium of the snowpack system, thereby invalidating results. Techniques used in previous studies to assess water movement through the snowpack include lysimeter measurements of water discharge at depth (Haupt, 1969; Colbeck and Anderson, 1982; Jordan, 1983a; Marsh and Woo, 1985; Harrington and Bales, 1998), thermistors measuring the change in heat flux caused by percolating meltwater (Conway and Raymond, 1993; Sturm and Holmgren, 1993; Conway and Benedict, 1994), capacitance meter measurements of snowpack liquid water content (Gerdel, 1954; Singh et al., 1999), monitoring of the water level at the snow-ice interface (Schneider, 2001), pumping and slug tests to determine hydraulic conductivity of the saturated layer (Fountain, 1989; Schneider, 1999), and observations of dye movement (Gerdel, 1954; Schneebeli, 1995; Kattelmann and Dozier, 1999; Waldner et al., 2004). In this study dye tracer tests are used as the primary method of obtaining information about water flow through the snowpack. Supplementary information to aid in the interpretation of snowpack hydrological behaviour is provided by a number of other techniques that monitor aspects of water movement through the snowpack, snowpack properties, meteorological conditions, and proglacial runoff.

3.5 LOCATION AND TIMING OF EXPERIMENTS

An initial aim of this study was to collect information about snowpack hydrological behaviour at a number of sites across the altitudinal range of the glacier, thereby allowing assessment of the spatial variability of meltwater runoff expected due to the different timing of snowpack maturation and ablation caused by the lapse of temperature with altitude.

However, regular movement of the dye tracing equipment proved difficult and caused much time to be lost. Moreover, altitudinal variation in snowpack behaviour may not be particularly significant at Arolla due to the small altitudinal range of the glacier, with variation in snowpack ablation more influenced by topographic shading and initial snow depth variations due to wind drifting. The majority of work in 2004 was carried out at a site 1 km upglacier from the glacier snout at approximately 2750m elevation (known as L (Lower); Figure 3.1), and provides a detailed picture of snowpack evolution at this site. Additional work was carried out at sites further upglacier (known as sites M (Middle; at approximately 2850m elevation) and U (Upper; at approximately 2950m elevation); Figure 3.1). The majority of dye tracing work in 2003 was carried out at U, as warm weather conditions resulted in rapid loss of the snowpack at L and M. The few experiments carried out at L and M in 2003 can be compared to results from U to provide some information about the spatial variability of snowpack hydrology.

Snowpack hydrological behaviour at L is of particular interest for two reasons. Firstly, the site is c.100m upglacier from a number of moulins which act as the lowest major point on the glacier tongue for meltwater input to the englacial and subglacial drainage systems. The way in which the snowpack at this site influences water runoff would therefore be expected to show some relationship to ice dynamics across the lower glacier tongue, and investigation of this relationship is an aim of this study. In previous years, significant increases in ice velocity have been observed in this area during the spring speed-up event (Mair et al., 2001). Secondly, the snowpack at this point is expected to be completely removed by the end of the field season, such that data can be collected to illustrate the hydrological behaviour of a supraglacial snowpack at all stages of its evolution.

During each field season a number of pits (typically 4 or 5) at each study site were used in rotation for dye tracing work. Sufficient time was allowed between work at one pit to ensure that dye from previous experiments was flushed naturally out of the system before the next experiment there was carried out. Repeat surface injections at a pit were carried out on the same area of the snowpack surface. This will help to reduce variation in return times caused by spatial differences in snowpack structure (for example, the presence of particularly efficient preferential flow features or impermeable ice layers, which could render return curves even from two adjacent areas at the same time of the melt season completely different) or different flow rates at the snowpack base, and therefore render curves obtained from the same pit comparable across the melt season.

Dye injections were carried out early in the day whenever possible, such that experimental results could be obtained before any overnight refreezing in the snowpack could interfere with water movement.

3.6 DYE TRACING EXPERIMENTS

The dye tracing technique involves the use of coloured dye to label water entering a hydrological system of interest, with the tracer detected after flow through the system and used to infer information about the nature of water flow. Dye tracing has been extensively used in en- and subglacial hydrology (e.g. Seaberg et al., 1988; Hock and Hooke, 1993; Willis et al., 1990; Nienow et al., 1996a, b; 1998) and in other hydrological systems (Leibundgut, 1995; Käss, 1998) to investigate drainage system structure and storage mechanisms. Dye also has a long history of use in snow hydrology, but in the past has generally provided only a visual indication of patterns of water movement in snow (referred to from here on as *qualitative* dye tracing). For the first time (with the exception of several experiments carried out by Grust (2004)), this study uses a down-borehole fluorometer installed at the snow-ice interface to accurately detect dye concentrations and recover quantitative information about rates of dye movement and dispersion through the snowpack. Qualitative dye tracing, however, remains important for the information it can provide about patterns of water flow in the snowpack and possible controls on runoff. Dye experiments were designed to investigate the nature of flow through snow in both the unsaturated (percolation) and saturated regimes. Injections on the snowpack surface provided information about percolation through the snowpack depth while injections directly into the basal saturated layer provided information about lateral flow across the glacier ice surface in the saturated layer. This section first describes the dyes chosen for use in this study, before discussing the injection, detection, and analysis methods adopted for both qualitative and quantitative dye experiments.

3.6.1. Tracer selection

Potential tracers must fulfil a number of requirements in order to be suitable for use in water tracing; these requirements together with the properties of commonly used tracers are described in detail in Smart and Laidlaw (1977) and Käss (1998), and summarised here. If experiments are to yield results representative of the behaviour of water under natural conditions, it is essential that the hydraulic behaviour of the tracer is the same as, or very similar to, that of water (Hotzl, 1990). Tracers must also be highly soluble in water, physically and chemically stable, and resistant to adsorption onto any sediment with which they may come into contact, though this consideration is less important in snowpack dye tracing than in subglacial environments. They must also occur at low concentrations in nature, be non-toxic to plant and animal life as well as humans, and ideally cost effective. The detection of dye concentrations should be unaffected by water temperature, pH, and turbidity.

Fluorescent dyes have become widely used in water tracing, their fluorescent properties giving them the advantage of accurate detection using a standard optical system of lamps and photodetectors. Some dyes can be detected by a fluorometer at concentrations as low as 0.05 μgl^{-1} (Smart et al., 1986), allowing the use of relatively small quantities of dye (Hubbard and Nienow, 1997). For qualitative dye tracing, some dyes are visible to the naked eye at concentrations as low as 40 $\mu g\ l^{-1}$ in clear water (Käss, 1998).

The fluorescent dyes fluorescein and rhodamine-WT were used in this study. Fluorescein has been successfully used as a tracer since the late nineteenth century, but care must be taken with its storage and use due to its very poor stability under exposure to sunlight (Dole, 1906; Smart and Laidlaw, 1977). Rhodamine-WT was developed in the 1960s specifically for use in water tracing, in response to the poor resistance to adsorption and comparative expense of earlier rhodamine dyes (Smart and Laidlaw, 1977). Both of the dyes selected exhibit the necessary properties for use in water tracing. The effect of fluorescein decay in the presence of sunlight was minimised by using this dye where possible for experiments beneath the snowpack surface. When fluorescein was used for injections on the snowpack surface, some degree of loss is expected due to photochemical decay but is considered unimportant in this case, as interpretation of results in no way relies on the amount of dye recovered. Rhodamine-WT and fluorescein fluoresce at different wavelengths (approximately 580 and 520 nm respectively (Smart and Laidlaw, 1977)) and can therefore be detected separately in the same sample, allowing quantitative experiments to be carried out which use both dyes simultaneously. Fluorescein appears as an acid yellow colour when dilute and rhodamine-WT as brilliant pink, making them clearly visually distinguishable in qualitative experiments.

For qualitative experiments in which only a visual impression of dye movement through the snowpack was required, food colouring was sometimes used instead of fluorescent dye. This enabled observations of water flow paths to be collected close to the location of quantitative experiments without risk of interfering with dye concentrations detected by the fluorometer.

3.6.2 Dye injection procedure

The same dye injection procedures were used regardless of whether dye movement was to be monitored simply visually or using fluorometry, and these are described here first for surface and then for basal injections.

3.6.2.1 Surface injections

For all surface injections, dye was spread in solution on the undisturbed snowpack surface using a spray dispenser and the minimum possible amount of water (typically 70 ml water

plus 5 ml of 20% dye solution over 1 m^2; Figure 3.3), in order that the added water would not significantly affect the natural development of the snowpack. Dye solutions were cooled by contact with isothermal snow prior to injection so that they would not interfere with the temperature equilibrium of the snowpack. Care was taken not to disturb the snowpack surface where surface injections were carried out. Using the spray dispenser, a fine mist of dye solution could be evenly applied across the injection area, minimising the risk of causing unnatural heterogeneous flow patterns due to uneven water application. Rhodamine-WT was used whenever possible for surface injections due to its stability in light and visibility to the naked eye at depth in the snowpack, but fluorescein was also used if the experiment called for the simultaneous use of two dyes. Although some degeneration of the fluorescein fluorescence is expected during exposure to sunlight at the snowpack surface, sufficient dye was injected such that its signal could still be clearly detected by a fluorometer several metres downglacier.

The application of coloured dye to the snow surface will alter the natural albedo of the snowpack and therefore change the melt rate, and this has been cited as a key disadvantage of dye techniques (Albert et al., 1999). However, melt rates will still lie within the naturally-occurring range and results therefore give useful information about water flow through snow, even if not under the precise conditions which would have existed naturally had dye not been used. Furthermore, no lowering of the snowpack surface across the injection area that would be caused by enhanced ablation relative to the surrounding

Figure 3.3: Injection of dye solution onto the snowpack surface using spray dispenser.

snowpack surface was observed, suggesting that albedo change due to dye addition is not an issue of concern.

3.6.2.2 Injections in the basal saturated layer

To investigate water flow in the basal saturated layer, 2 to 3 ml of 20% dye solution was injected through a borehole in the snowpack directly to the snow-ice interface. The borehole was first made with a plastic pipe of diameter c. 4cm and probed repeatedly to ensure that it was snow-free at the base, as dye retention in any snow at the base of the borehole would lead to unrepresentative return times. A thinner plastic pipe was then inserted into the borehole, reaching right to the base, and the dye poured through it, noting the injection time.

3.6.3 Qualitative dye injections

For qualitative dye injections, dye was spread on the snowpack surface as described in section 3.6.2.1 above and allowed to percolate naturally through the snowpack (i.e. advected with the percolating surface meltwater) for a known time (between 1 and 4 hours) before excavations were made into the snowpack beneath or downslope from the injection area, enabling examination of meltwater flow patterns. These observations provide valuable qualitative information about patterns of water flow, which can be used to aid interpretation of dye return curves and suggest explanations for the snowpack's influence on runoff. Excavations of two types were made: into the upglacier wall of a snowpit (e.g. Figure 3.4a), to examine percolation through the snow section across-slope, and into the side wall of a snowpit (e.g. Figure 3.4b), to examine the distribution of dye movement in the downslope direction over sloping ice layers within the snowpack. Excavations in these two directions are necessary to fully appreciate the three-dimensional impact of snowpack stratigraphy (particularly ice layers) on water flow. For each excavation the snowpit wall was dug back around 30 cm, in order to remove snow that might have been influenced by exposure to melting and/or refreezing due to its proximity to the pit wall. Beneath a surface injection area of 1 m^2 three excavations could generally be carried out, either immediately after one another, to examine the variation in dye flow patterns through space, or spread over the course of the day to examine the evolution of flow patterns through time.
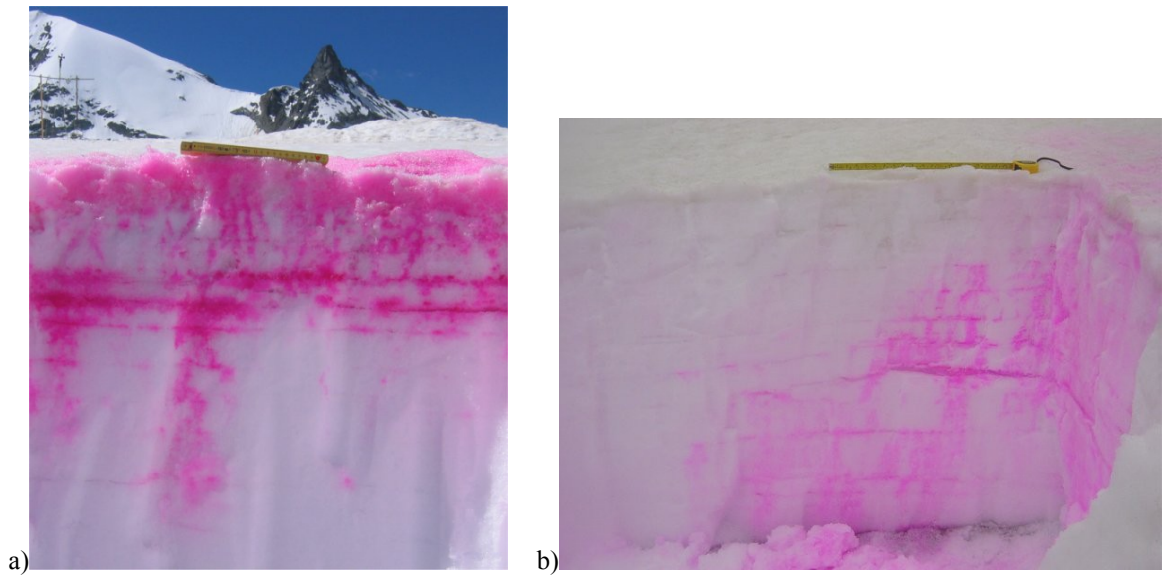
Figure 3.4: The two types of excavation carried out after qualitative surface dye injections: a) into the upglacier wall of a snowpit, to examine percolation through the snow section across-slope, and b) into the side wall of a snowpit, to examine the distribution of dye movement in the downslope direction over sloping ice layers within the snowpack.

Photographs of dye flow patterns were taken immediately after excavation: with a conventional camera in 2003, and with a 4 megapixel digital camera in 2004. Observations were made quickly before dye from saturated zones above ice layers spilled down the pit face and obscured natural flow patterns. Depths of dye propagation were examined to assess the rate of dye percolation and dye flow patterns examined to visually assess the extent to which the dye pulse is spread out, or dispersed, due to passage through the snowpack. Snowpit stratigraphic features were noted to help identify the controls on flow patterns.

3.6.3.1 Image analysis

Image classification is a relatively novel technique in dye tracing, but in recent years has been successfully used to provide detailed information about flow patterns through snow (Waldner et al., 2004). In particular, the ability to accurately identify the proportion of percolation taking place via preferential flow channels has the potential to contribute to better understanding of the role that this plays in enhancing percolation velocities (section 2.2.2.3). Analysis of high-resolution digital photographs of dye flow patterns taken during the 2004 field season enabled investigation of the proportion of flow taking place via preferential flow zones in the snowpack at Haut Glacier d'Arolla, and any evolution of this through time. In this way, quantitative information was extracted from a technique that was initially qualitative. The method of image analysis used was based on work carried out for an undergraduate dissertation by A. Clarke, a field assistant during the 2004 field season at Haut Glacier d'Arolla (Clarke, 2005). Each pixel in an image was classified according to

the intensity of the colour red (rhodamine WT being the dye used in almost all qualitative surface injections), with darker red shades assumed to represent more concentrated, preferential flow patterns.

Photographs showing representative dye flow patterns were selected for further image analysis and cropped to exclude areas of the snowpack exhibiting dye retention above ice layers (which would be incorrectly identified as areas of preferential flow in subsequent analysis) and areas low in the snowpack which dye percolation had not yet reached. Images were then pre-processed in order to reduce errors in subsequent analysis that would be caused by variable illumination of the snow surface. Photographs of dye flow patterns were frequently influenced by variable illumination due to areas of the snowpit wall being sunlit while others were shaded either by the surrounding walls or by small-scale unevenness of the excavated snowpit face. The resulting variations in brightness could mask spectral variations caused by differing dye concentrations, leading to errors in classification. Using software developed for Clarke (2005), the original colour digital photographs were converted to greyscale ratio images in which the shade of each pixel is a function of its colour intensity value in the red spectral band (indicating presence of rhodamine WT dye) divided by that in the green spectral band (chosen due to the low correlation between reflectance in the red and green bands in these images). Variable illumination operates equally in all colour bands, rendering pixel values in shadowed areas significantly lower. Ratio values however remain unchanged by changing illumination (Clarke, 2005; Lillesand et al., 2004; Figure 3.5). The ratio images therefore emphasize changes in colour content over brightness variation.
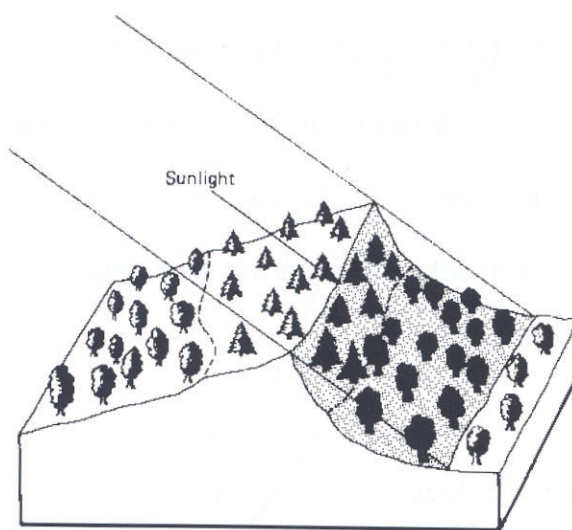
Land cover/ Illumination	Band A	Band B	Ratio (Band A/ Band B)
Deciduous			
Sunlit	48	50	0.96
Shadow	18	19	0.95
Coniferous			
Sunlit	31	45	0.69
Shadow	11	16	0.69

Figure 3.5: Reduction of scene illumination effects through spectral ratioing. Although the values of Band A and Band B change under different illumination, the ration of Band A/Band B remains the same. Modified from Sabins (1997) in Lillesand et al. (2004).

Ratio images were then opened in ERDAS Imagine software and the 'unsupervised classification' function used to automatically classify image pixels based on natural clusters in pixel values. Comparison of the original and classified images then enabled selection of the pixel classes which corresponded with preferential flow zones in each individual image. This manual method of choosing the classification scheme for each separate image introduces an element of subjectivity into this analysis, but due to the generally very clear delineation between areas of preferential flow and the surrounding snow, any errors in the preferential flow area calculated are expected to be small. The number of pixels falling into the preferential flow category was totalled using the 'Histogram' function in ERDAS Imagine and then used to calculate the percentage area occupied by preferential flow zones.

3.6.4 Quantitative dye injections

In quantitative dye tracing tests a known quantity of dye is injected in solution into the hydrological system of interest, allowed to flow naturally through the system, and its concentration sampled by a fluorometer located at a detection site downstream. Samples may be collected manually but more commonly by pump or gravity-driven continuous flow, in which case automatic data logging can record tracer concentration at regular and frequent time intervals (Hubbard and Nienow, 1997). The resulting dye return curve is analysed to obtain quantitative parameters that describe the nature of flow between the injection and detection points. Analysis of dye return curves is described in section 3.6.4.3. When dye is used to investigate flow through a porous material such as snow and detection is at a single point, the total quantity of dye detected at the fluorometer will be significantly less than 100% of that injected. Analysis of dye return curves here is therefore in no way based on measured dye concentration values, but makes use of the timing and shape of the curve.

The success of quantitative dye tracing tests in subglacial drainage systems (e.g. Seaberg et al., 1988; Hock and Hooke, 1993; Willis et al., 1990; Nienow, 1993) suggests that the technique may also be usefully applied to the supraglacial snowpack. Quantitative dye tracing enables velocity and dispersion values for water movement through snow to be calculated and is non-destructive, allowing repeated measurements to be made at the same site and the evolution of snowpack hydrological behaviour through time to be investigated. Lysimeters have been used to gather similar data in non-glacial settings in the past, but are less easy to operate in remote glacial locations where equipment cannot easily be installed prior to the onset of winter snowfall. The availability of a down-borehole GGUN-FL fluorometer (developed by the Institute of Geology at the University of Neuchâtel, Switzerland) presented the opportunity to investigate the usefulness of quantitative dye tracing techniques for work in snow, and to develop a suitable technique for their use.

Two separate types of quantitative dye experiment were carried out in the supraglacial snowpack for this study, corresponding to the two distinct types of flow occurring within the snowpack. In the first, dye was injected on the surface of the snowpack as described in section 3.6.2.1 and its concentration measured in the basal saturated layer as it emerged in a snowpit a few metres downglacier. The resulting dye return curves therefore give information about flow between these two points, including percolation through the snowpack depth and flow in the basal saturated layer. Injections on the snowpack surface were generally intended as stand-alone indications of the nature of water flow through the snowpack at a certain time, but during the 2003 field season two surface injections were often carried out simultaneously in combinations designed to enable consideration of the influence on runoff characteristics attributable to the difference in flow paths between the two injections. Experiment variations included simultaneous surface injections above snow of different depths (to assess the difference in return curve form and timing caused by this difference in snow depth), at different distances upglacier from the detection point (to assess the role of increased basal flow distance), and above and below an excavated ice layer.

In the second type of experiment, dye was injected through a borehole in the snowpack directly into the basal saturated layer (as described in section 3.6.2.2) and again detected in a snowpit a few metres downglacier, with results thereby giving information about flow through the basal saturated layer alone. The methods adopted for these two types of investigation are described in turn here.

3.6.4.1 Experimental set-up

The typical experimental set-up for quantitative injections on the snowpack surface is shown in Figure 3.6. Dye was injected onto the snowpack surface as described in section 3.6.2.1 and allowed to percolate naturally through the snowpack and flow laterally downslope across the glacier ice surface until it reached a snowpit a known distance downglacier (typically 3 to 4 metres), where the fluorometer was installed at the snow-ice interface to detect dye arriving in the basal saturated layer. The depth of snow through which dye was percolating in each experiment could not be precisely determined as any depth probing would provide an artificially fast route for percolation and therefore invalidate dye tracing results. Instead, snow depth was measured a short distance (0.5 to 1 m) upglacier, frequently coinciding with a borehole for injections into the basal saturated layer.

Figure 3.6 also shows the experimental set-up for injections in the basal saturated layer. Dye was injected directly into the basal saturated layer and flowed in the basal saturated layer until reaching the detection point in a snowpit a known distance (typically 4 to 5 metres) downglacier.
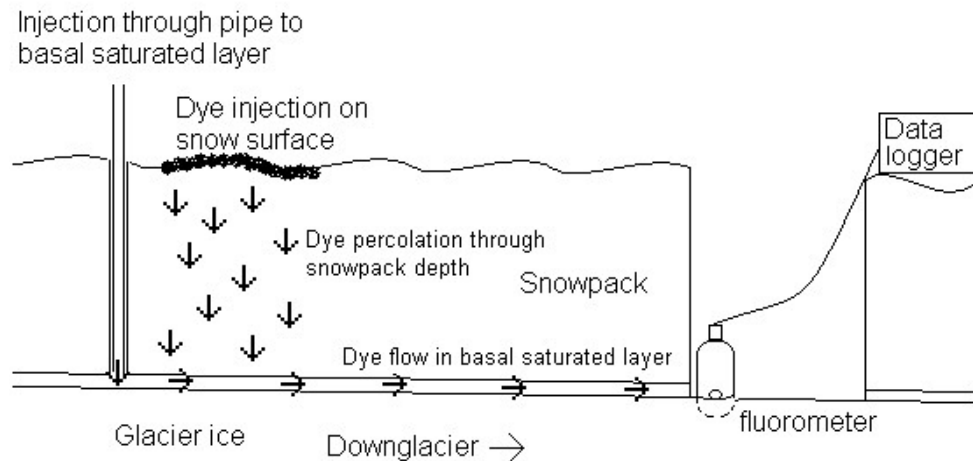
Figure 3.6: Experimental set-up for quantitative dye injections at the snowpack surface and at the snow-ice interface.

3.6.4.2 Tracer detection

For both types of quantitative dye experiment, the GGUN-FL down-borehole fluorometer was installed beside the upglacier wall of a snowpit a known distance downglacier to detect dye arriving in the basal saturated layer (Figure 3.7). Early experiments at each studied snow pit showed the location at which dye was likely to emerge and were used to guide placement of the fluorometer. Even when dye was injected over approximately 1 m^2 of the snowpack surface, it generally emerged through the saturated layer as a single plume less than 20 cm wide, as water percolating through the snowpack had been reorganized by either preferential flow zones within the snowpack depth or channelised flow on the ice surface. The fluorometer was installed at a single point within the area of dye emergence and is believed to have captured the pattern of emerging dye concentrations well.

The optical system used for detecting fluorescent dyes in the GGUN-FL fluorometer is located several centimetres above the base of the equipment, requiring it to be submerged in flowing water to a depth of about 4 cm in order for water to flow past the sensors. In some snowpits the basal saturated layer was sufficiently deep that the sensors were submerged as the fluorometer rested on the glacier ice surface. In pits in which water depth was much deeper than ~5 cm, however, recovered dye return curves were frequently poor, possibly due to movement of water around the fluorometer. Where basal water depth was less than 4 cm, a hole was made in the glacier ice using an ice drill and the fluorometer placed in this hole such that the sensors were submerged in water. This method of fluorometer installation was frequently successful even where no visible saturated layer was present on the ice surface, with the fluorometer hole observed to fill naturally within minutes with water flowing in a thin film

Figure 3.7: Fluorometer installation beside the upglacier wall of a snowpit to detect dye arriving in the basal saturated layer. The glacier ice surface slopes downslope towards the camera; dye was injected upglacier and can be seen arriving in the saturated layer behind the fluorometer. The fluorometer is sitting in a shallow borehole to ensure that water flows past its sensors.

across the ice surface. The fluorometer was positioned in all cases so that its sensors were aligned with the flow direction of the water (Figure 3.7). Each time the fluorometer was installed, the flow of water past it was observed carefully to ensure it was not pooling in the hole and therefore interfering with the passage of the dye wave. On several occasions where the saturated layer was shallow, small channels had to be dug in the ice surface downslope from the fluorometer in order to allow water to flow freely away.

The hole drilled into the glacier ice was useful in maintaining the fluorometer in an upright position, necessary to avoid interference with the fluorescence signal resulting from air bubbles. However, warm air temperatures caused gradual expansion of the hole and fluorometer positioning had to be regularly checked. A greater problem was encountered when surface layers of less dense glacier ice into which the hole had been drilled became permeable after continued exposure to warm air temperatures and caused the water around the fluorometer to drain. On several occasions experimental results went undetected because of this. Covering the fluorometer and surround ice with snow helped solve this problem.

Slush particles in the water flowing past the fluorometer sensors are thought to interfere with measurements of dye concentration, so entry and exit points to the sensing chamber were covered with plastic netting fine enough to prevent passage of slush but not to retard water movement.

The GGUN-FL fluorometer is provided with a dedicated data logger in a waterproof logger box. Data is recorded onto memory cards which can later be downloaded onto a laptop computer. In 'continuous acquisition' mode, the concentration of both fluorescent dyes is recorded at 10 second intervals. As the data logger has no internal clock, the time at which the fluorometer is turned on or off must be recorded manually.

Under ideal conditions, the GGUN-FL fluorometer is capable of detecting dye concentrations as low as 5×10^{-11} g ml^{-1} and is sensitive to variations in dye concentration as low as 0.05 ppb (GGUN-FL Fluorometer User Manual). Fluorometer calibration was checked prior to each field season. As subsequent analysis of dye return curves is based entirely on their shape and timing, and not in any way on the volume of dye recovered, the accuracy of dye concentrations detected by the fluorometer is believed to be sufficient.

3.6.4.3 Return curve interpretation

Tracer concentration breakthrough curves measured by the fluorometer can be analysed to yield a number of parameters describing the character of flow through the snowpack. The widespread use of dye tracing techniques in englacial and subglacial drainage systems has established the information that can be obtained from dye return curve analysis. An explanation of the parameters used in subglacial drainage studies can be found in many papers including Hubbard and Nienow (1997). In studies of subglacial drainage systems, these parameters provide a measure of the efficiency of the drainage pathway that can then be used to infer the morphology of the drainage system (Nienow et al., 1998). Here, these parameters are used primarily to provide a quantitative measure of the efficiency or otherwise of water flow through snow. The nature of dye flow paths can be directly investigated using observations of dye movement, as in the qualitative dye experiments carried out in this study.

Analysis of dye return curve shape and timing

Inspection of the timing and shape of dye return curves provides initial quantitative information about the nature of water movement, with earlier and more peaked curves indicating more efficient transfer of water through the snowpack, and vice versa. Although water flow through the snowpack is likely to be highly complex and may take a wide variety of different routes, some generalisations can be made about the flow paths, and therefore snowpack properties, likely to cause certain idealised return curve characteristics. These links between flow path and return curve characteristics are summarised in Figure 3.8, for reference to when interpreting dye return curves obtained in the field.
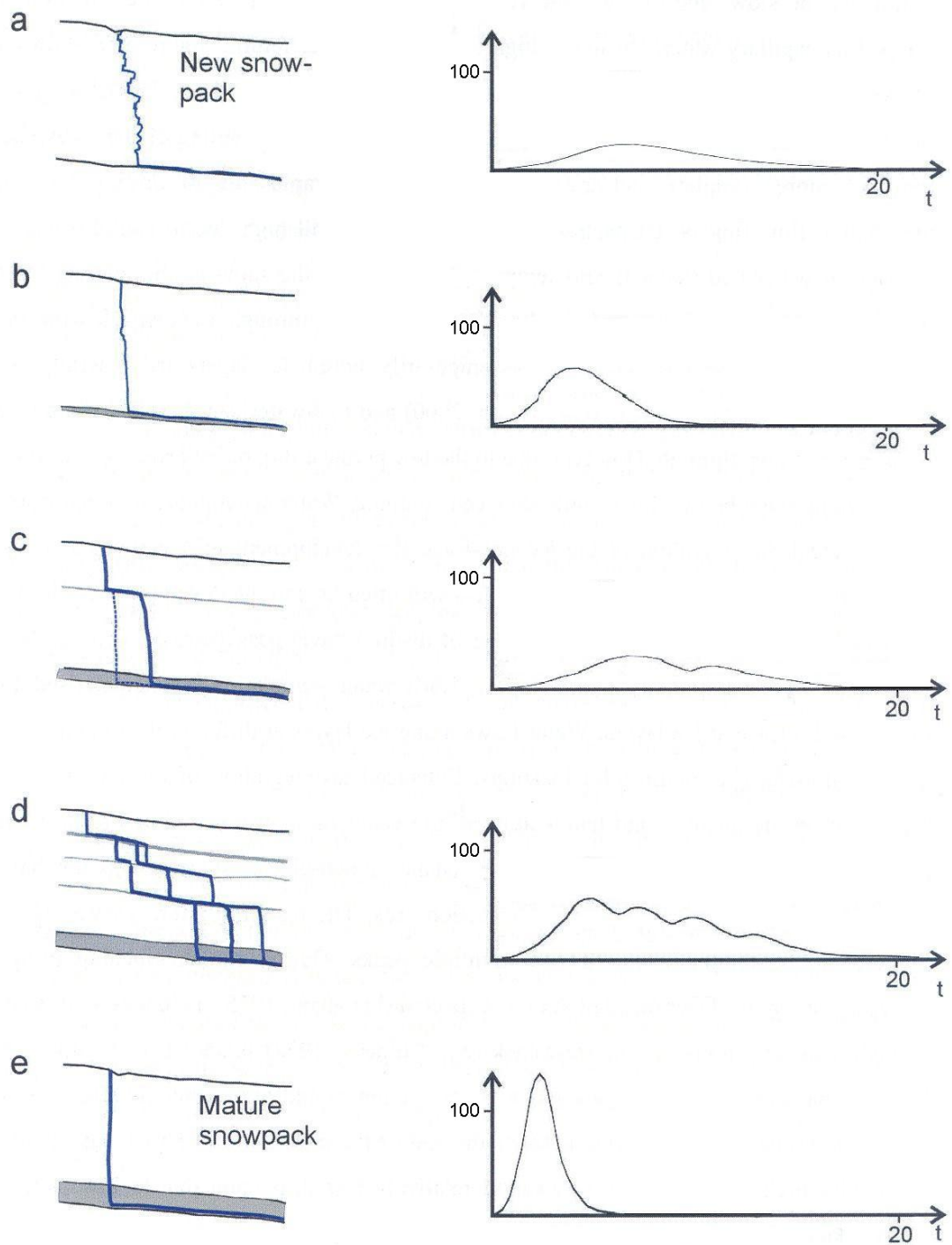
Figure 3.8: Idealised return curves for the passage of tracer through different configurations of glacial snowpack. x-axis scales are estimated in hours. Values on y-axes are relative, not absolute ppb values. Modified from Grust (2004), Figure 3.5.

_____

Quantitative parameters derived from dye return curves

A number of quantitative parameters can be derived from dye return curves, each providing a measure of the efficiency with which water has been transmitted through the hydrological system. The simplest of these are the return times to first dye detection at the detection site, t_{min}, detection of peak dye concentration, $t_{dominant}$, 50% dye recovery, t_{mean}, and last dye detection, t_{max}. Corresponding with these recovery times, four different through-flow velocities can be calculated for each return curve (Käss, 1998). These are:

   i)   the *maximal flow velocity v_{max}*, corresponding to the velocity of the fastest moving dye particles and obtained by dividing the straight-line distance from injection to detection site by t_{min};

   ii)   the *dominant flow velocity v_{dom}*, obtained by dividing the straight-line travel distance by t_{dom};

   iii)   the *mean flow velocity*, obtained by dividing straight-line travel distance by t_{mean}, and

   iv)   the *minimum flow velocity*, corresponding to the velocity of the slowest moving dye particles and obtained by dividing the straight-line travel distance by t_{max}. However, due to frequently extended trailing limbs of return curves and the need to move the fluorometer for work elsewhere, t_{max} (and therefore also minimum and mean flow velocity) was often unknown.

Due to the complexity of flow patterns as water percolates through snow, the true distance travelled by dye is expected to be greater than the straight-line travel distance. Velocities calculated as described above will therefore be a minimum estimate of the actual velocity at which dye (and water) has moved. However, they give a good indication of the net velocity at which meltwater travels through the snowpack, which controls the timing of runoff into the rest of the glacier hydrological system.

As water flow through the supraglacial snowpack takes place through two fundamentally different regimes (unsaturated percolation and saturated lateral flow at the snowpack base), it is of interest to investigate the differing roles that these two modes of flow play in influencing runoff. As return curves from injections on the snowpack surface are the net result of percolation through the snowpack depth plus flow along the basal saturated layer, percolation velocities must be calculated by subtracting the travel time for flow through the basal saturated layer from net dye transit time. As corresponding basal flow velocities were rarely available for each surface injection, lower and upper limits for basal flow velocity were assumed based on the complete basal dye injection data set and used to calculate upper

and lower estimates for percolation velocity respectively. Dye injections into the basal saturated layer provide direct information about flow in this flow regime.

The shape of a dye return curve is determined by dispersive processes that spread dye out during its passage through the hydrological system (Taylor, 1954; Fischer, 1968). The dispersion of the dye cloud is of interest in snow hydrology as it indicates the degree to which flux values are attenuated by passage through the snowpack and therefore the snowpack's influence on the magnitude of discharge flowing into the englacial drainage system.

The most common measure of dye dispersion derived from return curves is *dispersivity* (*d*, unit = m), which represents the rate at which the tracer cloud is spread out (described by the *dispersion coefficient*, *D*, in m^2 s^{-1}) relative to the rate of advection of dye through the system (the net flow velocity *u*, in m s^{-1}, for the passage of dye between the snowpack surface and the fluorometer) (Fischer, 1968; Seaberg et al., 1988; Hock and Hooke, 1993; Hubbard and Nienow, 1997):

$$d = D / u \tag{3.1}$$

In glaciology, a widely adopted method of calculating the dispersion coefficient *D* follows that of Brugman (unpublished) (Seaberg et al., 1988), in which

$$D = \frac{x^2 (t_m - t_i)^2}{4 t_m{}^2 t_i \left[2(t_m / t_i)^{1/2} \right]} \tag{3.2}$$

where *x* is the travel distance between the injection and detection points, t_m is the time to peak dye recovery (seconds) and t_i represents t_1 and t_2, the time to half peak concentration on the rise to and decline from the peak respectively. The equation is defined for both values of t_i and solved iteratively to find a consistent value of *D*.

3.7 OTHER TECHNIQUES FOR INVESTIGATING SNOWPACK HYDROLOGY

While quantitative dye tracing offers valuable possibilities for gathering information about water flow through the snowpack (in particular, rates of water movement and measures of dispersion), there are other techniques which can also be useful here in providing other types of information about snowpack hydrology. Lysimeters, for example, give information about discharge fluxes through the snowpack, which dye tracing techniques do not. Pressure transducers can be used to monitor water depth in the basal saturated layer, a measure of discharge through or storage in that part of the snowpack system. The data supplied by these techniques aids in the interpretation of dye tracing results and adds support to conclusions drawn.

3.7.1 Lysimeter discharge measurements

Lysimeters have been quite widely used within studies of snow hydrology to provide information about meltwater discharge through a snowpack at depth (Haupt, 1969; Colbeck and Anderson, 1982; Harrington and Bales, 1998; Fox et al., 1999). A lysimeter, essentially any gauging structure of known area, collects water arriving at a known depth in the snowpack. Water then runs off and is continuously measured, providing direct information about the volume of water passing through the snowpack at any time. Lysimeter investigations were carried out during the 2004 field season at Haut Glacier d'Arolla in order to supplement data from dye tracing investigations.

3.7.1.1 Lysimeter design

In this study, lysimeters were initially constructed from large (73 x 55 x 16 cm) white plastic storage trays, which were inserted into the walls of snow pits in mid to late May (Figure 3.9a) and packed in with snow in an attempt to preserve natural temperature conditions in the snowpack around the lysimeter despite proximity to the pit wall. The layout of lysimeter apparatus is summarised in Figure 3.10. However, the tipping bucket rain gauges (Figure 3.9b) into which water was diverted failed to register significant runoff even in late June, when other observations showed clearly that water was percolating through the snowpack. On excavation, the snow immediately above the lysimeters was found to have formed a c.1-2 cm-thick crust of hard icy snow, believed to be formed when water retained by capillary retention above the snow-air boundary repeatedly froze. This layer had not been destroyed by subsequent contact with liquid water and continued to prevent runoff into the lysimeter.
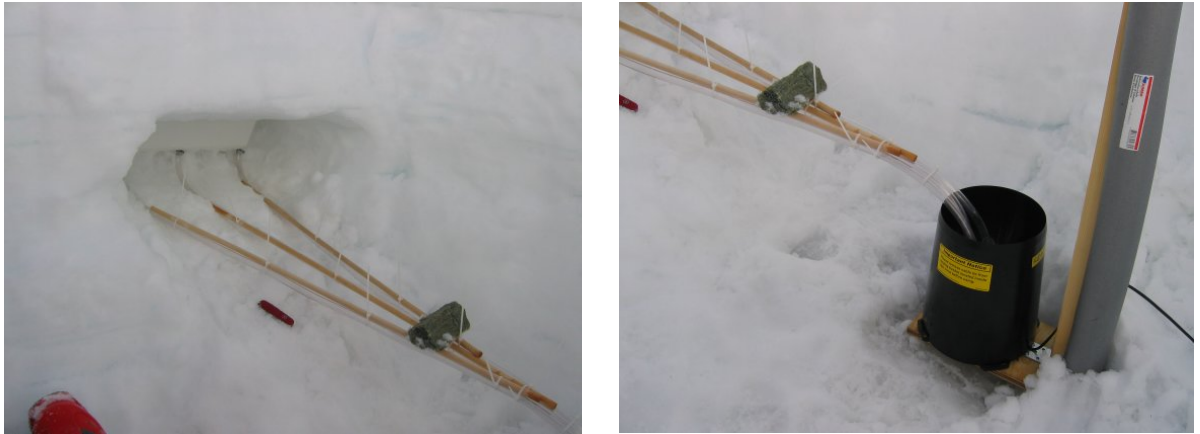
Figure 3.9: Initial lysimeter design: a) installation of white tray lysimeter into snowpit wall, with three drainage hoses (straightened with wooden dowels) leading from the lysimeter base; b) hoses draining into the tipping bucket rain gauge which measures runoff volume. The rain gauge is mounted on a wooden stake drilled into glacier ice to keep it level and out of pooling water. After installation, the tops of rain gauges were covered with plastic sheeting to keep out precipitation.

From early July, the tray lysimeters were replaced by smaller lysimeters constructed from lengths of gutter drainpipe (Figure 3.11a). As these were smaller and had no rear wall, they could be easily hammered into a snowpit wall such that the drainpipe was filled with snow and there was no snow-air boundary at which water could be retained. Immediately after installation, water was seen to saturate the snow at the base of the lysimeter (Figure 3.11b) and then to run off through the plastic tubing that led from the front of the lysimeter to a tipping bucket rain gauge nearby. Lysimeters were installed at a slightly sloping angle to ensure that runoff along the lysimeter base was rapid and did not influence the timing of runoff detected at the tipping bucket rain gauge.
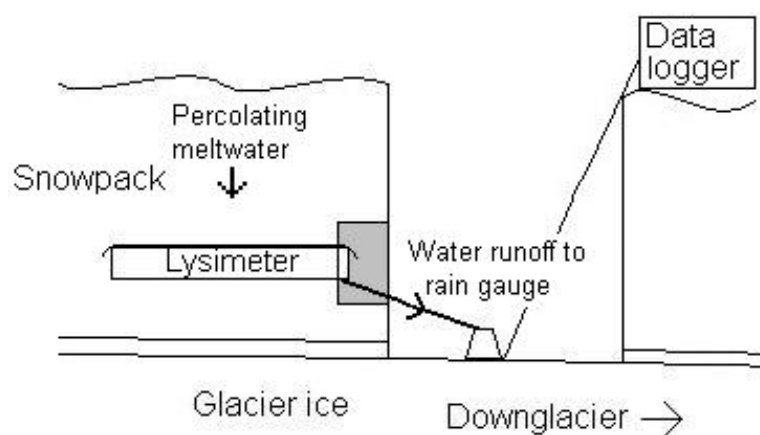
Figure 3.10: Layout of lysimeter apparatus. Meltwater percolating through the snowpack is collected by the lysimeter structure and then drains under gravity into a tipping bucked rain gauge which continually measures runoff volumes. A small area of the snowpit wall (shaded grey) was dug out so that lysimeters could be installed in snow not affected by air temperature, and refilled after installation.

Figure 3.11: Drainpipe lysimeter installation: a) lysimeter installed in pit wall; b) water saturating the snow in the lysimeter immediately after installation into the snowpack.

Due to the heterogeneous nature of water percolation through snow, large lysimeter sizes are desirable in order to obtain more representative results that average flow over a larger area. The smaller size of the drainpipe lysimeters used in this study (each around 0.1 m^2) means that they may be situated in areas of the snowpack through which unrepresentatively low or high flow is taking place. However, the majority of observations of percolation patterns at Haut Glacier d'Arolla (section 4.4) showed that flow fingers are small and closely spaced, making lysimeter size less of a concern. In addition, for some periods 2 to 3 small lysimeters were connected to the same tipping bucket rain gauge, increasing the effective sampling area of the lysimeter to around 0.3 m^2.

3.7.1.2 Measurement of runoff

Tipping bucket rain gauges (Figure 3.9b; model: Rain Collector II (7852M) by Davis Instruments, California) were used to collect water running off through the lysimeters and the number of tips in each 5 minute interval was recorded on Campbell Scientific CR10X or CR23X data loggers for later conversion to a volume of water. Rain gauges were calibrated before the field season and one tip found to equal 5 ml.

It was important that rain gauges be located sufficiently below the height of the lysimeter such that water flow in the tubing connecting the two was rapid and did not affect the timing of runoff measured. Lysimeters could therefore not be placed at the very base of the snowpack. Rain gauges also had to be kept level, and were therefore mounted on wooden stakes slightly above the sloping ice surface (Figure 3.9b). After installation, the tops of rain gauges were sealed with plastic to keep out precipitation.

_____

3.7.2 Pressure transducer measurements of basal water table height

Pressure transducer measurements of the depth of water in the basal saturated layer were made throughout both field seasons at each of the three study sites L, M and U. To install each pressure transducer, a borehole was made to the base of the snowpack using a plastic pipe of diameter c.4 cm and cleared of snow. The pressure transducer was then fastened inside the plastic pipe using cable ties such that the end of the instrument protruded slightly from the end of the pipe (Figure 3.12). In this way, the pressure transducer could be inserted directly to the snow-ice interface and kept in position over time. Slits cut in the pipe allowed water from the basal saturated layer to flow past the pressure transducer within the pipe and ensured that water levels inside and outside the pipe were equal. Pressure transducers were connected to Campbell Scientific CR10X or CR23X data loggers and 10-second readings averaged and recorded at 15-minute intervals.
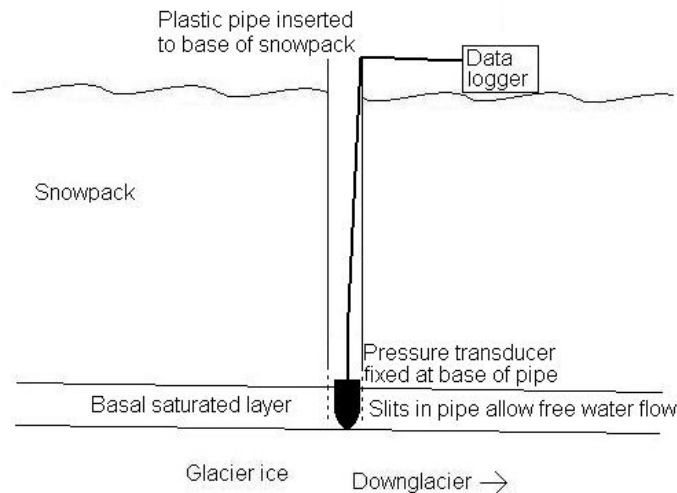
Figure 3.12: Pressure transducer set-up, showing pressure transducer fixed at the end of a plastic pipe and inserted into the basal saturated layer, with slips in the pipe ensuring that water levels inside and outside the pipe are equal.

3.7.3 Other observations of basal water table variations

Other observations of the depth and variability of the basal water table were made during work in snowpits. In order to examine the basal saturated layer across a wider area, two transects were surveyed for water table depth in late July. In each, a line (14 m long in the first transect, 10 m in the second) was marked out on the snowpack surface across-slope and a dry wooden dowel used to probe to find the depth of the water table every 25 cm along this line. Accompanying measurements of snow depth and surface slope enabled construction of cross-profiles showing the topography of the ice surface and the distribution of the water table along the transect.

3.8 SUPPLEMENTARY INFORMATION

3.8.1 Snowpack properties

Various techniques were employed to collect information about the properties of the snowpack and their evolution through time, for use in assessing which factors are important in controlling runoff characteristics. Factors thought likely to play a role include snowpack extent, depth, density, stratigraphy (particularly grain size and the presence of ice layers), wetness and temperature.

The extent of the snowline and the pattern of snowline retreat were monitored throughout each field season in a series of photographs taken from vantage points in front of the glacier. Campbell Scientific SR50 ultrasonic depth gauges mounted adjacent to each of the three study sites (Figure 3.13) provided a continuous record of snowpack depth changes to an accuracy of ±1 cm (Campbell Scientific SR50 Sonic Ranging Sensor User Guide). UDG distance measurements were corrected automatically for variations in air temperature using information from Campbell Scientific 107 thermistors mounted adjacent to each UDG. Manual depth probing at known distances along the glacier centreline using an avalanche probe provided additional information about the spatial variation of snow depth, and resistance of the snowpack to the insertion of the probe could be used to estimate the number and depths of ice layers present.

Figure 3.13: Ultrasonic depth gauge (UDG) mounted on 'H' frame and anchored using guy ropes to decrease instrument movement in windy conditions and therefore increase measurement stability. The thermistor used to correct UDG distance measurements for air temperature is mounted inside the radiation shield on the right hand post.

Snowpack stratigraphic properties were monitored throughout both field seasons by taking profiles of crystal type, grain size, snow hardness, wetness, temperature and density every 3 to 4 days, either in pits used for dye injections or at adjacent sites, following the methods outlined by Colbeck et al. (1990). All apparent stratigraphic boundaries within the snowpack were noted at the start of each period of data collection and observations made in each layer. Snow wetness and hardness were assessed using the hand tests outlined in Tables 3.1 and 3.2. For wetness, a scale is used which relates the ability of the snow to form a snowball and the amount of water that can be squeezed out of the snow to wetness. The ease with which objects of different surface area can be pushed into the snowpack provides an index of snow hardness.

Table 3.1: Snow wetness hand test scale (adapted from Colbeck et al. (1990)).

Term	Test	Water content (% of snowpack)
Dry	Disaggregate snow grains have little tendency to adhere to each other when pressed together – can't form a snowball	0%
Moist	When lightly crushed, the snow has a distinct tendency to stick together – can form a snowball	<3%
Wet	Snow wets glove when held in hand	3-8%
Very wet	Water can be pressed out by moderately squeezing the snow in the hands	8-15%
Slush	The snow is visibly flooded with water	>15%

Table 3.2: Snow hardness hand test scale (adapted from Colbeck et al. (1990)).

Term	Largest object which can be inserted into snow
Very low	Fist
Low	4 fingers
Medium	1 finger
High	Pencil
Very high	Knife blade
Ice	None

Snow grains were examined under a hand lens with the aid of 1, 2, and 3 mm^2 grids to assess grain size. Grain size, shape, and the degree of contact between grains were noted for each stratigraphic layer using the classification presented by Colbeck et al. (1990) (Appendix A). The dimensions of any ice masses present in the snowpack were also noted, including the thickness, lateral extent, and solidity of any ice layers or lenses. Further information about the occurrence of ice layers across the wider glacier extent was gathered during manual snow depth probing, with ice layer presence detected by their resistance to the lowering of the avalanche probe and their depths noted.

For measurement of snow density, samples of known volume were taken from each snow layer using a cylindrical sampling tube. Samples were weighed using a spring balance to 1 g accuracy and density calculated as sample mass divided by sample volume. Where possible,

measurements containing ice layers were kept separate from those containing only snow, as the presence of ice layers in a sample would lead to the calculation of density values unrepresentative of snow layers.

Snow temperature was measured at regular intervals through the snowpack depth using a TME MM2040 handheld temperature probe precise to $\pm 0.2\ ^{\circ}C$.

3.8.2 Meteorological data

During both field seasons, meteorological data was provided by two automatic weather stations (AWSs; Figure 3.14) operated by ETH Zürich and located at approximately 2800 (AWS_M) and 3000m (AWS_U) altitude on the glacier surface (Figure 3.1). Each AWS collected full energy balance data, as shown in Table 3.3, averaged and recorded at 5-minute intervals (more detailed information regarding the set-up of ETH AWSs can be found in Pellicciotti et al. (2005) and Strasser et al. (2004)). A further permanent AWS in the proglacial area (AWS_progl; Figure 3.1) provided full energy balance data year-round.
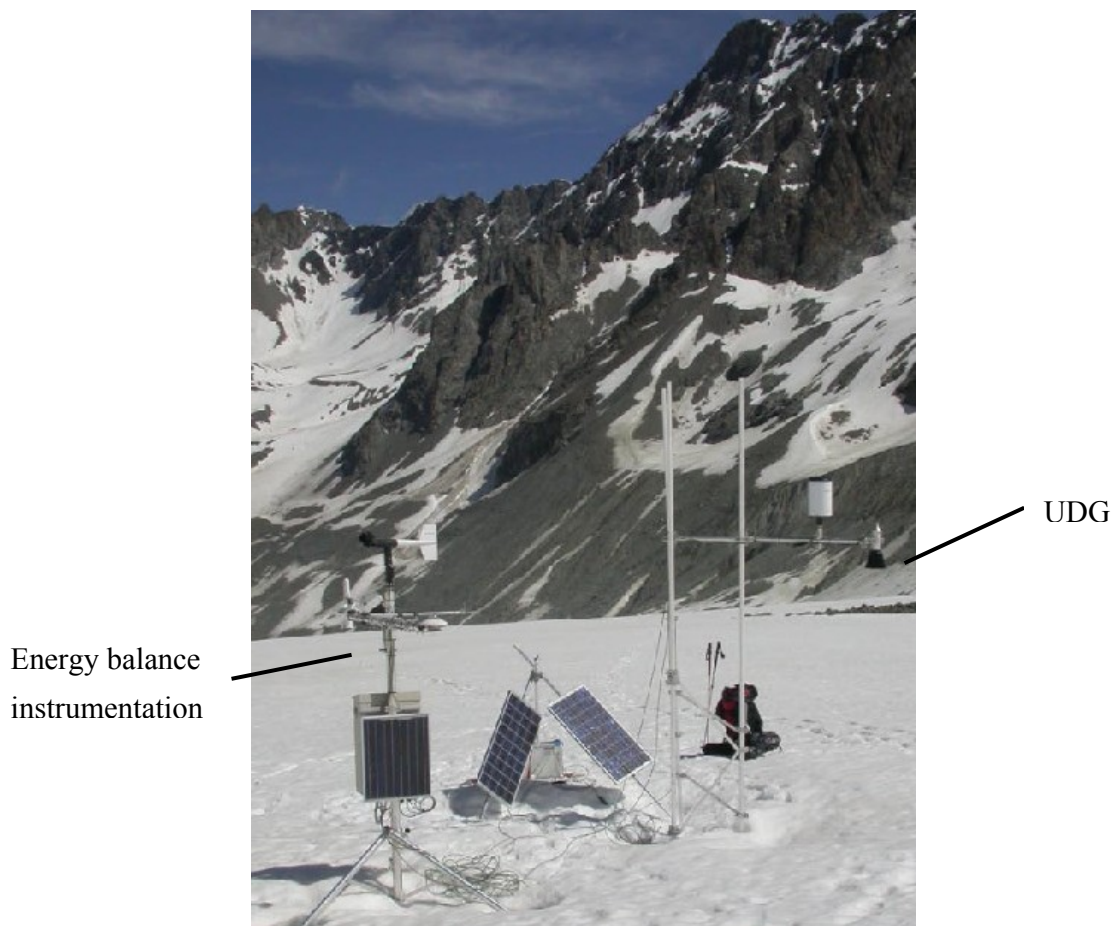
Figure 3.14: AWS_M, installed and maintained by ETH Zürich, in summer 2004. The UDG is mounted on a horizontal arm on the right hand side of the image; instruments for collection of energy balance data are mounted on the tripod on the left. Also seen are solar panels used to power AWS instruments throughout the season. Photo: ETH Zürich.

Table 3.3: Energy balance data collected by each automatic weather station.

Variable	Unit	Collected at AWS_M and U?	Collected at AWS_L?
Relative humidity	0:100%	√	√
Air temperature	^{o}C	√	√
Incoming shortwave radiation	W m^{-2}	√	√
Outgoing shortwave radiation	W m^{-2}	√	√
Net allwave radiation 0.2-100μm	W m^{-2}	√	-
Wind speed	m s^{-1}	√	√
Wind direction	0:360°	√	√
Precipitation	mm	√	-
Snow height	m	√	-

During the 2004 field season an additional AWS (AWS_L) was maintained adjacent to the main snow study site at L. This station measured a reduced range of meteorological variables (Table 3.3).

3.8.3 Proglacial stream data

The characteristics of proglacial runoff, including hydrograph timing and magnitude and water electrical conductivity (EC) and turbidity, provide information about runoff from the glacier system as a whole and conditions in the subglacial environment (Richards et al., 1996). This data can be used to consider the wider role of supraglacial snowpack hydrology in the glacier system. Bulk water discharge data for the Haut Glacier d'Arolla catchment is collected by the hydroelectric company Hydro Exploitation SA at a gauging station approximately 1km downstream from the glacier snout (Figure 3.1), and has kindly been provided for use in this study. A Dexion structure was assembled in each field season to position EC and turbidity sensors in the main proglacial channel approximately 50 to 100m from the glacier snout (Figures 3.1 and 3.15). Sensors were positioned away from the banks of the channel, in freely flowing, well-mixed water. Data was collected from 12th May onwards in 2003; in 2004, due to thick snow cover in the proglacial area early in the melt season, the proglacial stream could not be accessed to install equipment until 29th May. Measurements were taken every 10 seconds and mean values recorded to a Campbell Scientific CR10X data logger every 15 minutes.

Electrical conductivity was measured by a Campbell Scientific 247 combined conductivity and temperature probe. Ultimately, EC measurements were not corrected for variations in water temperature due to the narrow range of water temperatures observed. Water turbidity was measured using a Partech IR40C infrared turbidity sensor, which measures suspended sediment concentration by passing an infrared beam between an emitter and receiver spaced 40mm apart and detecting the degree to which the beam is attenuated. The sensor was not calibrated but is used to show relative variation in water turbidity through time. On several occasions in both field seasons, turbidity values exceeded the maximum that could be

measured by the sensor, resulting in short gaps in the data series. Further information about the collection of proglacial stream turbidity data at Haut Glacier d'Arolla can be found in Swift et al. (2005).

Figure 3.15: Gauging structure on the proglacial stream during the 2003 field season.

3.8.4 Surveying of glacier dynamics

In order to monitor variations in glacier surface dynamics, for later correlation with changes in supraglacial snowpack hydrological behaviour, a line of velocity stakes (5 in 2003, 7 in 2004) was established along the glacier length at the start of each field season (Figure 3.16). A single line of survey stakes was sufficient as it was primarily longitudinal spatial patterns of ice velocity that were of interest. In the absence of any exposed bedrock on which to mount a tripod, the survey station (LS; Figure 3.16) was established on moraine at the eastern edge of the main glacier tongue.

Stakes were inserted into the snowpack at the start of each melt season and regularly pushed lower into the snow to reduce errors associated with stakes swaying in the wind or leaning over. As snow depths decreased, stakes at lower altitudes were drilled into the ice surface.
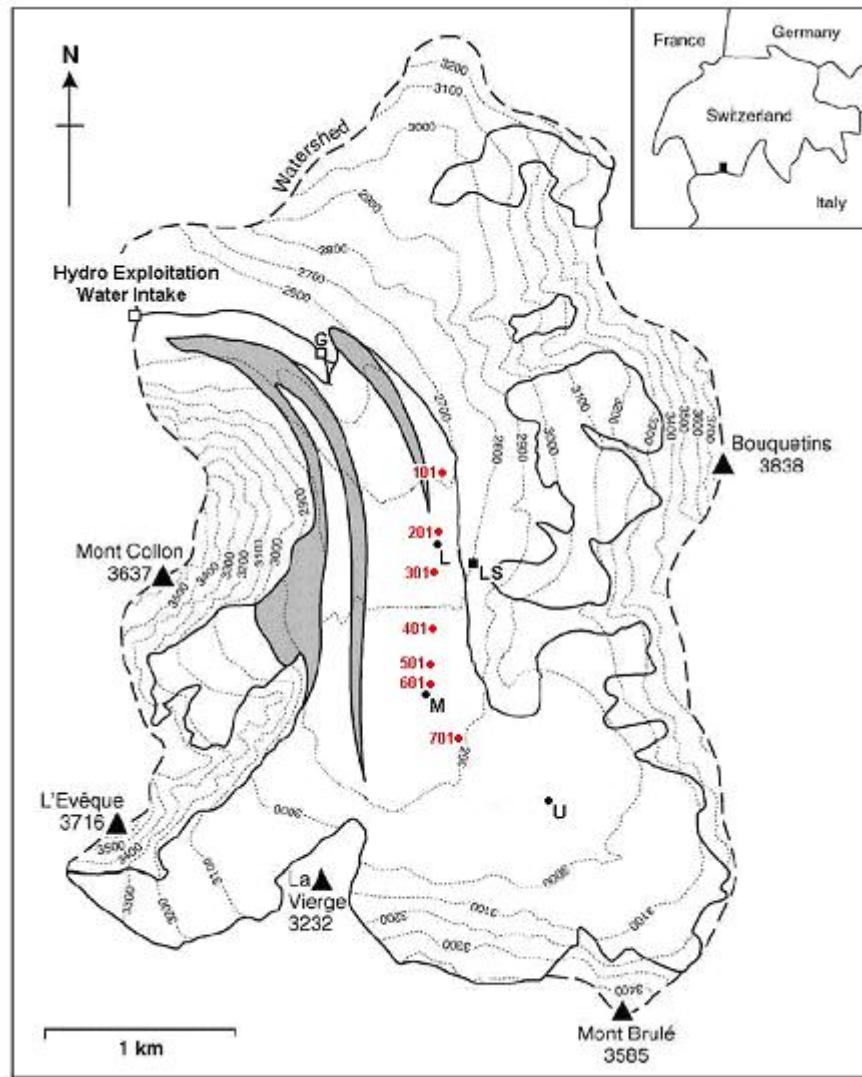
Figure 3.16: Map showing locations of survey stakes. Stakes 501 and 701 were not used in 2003. Base map taken from Figure 1 in Swift et al. (2005).

A Leica Wild T1010 theodolite with attached Wild DI1001 distomat was used for dynamic surveys in 2003 and a Geodimeter System 500 total station was used in 2004. The horizontal angle *HA*, vertical angle *VA* and straight-line distance *SD* to reflector prisms mounted on each survey stake were determined at regular intervals during each field season. A prism mounted on bedrock near the survey station acted as a reference. Typically, 2 to 4 readings were taken for each stake during each survey and averaged.

Inspection of *SD* to the reference prism revealed that there was considerable movement of the survey station during both field seasons due to its location on unfixed lateral moraine (Figure 3.17). The distance between the survey station and the reference prism increased by a total of 74 cm in 2003 and 77 cm in 2004, and this movement in both years took place initially at a more gradual rate (around 0.5 cm day^{-1}) and then more rapidly (at a rate of over

3 cm day^{-1}) (Figure 3.17). *VA* measurements between the survey station and reference prism also showed that the survey station had decreased in altitude significantly through time. As only one reference prism was available it was not possible to correct measured horizontal and vertical angles to the survey stakes for this degree of survey station movement. Instead, subsequent analysis made use only of the measured distance *SD* to survey stakes. The analysis method for calculation of glacier surface velocities from *SD* data is outlined in section 3.8.4.1. Errors in this analysis are discussed in Appendix E.
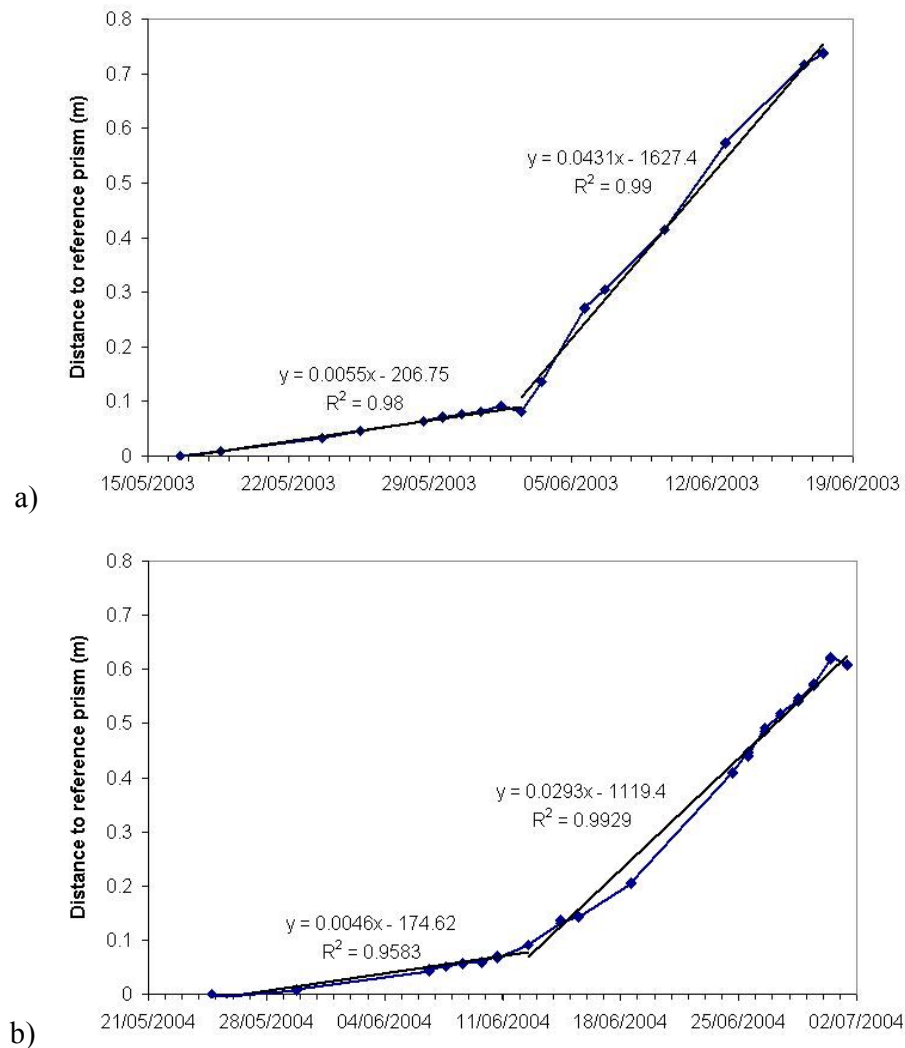
Figure 3.17: Movement of survey station away from reference prism in a) 2003 and b) 2004. The coefficient of x in each fitted trendline indicates the rate of survey station displacement (m day^{-1}) during each interval.

3.8.4.1 Calculation of ice surface velocity from distance data

When errors in *HA* are expected to be significant, ice surface velocities can be calculated using only the measured change in *SD*. The method used in this study followed that of Chandler (2005, p. 59), with additional adjustments to allow for the movement of the survey station. In this method, stake velocity *v* over a time interval *T* is

$$v = \frac{\Delta(SD)}{T} \frac{1}{\cos\alpha}$$

(3.3)

where α is the direction of stake movement relative to the line of sight between survey station and stake and Δ(*SD*) is the change in sighted distance *SD*. The direction of movement of all stakes on the tongue of Haut Glacier d'Arolla was assumed to be northwards and α for each stake was assumed to be constant, which requires that the flow direction is constant and that *SD* >> Δ(*SD*). Error in *α* will give rise to error in calculated velocities but this error will be constant, and *relative* changes in stake velocity are independent of *α* (Chandler, 2005). The change in sighted distance *SD* is most representative of change in actual stake movement for furthest away stakes which are moving approximately towards or away from the survey station. Data for stakes 301 and 701 was therefore discounted from further analysis.

The velocity of each survey stake in the northwards direction was calculated using Equation 3.3 for each interval between surveys. The northwards velocity v_{ss} of survey station motion due to moraine movement was then calculated as

$$v_{ss} = \frac{\Delta(SD_{ref})}{T} \frac{1}{\sqrt{2}}$$

(3.4)

with the assumption that its movement was towards the north-west.

The net velocity v_{net} of each survey stake was then calculated as

$$v_{net} = v + v_{ss}$$

(3.5)

3.9 SUMMARY

This chapter has introduced the Haut Glacier d'Arolla as the field site for this study and explained the methods which were employed in order to investigate the hydrological behaviour of the supraglacial snowpack, its evolution during the summer melt season, the factors controlling this behaviour, and possible implications for the rest of the glacier system. Chapters 4 and 5 present, analyse and discuss the field data collected.

Chapter 4. Supraglacial snowpack hydrology at Haut Glacier d'Arolla - snowpack properties and dye flow patterns

4.1 INTRODUCTION

As shown by the literature review presented in Chapter 2, the supraglacial snowpack is likely to play a key role in mediating the delivery of meltwater produced at the snowpack surface to the rest of the glacier system, with potential implications for both proglacial runoff and the timing and magnitude of glacier motion induced by changes in subglacial water pressure. However, there have been few observations of the hydrological behaviour of supraglacial snowpacks or of the way in which this behaviour evolves during the melt season.

This study aims to enhance our understanding of runoff processes in the supraglacial snowpack, primarily through the use of dye tracing techniques to yield both qualitative and quantitative information about water flow through the snowpack. Other field techniques, as outlined in Chapter 3, provide valuable additional information to help establish the factors controlling water movement through the snowpack and the importance of their roles. Specifically, fieldwork in the supraglacial snowpack aimed to:

  i)   determine the nature of water flow through the supraglacial snowpack of the study glacier;
  ii)   establish if, and in what way, this evolves over the course of the melt season;
  iii)   establish what are the factors controlling water movement through the snowpack, and the importance of their roles; and
  iv)   provide quantitative information about snowpack hydrological behaviour that can inform future modelling studies.

Results and analyses of field data collected at Haut Glacier d'Arolla during the 2003 and 2004 melt seasons are presented here and in Chapter 5. This chapter first presents information about factors likely to influence snow hydrological behaviour, namely the production of meltwater at the snowpack surface (section 4.2) and the physical properties of the snowpack both at the surface and at depth (section 4.3). Qualitative observations of dye flow patterns are then reported and discussed (section 4.4). Conclusions are then drawn about the nature of snowpack percolation as observed at Haut Glacier d'Arolla, the factors

influencing flow patterns, and their relative importance (section 4.5). Quantitative measurements of water flow through the snowpack are presented in Chapter 5, and data considering the wider importance of supraglacial snowpack hydrology - assessing the links between changing snowpack hydrological behaviour, the rest of the glacier hydrological system, and ice dynamics - is presented and analysed in Chapter 7.

The locations of measurement sites referred to in this chapter are marked on Figure 3.1.

4.2 MELTWATER INPUTS TO THE SUPRAGLACIAL SNOWPACK

This section presents data concerning the meltwater flux entering the supraglacial snowpack during the 2003 and 2004 melt seasons. As flux volume is a key control on snow permeability in the unsaturated regime (section 2.2.2.2), the data presented in this section is important for the subsequent interpretation of dye-tracing tests and other aspects of the snowpack's hydrological behaviour.

4.2.1 Overview of 2003 and 2004 snow and melt conditions

Snow observations made across Switzerland by the Swiss Federal Institute for Snow and Avalanche Research (SLF) provide an overview of snow and melt conditions during the study years (SLF Winter Aktuell website - http://wa.slf.ch/). Data from the permanent automatic weather station (AWS) maintained by ETH Zurich near the Hydro Exploitation water intake (Figure 3.1) also enables consideration of winter temperature conditions that will have influenced snowpack properties. Figure 4.1 shows the temporal pattern of snow accumulation recorded by SLF monitors at Zermatt (1600m; assumed to indicate the trend in snowpack accumulation across the wider Valais area) together with air temperature measured at the AWS in front of Haut Glacier d'Arolla during the winters preceding each field season.

Comparison of Figures 4.1 a and c indicates earlier accumulation of the winter snowpack in 2002-2003, with little further snowfall after early February. Air temperature records show unusually warm temperatures in April and May 2003 (Figure 4.1b), which triggered early melting of the snowpack. In winter 2003-2004, in comparison, there was continued snowfall throughout February, March and April (Figure 4.1c). In both years, but particularly 2003-2004, periods can be identified in which air temperature rises above 0°C before falling again, and these episodes are expected to lead to the formation of ice layers in the snowpack.

Summer 2003 saw unusually warm temperatures across Europe (Haeberli et al., 2006), with rapid snow melt in the Swiss Alps during June resulting in atypically early removal of the

snowpack in many areas (SLF, 2003). In contrast, summer 2004 saw renewed winter conditions and snowfall during May, more mixed conditions in June and July, and longer survival of the snowpack (SLF, 2004). As a result, fieldwork in the supraglacial snowpack at Haut Glacier d'Arolla was limited in summer 2003, with summer 2004 providing more opportunity for effective data collection throughout both June and July.
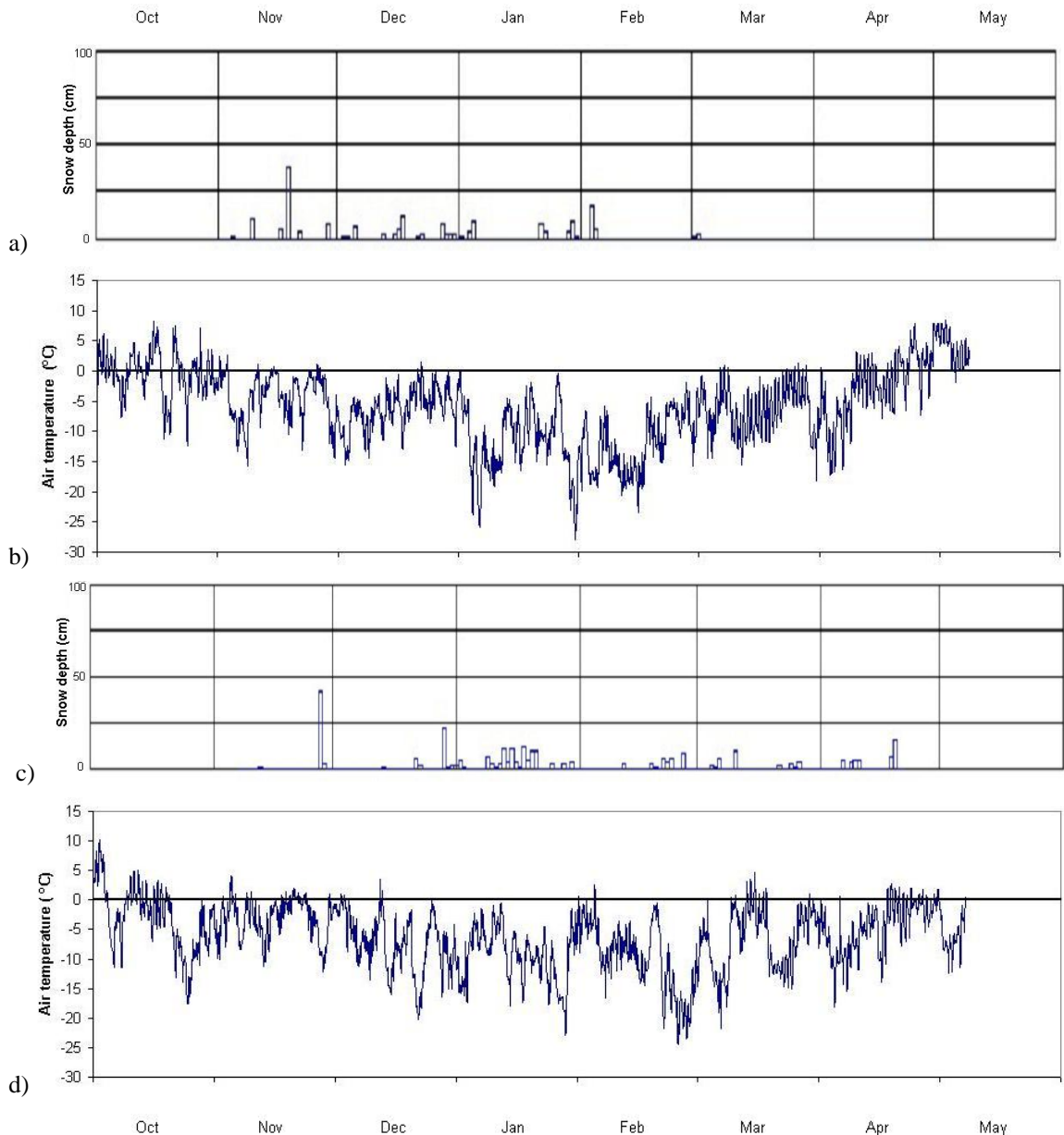
Figure 4.1: New snowfall depth measured at Zermatt (1600m) (SLF WinterAktuell online) and air temperature at ETH AWS for a-b) winter 2002-2003 and c-d) winter 2003-2004. Notable are the warm temperatures in April and May 2003 (b) which triggered early melting of the snowpack. In 2004, in comparison, there was continued snowfall throughout February, March and April (c). In both years, but particularly 2003-2004, periods can be identified in which air temperature rises above 0°C before falling again, and these episodes are expected to lead to the formation of ice layers in the snowpack.

4.2.2 Surface energy balance

Figure 4.2 presents time series of the meteorological data collected during summers 2003 and 2004 by the ETH AWS situated at around 2800m altitude on the glacier (AWS_M on Figure 3.1). As this on-ice AWS was not installed until 17th June in 2003, air temperature data from radiation-shielded Campbell Scientific 107 temperature probes mounted at L and M was used to give season-long information. Precipitation data collected proglacially was used to fill the data gap in the early season. The AWS was installed earlier in 2004 and full energy balance data is available for the duration of that field season. The higher June air temperatures in 2003 are apparent in Figure 4.2a when compared to data from 2004 (4.2d).

a)

b)

c)

d)
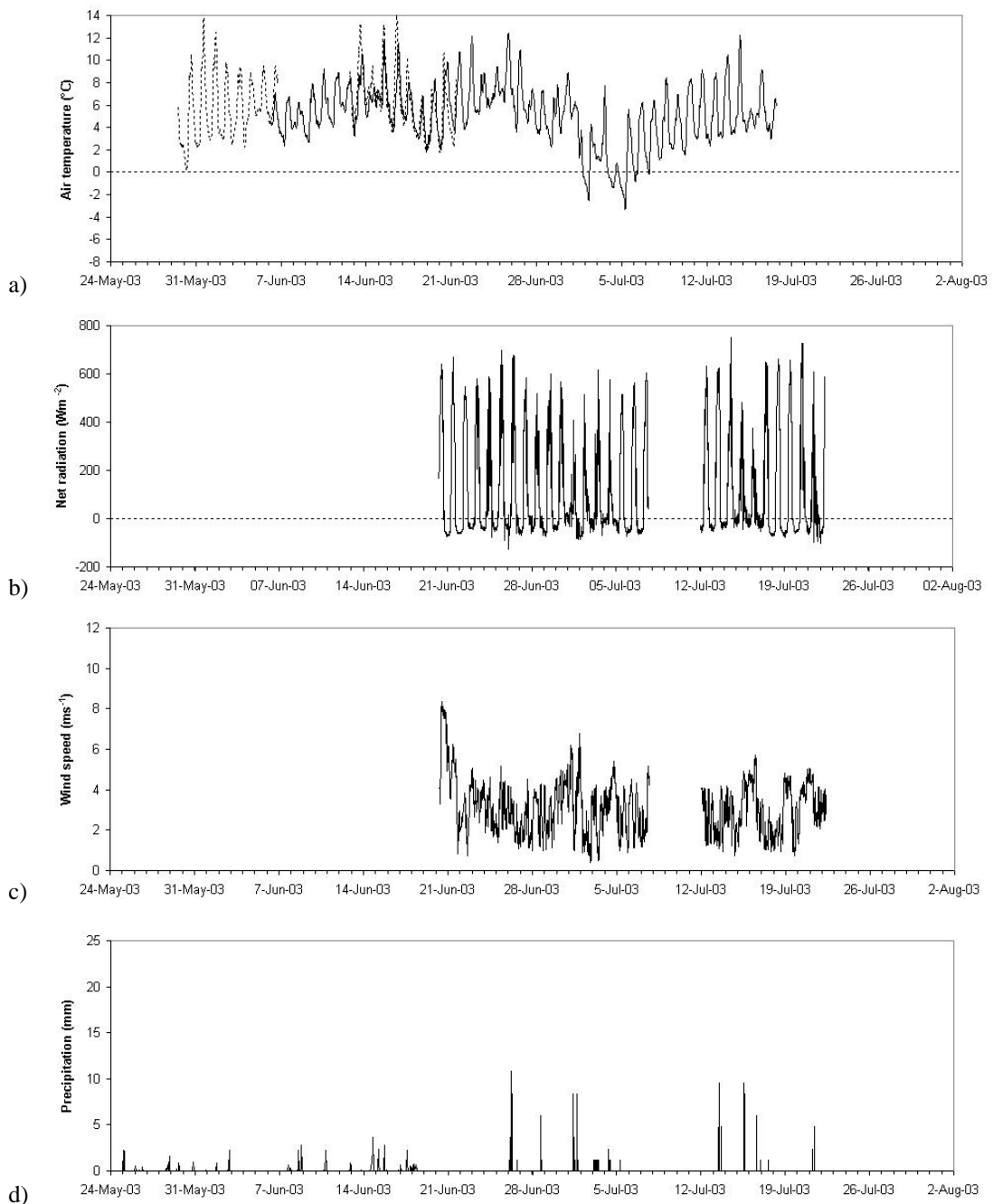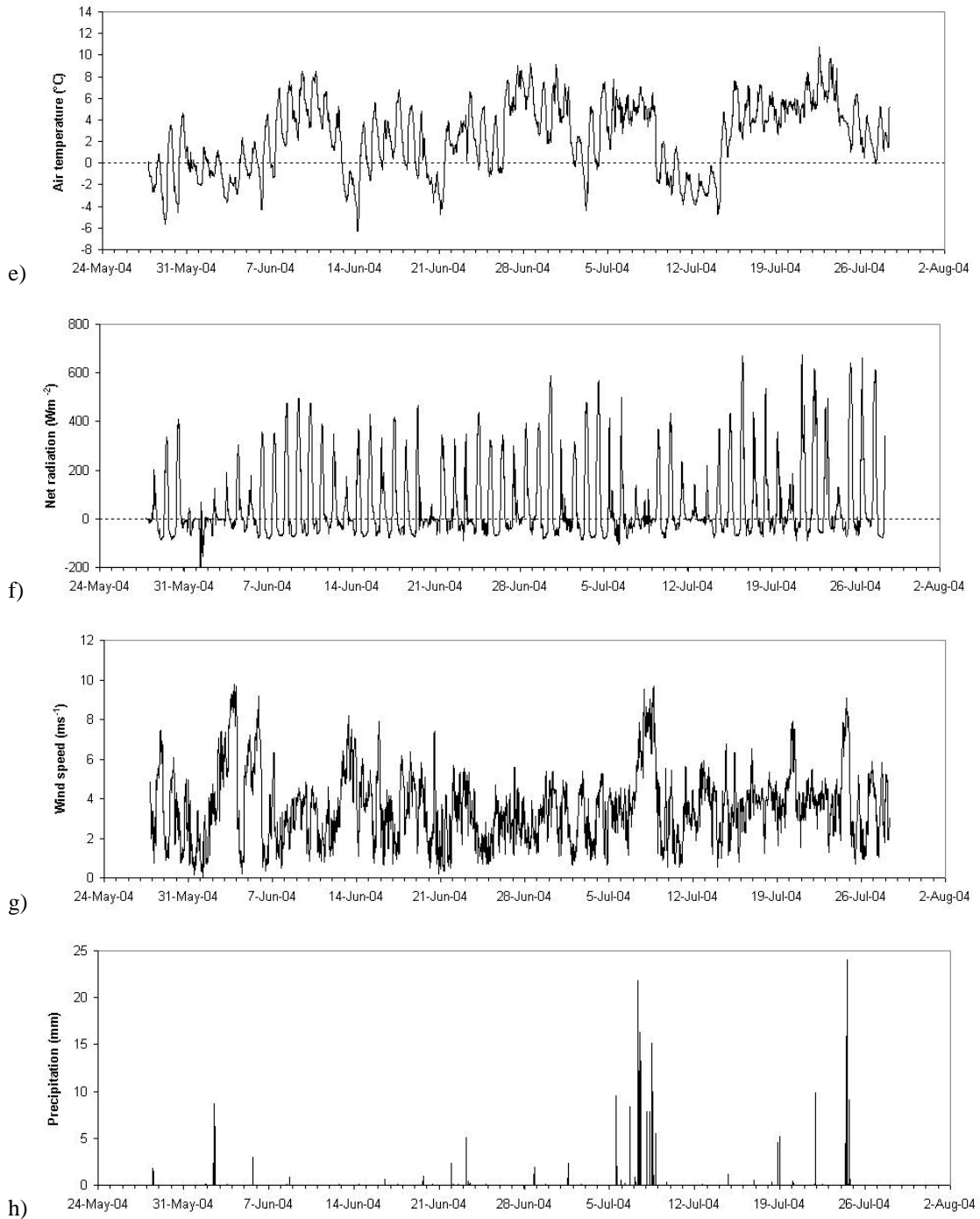
Figure 4.2: Meteorological time series data for the 2003 field season collected at AWS_M (Figure 3.1). On previous page: a) hourly air temperature (from L (dotted line) and M (solid line)), b) hourly net radiation, c) hourly wind speed, d) hourly precipitation. e) to h) as for a) to d), but for 2004 field season.

Surface melt was calculated from meteorological data using the energy balance model of Brock and Arnold (2000) (Figure 4.3). The key components of this model and the appropriateness of its use in this study are discussed in Appendix B. Model output showed that, as expected, peak melt rates were in general higher in 2003 than in 2004 (Figure 4.3). This would also be the case during early June, when full energy balance data was not

available in 2003 but high temperatures were recorded (Figure 4.2a). Modelled melt rates for 2004 are on the whole somewhat lower than those reported by Richards et al. (1996), Willis et al. (2002) and Fox (2003) for previous melt seasons at Haut Glacier d'Arolla, with hourly melt rarely reaching 0.004 m hr^{-1}.

The energy balance contribution of liquid precipitation is not included in the Brock and Arnold (2000) as it is argued to be important only in exceptional circumstances (Appendix B). However, rainfall can play a role in enhancing the hydrological efficiency of the snowpack (by causing coarsening of snow grains and possibly also encouraging the formation of an undulating snowpack surface, thereby encouraging preferential flow (Conway and Benedict, 1994; Singh et al., 1997)). June 2003, as well as seeing unusually warm temperatures, saw frequent heavy rainfall, often in the evening or as short showers during the day (Figure 4.2d and field notes). Rainfall was less frequent in 2004 and fewer episodes of heavy rain were noted (Figure 4.3h and field notes). In both years, however, periodic rainfall throughout the melt season may have contributed to the development of snowpack hydrological efficiency.

It was intended that ultrasonic depth gauge records would be used to calculate surface melt rates based on snowpack depth change. However, UDG records, while reliable over longer timescales, were very 'noisy' within each day and were therefore unsuitable for calculation of melt rates. Instead, hourly surface melt rates calculated using the Brock and Arnold (2000) model for 2004 data (Figure 4.3b) were converted to the corresponding snowpack depth change using an assumed surface snow density of 560 k gm^{-3} (a mean value of snow densities sampled in the field - see section 4.3.4), and in this way the modelled melt series could be verified by comparison to the UDG record (Figure 4.4). In general, surface melt rates calculated using Brock and Arnold (2000) match the rate of depth loss well (with the exception of snowfall events, which are not taken into account in the modelled data). This provides confidence in the modelled melt rates.

a)

b)
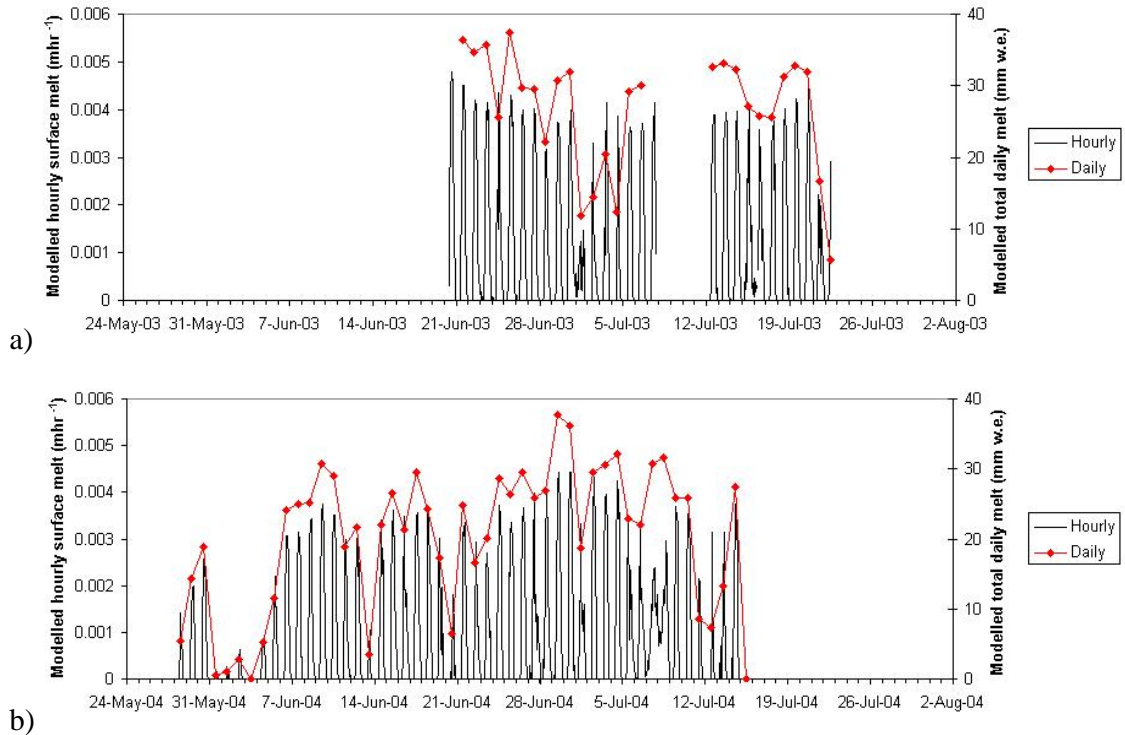
Figure 4.3: Hourly and daily surface melt rates for a) summer 2003 and b) summer 2004, modelled using the Brock and Arnold (2000) energy balance model (Appendix B). Peak melt rates can be seen to be generally higher in 2003 than in 2004, and although energy balance data is not available for early June 2003, the high temperatures observed in that time (Figure 4.2a) show that melt would also be high then. Modelled melt rated for 2004 are on the whole lower than those observed previously at Haut Glacier d'Arolla.
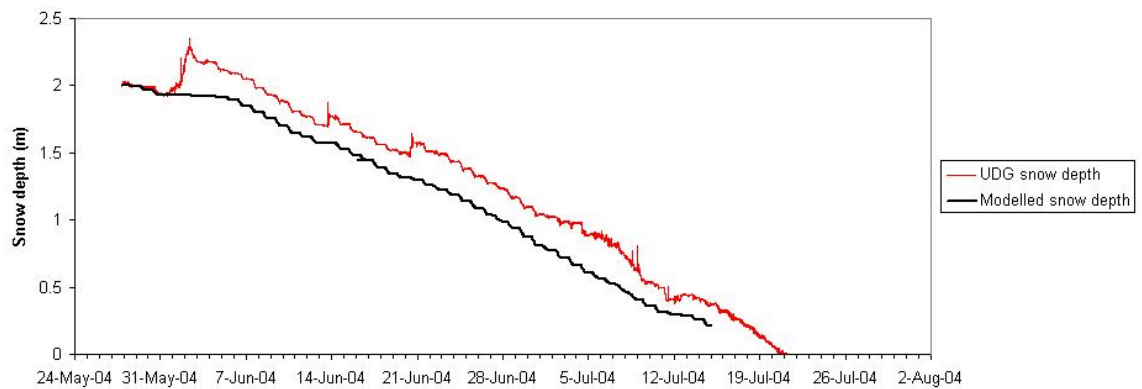
Figure 4.4: Verification of melt rates modelled using Brock and Arnold (2000) (Appendix B) by comparison of snow depth change corresponding to modelled melt rates to UDG data. The rate of depth loss is in general modelled well, giving confidence in modelled melt rates.

4.3 SNOWPACK PROPERTIES

The physical properties of the snowpack, in addition to input melt flux, are key controls on runoff. This section presents the results of field investigations monitoring snowpack depth, surface characteristics, stratigraphy, temperature and density throughout both field seasons.

4.3.1 Snowpack depth change – spatial and temporal patterns

Knowledge of snowpack depth and its spatial and temporal variability is necessary for subsequent assessment of the role that this plays in controlling runoff. Snow depth probing along the glacier centre-line near the start of both field seasons showed the spatial variation of snowpack depth (Figure 4.5). Data for 2004 shows significant evidence ($p < 0.05$) of an upglacier increase in snowpack depth, which would be expected as a result of increasing altitude, but there is also considerable variation within this trend. A weaker upglacier increase in snow depth was observed in 2003. The limited altitudinal range of the glacier and its variable longitudinal slope, combined with complex patterns of snow redistribution by wind and the different number of melt days which the snowpack had experienced each year before depth measurements were made, explain variations in this upglacier trend. The difference in snow conditions between 2003 and 2004 is also clear from Figure 4.5, with generally lower snow depths measured in 2003 despite depth probing being carried out two weeks earlier.
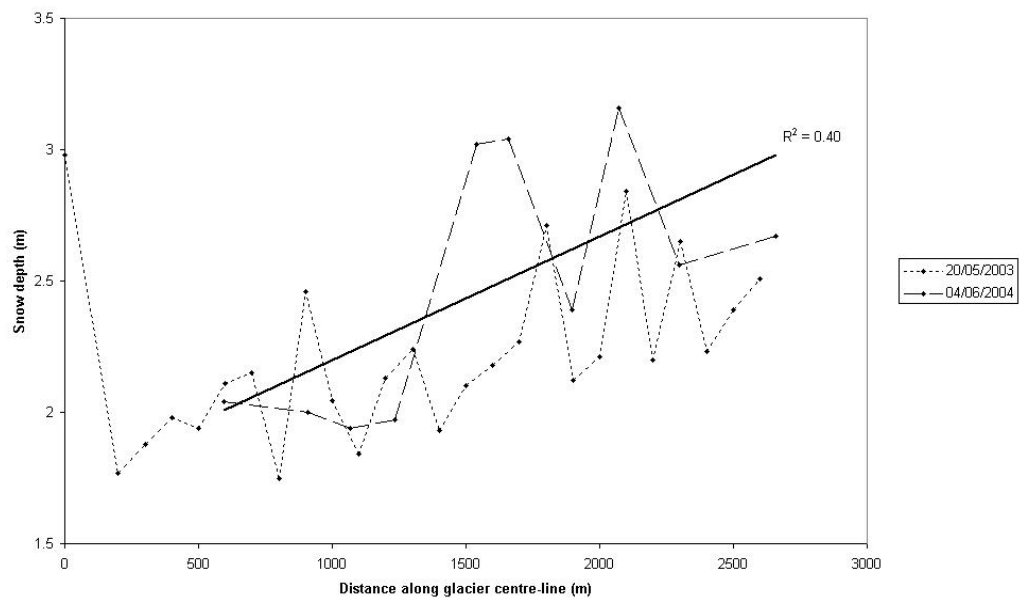
Figure 4.5: Variation in snowpack depth along the glacier centre-line at the start of both field seasons. Trendline and r^2 value shown for 2004 data. There is significant evidence ($p < 0.05$) of an upglacier increase in snow depth in 2004, which would be expected as a result of increasing altitude, but also considerable variation within this trend. A weaker upglacier increase in snow depth is seen in 2003 data. The difference in snow conditions between 2003 and 2004 is clear, as generally lower snow depth were measured in 2003 despite depth probing being carried out two weeks earlier in the summer.

Ultrasonic depth gauge (UDG) records from several locations on the glacier show the change in snowpack depth with time through both melt seasons (Figure 4.6). Snow depths at the start of the 2003 field season were lower than in 2004 due to the early onset of warm weather in April. Rates of surface lowering throughout 2003 were noticeably more rapid than in 2004, particularly at the lower station, and snowpack removal occurred earlier. In addition, snowpack survival in 2004 was aided by over 30cm of new snow accumulation in late May/early June and two smaller snowfalls in June. Taking into account only the period after the last significant snowfall of each year (24th May onwards in 2003 and 3rd June onwards in 2004), UDG records of snowpack depth change correspond to average rates of snowpack surface lowering at the lower snow study station of 6.1 cm per day in 2003 compared to 4.1 cm per day in 2004.
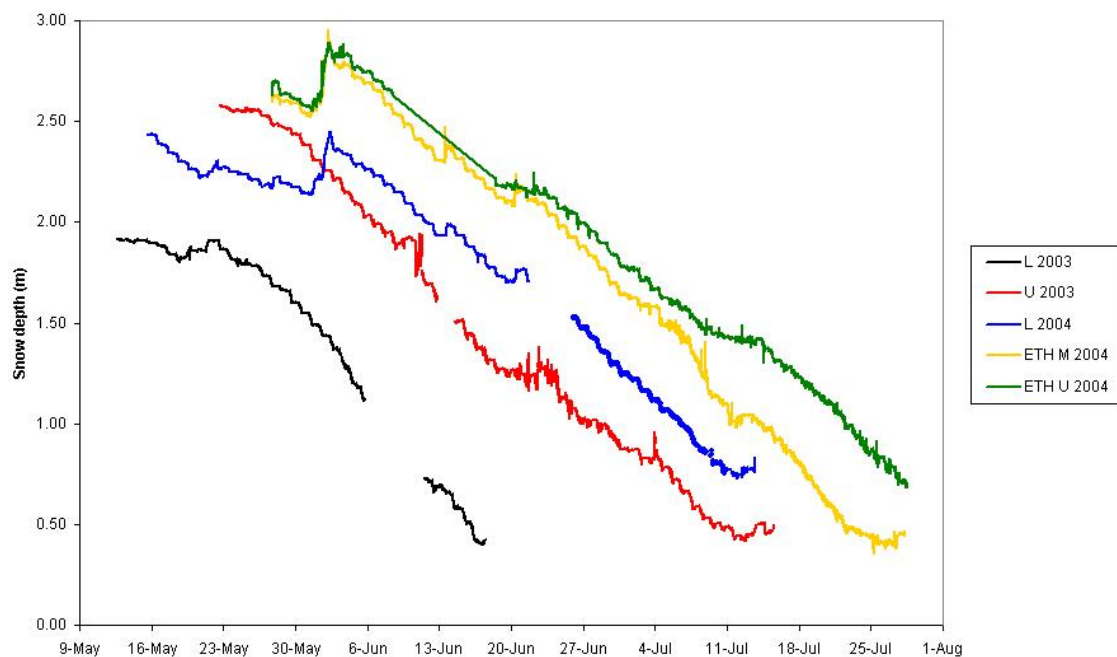
Figure 4.6: Ultrasonic depth gauge (UDG) records of snowpack depth for both field seasons. No data is available for M in 2003 as the UDG malfunctioned. It can be seen that surface lowering took place more rapidly in 2003 and snowpack removal occurred earlier.

The pattern of snowpack depletion during the 2004 field season is shown by the series of photographs in Figure 4.7, illustrating the spatial variability of snowpack depth (due to a combination of variable snow accumulation and variable ablation rate) and the uneven nature of snowline retreat. Patches of bare ice were first revealed at the end of June near the western margin of the glacier 800m from the snout, with patches of bare ice appearing lower on the snout in early July (Figure 4.7a). By mid-July much of the main glacier tongue was free of snow on its western flank to around 1.5 km from the terminus, but snow remained across the eastern flank (Figure 4.7b). By the end of July (Figure 4.7d) the main glacier tongue was almost entirely free of snow and several large patches of bare ice were exposed in the eastern upper basin.

a)

b)

c)

d)
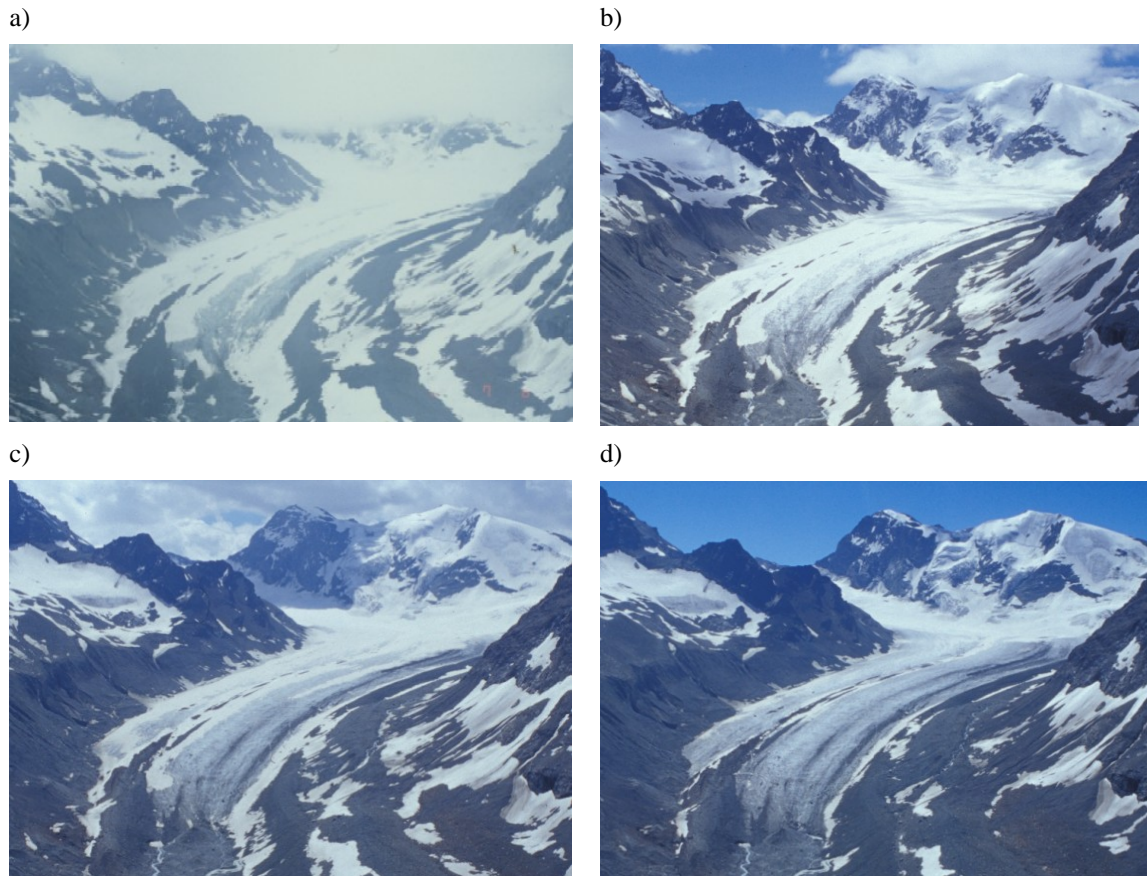
Figure 4.7: Pattern of snowpack depletion during the 2004 melt season, as recorded by a permanently-installed camera maintained by ETH Zurich. Photographs taken on: a) 8th July, b) 15th July, c) 21st July, d) 29th July. The uneven nature of snowline retreat is clear.

Due to warmer temperatures in summer 2003, snowpack removal proceeded almost one month earlier than in 2004. Patches of bare ice were exposed on the lower tongue of the glacier in early June (Figure 4.8a) and much of the main glacier tongue was snow-free across the western flank by mid-June (Figure 4.8b). By early July, most of the eastern upper basin, and therefore almost the entire glacier surface, was also free of snow.

a)

b)
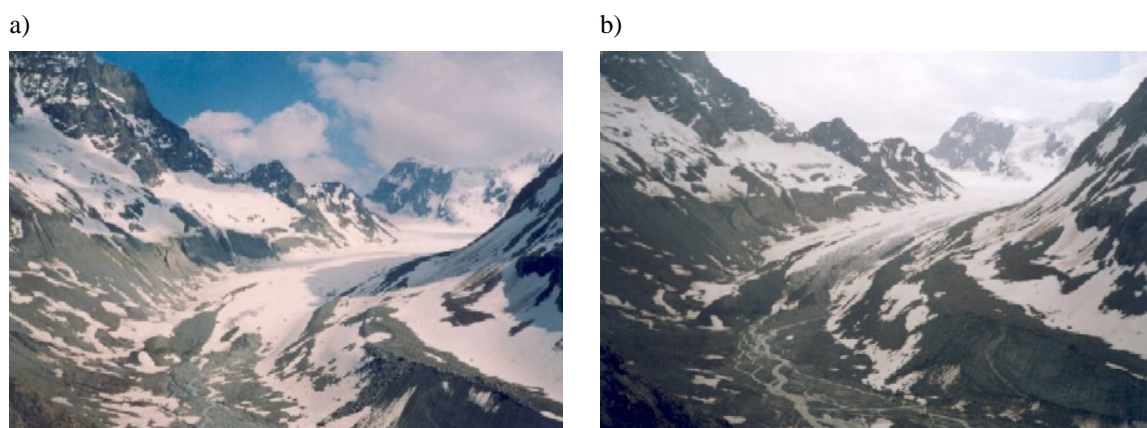
Figure 4.8: Pattern of snowpack depletion during the 2003 melt season. Photographs taken on: a) 8th June, b) 14th June. Snowpack extent in b) is comparable to that in Figure 4.7b, taken on 15th July 2004, thereby illustrating the ~one month advance of melt conditions during summer 2003. Comparison to Figure 4.7 shows that snowpack removal proceeded almost 1 month earlier in 2003 than in 2004.

4.3.2 Snowpack surface characteristics

Photographs taken throughout both field seasons illustrate changes in snowpack surface characteristics that may both reflect the hydrological state of the snowpack beneath and influence the production and subsequent movement of water (section 2.2.2.3) (Figures 4.9 – 4.14). Data from 2004 is considered first due to the greater number of observations made in that year.

2004 field season

Early in the melt season, in mid-May, the snowpack surface was observed to have an undulating topography, with elongated shallow depressions (hereafter referred to as 'rills') running in a downslope direction with spacing of around 1 to 1.5 metres (Figure 4.9). A link between snow surface topography and water distribution within the snowpack has been suggested by a number of studies, including Gerdel (1954), Wankiewicz (1979), Kattelman (1989) and Williams et al. (1999) (section 2.2.2.3). These workers suggest that surface depressions both enhance melt by reflection and collect water flowing downslope from the surrounding area, and thereby concentrate percolating meltwater creating higher saturation and faster percolation velocities. The concentration of percolating meltwater and resulting grain growth and densification in more saturated areas of the snowpack then triggers a positive feedback by enhancing surface lowering.

It was therefore considered that rill forms on the snowpack surface might indicate the presence of water regularly distributed within the snowpack. If rill forms observed at Haut Glacier d'Arolla in May 2004 are an expression of flow organisation within the snowpack, the extent to which these features are developed early in the melt season is perhaps surprising. Observations of dye percolation patterns later in 2004 (reported in section 4.4) did not show evidence of flow organisation at this scale, but investigations were few and observations may have been masked by the intense heterogeneity of flow patterns at the smaller scale. Further field observations of water flow within the snowpack are required before this link can be further considered.

Figure 4.9: Rill topography on the snowpack surface between M and L, 20th May 2004.

From mid-May onwards the snowpack surface developed small-scale melt forms after two or three days of continuous melt (Figure 4.10).

Figure 4.10: Typical early melt season snowpack surface after good weather, with small-scale melt forms developing (20th May 2004).

Undulating surface topography and downhill-trending rills continued to be visible throughout June, often made more clearly visible by bright white new snow drifting into depressions (or persistence of new snow in depressions as snow melted away after a snowfall) (Figure 4.11). At the smaller scale, the snowpack surface developed a more rippled form after continued melt, which was superimposed on the larger scale rills (Figure 4.12).

Figure 4.11: Undulating snow surface topography on the main glacier tongue near L in June 2004, with depressions picked out by new white snow.

Figure 4.12: Developing 'ripple' melt forms on the snowpack surface at L, superimposed on larger scale undulations ('rills') running left to right across the image (10th June 2004). Yellow rule is 2m long.

From the beginning of July, the snowpack surface developed a more 'wavy' topography (Colbeck et al., 1990) at the small scale, with small (c. 10 to 15 cm deep) depressions known as 'suncups' (USGS definition) or 'ablation hollows' spaced irregularly at approximately 20 to 40 cm intervals (Figure 4.16). Suncups, as described by Betterton (2001) and Herzfeld et al. (2003) and in a similar manner to that described for rills above, have been identified as playing a role in altering surface energy balance and concentrating melt production in depressions. Their undulating topography may also direct meltwater to topographic lows, further varying the distribution of flux within the snowpack. Evidence for this was not seen in dye observations in 2004, but observations from 2003 which support this idea are discussed in section 4.4.5. Suncups developed first across the lower glacier and subsequently spread upglacier. Sediment accumulated in suncup troughs (Figure 4.13b) and will have triggered a positive feedback process by increasing surface albedo in depressions.
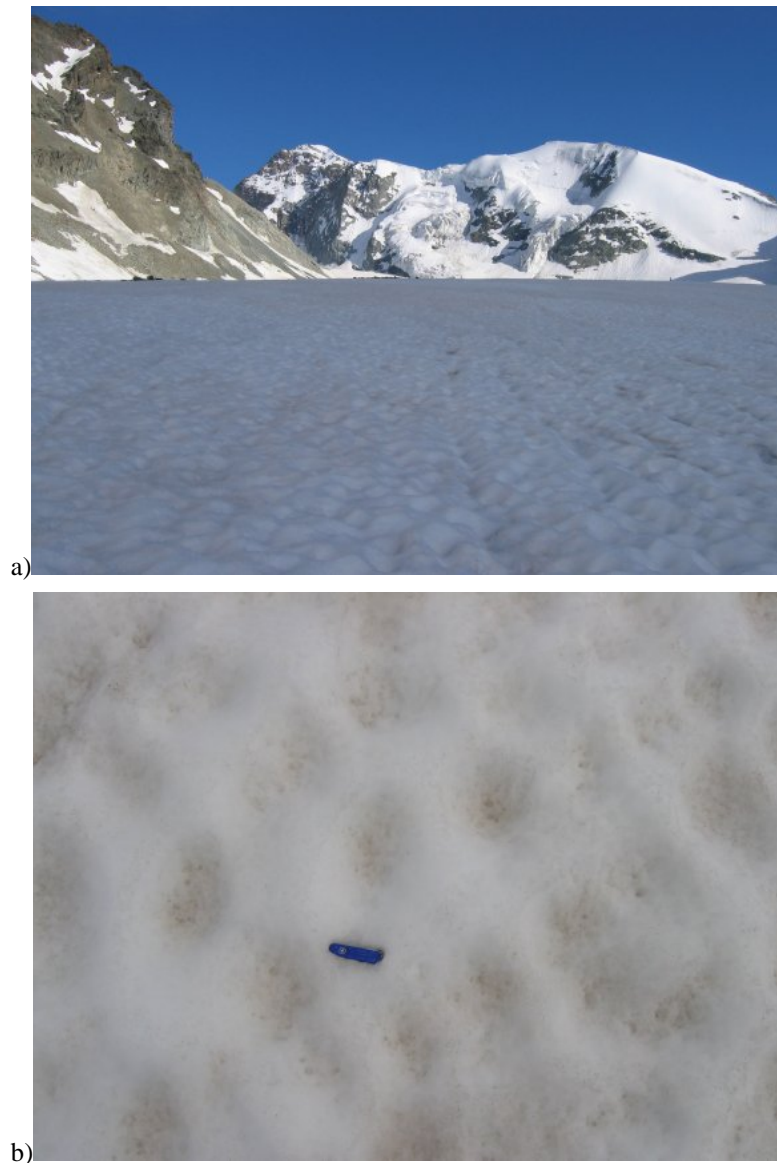
Figure 4.13: Suncupped snow surface on the main glacier tongue near L, early July 2004. b) shows sediment concentration in suncup troughs.

2003 field season

In accordance with the earlier onset of melt and warmer weather in 2003, suncup forms had already appeared on the snowpack surface across the lower glacier in late May (Figure 4.14) and had developed at U by mid-June. Observations of dye percolation patterns (presented in section 4.4.5) appeared to show some concentration of percolating meltwater beneath suncup depressions, supporting the suggestion that snow surface topography can play a role in spatially concentrating flux and thereby enhancing runoff efficiency, as suggested above.

Figure 4.14: Suncupped snow surface on the main glacier tongue in early May 2003.

4.3.3 Stratigraphic evolution

Representative snowpit stratigraphic profiles from both field seasons are shown in Figures 4.15 and 4.16. Profiles measured at each of the three snow study sites L, M and U at the start of the 2003 field season gave some indication of snowpack properties across the spatial extent of the glacier (Figure 4.15 a, c and e). Repeat observations approximately one month later showed the snowpack stratigraphy after exposure to considerable melt (Figure 4.15 b, d and f). As most work in 2004 was carried out at L, a more detailed sequence of four stratigraphic profiles between 20th May and 10th July is presented (Figure 4.16), showing the evolution of snowpack stratigraphic properties through time at a single pit location.

In every case, stratigraphic profiles from May showed the presence of a large number of ice layers within the snowpack. On 20th May 2004 over 22 hard, high-density layers could be

identified in the 2.25 metre-deep snowpack at the study site, three of which were over 1 cm thick. Ice layers in general varied in thickness from a few millimetres to around 2 cm, with 'complexes' of ice layers up to 5 cm thick sometimes formed by multiple smaller ice layers formed closely one upon the other. Some were observed to be discontinuous across the c.1.5 m width of the snowpit wall, but many others appeared solid and continuous across a distance of tens of metres. In all early-season profiles, ice layers were distributed through the snowpack depth with a lower concentration near the base. As a result, when snowpack depth decreased below around 1 m, typically only 2 or 3 ice layers remained in the snowpack, although these often remained spatially continuous and solid in appearance despite prolonged exposure to liquid water moving through the snowpack (Figure 4.27 later in this chapter). In this respect, observations of ice layers at Haut Glacier d'Arolla disagree with Gerdel (1954), who suggested that ice layers decay rapidly in the presence of liquid water and therefore have little further effect on water flow. In 2004, the snow above ice layers was sometimes observed to be saturated with water, suggesting impermeability to water flow and retardation of downwards water percolation. This effect was also observed in the profile taken on 3rd July 2004 above an ice layer exposed to percolating meltwater for over one month and now just 10 cm from the snowpack surface (Figure 4.24 later in this chapter), further contradicting Gerdel (1954).

Throughout both seasons the entire snowpack (with the exception of early-season surface and depth hoar, and rounded, unbonded grains present through the whole snow depth at L in early 2004) was composed of rounded, bonded snow grains characteristic of a snowpack which has experienced wet snow metamorphism and refreezing (Colbeck et al., 1990). Grain sizes, however, remained small (around 1 mm diameter) throughout both seasons, with only a few layers attaining the 2 mm diameter often said to characterise a mature snowpack (Colbeck, 1978a).

Temperatures within the snowpack were measured concurrently with stratigraphic profiles and are presented alongside early-season profiles in Figures 4.15 and 4.16. The snowpack was found to be isothermal at 0° from the onset of both field seasons.

a)

b)
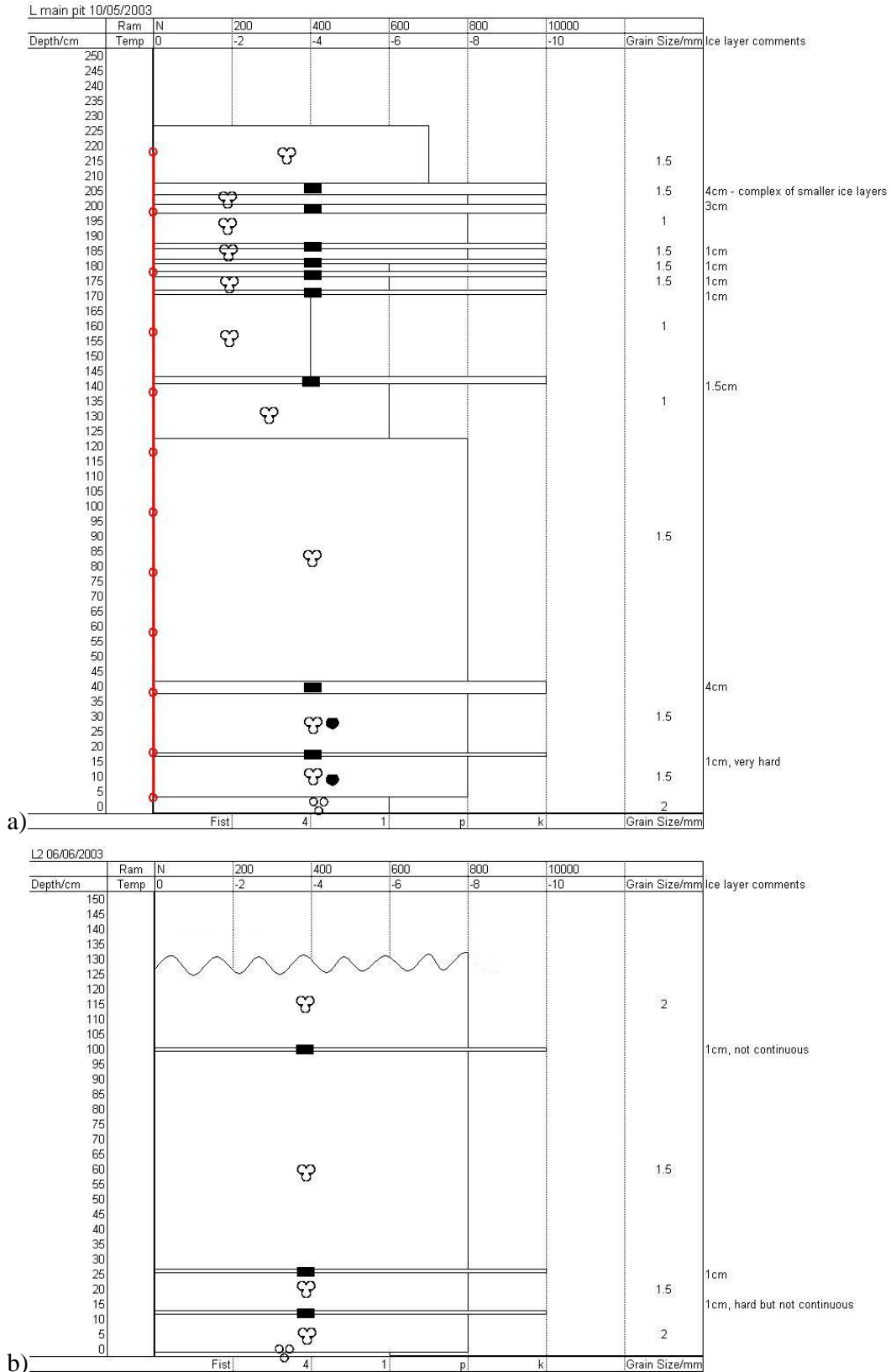
Figure 4.15: Snowpack stratigraphy at L during summer 2003, on a) 10th May and b) 6th June, at M on c) 14th May and d) 13th June, and at U on e) 15th May and f) 20th June. Observations of snowpack surface topography (section 4.3.2) are represented by the line forming the upper boundary of each stratigraphic section. Snowpack temperature measurements are represented by the red line on the first stratigraphy from each location (all snow was isothermal from the first measurements). Drawing of stratigraphies was based on the Excel-based plotting tool of Ream (2000), which uses the Colbeck et al. (1990) snow grain classification (Appendix A). A key to snow grain types is provided after Figure 4.16.

M main pit 14/05/2003

Depth/cm	Ram Temp	N 0	200 -2	400 -4	600 -6	800 -8	10000 -10	Grain Size/mm	Ice layer comments
260									
255									
250									
245				V				2	
240				■				1	3mm
235									3mm
230				■				1	
225									
220									
215				☘				1	
210									
205									
200				■					3mm
195				■					IL complex
190									
185				☘				1	dense, icy snow
180									2cm, continuous
175									
170				☘				1	
165									4mm, non-continuous
160				☘				1	
155				■					8mm
150									
145				☘					dense icy snow, angular
140								1	
135									
130				■					3cm, non-continuous
125								1	
120				■					1.5cm, non-continuous
115				☘				1	
110				■					1.5cm, continuous
105									
100									
95									
90									
85								1	
80				☘ ⌂					
75									
70									
65									
60									
55									
50									
45				■					7cm, continuous
40				⌂				1	
35									
30									
25									
20								1	
15				Λ					
10									
5									
0									
		Fist	4	1	p	k		Grain Size/mm	

c)

M3 13/06/2003

Depth/cm	Ram Temp	N 0	200 -2	400 -4	600 -6	800 -8	10000 -10	Grain Size/mm	Ice layer comments
150									
145									
140									
135									
130									
125									
120									
115								1.5	
110				☘					
105									
100									
95									
90									
85									
80				☘				1.5	
75									
70									
65									
60									
55									
50				■					0.6-2cm, continuous
45									
40				☘				1.5	
35				■					1.5cm, solid
30									
25				☘				1.5	1cm, grainy, disintegrating
20				■					
15				☘				1.5	
10									
5									
0				☘☘				2	5cm pooling water
		Fist	4	1	p	k		Grain Size/mm	

d)

e)

f)

Figure 4.16: Snowpack stratigraphy at L during summer 2004, on a) 20th May, b) 21st June, c) 3rd July and d) 10th July. See caption for Figure 4.15 for information. A key to snow grain types is provided after d).

L New pit 03/07/2004

Ram	N	200	400	600	800	10000		
Depth CM	Temp	0	-2	-4	-6	-8	-10	Grain Size/mm	Ice layer observations

Depth CM: 150, 145, 140, 135, 130, 125, 120, 115, 110, 105, 100, 95, 90, 85, 80, 75, 70, 65, 60, 55, 50, 45, 40, 35, 30, 25, 20, 15, 10, 5, 0

Grain Size/mm values: <1, 1, <1, 1, 1-1.5, 1.5, 2

Ice layer observations: 5mm grainy, decayed?; 4mm solid; 8mm, 1cm saturated above; 6mm-1cm, very solid

Bottom axis: Fist | 4 | 1 | p | k | Grain Size/mm

c)

L New pit 10/07/2004

Ram	N	200	400	600	800	10000		
Depth CM	Temp	0	-2	-4	-6	-8	-10	Grain Size/mm	Ice layer observations

Depth CM: 100, 95, 90, 85, 80, 75, 70, 65, 60, 55, 50, 45, 40, 35, 30, 25, 20, 15, 10, 5, 0

Grain Size/mm values: 1, 1, <1.5, <1.5, 1.5, 2

Ice layer observations: 5mm, still solid; 3cm; no sat layer

Bottom axis: Fist | 4 | 1 | p | k | Grain Size/mm

d)

Key to snow grain types used in stratigraphic profiles, following the Colbeck et al. (1990) International Classification for Seasonal Snow on the Ground (Appendix A):

Rounded grains (monocrystals):
- large rounded particles
- mixed forms

Faceted crystals:
- mixed forms

Wet grains:
- clustered rounded grains
- rounded polycrystals
- slush

depth hoar

surface hoar

ice layer

In stratigraphies observed in early 2004 a yellow layer could be seen around 1.30 m above the ice surface (Figure 4.16a), formed by the deposition of Sahara dust onto the snowpack surface during a föhnstorm on 21st February (SLF WinterAktuell, 2004). This layer was observed to melt out to the snowpack surface at L around 10th June, after which time it will have played a role in lowering surface albedo and enhancing melt.

As the presence of ice layers within the snowpack is expected to be of hydrological importance, probing was undertaken in 2003 (following the method described in section 3.8.1) to investigate their wider occurrence across the altitudinal range of the glacier. A large number of ice layers was present at all locations along the glacier centre-line (Figure 4.17), with an average of 11 ice layers (minimum 6, maximum 20) detected at each location. A higher frequency of ice layer occurrence in the upper ~0.5 m of the snowpack was also apparent at most of the locations probed. Stratigraphic profiles taken early in the 2004 melt season (e.g. Figure 4.16a) show that this phenomena existed in that year too. As the formation of ice layers is a result of melting and refreezing events, their distribution through the snowpack suggests that such events are rare in the first months of winter and frequent towards the end, when warm and cold periods alternate. Air temperature and snow accumulation data (Figure 4.1) show evidence for alternating periods of melting and refreezing in combination with intermittent snowfall, which will have resulted in ice layer formation and burial. That ice layer formation should be most frequent at the end of winter, however, is not immediately apparent from Figure 4.1. Whether this is likely to be a general occurrence in alpine snowpacks is a matter for further investigation, and could have important implications for the hydrological behaviour of supraglacial snowpacks.
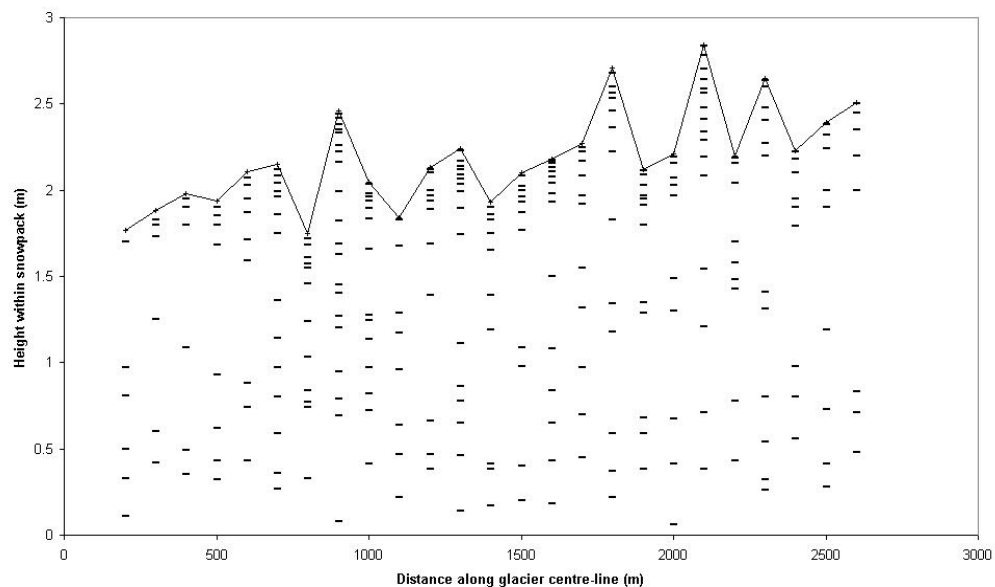
Figure 4.17: Ice layer occurrence through the snowpack depth across the glacier altitudinal range, measured by probing on 19th May 2003. - represents an ice layer; solid line represents the snowpack surface. A large number of ice layers are present at all locations and show a tendency to be concentrated in the upper ~0.5 m of the snowpack. Ice layers will have been formed by the melting and refreezing events identified in Figure 4.1.

4.3.4 Density

Density measurements taken throughout the melt season in 2004 (Figure 4.18) showed values of, on average, 560 ± 82 kg m^{-3}. Density varied with depth through the snowpack in each profile but there was considerable variability between profiles, making it difficult to pick out a consistent pattern. No clear evolution of density through time could be seen. The destructive nature of density measurements and the resulting necessity of taking repeat measurements at different locations make it difficult to separate temporal variations in density from spatial variations without multiple density profiles taken concurrently.

a)   b)

c)   d)
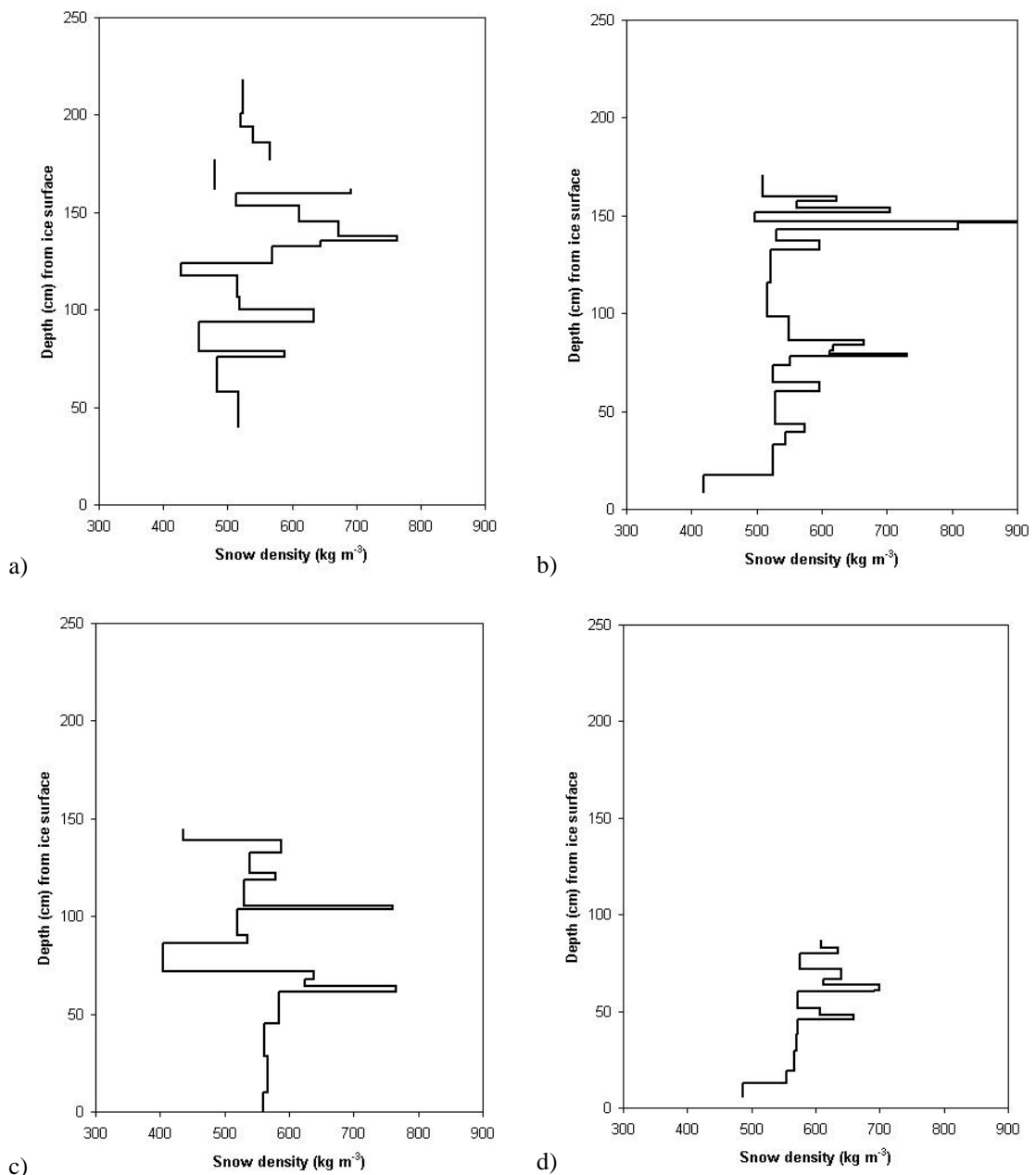
Figure 4.18: Snow density data for 2004, measured at L on a) 25th May, b) 19th June, c) 25th June and 6th July. Thin, high-density layers are ice layers. Mean density of snow containing no significant ice layers is 560 kg m^{-3} and no clear evolution of density through time can be seen.

4.4 WATER FLOW THROUGH THE SNOWPACK - QUALITATIVE OBSERVATIONS

Photographs are presented to illustrate patterns of dye movement observed in the snowpack at different points during each melt season. Qualitative dye injections confirm previous observations from non-glacial snowpacks that show water flow in snow to be highly heterogeneous (Gerdel, 1954; Wankiewicz, 1979; Marsh and Woo, 1985; McGurk and Marsh, 1995; Schneebeli, 1995; Kattelman and Dozier, 1999; Waldner et al., 2004). This heterogeneity, as described in section 2.2.2, may take three forms: interaction of percolating water with ice layers within the snowpack, influence of other textural horizons, and formation of preferential flow fingers (which may be related to spatially variable ice layer permeability, other stratigraphic boundaries, snow surface topography, or inherent flow instability). Each of these, to varying degrees, was observed in the snowpack at Haut Glacier d'Arolla, serving as a reminder that such heterogeneous flow features must be taken into account in the glacial context too. Observed patterns of dye flow in 2004 are described in sections 4.4.1 and 4.4.2 for vertical and lateral flow respectively. The role of preferential flow fingers is further investigated in section 4.4.3, in which image analysis is used to examine the proportion of snowpack volume through which flow takes place. Qualitative dye observations from the 2003 field season, which are fewer in number but useful in enabling comparison to flow patterns seen in 2004, are presented in section 4.4.4. Finally, conclusions regarding the nature of snowpack percolation as observed at Haut Glacier d'Arolla, the factors influencing flow patterns, and their relative importance are presented in section 4.4.5.

4.4.1 Observed patterns of vertical dye movement - 2004

In the earliest qualitative dye injection undertaken in 2004, on 16th May, excavation after 1½ hours showed much of the dye to be retained above ice layers just 10 cm below the snow surface (Figure 4.19). Elsewhere in the section examined, dye had passed these top layers and reached an ice layer 17 cm from the surface. Dye was observed on this ice layer even while the snow above it remained completely white, showing that dye reaching the ice lens further upslope was flowing forward along it. At one point, a plume of dye around 15 cm wide had passed below this ice layer at 17 cm depth to reach a maximum depth of 33 cm below the snowpack surface (Figure 4.19).
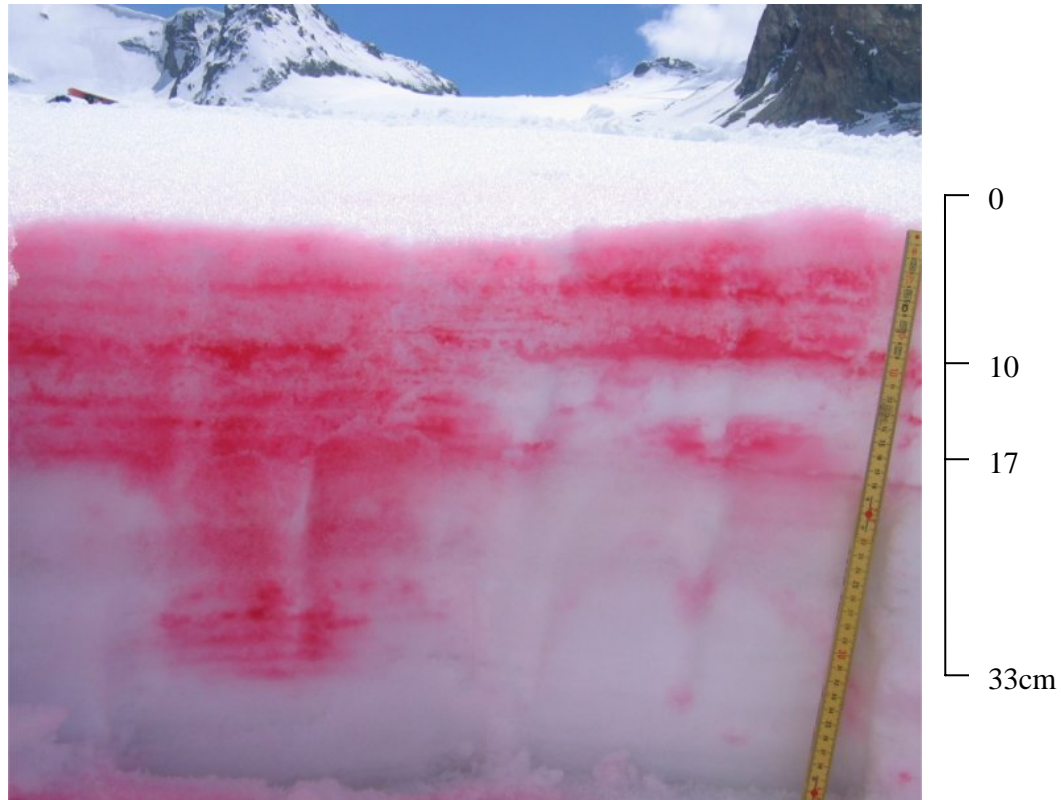
Figure 4.19: Percolation pattern at L on 16th May 2004, 1½ hours after dye injection, showing that much of the dye is retained above the ice layer at 10 cm below the snow surface but has also reached the ice layer at 17 cm depth to be retained there, and at one point has passed further downwards (to a maximum depth of 33 cm) in a plume ~15 cm wide. Scale to right of image indicates depths (cm) from the snowpack surface.

On 29th May, dye across a 1m-wide section had percolated to a major ice layer 22 cm from the snowpack surface after 45 minutes, with the darker pink appearance of snow above this ice layer indicating retention of the percolating meltwater (Figure 4.20). The area through which dye had percolated had a 'marbled' appearance, with pink areas unevenly interspersed with white, un-dyed snow. Upon closer inspection, dye percolation appeared to have taken place via multiple small (~1 to 2 cm in diameter) flow fingers spaced unevenly through the snowpack.

Thinner ice layers in the top 20 cm of snow showed some evidence of retaining percolating meltwater (Figure 4.21) but in general had not prevented flow reaching deeper. The passage of dye also picked out multiple horizontal lineations in the snowpack which had not been observed in un-dyed snow (Figure 4.21). These may be thin buried surface crusts or glazes formed by rain, melt or wind, or boundaries between snow layers, and may have had some slight effect on percolation.

Figure 4.20: Percolation pattern at L on 29th May 2004, 45 minutes after dye injection. Dye has percolated to a major ice layer 22 cm from the surface and is retained above it. Dye percolation has taken place via multiple small (~1 to 2 cm diameter) flow fingers, giving the dyed area a 'marbled' appearance.

Figure 4.21: Close-up of small ice layers and other horizontal lineations in the dyed area of Figure 4.20 (29th May 2004). These are likely to have had some effect on dye percolation but in general had not prevented flow reaching deeper.

A qualitative surface injection on 7th June showed percolation taking place via large flow zones around 20 cm wide, with the intervening snow largely untouched by dye (Figure 4.22, taken 1 hour 15 minutes after dye injection). The location of flow zones was not related to depressions on the snowpack surface and no obvious cause for their placement could be seen. When flow reached the large ice layer now at c.27 cm from the snowpack surface (due to new snowfall in the preceding week), it passed beyond it without significant lateral diversion to reach a maximum depth of around 40 cm. Within these larger zones, flow appeared fairly even. When the snowpit was excavated 0.5 m further back 30 minutes later, the same flow pattern was seen.
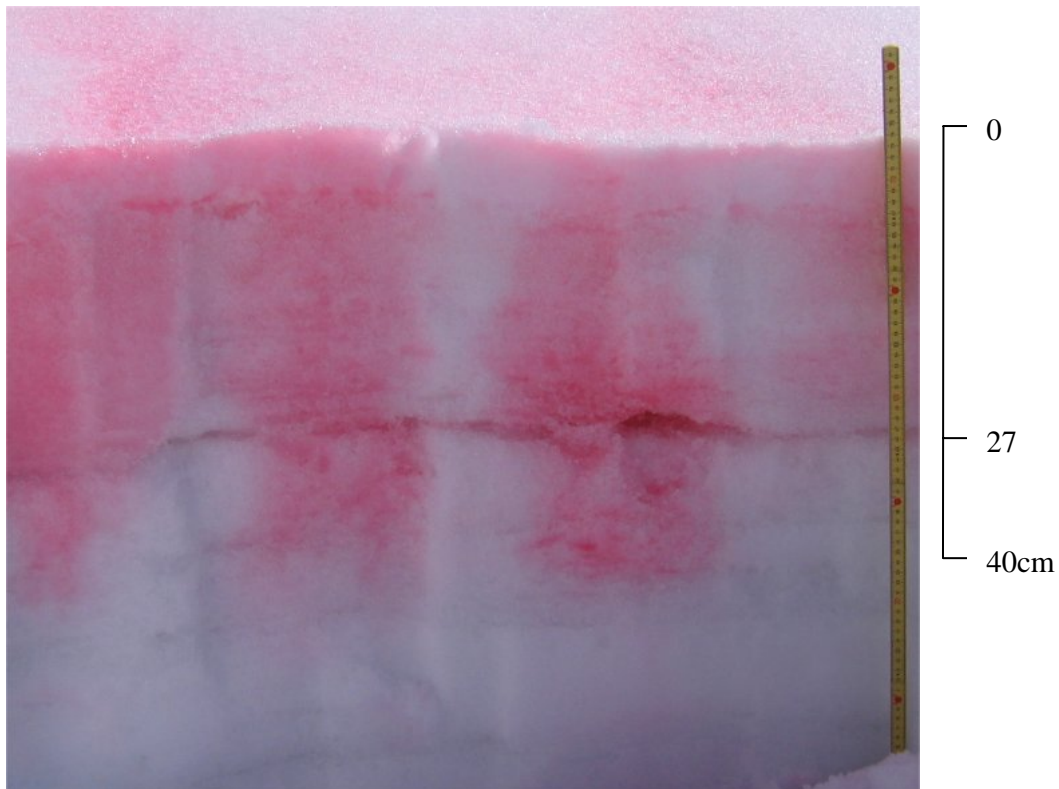
Figure 4.22: Percolation pattern at L on 7th June 2004, 1hr 15mins after dye injection. Dye percolation has taken place via large flow zones around 20 cm wide but no obvious cause for the existence of these flow zones (e.g. surface topography) could be seen. The ice layer at 27 cm depth has had no significant effect on the flow pattern and the flow zones continue beneath it.

Figure 4.23 shows the pattern of dye percolation observed on 16th June two hours after dye injection. Dye had percolated fairly evenly through the top 21 cm of snow despite the presence of two large ice layers. Beneath that, flow again proceeded via multiple small flow fingers while a large proportion of the snowpack remained untouched by dye. Flow was retained above the ice layers at 66 and 72 cm depth but also passed beyond to reach a maximum depth of c.110 cm. The majority of colour remained in the top 20 cm of the snowpack.

Figure 4.23: Percolation pattern at L on 16th June 2004, 2 hours after dye injection, showing fairly even percolation through the top 21 cm of the snowpack despite the presence of two large ice layers and, beneath that, further percolation to a maximum depth of ~110 cm via multiple small flow paths. Ice layers at 66 and 72 cm depth have retained some dye but allowed some to pass.

Following a surface dye injection for fluorometric detection on 21st June, dye was seen flowing downslope along an ice layer just 10 cm below the snowpack surface even 1.5 hours after injection (Figure 4.24). This layer is believed to have been located close to the snowpack surface before burial by a few centimetres of new snow on 20th June. Within the next 1.5 hours the pink colour near the surface faded until it was barely visible. This ice layer was seemingly of low permeability, but allowed dye to pass through it slowly (alternatively, the fading of dye near the surface may have been caused by dilution by subsequent meltwater). In a previous surface injection at the same location on 18th June, no such influence of this near-surface ice layer had been observed, but temporary cold temperatures and refreezing of water in the layer may have lowered its permeability.

Figure 4.24: Retention of dye above a near-surface ice layer on 21st June 2004 (~1.5hrs after injection), believed to be triggered by refreezing of the ice layer in cold weather. Photograph looks in the upglacier direction. Ruler in foreground is 1m in length.

On the same day (21st June), a qualitative dye injection excavated after approximately 4 hours (Figure 4.25) showed that dye had successfully percolated beyond near-surface ice layers but was largely retained above an ice layer c.35 cm from the surface. Percolation beyond that ice layer was confined within one zone which reached a maximum depth of 90 cm from the snow surface. Within this zone flow took place via small flow fingers and generally passed through further ice layers with minimal lateral diversion.
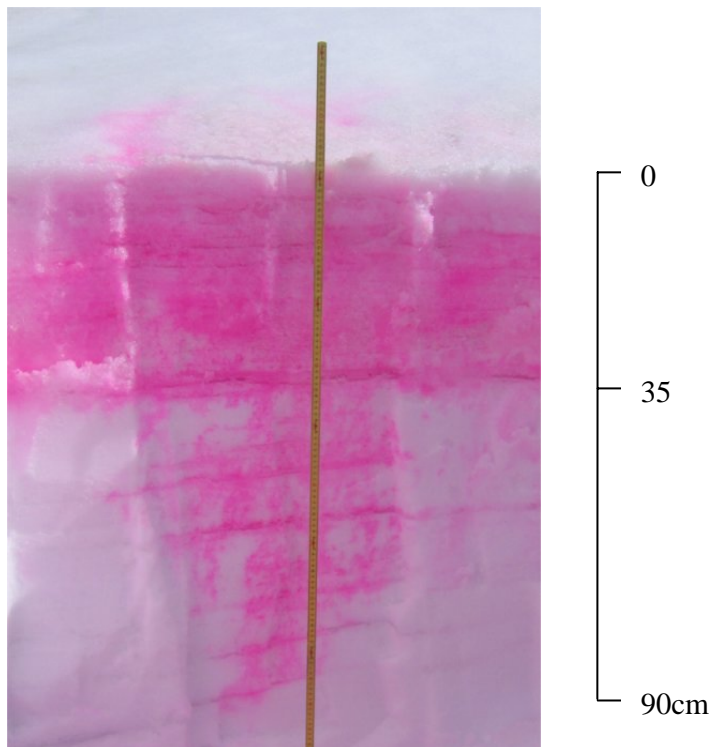
Figure 4.25: Percolation pattern at L on 21st June 2004, 4 hours after dye injection, showing dye retention above the ice layer at 35 cm depth and further percolation to 90 cm depth via small flow fingers within one zone, within which dye successfully passes through further ice layers.

On 27th June, approximately 1.5 hours after dye injection, small flow fingers around 1 cm in diameter were the primary mode of flow observed, carrying flow at isolated locations as deep as 60 cm while other dye was retained above ice layers at 20 to 30 cm depth (Figure 4.26).
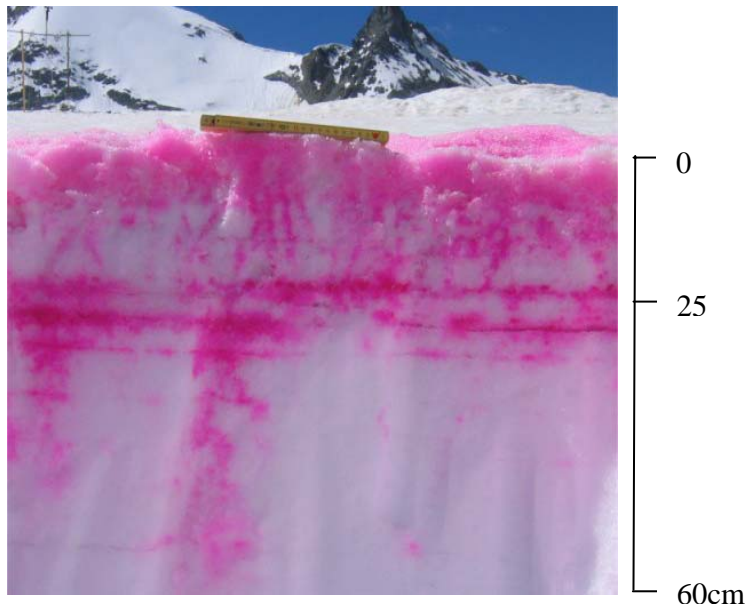
Figure 4.26: Percolation pattern at L on 27th June 2004, 1½ hours after injection, showing small flow fingers carrying flow at isolated locations as far as 60 cm depth and retention by ice layers elsewhere.

In late July 2004 qualitative dye experiments were undertaken at the middle snow study site, where the remaining c.70 cm of snow had been exposed to prolonged melt. Dye percolation on 25th July (Figure 4.27, c.2.5 hours after dye injection) was visibly more homogeneous than in previous experiments, yet an ice layer ~30 cm above the ice surface continued to retain dye above it and allow continued downwards flow only at certain points.
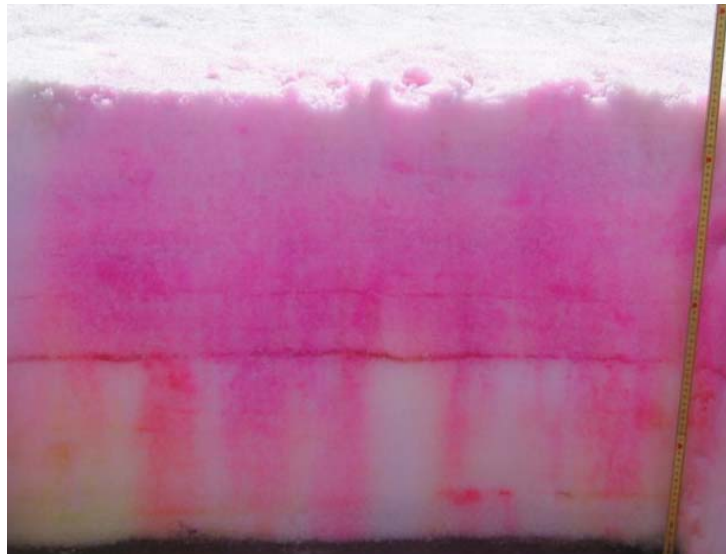
Figure 4.27: Percolation pattern at M on 25th July 2004, 2½ hours after dye injection, showing more homogeneous percolation than in previous experiments. The ice layer 30 cm above the ice surface, however, continues to retain dye above it and allow continued downwards flow only at certain points.

4.4.2 Observed patterns of lateral dye movement - 2004

Excavations into the sidewall of snowpits showed the distribution of dye movement in the downslope direction over sloping ice layers in the snowpack. Experiments on 29th May and 24th and 27th June 2004 illustrate typical lateral flow patterns and their evolution through time.

On 29th May, when excavated 2.5 hours after injection, dye was observed to have flowed almost 80 cm forward from the front of the injection area along the highest ice layer in the snowpack, 21 cm below the surface (Figure 4.28). Pink colouring beneath this ice layer to 60 cm in front of the injection area indicated that it was allowing some water to pass through it while that trapped above flowed forwards downslope. Dye in this way also reached ice layers at 31, 38 and 52 cm depth, again being carried forward to between 60 and 80 cm in front of the injection area. No dye was seen more than 60 cm below the snow surface. In this instance, downglacier lateral flow along ice layers was therefore more rapid than vertical percolation.
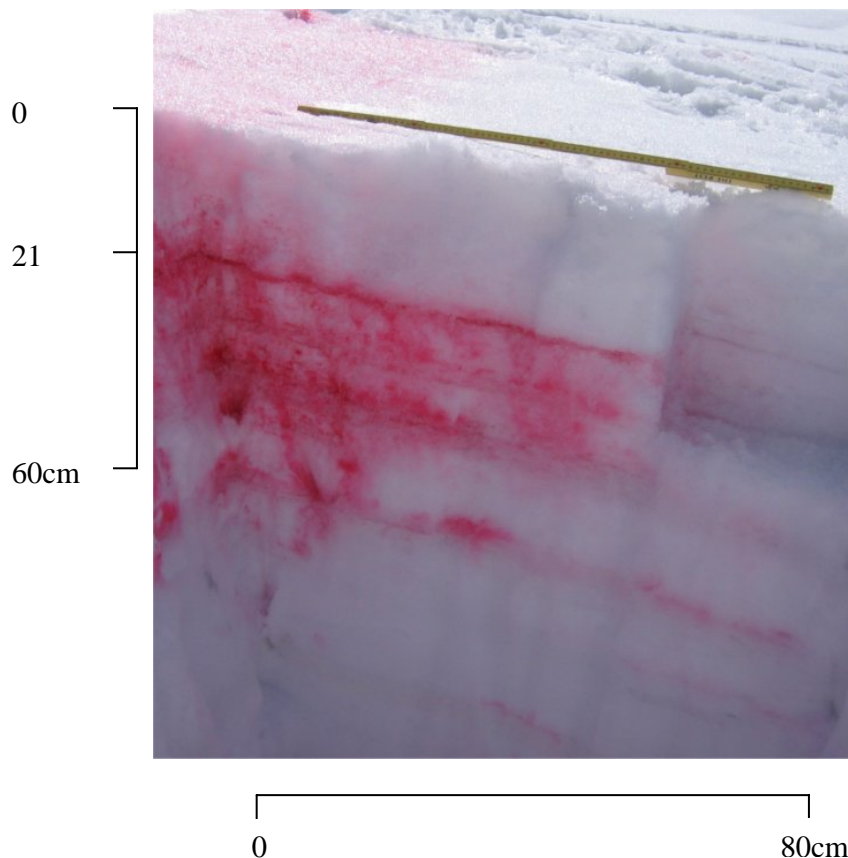
Figure 4.28: Downslope dye movement along ice layers at on 29th May 2004, 2½ hours after dye injection, showing that downglacier lateral flow (reaching up to 80 cm in front of the injection area) is taking place faster than vertical percolation (which reaches only 60 cm below the snowpack surface).

Almost one month later, on 24th June, excavation after 2 hours (Figure 4.29a) showed dye percolation to greater depth (having reached the base of the c.1.3 m-deep snowpack within 2 hours) but still indicated significant downslope diversion of dye by ice layers. Dye could be seen along the highest ice layer in the snowpack (10 cm from the snow surface) to 1.8 m in front of the injection area. Further ice layers at greater depth also diverted percolating dye forward, such that dye did not percolate directly downwards beneath the injection area but instead first reached the base of the snowpack around 85 cm in front of the injection area. Further excavation one hour later (3 hours after injection; Figure 4.29b) showed more dye towards the right of the section, indicating that more water was percolating directly downwards rather than being diverted forwards along the ice layers. Correspondingly, dye now reached the base of the snowpack just 37 cm in front of the injection area.

a)   b)

1.8m   0.85   0   1.2m   0.37   0
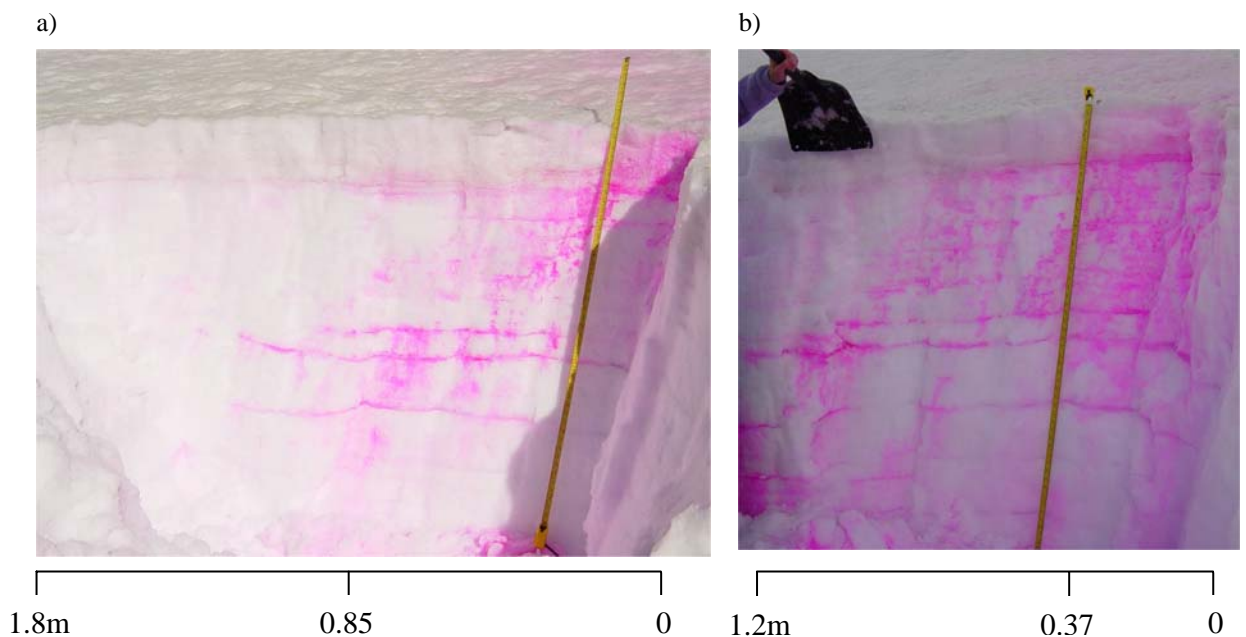
Figure 4.29: Downslope dye movement along ice layers at L on 24th June 2004, a) 2 hours and b) 3 hours after dye injection. The area of dye injection on the snow surface can be seen in the top right of each picture; the glacier surface and ice layers within the snowpack slope gently downwards towards the left hand side of the picture. Diversion by multiple ice layers can be seen to cause dye to reach the snowpack base not directly beneath the injection area, but some distance downglacier.

Excavations 2 and 4 hours (Figures 4.34a and 4.34b respectively) after an injection on 27th June showed a similar pattern, with the combined effect of obstruction and diversion by multiple ice layers of varying sizes causing percolation through the snowpack to take place in a stepped fashion, reaching the base of the snowpack between 0.3 and 2 m downglacier from the injection area.

a)   b)
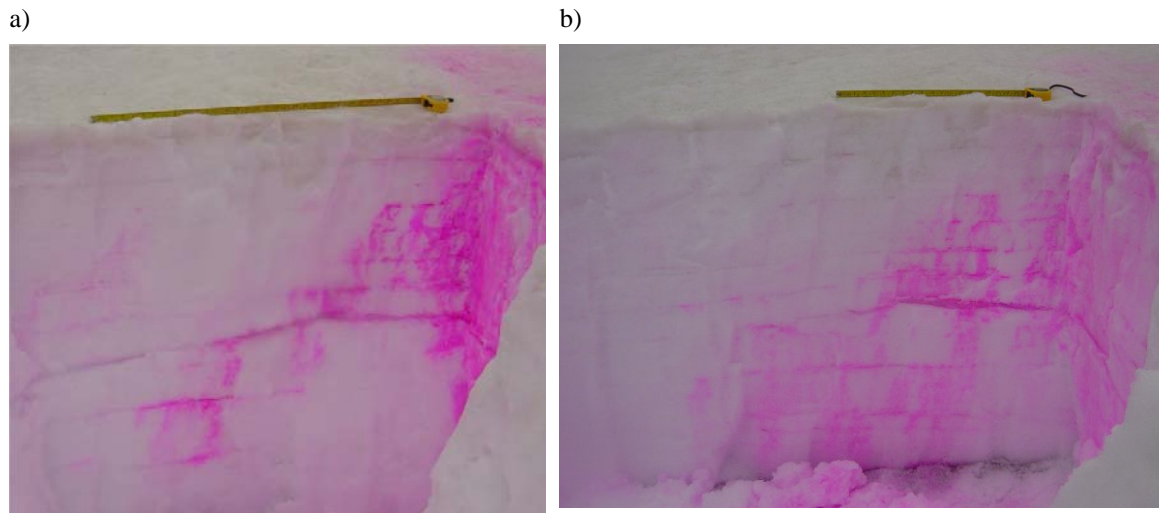
Figure 4.30: Downslope dye movement along ice layers at L on 27th June 2004, a) 2 hours and b) 4 hours after dye injection. The area of dye injection on the snow surface can be seen in the top right of each picture; the glacier surface and ice layers within the snowpack slope gently downwards towards the left hand side of the picture. Yellow ruler = 1 m. As in Figure 4.29, diversion by multiple ice layers carries dye forwards to reach the snowpack base downglacier of the injection area.

4.4.3 Image analysis – preferential flow area

In order for the effect of preferential flow on runoff to be better understood, more quantitative information is needed about the degree to which preferential flow channels alter the concentration of flux within the snowpack (section 2.2.2.3). Multi-compartment lysimeter data can provide information about flux variation directly (Marsh and Woo, 1995); alternatively, observations of the area occupied by flow fingers can be used following Wankiewicz (1979) (Equation 2.2) to calculate the amount by which flux within flow channels is amplified relative to uniform flow. The area occupied by flow fingers in the snowpack at Haut Glacier d'Arolla in 2004 was investigated by analysis of digital photographs of qualitative dye tracing experiments as described in section 3.6.3.1. In this way, quantitative information is extracted from a technique that was initially qualitative.

The 14 images that were analysed are shown in Figure 4.31, and the calculated percentage flow areas are presented in Table 4.1. Values vary quite widely, as would be expected given the natural heterogeneity of water percolation through snow. In addition, variation may be related to flux conditions at the time of dye injection and in previous days or to snow and ice layer properties at different locations. No significant evidence of evolution through time can be seen (Figure 4.32); as shown in photographs presented previously (Figures 4.19 to 4.27), dye flow patterns were characterised by great heterogeneity for the duration of work at L, with more homogeneous flow only seen at M in late July.
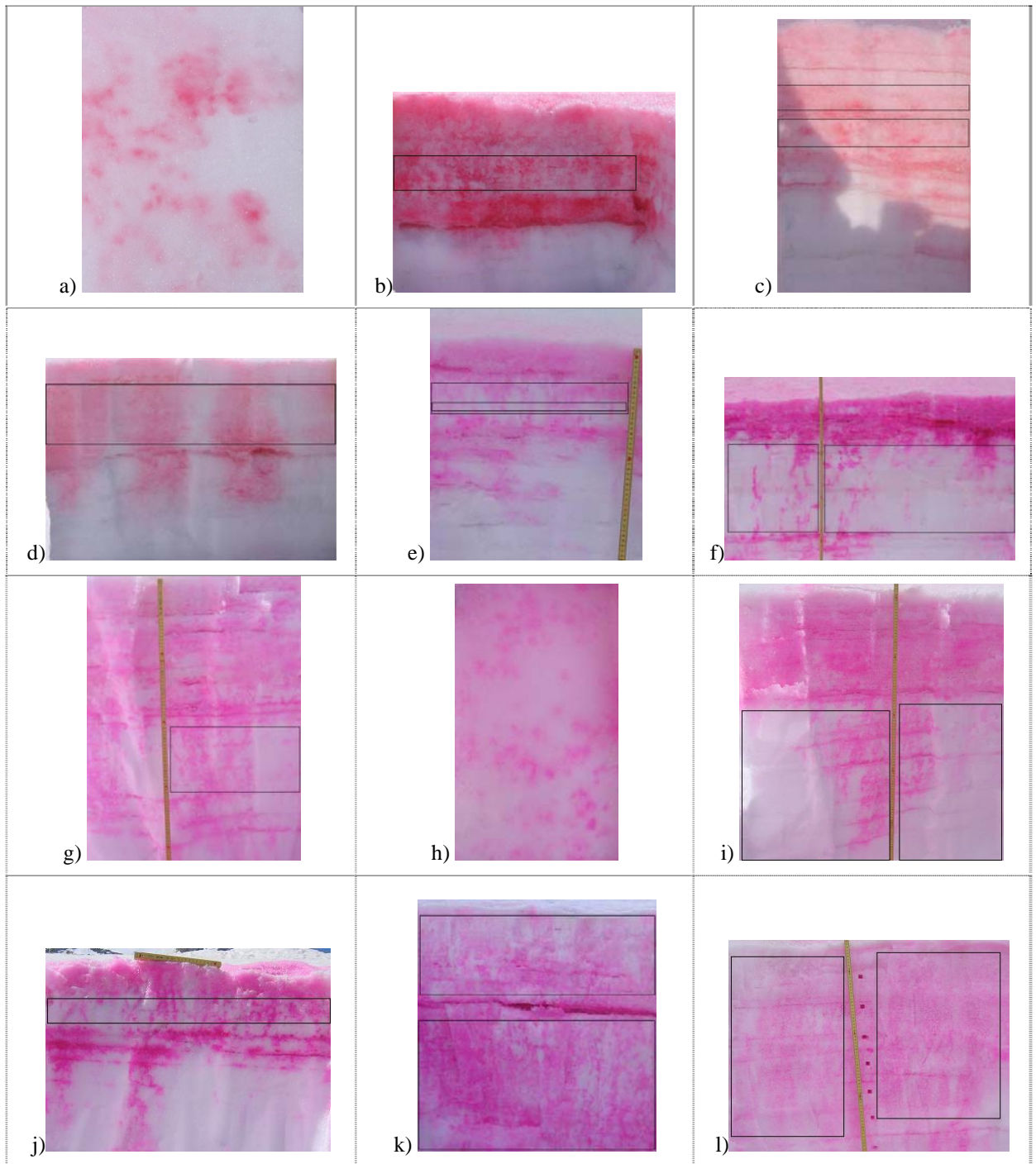
Figure 4.31: Photographs used for image analysis of preferential flow area. Black rectangles indicate the sub-sections of images that were selected for analysis in order to omit the influence of ice layers on flow. Images a) and h) are viewed from above; all others are pit walls. For each image, sub-section results were combined to find an average value. The dates on which each photograph was taken are shown in Table 4.1.

Overall, values for preferential flow area ranged between 15 and 52 percent, and while errors in image classification will cause some inaccuracy, this gives a good indication of the approximate snowpack volume through which preferential flow may take place. From Wankiewicz (1979; Equation 2.2), a preferential flow area of 15 to 52 percent corresponds to amplification of surface flux by a factor of between 1.9 and 6.6. The implications of this for runoff are considered in section 6.3.4 using the predictions of a physically-based model of water percolation through snow.

Table 4.1: Percentage preferential flow areas calculated by image analysis.

Date	Figure	Percentage preferential flow area
16/05/2004	4.37a	23
29/05/2004	4.37b	27
30/05/2004	4.37c	32
07/06/2004	4.37d	52
12/06/2004	4.37e	37
16/06/2004	4.37f	15
18/06/2004	4.37g+h	20
21/06/2004	4.37i	22
27/06/2004	4.37j	29
14/07/2004	4.37k	18
21/07/2004	4.37l	25
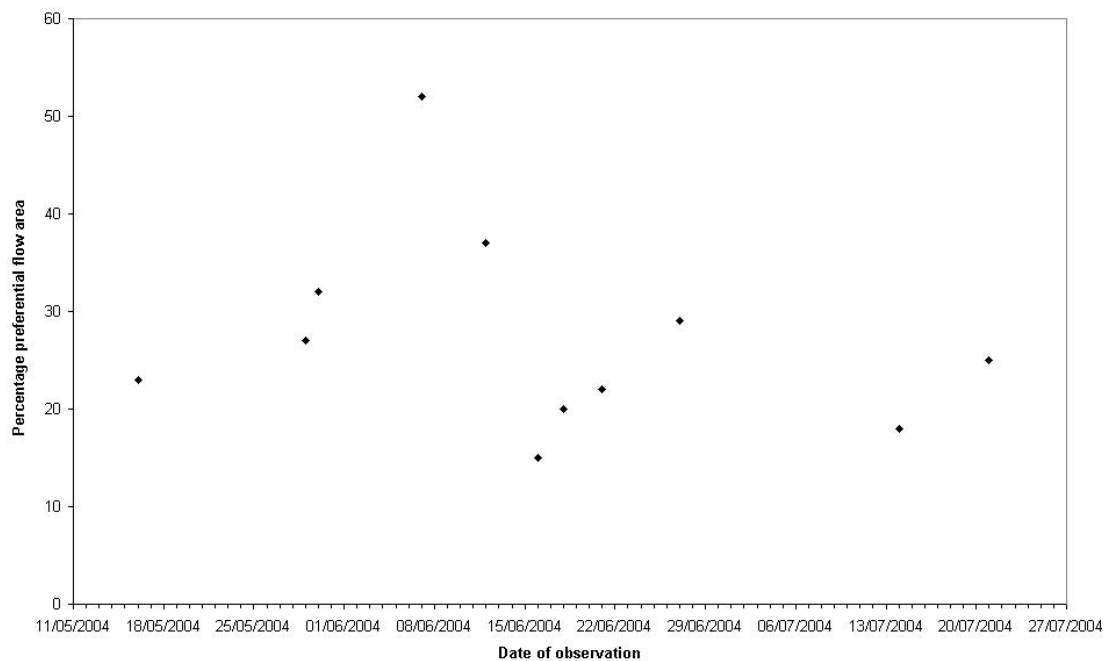
Figure 4.32: Variation in percentage preferential flow area derived from image analysis with time. No significant evidence of a change in percentage preferential flow area through time is seen.

4.4.4 Water flow through the snowpack - qualitative observations 2003

Figures 4.33 and 4.34 illustrate patterns of dye movement observed in the snowpack during the 2003 melt season. Dye percolation was seen to be different from that in 2004 in several ways. Surface dye injections in late May/early June 2003 showed percolation taking place in a very uniform manner, with little evidence of preferential flow or influence of ice layers (Figure 4.33, taken on June 1st). On June 13th (Figure 4.34), when pronounced suncup forms had become established on the snowpack surface, dye percolation was organised in fairly large (c.10-20 cm wide) zones, with flow within these zones remaining fairly homogeneous. These zones of preferential flow appeared to be situated beneath topographic lows on the suncupped snowpack surface (Figure 4.34), suggesting that snow surface topography (by enhancing melt in hollows due to radiation reflections and/or by lateral diversion of meltwater by surface slope) was playing a role in controlling the distribution of percolating meltwater within the snowpack, as suggested in section 4.3.2 above.

In general, few solid ice layers remained in the snowpack in June 2003, but those occurring near the base of the snowpack were observed to play a continuing role in inhibiting dye percolation and diverting flow.

Figure 4.33: Homogeneous flow pattern seen at L on 1st June 2003.
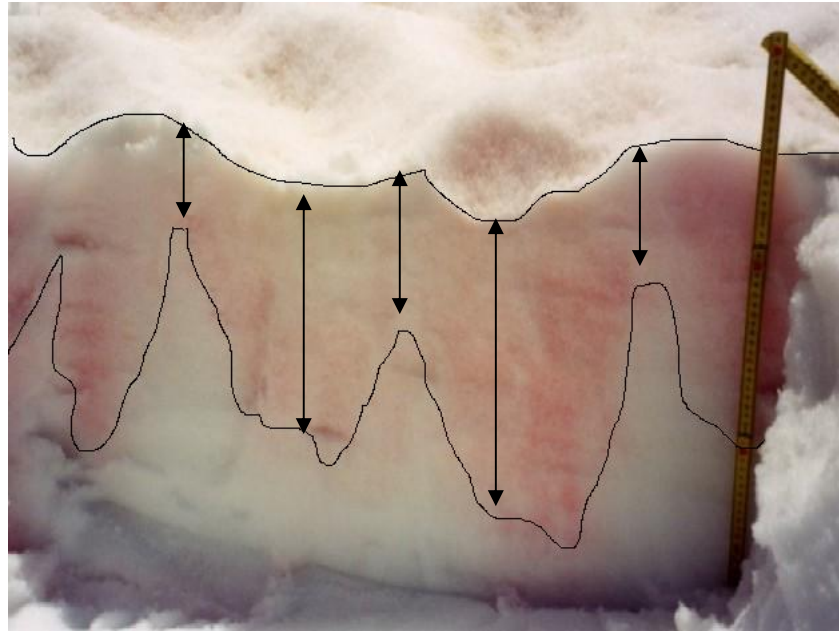
Figure 4.34: Preferential flow zones beneath suncup hollows (13th June 2003). Arrows indicate the different depths to which dye has percolated beneath suncup topographic highs and lows. Photograph by C. Colls.

4.5 CONCLUSIONS: NATURE OF SNOWPACK PERCOLATION AT HAUT GLACIER D'AROLLA

Observations of meltwater inputs (section 4.2), snowpack physical properties (section 4.3) and dye flow patterns (section 4.4) are drawn together here to summarize the nature of water percolation through the snowpack at Haut Glacier d'Arolla, the factors influencing this, and the relative importance of these factors. Qualitative dye injections showed percolation to take place in a highly heterogeneous manner. Three forms of heterogeneity - interaction of percolating water with ice layers, influence of other textural horizons, and formation of preferential flow fingers – are considered in turn.

4.5.1 Influence of ice layers

The many ice layers that were present in the snowpack at Haut Glacier d'Arolla (section 4.3.3) were observed to have a complex effect on dye movement. Previous studies (section 2.2.2.3) have identified three ways in which ice layers affect water movement through snow, namely the formation of static internal ponds above dips in ice layers, dynamic detention of flowing water, and diversion of flow along sloping ice layers (Langham, 1974a, b, c), and each of these effects was observed during qualitative dye tracing experiments.

Ice layers exhibited variable permeability as proposed by Langham (1974a), who showed theoretically that the size of veins between ice crystals, and therefore ice layer permeability, would respond continuously to changing temperature, pressure, and dissolved air concentration around the layer. A marked example of this was seen following an injection at L on 21st June (Figure 4.24), when a near-surface ice layer caused temporary retention of dye and flow downslope along the ice layer due to temporary cold temperatures, partial refreezing, and decreased permeability of the layer. In a previous experiment on the same area of the snowpack surface, under warmer conditions, this ice layer had no such effect on dye percolation.

In Figures 4.19, 4.20, 4.23, 4.25, 4.26 and 4.27 ice layers can be seen impeding the downward movement of dye, with continued downward flow taking place only from limited points. In Figure 4.25, taken on 21st June, the vast majority of dye is retained above a major ice layer situated 35 cm from the snow surface even 4 hours after dye injection, suggesting that ice layers may cause a significant delay in runoff. Spatial variability in ice layer permeability results in concentration of further downward propagation of flow within only a fraction of the snowpack volume, with multiple small flow fingers either spread throughout the snowpack as in Figures 4.20, 4.23 and 4.26 or concentrated within larger zones as in Figure 4.25. Following Equation 2.12 (Colbeck, 1972), this concentration of flux within the snowpack volume may have important implications for water flow rates; this is considered further in section 6.3.4 using the predictions of a physically-based model of water percolation through snow.

In the sloping supraglacial snowpack at Haut Glacier d'Arolla the downslope advection of percolating meltwater along ice layers appears to be widespread. In the first fluorometric experiment of the 2004 season, on 29th May, dye injected on the snowpack surface was seen to emerge in a pit 3m downglacier not at the snow-ice interface but along ice layers between 1.2 and 1.7 m above the ice surface, in plumes 10-15 cm wide (Figure 4.35). On 8th June 2004, in an experiment at the same location, dye emerged along ice layers closer to the snowpack base, and on 12th June dye again reached closer to the snowpack base. In all later experiments dye was observed to arrive at the pit wall in the basal saturated layer, enabling detection using the borehole fluorometer. During the early melt season, ice layers in the snowpack were clearly causing significant lateral redistribution of percolating meltwater, and this effect decreased through time. This effect was most clearly shown in excavations down-glacier of surface dye injections (Figures 4.29 and 3.30), which showed percolation taking place in a stepped fashion and arriving at the base of the snowpack not directly beneath but some distance downglacier from the surface injection area.

As the melt season progressed, ice layers in the remaining snowpack continued to play a role in retaining percolating meltwater, as seen in Figure 4.27, taken on July 25th 2004. This is in accordance with stratigraphic observations (section 4.3.3) that showed that ice layers near the base of the snowpack often remain solid in appearance throughout the melt season, rather than disintegrate in the presence of liquid water as suggested by Gerdel (1954). Notably however, there were fewer ice layers left in the snowpack later in each melt season as those closest to the surface had melted out during ablation, and their net effect is therefore expected to decrease. As ice layers occurred more frequently near the top of the snowpack (section 4.3.3), their influence in retaining percolating meltwater will have decreased most quickly as the upper snowpack ablated, introducing a non-linearity to the snowpack's effect on runoff that has not previously been considered.

Figure 4.35: Emergence of dye from a surface injection on 8th June along ice layers between 1.2 and 1.7 m above the glacier ice surface. Multiple individual plumes of dye emerging along the ice layer at 1.2m from ice surface have merged together to form a continuous line of pink.

4.5.2 Influence of stratigraphic horizons

On occasion, percolating dye was also observed to stop its downward motion and spread horizontally where no ice layer was apparent. Stratigraphic variations in texture and density within the snowpack are expected to impede, accelerate, or have no influence on water

percolation as described by Wankiewicz's (1979) FINA model; although such layer boundaries could not be identified by eye as the cause of dye retention in this case, they are expected to be responsible. Observations of these effects at the field site were rare, possibly due to the fairly advanced stage of metamorphism of the snowpack and its relative homogeneity (with the exception of ice layers; stratigraphic investigations showed the snowpack to be composed largely of rounded melt grains throughout both field seasons (section 4.3.3)). As a result, textural and density variations may be disregarded as an important influence on meltwater runoff through the summer snowpack at Haut Glacier d'Arolla in these years.

4.5.3 Preferential flow patterns

Qualitative dye experiments showed preferential flow to take place at a range of scales, from the 1cm-wide flow fingers in Figures 4.23 and 4.26 to the 20 to 40 cm-wide preferential flow zones shown in Figures 4.22 and 4.25. The proportion of the snowpack occupied by preferential flow fingers varied widely between 15 and 52 % (section 4.4.3). The controls on this organization of flow are hard to identify. In some cases it may result from the variable permeability of ice layers above; in others the topography of the snowpack surface may play a role in concentrating flow, as suggested by Figure 4.34. In other cases no obvious control is apparent. Whatever the cause, preferential flow results in the concentration of flux within some areas of the snowpack, with the potential to therefore increase permeability in those areas and make runoff correspondingly more efficient. The observed patterns of preferential flow, together with dye retention above ice layers, also make it clear that percolating meltwater is moving through the snowpack at a range of rates and therefore introducing an element of dispersion to the meltwater wave, which may play a role in attenuating peak flux values in the runoff hydrograph.

Chapter 5. Supraglacial snowpack hydrology at Haut Glacier d'Arolla - quantitative measurements of water flow through the snowpack

5.1 INTRODUCTION

A key aim of this study was to collect quantitative information about snowpack hydrological behaviour that can inform future modelling studies, and results and analyses from quantitative investigations of snow hydrology are presented in this chapter. Dye tracing experiments with fluorometric detection of dye concentrations were the primary source of quantitative information about water flow both vertically through the snowpack depth (section 5.2) and laterally through the basal saturated layer (section 5.4). Lysimeter discharge records provided additional information about water percolation through the snowpack (section 5.3). The operation of snow hydrology at the catchment scale was also investigated (section 5.5), as it is the net effect of the snowpack across a wider area of the supraglacial drainage system that will control water discharge into the englacial drainage system. Data considering the wider importance of supraglacial snowpack hydrology - assessing the links between changing snowpack hydrological behaviour, the rest of the glacier hydrological system, and ice dynamics - is presented and analysed in Chapter 7.

5.2 QUANTITATIVE DYE TRACING TESTS ON THE SNOWPACK SURFACE

This section first presents results and analyses of quantitative surface dye injections in 2003, considering dye return curve characteristics (section 5.2.1) and quantitative parameters derived from return curves (section 5.2.2 – 5.2.5). Results from quantitative dye injections in 2004 are then considered, following the same order (section 5.2.6 – 5.2.10). Difficulties in reliably detecting the dye pulse emerging in the basal saturated layer (discussed in section 3.6.4.2) resulted in the results of around half of the dye experiments being undetected or unreliable. A full chronological list of all dye injections carried out for quantitative detection during this project is provided in Appendix C, and the success rate of this technique, and the possible reasons for experiment failure, are discussed. Dye return curves from successful experiments were analysed with the aim firstly of describing the characteristics of water percolation through the snowpack at Haut Glacier d'Arolla, and secondly of identifying any changes in the hydrological behaviour of the snowpack as the melt season progressed. Quantitative dye tracing data exhibited significant variability that in all cases can be attributed to the natural heterogeneity of flow through snow (as was clearly illustrated by qualitative dye observations in section 4.4) together with the varying flux conditions and snowpack characteristics under which dye injections took place. Despite

this, it is possible to identify trends in snowpack hydrological behaviour that are not the result of random variability or differing flux conditions, but reflect a temporal change in the snowpack's mediating influence on runoff.

2003 field season

Quantitative surface injections in summer 2003 yielded a total of 13 useful return curves, obtained between 6th June and 5th July. Due to the rapid depletion of the snowpack at L only two successful return curves were obtained there before shallow snow depths made further dye tracing work meaningless and work was moved further upglacier. One useful return curve was obtained at M before further work (from 21st June until 5th July) was concentrated at U, where snowcover persisted longest. Experiments at U were carried out in 5 different snowpits, such that the 11 curves obtained there do not reflect snow depths consistently decreasing through time nor consistent basal flow conditions. Surface melt fluxes at the time of dye injections varied randomly between experiments, making the influence of flux magnitude in influencing percolation rates difficult to distinguish. As a result of these inconsistencies in experiment location and flux conditions, and also because returns were obtained across a period of only 15 days, the results obtained at U in 2003 are of limited use for investigating the evolution of snowpack hydrology with time through the melt season. However, they provide information about several aspects of snowpack hydrological behaviour at the time of each dye injection.

5.2.1 Nature of water flow: dye return curve shape and timing

A number of variations on the basic surface dye injection set-up were developed in 2003 in order to investigate specific aspects of snowpack behaviour (Chapter 3.6.4); these individual daily experiments are considered separately (section 5.2.1.1) before being brought together to summarise the general principles of snow percolation which they reveal, and to investigate possible trends through time (section 5.2.1.2).

5.2.1.1 Individual experiments

The two return curves obtained at L in early June 2003 exhibited rapid dye recovery and low dispersion of the dye pulse, with peak dye concentration after 2.01 hours on 6th June (snow depth 1.25 m) and after 2.17 hours on 10th June (snow depth 0.95 m) (Figure 5.1). The return curve for 6th June in particular was highly peaked (total dye recovery within ~4 hours) and showed little evidence of a trailing limb caused by dye moving slowly through the snowpack. This efficient transmission of dye through the snowpack can possibly be attributed to the relatively shallow snow depth, lack of ice layers, and advanced state of snow metamorphism following rapid melt in the preceding weeks (section 4.3). However, it could also be a result of the higher water flux added to the snowpack with dye during these early injections, which used more than twice the water of later experiments.
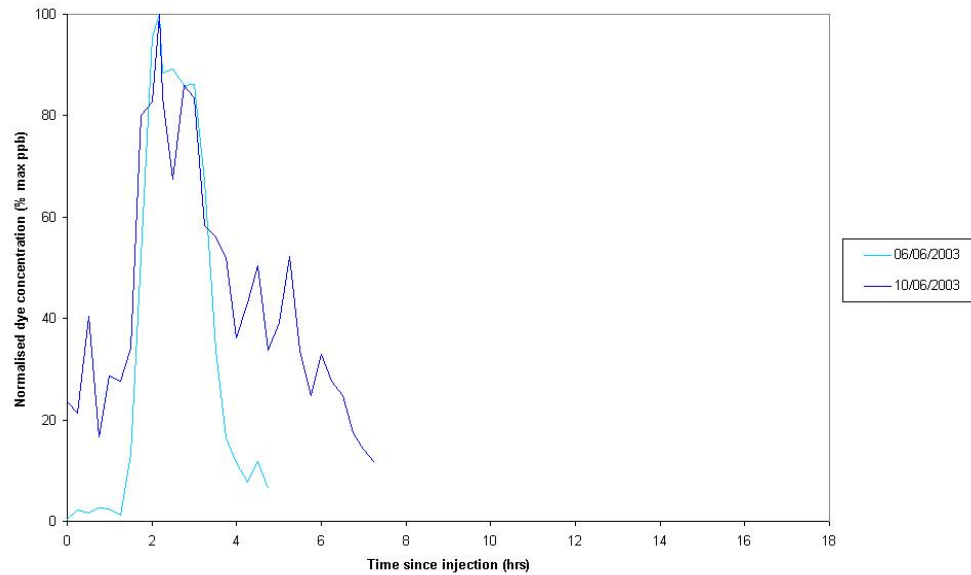
Figure 5.1: Dye return curves from L, 2003, through snow depths of 1.25m (6th June) and 0.95 m (10th June. In both cases peak dye concentration reaches the fluorometer quickly (in around 2 hours) and the return curves are peaked.
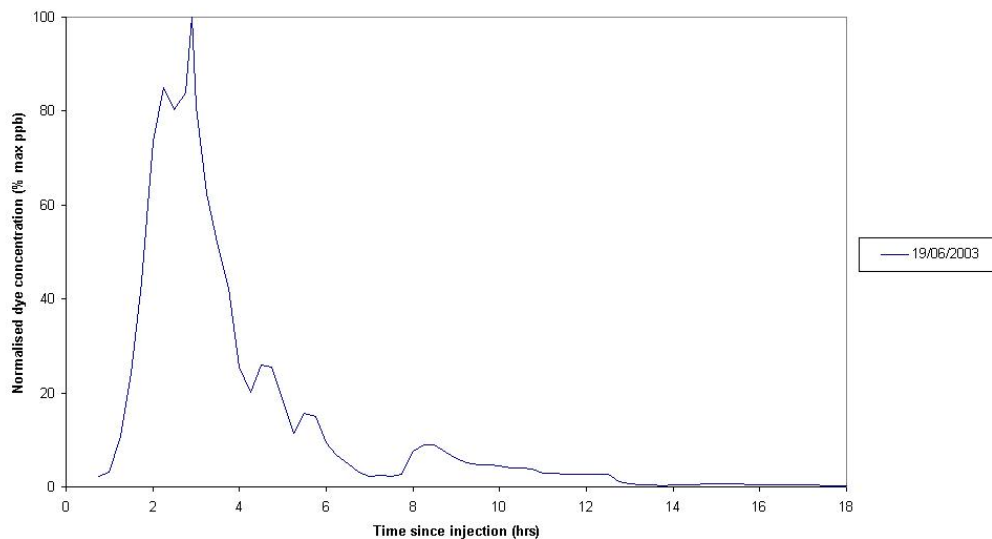
Figure 5.2: Dye return curve from injection at M, 2003, through a snow depth of 0.65m. Peak dye concentration is detected quite quickly (after 2.9 hours) and the curve is highly peaked, with only a very low magnitude trailing limb.

The single return curve obtained at M (Figure 5.2), on 19th June 2003, also indicated efficient meltwater transmission through the ~0.65 m-deep snowpack. The return curve has a peaked form and only a low magnitude trailing limb, and peak dye concentration is detected after 2.9 hours.

The first successful quantitative dye tracing experiment carried out at U in 2003 involved simultaneous injections of rhodamine WT and fluorescein onto the snowpack surface at distances of 3.5 - 4.0 m and 7.5 - 8.0 m upglacier from the fluorometer respectively, on snow depths of approximately 1.10 m (21st June 2003). With the assumption that

percolation through the snowpack will take place in approximately the same manner in each case, any difference in the resulting return curves can be attributed to the flow of water in the basal saturated layer between the two injection sites. The return curves for rhodamine and fluorescein were almost identical (Figure 5.3), indicating that flow along 4 m of the basal saturated layer did not impart any significant additional delay or dispersion to the fluorescein return. The agreement between the curves also provides confidence in the reliability of the dye tracing technique.

Return curves from this experiment at U were more delayed and dispersed than those for previous experiments at L and M, with peak dye concentration detected after 4.53 and 5.71 hours for rhodamine and fluorescein respectively and significant quantities of dye still passing the fluorometer 12 hours after injection (Figure 5.3). There is therefore some indication of spatial variation in snowpack hydrological behaviour, with lower altitude regions becoming efficient in transmitting water at an earlier date. Due to differing flux volumes used in dye injections, however, this trend cannot be further verified here.
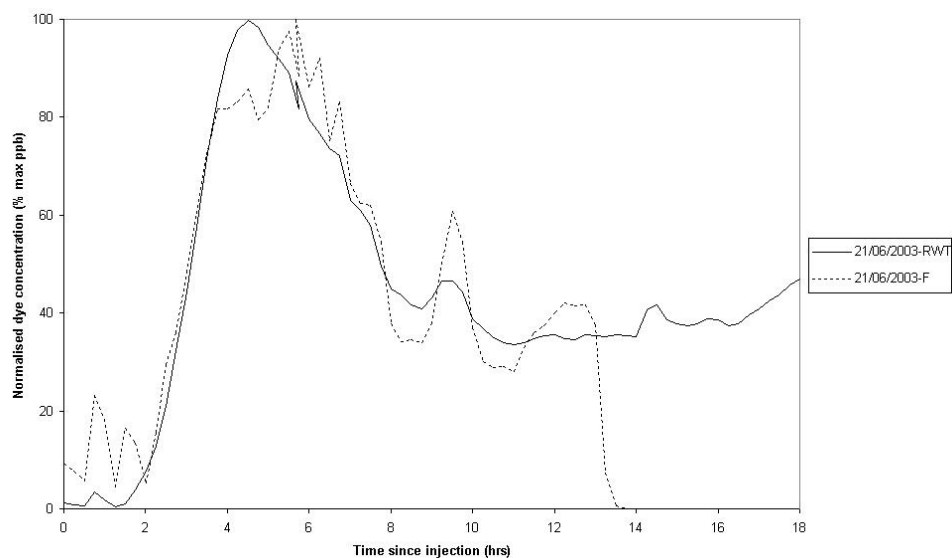
Figure 5.3: Dye return curves from simultaneous surface injections at different distances upglacier from detection point at U, 21st June 2003 (snow depths c. 1.10 m). The strong match between the curves indicates that the greater flow distance in the basal saturated layer for the fluorescein injection was not sufficient to alter the pattern of runoff. The curves here are notably more delayed and less peaked than those in Figures 5.1 and 5.2.

The experiment on 23rd June 2003 undertook simultaneous injections of fluorescein on the natural snowpack surface and rhodamine WT on an area of the snowpack that had been excavated to shallower depth. This was designed to allow consideration of the effect of differing snow depth on runoff, with both injections taking place under the same flux conditions in order to rule out flux variations as a cause of differing runoff. A clear difference in the timing and form of the resulting curves could be seen (Figure 5.4). The

rhodamine, percolating through just 0.30 m of snow, produced a faster, more peaked return compared to the wide, dispersed fluorescein curve formed by percolation through 0.96 m of snow. This marked difference in the delay and attenuation of the dye pulse resulted from percolation through an extra ~66 cm of snow.
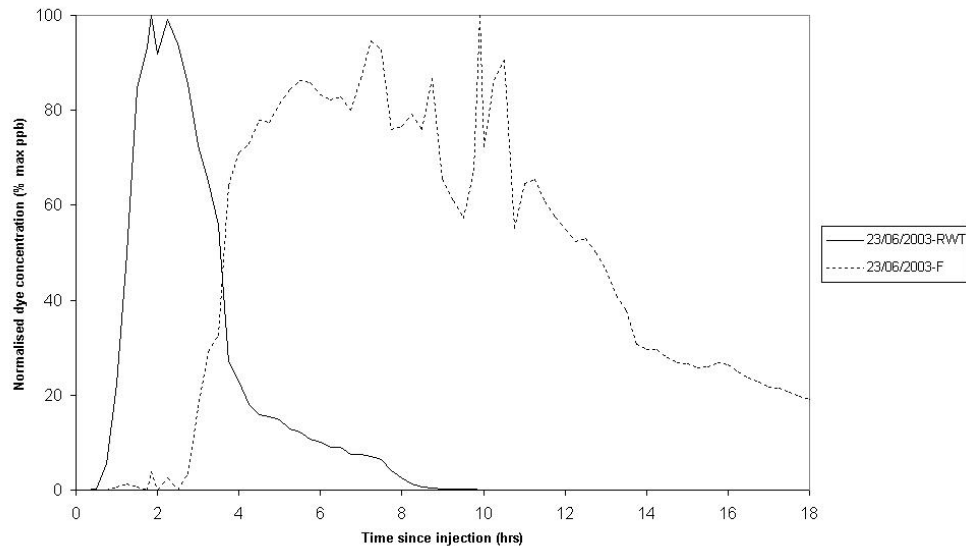
Figure 5.4: Dye return curves from simultaneous surface injections on different snow depths at U (rhodamine on snow 0.30 m deep, fluorescein on snow 0.96 m deep), 23rd June 2003. The marked difference in delay and attenuation of the dye pulse which resulted from percolation through an extra ~66 cm of snow is clear.

Simultaneous surface injections of rhodamine and fluorescein on 28th June 2003, both on the natural snowpack surface but 1.75 and 3.75 m upglacier from the fluorometer respectively, allowed consideration of flow characteristics imparted by percolation through adjacent areas of similar snow depth with only a slight difference in basal flow distance (Figure 5.5). The mismatch between the two return curves called for consideration of the variability of flow conditions within just 2 m lateral distance – the difference between curves seen here is in contrast to the two very similar curves recovered on 21st June (Figure 5.3) when the injection sites were 4 m apart. The good agreement of both the onset and end of dye recovery does however imply some match in flow conditions, although fluorescein concentrations dropped in the middle while rhodamine remained high. This suggests either some retention effect in the fluorescein flow path, or temporary diversion of the emerging fluorescein pulse away from the fluorometer.
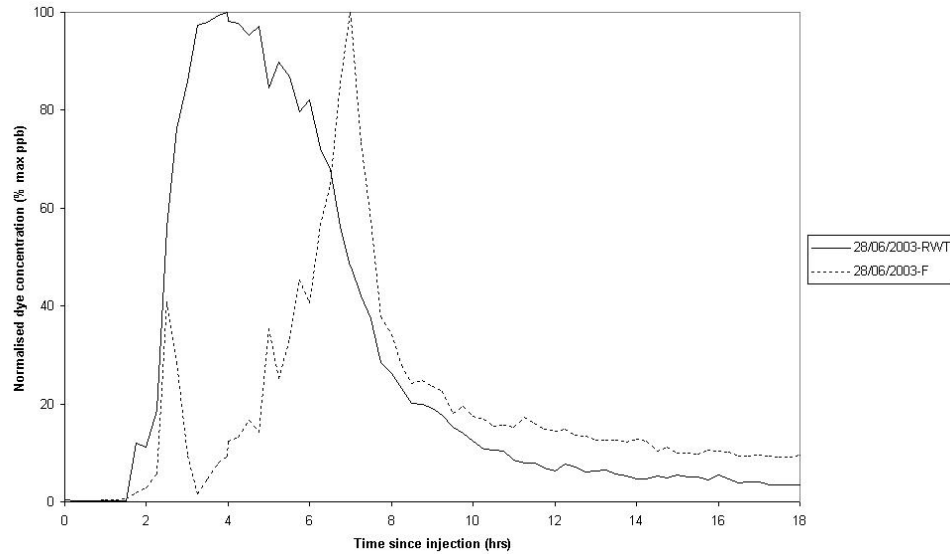
Figure 5.5: Dye return curves from simultaneous surface injections at U on 28th June 2003 (snow depth c. 0.58 m). See previous paragraph for explanation for the mismatch between the two curves despite the similar snow depths on which injections were carried out.

For an experiment on 30th June 2003 surface snow was removed down to an ice layer c.22 cm above the glacier ice surface in order to allow injection of rhodamine WT directly on top of the ice layer. The ice layer was covered with a layer of snow after dye injection to reduce its deterioration due to exposure to the sun. Fluorescein was injected on an adjacent area onto snow from which this ice layer and all snow above had been removed. Any difference between the resulting dye return curves would reflect the effect of this ice layer on water percolating through the snowpack, although some slight delay would also be expected due to the difference in snow depth. Both dyes were first detected at the fluorometer almost simultaneously (Figure 5.6), showing that some water was able to penetrate the ice layer with no delay. Peak dye concentrations, too, were recovered at approximately the same time. There was, however, a marked difference in the trailing limbs of the two curves, with rhodamine that had negotiated the ice layer delayed for many more hours (Figure 5.6). The ice layer therefore allowed some of the percolating dye to pass downwards immediately, but retained a significant quantity (over 65% if the area of the curve under the trailing limb is considered) that passed more slowly to form the trailing limb. The net effect of the ice layer was as a barrier delaying water throughput.

122
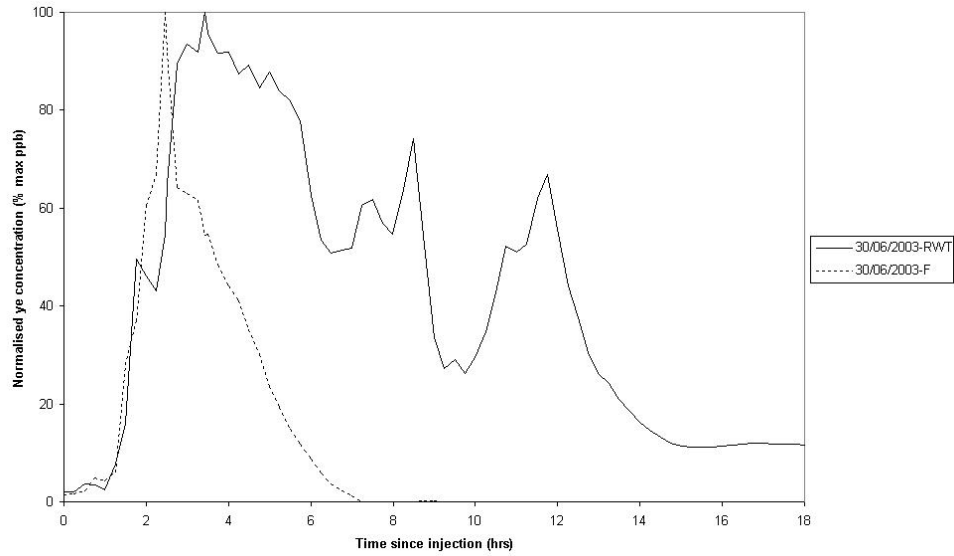
Figure 5.6: Dye return curves from simultaneous injections above (RWT) and below (F) an ice layer at U on 30th June 2003, showing the extended trailing limb caused by dye retention during passage through an ice layer.

Results from two simultaneous surface injections on 5th July 2003 (Figure 5.7; snow depth ~0.30 m) indicated more efficient dye transmission than previous surface injections, but although return curves were quite highly peaked, dye recovery remained delayed by 3 to 4 hours.
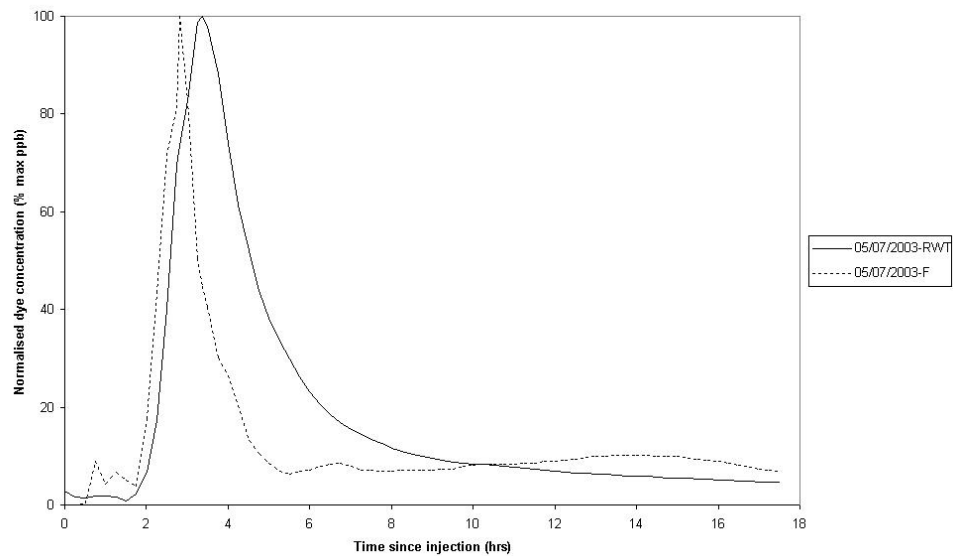
Figure 5.7: Dye return curves from simultaneous surface injections at U on 5th July 2003 (snow depth c. 0.30 m). Peak dye recovery remains delayed by 3 to 4 hours but curves are quite highly peaked, indicating an increase in the efficiency of water transmission through the snowpack.

5.2.1.2 Summary

The generally broad form of the return curves presented in Figures 5.1 to 5.7 above shows that dye added to the snowpack as an instantaneous slug injection moved through the snowpack at a range of rates. In general, return curves had an asymmetric form, the trailing limb indicating that residual dye moved through the snowpack much more slowly than the majority. The heterogeneous flow patterns seen in qualitative dye experiments (section 4.4), influenced by ice layers and preferential flow zones, are the likely cause of this dispersion of the dye pulse. The degree of return curve dispersion is considered important as an indication of the degree to which flux values are attenuated by passage through the snowpack and therefore the snowpack's influence on the magnitude of runoff. The experiment on 23rd June showed that both dispersion and delay of the dye pulse can be markedly decreased by flow through a lesser depth of snow (Figure 5.4). The experiment on 30th June also clearly showed the degree to which ice layers can retain percolating water, causing dispersion of the meltwater wave (Figure 5.6). These delaying and dispersive effects appear to be largely caused by vertical percolation, with lateral flow of up to 4 metres in the basal saturated layer having little effect on return curve timing and form (Figure 5.3). Taking all successful return curves obtained from injections on the natural snowpack surface at U in 2003 together, a general trend of decreasing lag time and decreasing curve dispersion through time is noticeable (Figure 5.8).
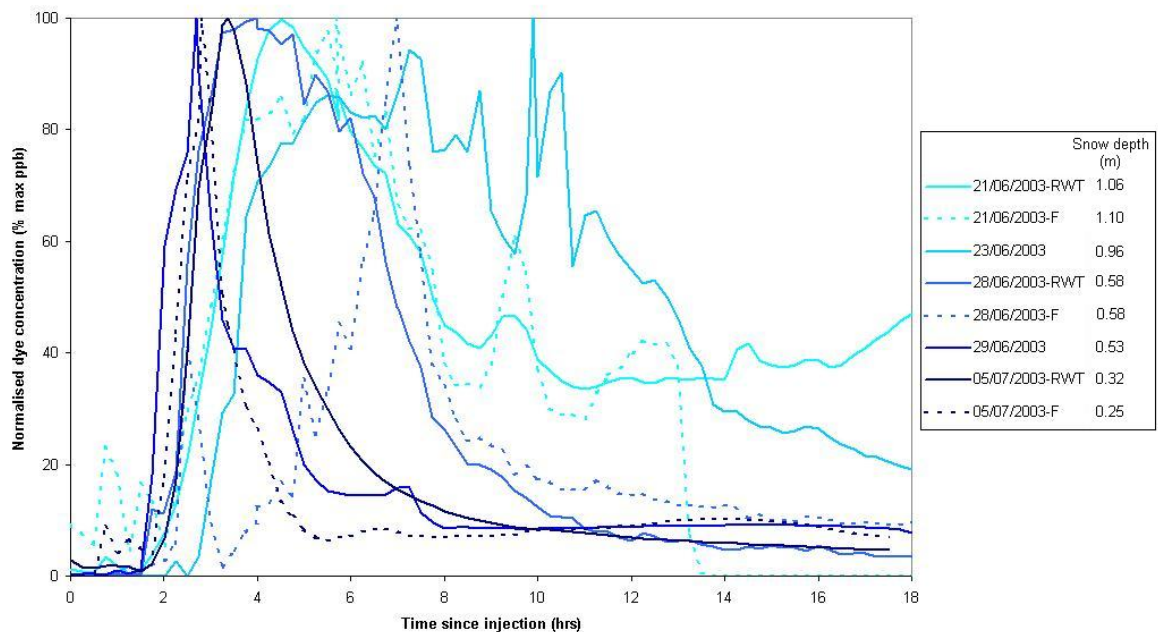
Figure 5.8: All return curves obtained from dye injections on the natural snowpack surface at U in 2003. For days when two injections were carried out these are distinguished by the labels RWT (rhodamine) and F (fluorescein) in the legend. Snow depths onto which injections were carried out are shown for reference in the legend. An impression of the order in which experiments were carried out is given by the darkness of line colour (first injection = light blue, last injection = dark blue).

5.2.2 Transit times for dye flow through the snowpack

Transit times for dye flow through the snowpack indicate the delaying effect that the snowpack imparted on runoff and the way in which this effect changed through time. The transit times to first dye detection, peak concentration, 50% dye recovery and last dye detection for each suitable return curve are presented in Table 5.1 along with information about the date, time, snow depth, and flux conditions (available from 17th June onwards, after installation of the ETH on-ice AWS) for each injection. In general, results indicate a time lag of between 1 and 2 hours required for the fastest-moving dye to pass from the snowpack surface to the fluorometer in the basal saturated layer, and between 2 to 7 hours for half of the dye to be recovered (Table 5.1). The most slowly-moving dye took up to 20 hours to pass through the snowpack. Injections carried out on the unexcavated snowpack surface at U show some evidence ($p < 0.1$) of a decrease in t_{dom} through time (Figure 5.9), in agreement with the trend observed in return curves (Figure 5.8).

Table 5.1: General information for, and transit times derived from, return curves from 2003.

Date	Locn	Distance	Time of injection	Snow depth (m)	Water flux (m hr^{-1})	t_{min} (hrs)	t_{dom} (hrs)	t_{mean} (hrs)	t_{max} (hrs)
06/06/2003	L3	RWT 3-3.5m upgl	12:50	1.25	-	1.24	2.01	2.61	5.00
10/06/2003	L3	RWT 3-3.5m upgl	11:00	0.95	-	1.33	2.17	3.29	7.44
13/06/2003	M3	RWT 3-3.5m upgl	13:06	0.99	-	2.25	-	-	-
19/06/2003	M1	RWT 3-3.5m upgl	14:10	0.64	-	0.86	2.90	2.89	7.00
21/06/2003	U1	RWT 3.5-4m upgl	14:43	1.06	0.0148	1.72	5.71	6.37	14.00
21/06/2003	U1	F 7.5-8m upgl	14:43	1.10	0.0148	1.36	4.53	-	-
23/06/2003	U1	RWT excav. surface	13:40	0.30	0.0259	0.43	1.85	2.56	9.86
23/06/2003	U1	F surface	13:40	0.96	0.0259	2.67	7.48	-	20.00
28/06/2003	U2	RWT 1.5-2m upgl	13:50	0.58	0.0099	1.60	7.00	7.42	19.00
28/06/2003	U2	F 3.5-4m upgl	13:50	0.58	0.0099	1.60	4.16	5.19	19.00
29/06/2003	U3	RWT 1-1.5m upgl	13:05	0.53	0.0120	1.67	2.70	-	-
30/06/2003	U4	RWT above IL	13:55	0.25	0.0112	1.00	3.44	6.16	15.25
30/06/2003	U4	F below IL	13:55	0.20	0.0112	1.00	2.46	3.12	7.20
05/07/2003	U5	RWT 1.5-2m upgl	14:20	0.32	0.0119	1.80	2.83	2.96	5.40
05/07/2003	U5	F 3.5-4m upgl	14:20	0.25	0.0119	1.80	3.38	4.10	12+

_____
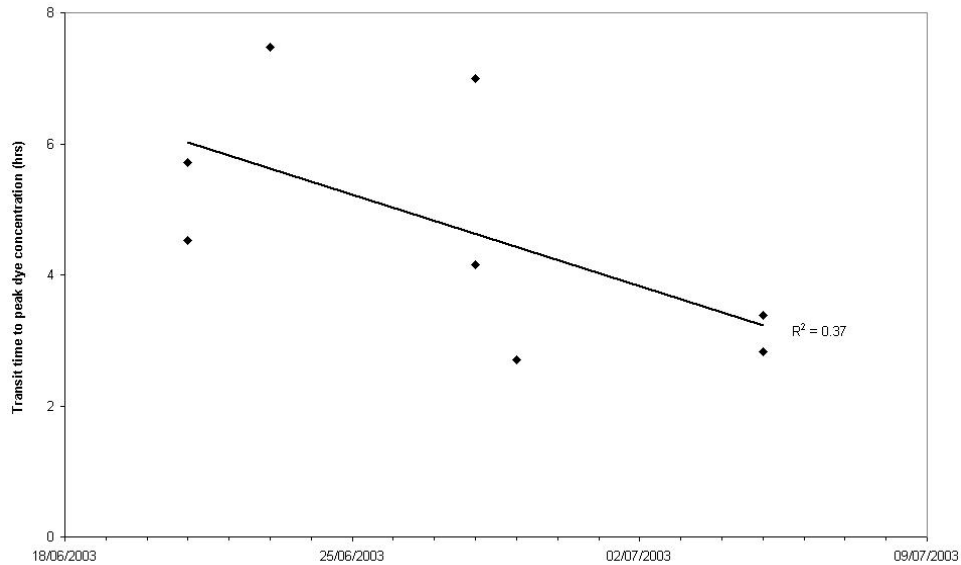
Figure 5.9: Variation in t_{dom} with date through 2003 melt season, showing some evidence ($p < 0.1$) of a decrease through the melt season.

5.2.3 Dye percolation rates

Transit times presented in Table 5.1 were used to calculate maximum, dominant, mean and minimum estimated percolation velocities for each suitable 2003 return curve using the method outlined in section 3.6.2.4 (Table 5.2). In accordance with the results of basal dye injections presented in section 5.4, water flow in the basal saturated layer was assumed to take place at a rate of between 3 and 25 m hr^{-1}, giving rise to upper and lower estimates of percolation velocity. The mean of these values was used in further work. Dominant percolation velocities were very high (0.65 and 1.00 m hr^{-1}) for the injections carried out at L in early June, but due to the high water flux added to the snowpack with dye during these experiments this cannot reliably be used as evidence for particular hydrological efficiency of the snowpack there at this time. Dominant percolation velocities from injections at U ranged between 0.08 and 0.28 m hr^{-1}, agreeing in general with the lower range of previous values found in snow (Table 2.1). Dominant percolation velocity showed evidence of a decrease through time ($p < 0.05$) (Figure 5.10). It appears, therefore, that although t_{dom} decreased through time (Figure 5.9), this could be attributed to decreasing snow depth, not an increase in efficiency of water flow. Water flux at the time of dye injection, however, also decreased through time ($p < 0.1$), and this will likely have contributed to this decreasing temporal trend in percolation velocity, possibly outweighing the influence of any increase in snowpack hydrological efficiency that took place.

Table 5.2: Percolation velocities derived from return curves from 2003.

Date	Locn	Experiment type	Time of injection	Snow depth (m)	Water flux (m hr^{-1})	v_{max} (m hr^{-1})	v_{dom} (m hr^{-1})	v_{mean} (m hr^{-1})	v_{min} (m hr^{-1})
06/06/2003	L3	RWT 3-3.5m upgl	12:50	1.25	-	4.66	1.00	0.66	0.29
10/06/2003	L3	RWT 3-3.5m upgl	11:00	0.95	-	2.36	0.67	0.36	0.14
13/06/2003	M3	RWT 3-3.5m upgl	13:06	0.99	-	0.65	-	-	-
19/06/2003	M1	RWT 3-3.5m upgl	14:10	0.64	-	1.95	0.29	0.29	0.10
21/06/2003	U1	RWT 3.5-4m upgl	14:43	1.06	0.0148	5.25	0.28	-	-
21/06/2003	U1	F 7.5-8m upgl	14:43	1.10	0.0148	3.62	0.28	0.24	0.09
23/06/2003	U1	RWT excav. surface	13:40	0.30	0.0259	1.55	0.19	0.13	0.03
23/06/2003	U1	F surface	13:40	0.96	0.0259	0.38	0.13	-	0.05
28/06/2003	U2	RWT 1.5-2m upgl	13:50	0.58	0.0099	0.47	0.15	0.12	0.03
28/06/2003	U2	F 3.5-4m upgl	13:50	0.58	0.0099	1.03	0.09	0.09	0.03
29/06/2003	U3	RWT 1-1.5m upgl	13:05	0.53	0.0120	0.37	0.22	-	-
30/06/2003	U4	RWT above IL	13:55	0.25	0.0112	0.32	0.08	0.04	0.02
30/06/2003	U4	F below IL	13:55	0.20	0.0112	0.35	0.10	0.07	0.03
05/07/2003	U5	RWT 1.5-2m upgl	14:20	0.32	0.0119	0.22	0.10	0.08	0.03
05/07/2003	U5	F 3.5-4m upgl	14:20	0.25	0.0119	0.30	0.13	0.12	0.05
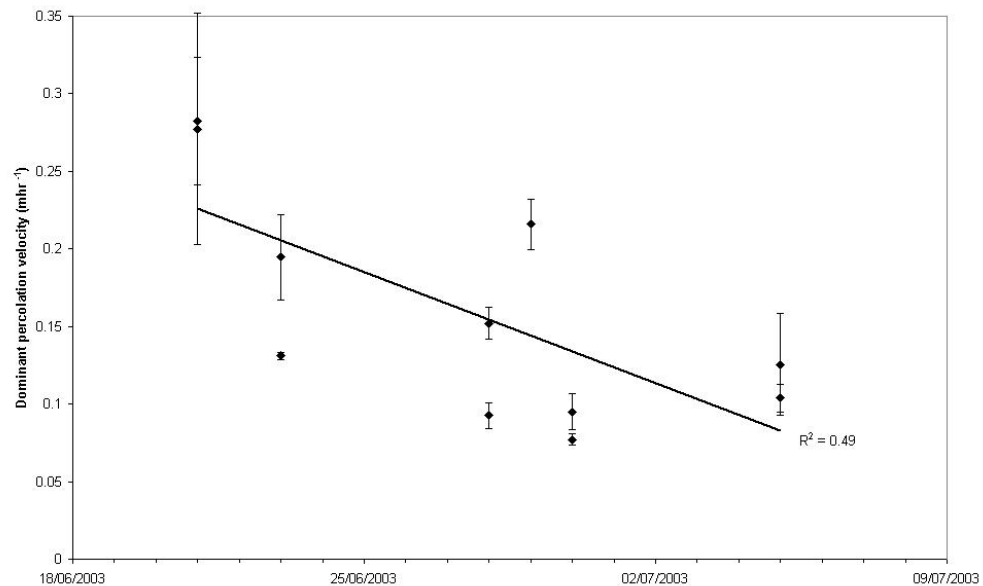
Figure 5.10: Variation in dominant percolation velocity with date through the 2003 melt season.

5.2.4 Dispersion of the dye pulse

The extent to which each dye pulse was dispersed or spread out during flow through the snowpack was considered quantitatively by calculating the dispersion coefficient *D* and dispersivity index *d* as described in section 3.6.2.4 (Table 5.3). These dispersion indices are considered important as an indication of the degree to which flux volumes are attenuated by passage through the snowpack and therefore the snowpack's influence on the magnitude of

discharge flowing into the englacial drainage system. Due to the varying distances over which injections took place, in addition to the variation in flux conditions, caution must be exercised in drawing conclusions from this data. D values range from 2.8×10^{-6} to 2.95×10^{-4} $m^2 s^{-1}$ and d values from 0.02 to 0.68 m. As such, values for D are in the range identified by Brugman (unpublished) as generally occurring in porous or natural granular media, and significantly less than occur in channelised systems such as surface or underground rivers or man-made pipes. This indicates that, as expected, the effect of flow through the supraglacial snowpack will be very different to that in open channels on the glacier surface, and points to the difference in runoff that is therefore likely to occur when the snowpack is removed and bare ice revealed.

Both D and d showed evidence of decrease through time (Figure 5.11; $p < 0.1$ for the decrease in D through time, $p < 0.05$ for decrease in d). As high values of d are associated with more dispersed curve forms and lower flow velocities, this decrease in d is indicative of increasing efficiency of flow through the snowpack hydrological system.

Table 5.3: D and d values for surface dye injections in 2003 along with information about the distance over which dye flowed and the net flow velocities used in their calculation.

Date	Locn	Experiment type	Snow depth (m)	Basal flow distance (m)	Total flow distance (m)	D ($m^2 s^{-1}$)	v net (m hr^{-1})	d (m)
06/06/2003	L3	RWT 3-3.5m upgl	1.25	3.25	4.50	2.47E-05	2.24	0.0398
10/06/2003	L3	RWT 3-3.5m upgl	0.95	3.25	4.20	1.05E-04	1.94	0.1943
19/06/2003	M3	RWT 3-3.5m upgl	0.64	3.25	3.89	5.96E-05	1.34	0.1599
21/06/2003	M1	RWT 3.5-4m upgl	1.06	3.75	4.81	9.08E-05	1.06	0.3078
21/06/2003	U1	F 7.5-8m upgl	1.10	7.75	8.85	2.94E-04	1.55	0.6839
23/06/2003	U1	RWT excav. surface	0.30	1.50	1.80	3.87E-05	0.97	0.1434
23/06/2003	U1	F surface	0.96	0.80	1.76	1.61E-05	0.24	0.2459
28/06/2003	U1	RWT 1.5-2m upgl	0.58	1.75	2.33	3.17E-05	0.56	0.2038
28/06/2003	U2	F 3.5-4m upgl	0.58	3.75	4.33	2.80E-06	0.62	0.0163
29/06/2003	U2	RWT 1-1.5m upgl	0.53	1.25	1.78	7.63E-06	0.66	0.0416
30/06/2003	U3	RWT above IL	0.25	1.05	1.30	2.25E-05	0.38	0.2143
30/06/2003	U4	F below IL	0.20	1.75	1.95	1.36E-05	0.79	0.0617
05/07/2003	U4	RWT 1.5-2m upgl	0.32	1.75	2.07	9.51E-06	0.61	0.0560
05/07/2003	U5	F 3.5-4m upgl	0.25	3.75	4.00	1.64E-05	1.41	0.0418
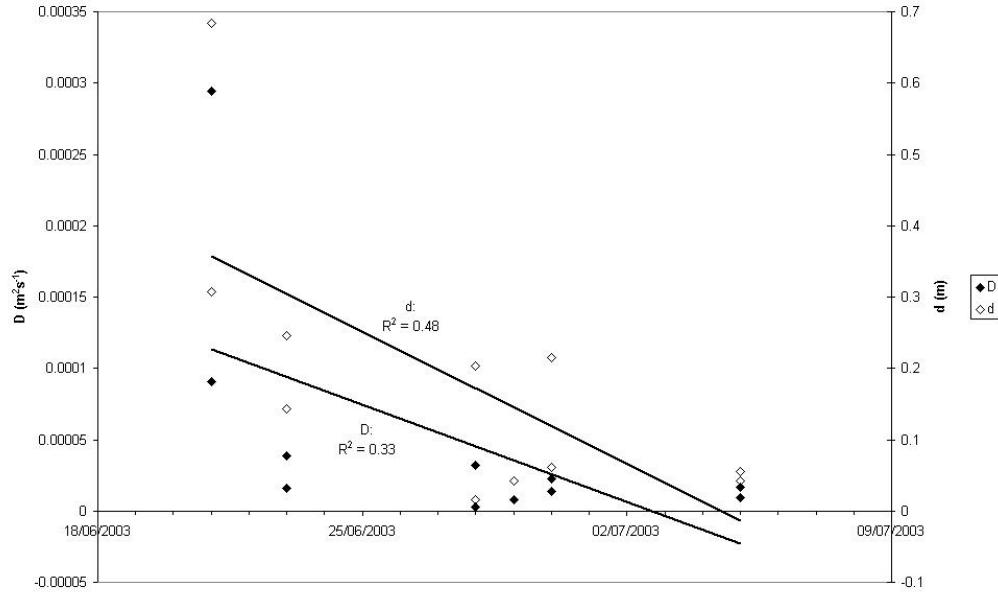
Figure 5.11: Variation in D and d with date through the 2003 field season ($r^2 = 0.33$ for D, 0.48 for d). There is evidence of decreasing D and d through time.

5.2.5 Snowpack permeability

Past measurements of snowpack permeability have used lysimeter discharge data and known input surface flux to calculate velocities of water movement between the surface and the base, and then back-calculated corresponding equivalent permeability values for the net snowpack depth using theory (Marsh, 1991). The flow velocities derived from dye return curves were used in a similar way to estimate the equivalent permeability of the snowpack at Haut Glacier d'Arolla at the time of each quantitative dye experiment.

Equation 2.12 (Colbeck (1978a); reproduced as Equation 5.1 below) presented a simple theoretical model of the rate of water percolation in snow and the factors controlling it:

$$\frac{dz}{dt}\bigg|_u = 3\alpha^{1/3}k^{1/3}\phi_e^{-1}u^{2/3} \qquad (5.1)$$

where $dz/dt|_u$ is the rate of water percolation through the snowpack (m hr^{-1}),

α is a constant representing the density and viscosity of water and gravitational acceleration,

k is snowpack permeability (m^2),

ϕ_e is effective snow porosity, and

u is the volume flux of water (m hr^{-1}).

_____

As the rate of water percolation through the snowpack, $dz/dt|_u$, was known from dye injections, Equation 5.1 could be used to calculate the permeability of the snowpack at the time of each experiment. u was known from energy balance modelling of surface melt flux (using the Brock and Arnold (2000) model; Appendix B) and the volume of water added with dye and ϕ_e from Equation 2.10 (with snow porosity ϕ known from density profiles). Although the calculation of ϕ_e from density measurements is subject to some error, sensitivity analysis of Equation 5.1 (Appendix D) shows that this will not cause significant error in the value of k calculated.

Although Colbeck's derivation of Equation 5.1 was based on the assumption of homogeneous percolation, shown by qualitative dye experiments to be incorrect for the snowpack at Haut Glacier d'Arolla (section 4.4), application of Equation 5.1 is believed to give a useful estimate of net snowpack permeability. Two sources of error are expected, both relating to the value of u used. Firstly, flux produced at the snowpack surface is concentrated at depth within multiple preferential flow channels; therefore, the value of u used in Equation 5.1 (calculated by adding the water flux added with dye to the surface melt flux predicted using the Brock and Arnold (2000) energy balance model) is likely to be lower than the real value and the resulting k a maximum estimate of snow permeability. Secondly, due to the dependence of percolation velocity on flux magnitude, dye percolating through the snowpack under conditions of decreasing flux (always the case due to the extra water added with injected dye) is likely to encounter other percolating meltwater produced at the surface before the time of dye injection, and thereby generate a larger flux. The instantaneous surface flux at the time of dye injection is again a minimum estimate of that actually traveling through the snowpack for most of its depth, and hence the value of k calculated using Equation 5.1 is expected to be higher than the real snow permeability. The impact of errors in flux values on values of k calculated is discussed fully in Appendix D.

Values of k corresponding to the dominant percolation velocities from dye injections in 2003 ranged between 2.02×10^{-13} and 1.47×10^{-11} m^2 (Table 5.4). These values are significantly lower than those found in previous studies (section 2.2.2.3). There was little evidence of a trend in k through time that would confirm the increase in flow efficiency suggested by dispersivity values (Figure 5.12); if anything, k values tended to decrease through time, with the earliest injections at U, on 21st June 2003, resulting in the highest k values.

Table 5.4: Permeability *k* values calculated for 2003 surface dye tracing data.

Date	k (m^2)
21/06/2003	1.47E-11
21/06/2003	1.39E-11
23/06/2003	1.57E-12
23/06/2003	2.02E-13
23/06/2003	4.78E-13
28/06/2003	5.11E-12
28/06/2003	1.16E-12
29/06/2003	9.94E-12
30/06/2003	5.24E-13
30/06/2003	9.77E-13
05/07/2003	1.12E-12
05/07/2003	1.98E-12
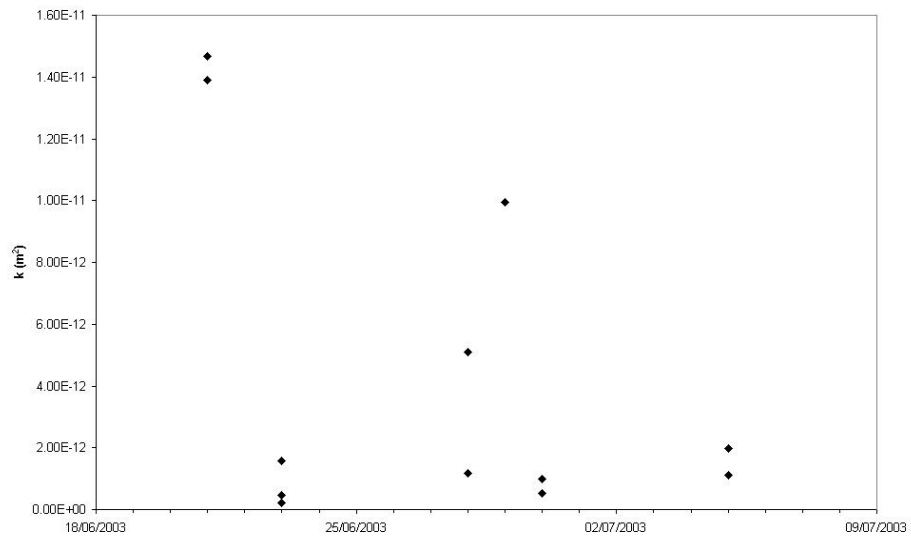
Figure 5.12: Variation in *k* with date through the 2003 field season. There is little evidence of any trend in *k* through time.

2004 field season

Quantitative surface dye injections in summer 2004 yielded a total of 14 useful complete return curves from the main study site at L. A further 3 curves showed the onset of dye arrival at the fluorometer before migration of the emerging dye plume or drainage of the detection pool resulted in the loss of the rest of the curve. Successful dye returns were obtained between 14th June and 10th July. Earlier experiments were unsuccessful as ice layers within the snowpack prevented dye from reaching the base of the snowpack within the 3 meters between the injection area and the fluorometer, with dye observed to emerge above ice layers in the middle of the pit face (Figure 4.35). Two adjacent snowpits at L (referred to as Pit A and Pit B) were used in rotation for the experiments reported here, with repeat injections at a pit carried out on the same area of the snowpack surface. This reduced variation in return times caused by spatial differences in snowpack structure and differing flow rates at the snowpack base, and therefore rendered curves obtained from the same pit comparable through time. The data obtained therefore provide a detailed picture of snowpack evolution over a c.1 month period at 2750m elevation.

5.2.6 Nature of water flow: dye return curve shape and timing

Return curves from tests carried out earlier in the melt season typically had a wide, dispersed form, with the dye wave frequently taking over 12 hours to pass the fluorometer (Figures 5.13 and 5.14). There was a decrease in curve dispersion through time, with curves from later injections generally more peaked. The timing of return curves also evolved, with earlier dye recovery through time. For injections at Pit A (Figure 5.13), dye arrived progressively earlier as the melt season progressed. For injections at Pit B (Figure 5.14), the decrease in transit time was less consistent but showed the same general trend.
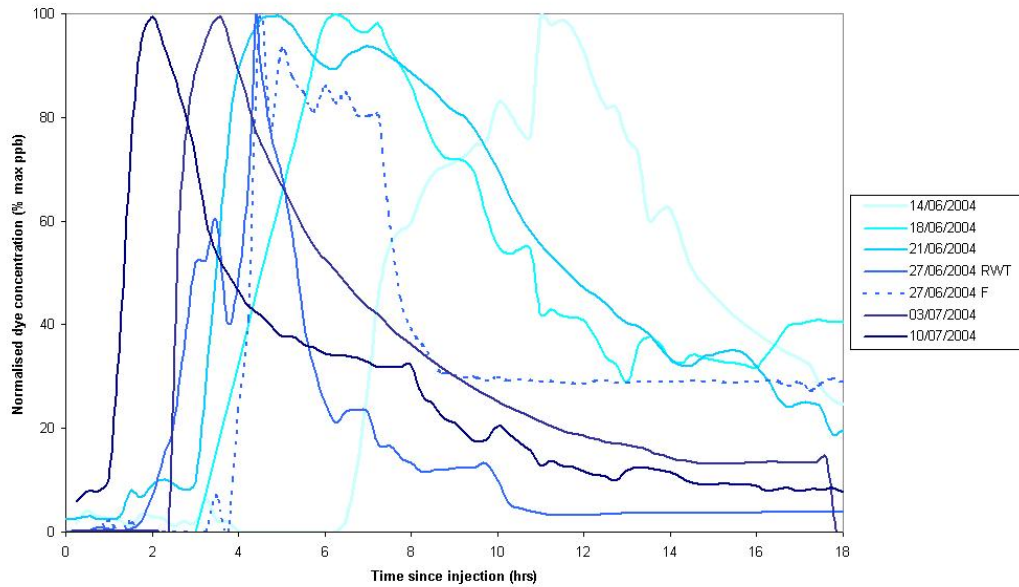
Figure 5.13: Dye return curves obtained from surface injections at Pit A in 2004. An impression of the order in which experiments were carried out is given by the darkness of line colour (first injection = light blue, last injection = dark blue).
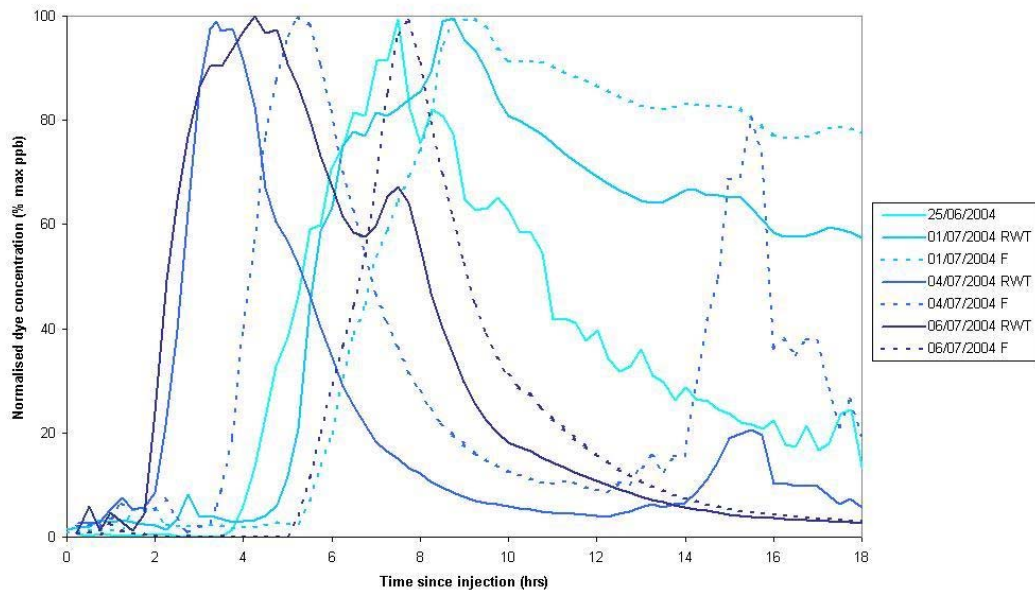
Figure 5.14: Dye return curves obtained from surface injections at Pit B in 2004. An impression of the order in which experiments were carried out is given by the darkness of line colour (first injection = light blue, last injection = dark blue).

5.2.7 Transit times for dye flow through the snowpack

The transit times to first dye detection, peak concentration, 50% dye recovery and last dye detection for each suitable return curve are presented in Tables 5.5 a and b for dye experiments at Pits A and B respectively.

133

Table 5.5: General information for, and transit times derived from, return curves from a) Pit A and b) Pit B.

a)

Date	Location	Time of injection	Snow depth (m)	Input water flux (m hr^{-1})	t_{min} (hrs)	t_{dom} (hrs)	t_{mean} (hrs)	t_{max} (hrs)
14/06/2004	Pit A	12:13	1.75	0.0043	6.25	10.90	11.57	45.67
18/06/2004	Pit A	12:54	1.54	0.0077	2.05	6.01	-	-
21/06/2004	Pit A	14:26	1.53	0.0085	1.40	4.60	-	-
27/06/2004	Pit A	11:30	1.23	0.0060	1.22	4.41	4.74	11.30
27/06/2004	Pit A	14:02	1.23	0.0049	3.75	4.40	5.95	8.80
29/06/2004	Pit A	10:37	1.15		-	0.99	-	-
03/07/2004	Pit A	15:48	0.92	0.0062	2.52	3.51	6.12	17.83
10/07/2004	Pit A	15:58	0.58	0.0040	0.93	1.95	4.48	15.00

b)

Date	Location	Time of injection	Snow depth (m)	Input water flux (m hr^{-1})	t_{min} (hrs)	t_{dom} (hrs)	t_{mean} (hrs)	t_{max} (hrs)
25/06/2004	Pit B	11:27	1.35	0.0058	3.59	7.52	9.01	19.03
25/06/2004	Pit B	15:37	1.35		-	4.33	-	-
01/07/2004	Pit B	12:03	1.03	0.0038	4.60	8.82	15.54	38.70
01/07/2004	Pit B	13:34	1.03	0.0027	4.00	7.90	15.66	37.40
04/07/2004	Pit B	12:18	0.89	0.0061	1.83	3.30	4.26	12.52
04/07/2004	Pit B	14:03	0.89	0.0060	1.56	3.53	4.14	10.77
06/07/2004	Pit B	10:31	0.79	0.0029	1.37	4.19	5.42	18.50
06/07/2004	Pit B	13:03	0.79	0.0043	2.52	5.16	5.76	16.00
09/07/2004	Pit B	15:06	0.64		-	0.39	-	-

In the first successful quantitative dye injection of 2004, on 14th June, dye was not detected at the fluorometer 3.25 m downglacier until 6.25 hours after injection. In all later experiments t_{min} was less, falling below one hour in the last experiments of the season in early July. There is some evidence of decreasing minimum transit time with date for both pits but considerable variability within this trend (p = 0.13, r^2 = 0.34 for Pit A; p = 0.08, r^2 = 0.66 for Pit B; Figure 5.15).
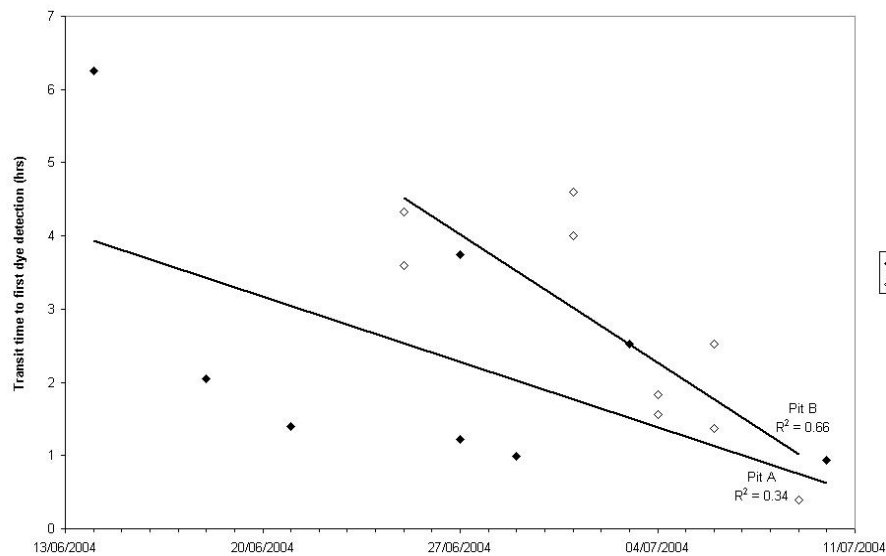
Figure 5.15: Scatter plot of time to first dye detection t_{min} against date of experiment, showing some evidence of decreasing minimum dye transit time with date for both pits but considerable variability within this trend ($p = 0.13$, $r^2 = 0.34$ for Pit A; $p = 0.08$, $r^2 = 0.66$ for Pit B).

Transit times to peak dye concentration t_{dom} are plotted against date of dye injection in Figure 5.16. For Pit A, t_{dom} decreased continuously over the period of study ($p < 0.05$). In the earliest injection (June 14th, snow depth ~1.75 m), almost 11 hours passed before detection of peak dye concentration, compared to just 2 hours in the last injection (July 10th, snow depth ~0.60 m). For injections at Pit B, the decrease in t_{dom} was less consistent but showed the same general trend ($p < 0.1$). For experiments at Pit A, input water fluxes at the time of dye injections generally decreased later in the season (Table 5.5a), such that the decrease in t_{dom} is believed to reflect a change in the snowpack's delaying influence on runoff that is the result of changing snowpack properties rather than higher input fluxes. The precise role of flux conditions cannot however be considered without undertaking further modelling of the interaction of percolating meltwater fluxes within the snowpack.
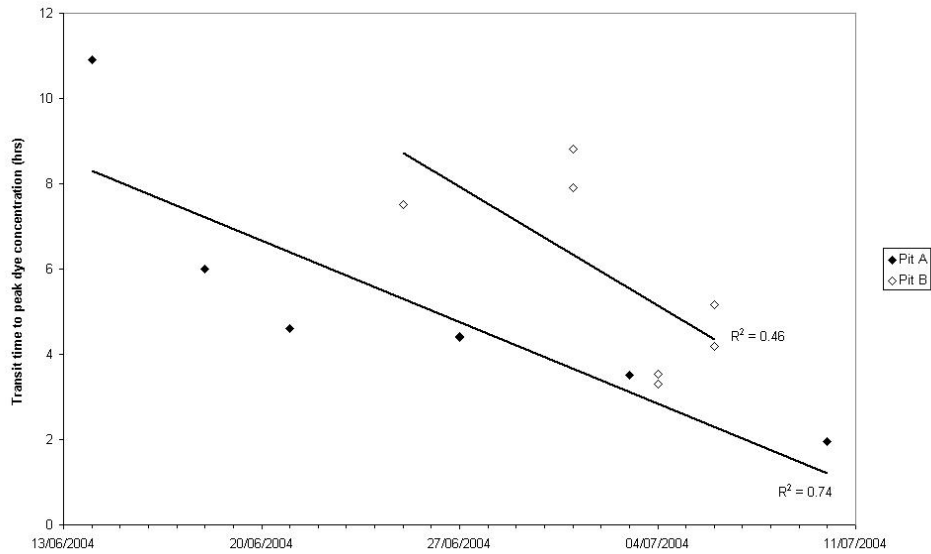
Figure 5.16: Scatter plot of time to peak dye detection t_{dom} against date of experiment, showing evidence of decreasing dominant dye transit time with date ($r^2 = 0.74$, $p < 0.05$ for Pit A injections, $r^2 = 0.46$, $p < 0.1$ for Pit B injections).

The derivation of t_{mean}, the transit time to 50% dye recovery, was often difficult due to the necessity of defining the end of the dye curve, which was frequently characterised by ongoing low dye concentrations and/or cut short by the start of a new experiment. The t_{mean} values produced therefore contain an element of subjectivity and the data set is smaller. Values showed little evidence of a decrease in transit time with date through the melt season.

For the same reasons, limited explanatory power is given to recovered values of t_{max}, the transit time to last dye detection. Those that were recovered indicate lags as high as 45 hours for the first injection of the season and a minimum of around 12 hours (Table 5.5).

5.2.8 Dye percolation rates

Estimated maximum, dominant, mean and minimum percolation velocities for each suitable 2004 return curve are presented in Table 5.6. Dominant percolation velocities v_{dom} provide the most complete record of dye flow rate. v_{dom} for percolation through the snowpack in 2004 ranged between 0.13 and 0.49 m hr^{-1}, therefore tending to be slightly higher than found in 2003 but again agreeing in general with the lower range of previous values found in snow (Table 2.1). Maximum percolation velocities v_{max} were an order of magnitude greater than v_{dom}, frequently above 1 m hr^{-1} and on occasion as high as 5 m hr^{-1}. Minimum percolation velocities v_{min} ranged between 0.03 and 0.15 m hr^{-1}.

Table 5.6: Percolation velocities derived from surface dye injections at a) Pit A and b) Pit B.

a) Date	Location	Time of injection	Snow depth (m)	Input water flux (m hr^{-1})	v_{max} (m hr^{-1})	v_{dom} (m hr^{-1})	v_{mean} (m hr^{-1})	v_{min} (m hr^{-1})
14/06/2004	Pit A	12:13	1.75	0.0043	0.31	0.17	0.16	0.04
18/06/2004	Pit A	12:54	1.54	0.0077	1.19	0.29	-	-
21/06/2004	Pit A	14:26	1.53	0.0085	3.01	0.39	-	-
27/06/2004	Pit A	11:30	1.23	0.0060	5.06	0.33	0.30	0.12
27/06/2004	Pit A	14:02	1.23	0.0049	0.40	0.33	0.23	0.15
29/06/2004	Pit A	10:37	1.15	-	2.37	-	-	-
03/07/2004	Pit A	15:48	0.92	0.0062	0.51	0.33	0.17	0.05
10/07/2004	Pit A	15:58	0.58	0.0040	1.39	0.49	0.15	0.04

b) Date	Location	Time of injection	Snow depth (m)	Input water flux (m hr^{-1})	v_{max} (m hr^{-1})	v_{dom} (m hr^{-1})	v_{mean} (m hr^{-1})	v_{min} (m hr^{-1})
25/06/2004	Pit B	11:27	1.35	0.0058	0.46	0.2	0.16	0.07
25/06/2004	Pit B	15:37	1.35	-	0.37	-	-	-
01/07/2004	Pit B	12:03	1.03	0.0038	0.26	0.13	0.07	0.03
01/07/2004	Pit B	13:34	1.03	0.0027	0.31	0.14	0.07	0.03
04/07/2004	Pit B	12:18	0.89	0.0061	0.86	0.34	0.25	0.07
04/07/2004	Pit B	14:03	0.89	0.0060	1.24	0.31	0.26	0.09
06/07/2004	Pit B	10:31	0.79	0.0029	1.69	0.22	0.17	0.04
06/07/2004	Pit B	13:03	0.79	0.0043	0.44	0.18	0.15	0.05
09/07/2004	Pit B	15:06	0.64	-	5.79	-	-	-

Results from Pit A showed significant evidence (p <0.05) of an increase in v_{dom} with time through the melt season (Figure 5.17). Pit B data showed no clear trend. The decrease in dye transit time with date through the melt season at Pit A that was noted in section 5.2.7 (Figure 5.16) was therefore not simply a function of decreasing snow depth, but also reflects faster water percolation through time. With changing flux magnitude ruled out as a possible cause of increasing percolation rates through time at Pit A, this increase in v_{dom} must be explained by some change in snowpack properties that has increased the efficiency with which the snowpack is able to transmit water. Increasing snow grain size and porosity and/or ice layer melt-out or decay are possible causes of increasing snow permeability. However, little temporal change in snow grain size or density was observed during stratigraphic investigations (sections 4.3.3 and 4.3.4). Instead, decreasing retention of percolating meltwater by ice layers is suggested as a likely cause of increasing snowpack hydrological efficiency. Ice layer impact on water percolation decreased through time for two reasons. Firstly, as snow depth decreased through the melt season ice layers closest to the snowpack surface melted out, decreasing the net effect of ice layers in retaining percolating meltwater. As ice layers were concentrated in the upper snowpack (section 4.3.3), net snowpack permeability will have increased most quickly as these upper layers melted out, introducing a non-linearity to the snowpack's hydrological behaviour. Secondly, although ice layers remaining in the snowpack often retained a solid appearance throughout

their lifetime and continued to restrict downward water movement (e.g. Figure 4.27), the individual permeability of each is expected to have increased through time following Langham (1973a, b). Evidence for this was seen in early 2004, when dye injected on the snowpack surface for the first quantitative experiments of the season had been observed to emerge not at the snow-ice interface but along ice layers up to 1.7 m above the ice surface (Figure 4.35). Over the following two weeks, dye emerged on ice layers lower in the snowpack and finally in the basal saturated layer, showing that ice layers were allowing percolating water to take a more direct path between the snowpack surface and base.
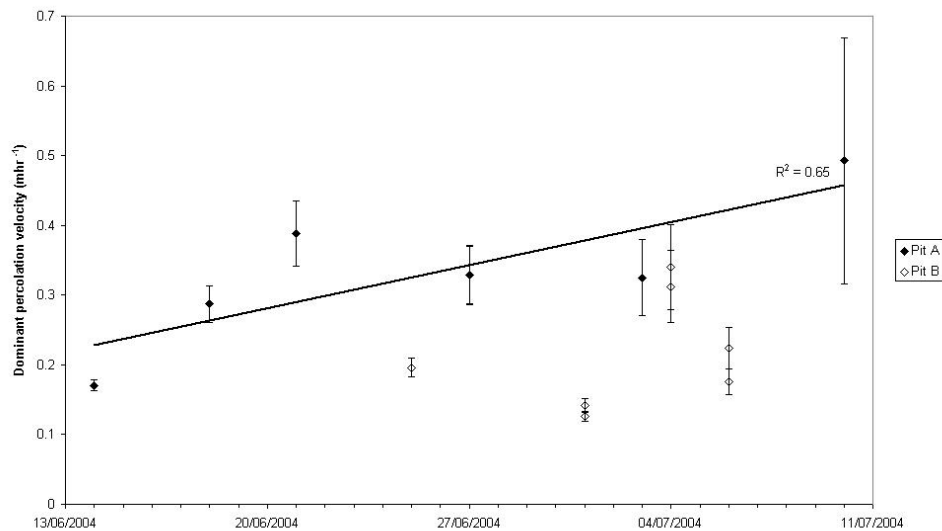
Figure 5.17: Variation in dominant dye percolation velocity with date for 2004 data. Calculation of percolation velocity from net dye transit time by assumption of basal flow taking place at a rate of between 3 and 25 m hr^{-1} gives rise to upper and lower estimates of percolation velocity; these are marked as upper and lower error bars on all subsequent graphs. For Pit A data there is significant evidence (p < 0.05) of an increase in v_{dom} through time; for Pit B data there is no clear trend.

5.2.9 Dispersion of the dye pulse

Calculated values of the dispersion coefficient *D* and dispersivity *d* along with the net flow velocities used in the calculation of *d* are presented in Table 5.7. Values for *D* range between 1.42×10^{-5} to 1.20×10^{-4} m^2 s^{-1} and values for *d* between 0.07 and 0.48 m. These values are comparable to those found from 2003 data, though extending across a narrower range. As in 2003, values for *D* are in the range expected for flow through porous or granular media (Brugman, unpublished) and point to the inefficiency of flow through the snowpack compared to open channel supraglacial flow once the snowpack is removed.

_____

Table 5.7: Calculated values of the dispersion coefficient *D* and dispersivity *d* for surface dye injections at a) Pit A and b) Pit B.

a) Experiment	v net (m hr^{-1})	D (m^2 s^{-1})	d (m)
14/06/2004	0.44	2.46E-05	0.20
18/06/2004	0.76	5.02E-05	0.24
21/06/2004	0.99	1.01E-04	0.37
27/06/2004 RWT	0.96	3.01E-05	0.11
27/06/2004 F	0.96	3.58E-05	0.13
03/07/2004	1.12	7.01E-05	0.23
10/07/2004	1.84	1.08E-04	0.21

b) Experiment	v net (m hr^{-1})	D (m^2 s^{-1})	d (m)
25/06/2004	0.58	2.69E-05	0.17
01/07/2004 RWT	0.46	5.05E-05	0.40
01/07/2004 F	0.51	6.62E-05	0.47
04/07/2004 RWT	1.18	5.25E-05	0.16
04/07/2004 F	1.10	5.83E-05	0.19
06/07/2004 RWT	0.90	1.20E-04	0.48
06/07/2004 F	0.73	1.42E-05	0.07

Neither *D* nor *d* showed evidence of a discernible trend through time (Figure 5.18). Therefore, although visual examination of return curve form (section 5.2.6) suggested a reduction through time in the dispersive effect of the snowpack on water flow, there is no quantitative evidence of a significant change.
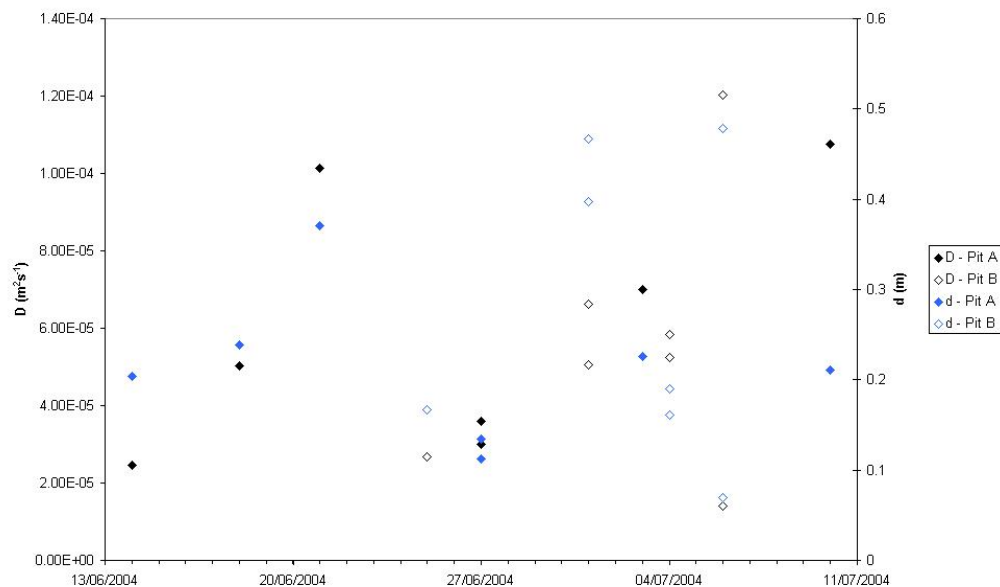
Figure 5.18: Variation of *D* and *d* values with date. There is no evidence of any trend in *D* or *d* through time.

5.2.10 Snowpack permeability

Dye velocity data presented in section 5.2.8 indicated an increase through time in the efficiency with which water was transmitted through the snowpack. Effectively, this must translate into an increase in snowpack permeability. Values of k corresponding to dominant dye percolation velocities found in 2004 are presented in Table 5.8. As a result of uncertainties in the value of u used in calculating k (see section 5.2.5), these values are not expected to be correct in absolute terms but instead should provide a maximum estimate of real snow permeability for comparison to permeability values found and used in other studies. Permeability values derived from Pit B experiments were generally lower than those from Pit A experiments, but no obvious explanation for this (e.g. more or thicker ice layers) was observed in the stratigraphy of the snowpits. Values of k for 2004 data range between 1.95×10^{-11} and 1.05×10^{-9} m^2 and are comparable to those found in studies of non-glacial snowpacks (section 2.2.2.3), but are in general somewhat lower.

Table 5.8: Calculated values of net snowpack permeability k for surface dye injections at a) Pit A and b) Pit B.

a) Date	Location	k (m^2)	b) Date	Location	k (m^2)
14/06/2004	Pit A	3.77E-11	25/06/2004	Pit B	3.14E-11
18/06/2004	Pit A	5.63E-11	01/07/2004	Pit B	1.95E-11
21/06/2004	Pit A	1.15E-10	01/07/2004	Pit B	5.45E-11
27/06/2004	Pit A	1.41E-10	04/07/2004	Pit B	1.50E-10
27/06/2004	Pit A	2.08E-10	04/07/2004	Pit B	1.21E-10
03/07/2004	Pit A	1.28E-10	06/07/2004	Pit B	1.84E-10
10/07/2004	Pit A	1.05E-09	06/07/2004	Pit B	4.20E-11

Modeling studies of water percolation through snow have frequently based their estimates of k on the formulation of Shimizu (1970; Equation 2.1, reproduced as Equation 5.2 below), in which k depends on snow grain size d and snow density ρ_s according to the formula

$$k = 0.077 d^2 \exp\left[-7.8\left(\rho_s / \rho_w\right)\right] \qquad (5.2)$$

(where ρ_w is the density of liquid water). Estimation of a likely minimum snow permeability value by Shimizu using a grain size of 0.5 mm (generally expected to be found only in early-season, hydrologically poorly-developed snowpacks) and a dry snow density of 600 kg m^{-3} (higher than that found from density profiling at Haut Glacier d'Arolla) results in a value (1.79×10^{-10} m^2) significantly higher than most of those found here (Figure 5.19). In comparison to the very low permeability values found in 2003 (section 5.2.5), this gap between estimated and observed values would be even more marked. The straightforward application of Shimizu's formula for the estimation of snowpack permeability is therefore

insufficient where the snowpack contains ice layers or other less permeable strata, as is frequently the case in (alpine) glacial snowpacks.

For *k* values derived from dye tracing tests at Pit A there is significant ($p < 0.05$) evidence of an increase in snowpack net permeability through time (Figure 5.19); the increase in *k* for pit B data is less clear ($p = 0.16$). Examination of the sensitivity of the calculated value of *k* to errors in *u* shows that this dependence is limited at the higher values of *u* generally considered here, and that for the results considered here, the variation in $dz/dt|_u$ will reflect a genuine increase in *k* (Appendix D). As discussed in section 5.2.8, reduced retention of percolating water by ice layers is suggested as an important cause of increasing snowpack hydrological efficiency. A change in the distribution of flux through preferential flow zones and any increase in snow grain size may also have contributed to increasing effective snow permeability, but no evidence of these was observed.
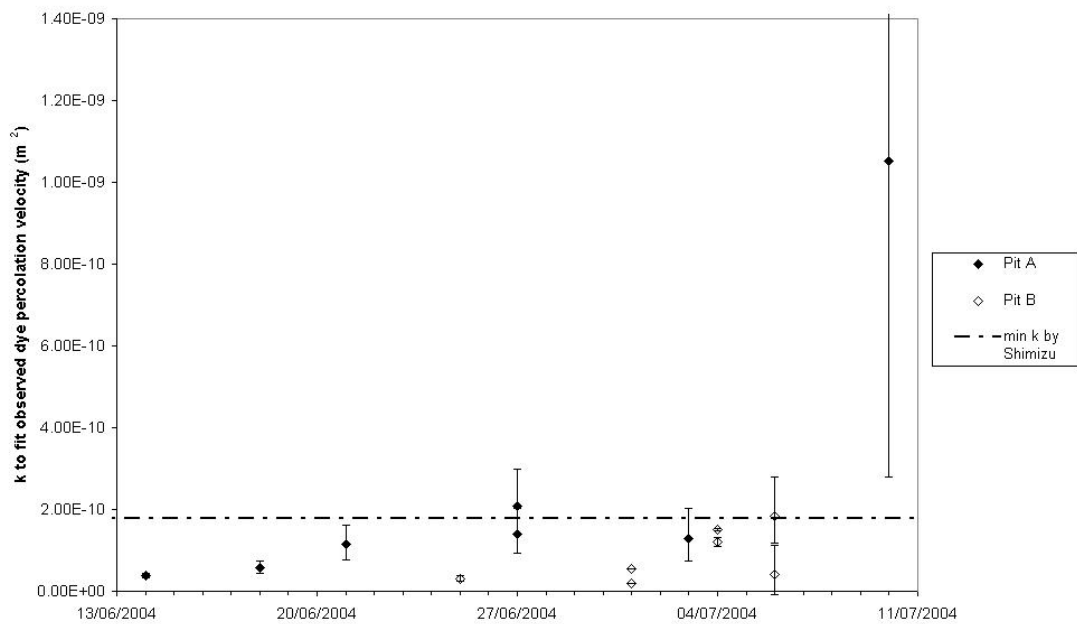
Figure 5.19: Variation in values of snowpack permeability *k* with date. For Pit A data there is significant ($p < 0.05$) evidence of an increase in snowpack net permeability through time; the increase in *k* for Pit B data is less clear ($p = 0.16$). The dashed line indicates the value for snow permeability predicted by Shimizu's (1970) equation (Equation 5.2) for snow of grain size 0.5mm and dry density 600 kg m^{-3}.

5.3 LYSIMETER-DERIVED INFORMATION ABOUT SNOW WATER PERCOLATION

Lysimeter measurements of water discharge through the snowpack during the 2004 field season provided an independent source of information about water percolation, for comparison to results from dye tracing work. Unfortunately, due to difficulties in lysimeter set-up (section 2.6.1.1), data was obtained only for a 10-day period in early July. Lysimeter data is therefore of limited use in considering the evolution of snowpack hydrology through time and does not give any information about the hydrological behaviour of the early-season snowpack. It does, however, enable confirmation of dye tracing results gathered concurrently and consideration of the merits of these two methods of snow hydrology investigation. Lysimeter data was analysed with reference to melt inputs at the snow surface in order to consider the delaying and attenuating effect of the snowpack on diurnal runoff hydrographs and to derive velocities of water percolation.

5.3.1 Lysimeter records

Data is available from three lysimeters located at L during the period 2nd – 12th July 2004. The first, Lysimeter A, consisted of a single section of drainpipe (area 0.10 m^2) and was located close to the snowpack surface until 4th July. Lysimeter B, consisting of three small drainage structures connected together to drain a total area of 0.32 m^2, was installed at the base of the snowpack on 4th July at an initial depth of 65 cm. Lysimeter C consisted of a single section of drainpipe (area 0.09 m^2) and was located close to the snowpack base throughout. Very heavy rain on 7th and 8th July led to irregular lysimeter records that could not be reliably related to surface input fluxes, and these days were therefore disregarded from subsequent analysis. Lysimeter data is presented in Figure 5.20.
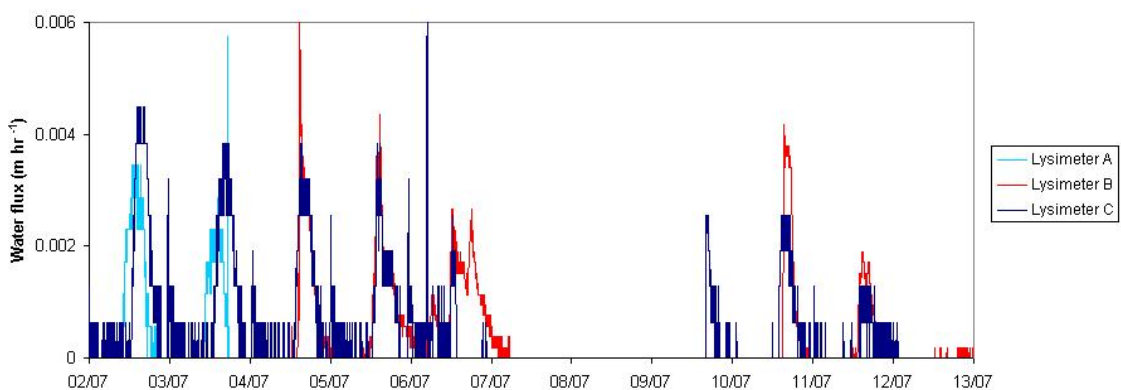
Figure 5.20: Water discharge through the snowpack as measured by lysimeters at L in 2004. Lysimeter depths were as follows: Lysimeter A – c. 25 cm on 2nd July, Lysimeter B – c. 65 cm on 4th July, Lysimeter C – c. 75 cm on 2nd July.

5.3.1.1 Analysis of lysimeter data

Initial visual inspection of the lysimeter records in Figure 5.20 raised two obvious points. Firstly, the delay caused by water percolation through the snowpack depth is clear from the lag between the hydrographs from Lysimeters A and C on the 2nd and 3rd July. Secondly, there is a very good match between records from Lysimeters B and C from 4th July on, which increases confidence in the reliability of data provided by these lysimeters, despite their small size.

Lysimeter data from the 2nd and 3rd July is shown in more detail in Figure 5.21, along with the surface melt flux for this period as modelled using Brock and Arnold's (2000) energy balance model (refer to Appendix B for information about energy balance model). Comparison of surface and lysimeter flux records enables consideration of the change in runoff hydrograph timing and magnitude that is caused by percolation through the snowpack. The delay caused by flow through the snowpack depth is clearly visible, with runoff at Lysimeter C (at ~75 cm depth) beginning to rise over 4 hours after the onset of surface melt. This corresponds to a percolation velocity of around 0.19 m hr^{-1}. Runoff at Lysimeter A, around 25 cm from the snowpack surface, was delayed by around 2 hours, equivalent to a percolation velocity of 0.12 m hr^{-1}. Also notable is a lack of dispersion of hydrograph form, even after percolation through 75 cm of snow to the depth of Lysimeter C – the form of the hydrograph peak was largely unaltered, with the exception of the formation of a slight trailing limb. In Lysimeter C records, peak flux magnitude at the lysimeter was on both days very similar to peak melt input at the surface, suggesting that flow through the snowpack had little attenuating influence on flux magnitude. Hydrographs from Lysimeter A in comparison show a loss of peak flux magnitude. It is unclear whether either of these effects (preservation of flux magnitude at Lysimeter C and loss of peak flux magnitude at Lysimeter A) reflects the true influence of the snowpack on hydrograph form or might be attributed to under- or over-catch of percolating meltwater due to heterogeneous flow patterns within the snowpack.

Lysimeters B and C, located at the same depth in the snowpack, both showed a lag of on average 4 hours between the onset of melt at the snowpack surface and discharge near the snowpack base during the period 4th – 12th July (Figure 5.22). As lysimeters were located around 60 cm from the surface, this lag corresponds to a percolation velocity of about 0.15 m hr^{-1}. Again, there was little visible dispersion of hydrograph form and peak flux magnitudes at lysimeter depth remained comparable to surface inputs (given the likely under- or over-catch expected at lysimeters).
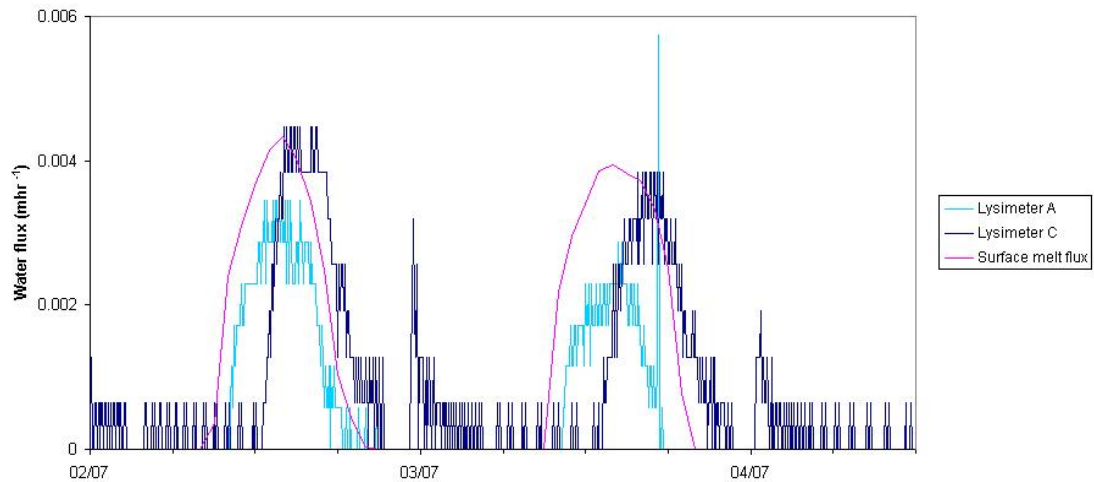
Figure 5.21: Comparison of input surface melt flux and discharge through the snowpack at lysimeters A and C, 2nd and 3rd July 2004. Lysimeter depths on 2nd July: Lysimeter A – 25 cm, Lysimeter C – 75 cm.
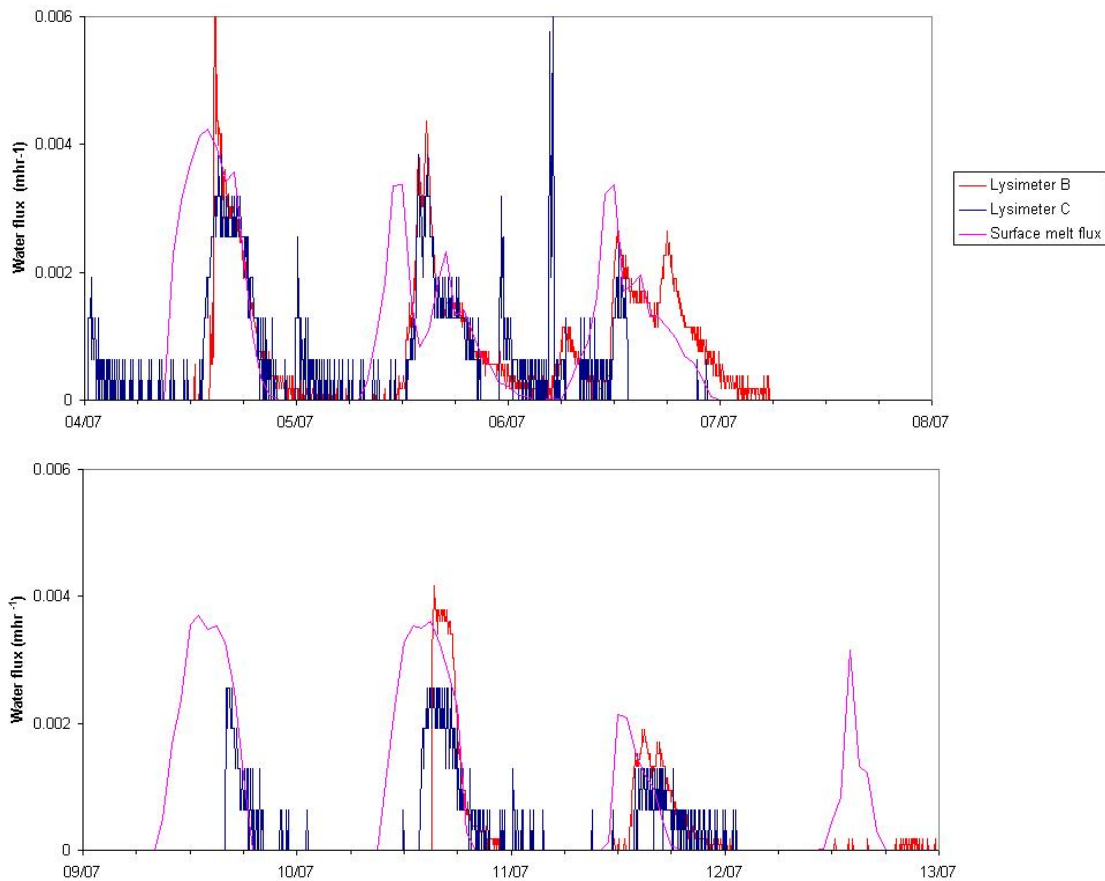
Figure 5.22: Comparison of input surface melt flux and discharge through the snowpack at lysimeters B and C, 4th – 12th July 2004. Both lysimeters were at a depth of c. 65 cm on 4th July.

Derivation of water flow velocities from lysimeter data followed the method described by McGurk and Kattelman (1986) and Fox et al. (1999). Discharge hydrographs from both the surface and depth were converted to cumulative percentage discharge curves and the lag between production of a cumulative flux value at the surface and detection of the same

cumulative flux at depth was found and converted to a flow velocity using the known depth of the lysimeter. Lysimeter data from the 3rd, 4th, 6th and 10th of July were selected for analysis as dye percolation velocities from quantitative surface dye injections on those days were available for comparison. Results based on 3rd and 10th July data gave best results due to the very regular form of the surface melt curve (Figures 5.21 and 5.22). The irregular form of the surface melt curve on 6th July (Figure 5.22) in contrast resulted in an unclear relationship between flux volume and percolation velocity, and data from this day was not considered further.

Percolation velocities calculated from lysimeter data ranged between 0.04 and 0.20 m hr^{-1}, with larger melt fluxes as expected moving at a faster rate (Figure 5.23). Percolation velocities were in general lower than those derived from dye tracing experiments (nine of the fourteen v_{dom} values found in 2004 exceeded 0.20 m hr^{-1}), but this may be attributed to the higher fluxes created by the addition of water with dye. The relationship between flux magnitude and percolation rate according to lysimeter data is similar for all three days (Figure 5.23). Figure 5.23 also shows the relationship between flux magnitude and percolation rate as predicted by Colbeck (1978a; Equation 2.12) for a snowpack with a permeability of 1.79×10^{-10} m^2 (identified in section 5.2.10 as an expected minimum value found when Shimizu's (1970) equation is used to predict snow permeability). This
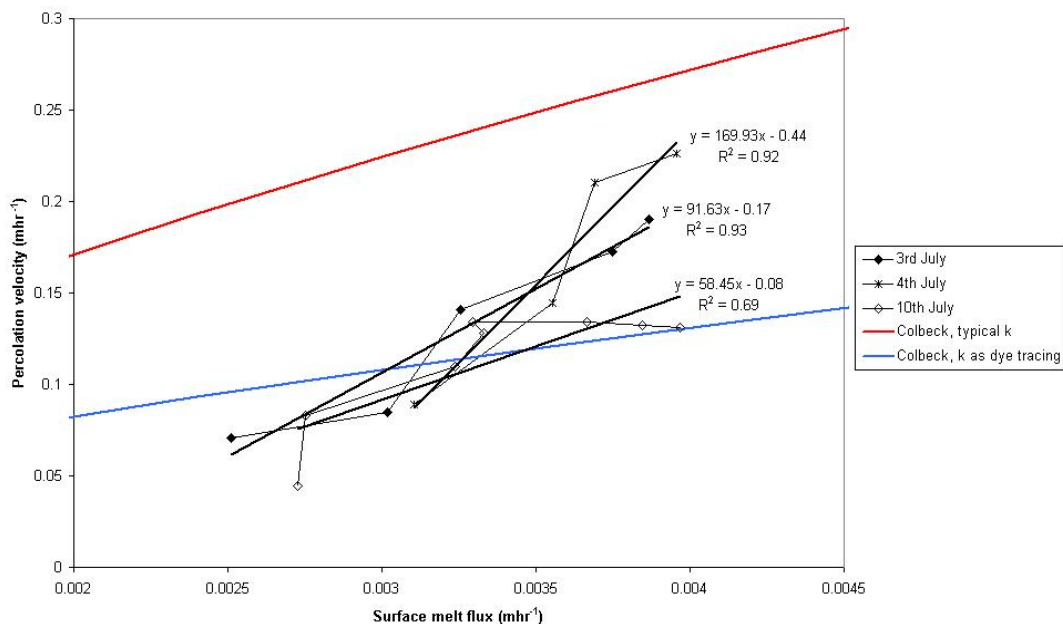
Figure 5.23: Relationship between surface melt flux and percolation velocity as derived from lysimeter data. Lysimeter for all 3 days analysed here indicates a flux-velocity relationship significantly different from that predicted by Colbeck (1978a; Equation 2.12 – red line) for a snowpack having permeability around the minimum often assumed in previous studies. Use of a lower permeability value as determined by dye tests in section 5.2.10 gives a better match to lysimeter data (blue line).

relationship predicts percolation rates significantly higher than were found from lysimeter data. Only the assumption of a lower snow permeability value similar to that found from early-season quantitative dye tracing tests in 2004 (2.0×10^{-11} m^2) will explain percolation velocities of this magnitude using Equation 2.12, with the blue line on Figure 5.23 seen to provide a better fit to lysimeter data. The analysis of lysimeter data therefore supports one of the major conclusions drawn from quantitative surface dye injections, namely that the permeability of a natural heterogeneous snowpack is likely to be significantly lower than often assumed, and that more reliable estimation of snowpack permeability is required if runoff patterns are to be properly understood.

Using the equations shown in Figure 5.23 for the relationship between flux magnitude and percolation velocity on the 3rd and 10th June, together with surface fluxes at the time of dye injections on those days (Table 5.5), the expected rate of dye percolation according to lysimeter data can be calculated. This produces estimated dye percolation velocities of 0.40 and 0.15 m hr^{-1} for 3rd and 10th June respectively, compared to observed dominant dye percolation rates of 0.33 and 0.44 m hr^{-1}. Dye percolation velocities are clearly not simply comparable to lysimeter data, although discrepancies could easily be attributed to precise flux conditions around the time of dye injections.

5.4 WATER FLOW THROUGH THE BASAL SATURATED LAYER

Water flow through the basal saturated layer is expected to be much more efficient than vertical percolation through the snowpack. This difference is primarily due to the increase in snow permeability to water flow as water saturation increases. The effect of ice layers through the snowpack depth inhibiting percolation and larger grain sizes in the saturated layer further enhance the difference in permeability between the unsaturated and saturated regimes. Cumulatively, these effects have been predicted to increase permeability in the basal saturated layer compared to that in the unsaturated regime by a factor of 10^6 (Colbeck, 1978a). Field observations have confirmed that flow rates at the base of the snowcover are significantly higher than observed percolation velocities (e.g. Fujino, 1971). It is therefore expected that for snowpacks of any significant depth, it is the unsaturated regime that primarily controls the snowpack's influence on runoff. Dye tracer investigations of water flow in the basal saturated layer at Haut Glacier d'Arolla are presented in this section, enabling the character of flow to be identified and its role in influencing runoff assessed.

5.4.1 Quantitative dye tests in the basal saturated layer

Dye injections into the basal saturated layer were intended primarily for fluorometric detection. However, return curves were frequently of poor quality, in which case the time of dye emergence in the snowpit was where possible noted visually to give an estimate of dye transit time and flow velocity. A full chronological list of dye injections carried out for

quantitative detection during both field seasons is presented in Appendix C, and the success rate of this technique, and the possible reasons for experiment failure, are discussed. Problems obtaining quantitative return curves from injections in the basal saturated layer are attributed to the difficulty of predicting the fluorometer location necessary to capture dye emerging from the saturated layer in a narrow plume, combined with other difficulties in reliably detecting the dye pulse as discussed in section 3.6.4.2. In addition, the failure of some dye injections to reach the snowpit may result from the retention of dye in unsaturated snow at the base of the injection borehole. In total, eleven successful dye tests through the saturated layer were carried out in 2003, and ten in 2004. Injections in both years were carried out at a number of different pits at all three study sites. As the slope of the glacier ice surface varied between sites, valid comparisons cannot be made between sites when attempting to infer changes in basal flow conditions. Dye experiments do, however, show the general nature of water flow in the basal saturated layer, enabling the role of this flow regime in influencing runoff to be considered.

5.4.1.1 Analysis of basal returns

Successful dye return curves for injections in the basal saturated layer are presented in Figures 5.24 and 5.25 for 2003 and 2004 respectively. Most injections yielded highly peaked return curves, with the majority of dye passing the fluorometer in less than 2 hours (and often less than 1 hour). An exception is the curve from 21st June 2004, when dye continued to be recovered for over 8 hours. Curves from 2nd June 2003 and 19th June 2004 also exhibited trailing limbs continuing for several hours although peak dye concentrations were observed between 1 and 2 hours after injection. As mentioned above, such a delay in dye movement might be attributed to retention of dye in unsaturated snow at the base of the injection borehole. It is also likely that some dye was injected onto drier areas of the ice surface (akin to local 'interfluves'), where any flow through the saturated layer would take place more slowly.

The times to first, peak, 50% and last dye recovery were derived from return curves and used to calculate maximum, dominant, mean and minimum velocities of dye movement through the basal saturated layer (Table 5.9). Visual observations of dye emergence times were usually of first dye emergence but could also include estimates of peak dye emergence (by brightest dye appearance) and last dye emergence; these are expected to yield less accurate estimates of dye flow velocity and are annotated as such in Table 5.9.

Flow velocities in the saturated layer reached a maximum of 28 m hr^{-1}, while dominant velocities ranged between 1.35 to 18.48 m hr^{-1}. Although there was much variability in the flow velocities observed, water flow in the basal saturated layer took place on average one
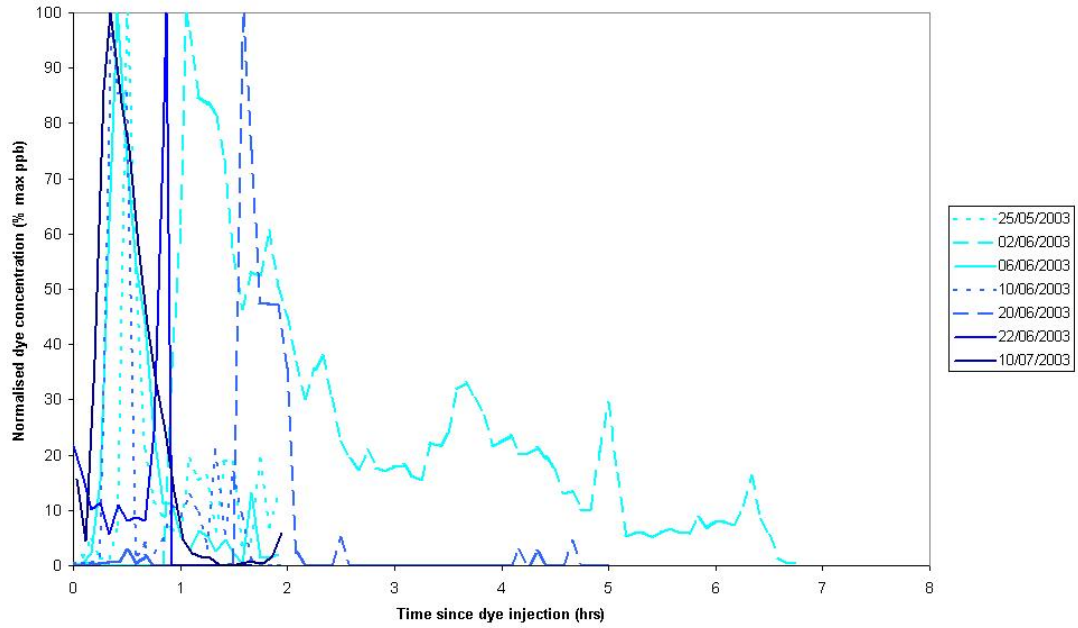
Figure 5.24: Return curves from quantitative dye injections in the basal saturated layer, 2003. An impression of the temporal sequence in which experiments were carried out is given by the line colour (light blue = first injection, dark blue = last injection).
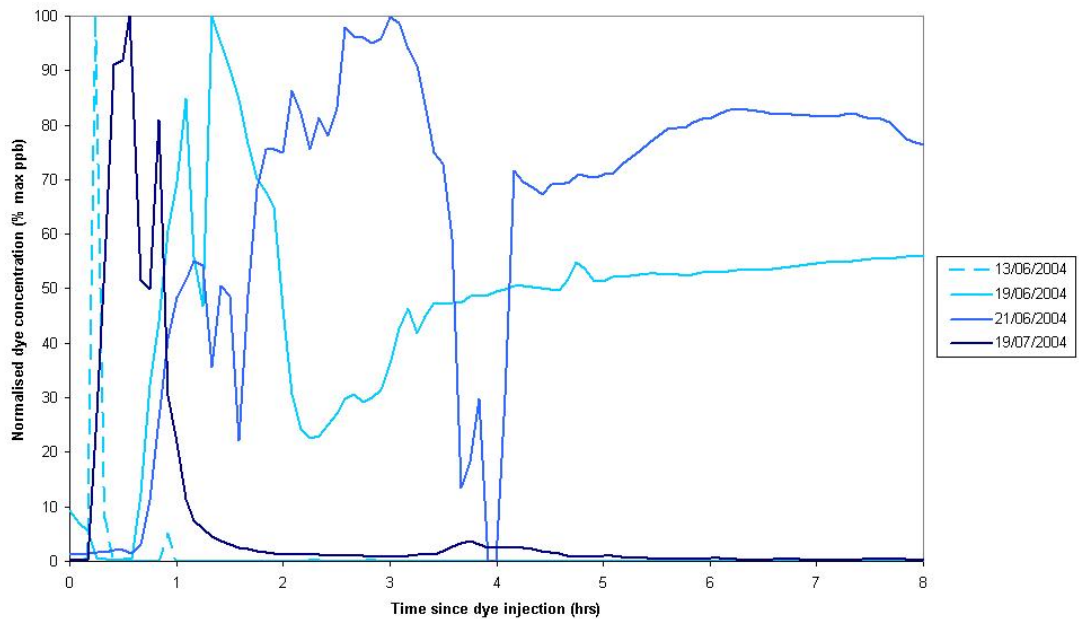
Figure 5.25: Return curves from quantitative dye injections in the basal saturated layer, 2004.

to two orders of magnitude faster than percolation in the unsaturated regime. Mean v_{dom} for all 2003 and 2004 results was 0.27 m hr^{-1} for percolation compared to 7.23 m hr^{-1} for water flow in the basal saturated layer.

Table 5.9: (continued on next page) Times and velocities derived from dye injections in the basal saturated layer. Data derived from visual observations of dye emergence is expected to be less reliable and is printed in grey. Refer to Figure 3.1 for the locations of study sites L, M and U. At each site multiple pits used for dye experiments were located close together.

Date	Location	Basal distance (m)	Injection time	t_{min} (hrs)	t_{dom} (hrs)	t_{mean} (hrs)	t_{max} (hrs)
25/05/2003	L1	4.00	13:21	0.41	0.49	0.55	1.08
02/06/2003	L2	4.00	09:24	0.82	1.06	-	-
			10:09	0.07	0.61	-	-
06/06/2003	L3	4.00	12:48	0.18	0.41	0.50	1.51
10/06/2003	L3	4.00	11:05	0.23	0.36	0.47	1.80
13/06/2003	M3	4.00	13:13	0.69	0.82	1.88	4.90
19/06/2003	M1	4.00	14:10	0.17	-	-	-
20/06/2003	U1	4.00	12:45	1.50	1.58	1.74	2.08
22/06/2003	U1 (F)	6.00	14:30	0.70	0.87	-	-
22/06/2003	U1 (RWT)	3.00	14:30	0.70	-	-	-
10/07/2003	U6 (F)	6.00	13:10	0.14	0.32	0.45	1.05
10/07/2003	U6 (RWT)	2.00	13:10	0.15	0.31	-	-

Date	Location	Basal distance (m)	Injection time	v_{max} (m hr^{-1})	v_{dom} (m hr^{-1})	v_{mean} (m hr^{-1})	v_{min} (m hr^{-1})
25/05/2003	L1	4.00	13:21	9.74	8.09	7.29	3.70
02/06/2003	L2	4.00	09:24	4.88	3.77	-	-
			10:09	57.39	6.55	-	-
06/06/2003	L3	4.00	12:48	22.86	9.66	8.05	2.66
10/06/2003	L3	4.00	11:05	17.32	11.17	8.47	2.22
13/06/2003	M3	4.00	13:13	5.81	4.90	2.13	0.82
19/06/2003	M1	4.00	14:10	24.00	-	-	-
20/06/2003	U1	4.00	12:45	2.66	2.53	2.30	1.92
22/06/2003	U1 (F)	6.00	14:30	8.57	6.90	-	-
22/06/2003	U1 (RWT)	3.00	14:30	4.29	-	-	-
10/07/2003	U6 (F)	6.00	13:10	43.26	18.48	13.33	5.73
10/07/2003	U6 (RWT)	2.00	13:10	13.36	6.54	-	-

Date	Location	Basal distance (m)	Injection time	t_{min} (hrs)	t_{dom} (hrs)	t_{mean} (hrs)	t_{max} (hrs)
12/06/2004	Wet Pit at L	4.00	14:04	-	0.93	-	-
13/06/2004	Wet Pit at L	4.00	12:00	0.17	0.25	0.26	0.34
15/06/2004	Pit A at L	4.00	13:50	0.25	-	-	-
18/06/2004	Pit A at L	4.00	14:40	0.17	0.42	-	1.52
19/06/2004	Pit B at L	4.00	12:49	0.64	1.14	-	-
21/06/2004	Pit A at L	4.00	14:25	0.66	2.97	-	-
19/07/2004	M2	4.00	13:28	0.23	0.43	0.61	2.00
21/07/2004	M2	4.00	11:51	2.22	2.89	2.94	-
21/07/2004	M2	4.00	15:31	0.21	0.38	1.53	-
26/07/2004	M5	4.00	12:30	0.74	1.46	1.77	-

Date	Location	Basal distance (m)	Injection time	v_{max} (m hr^{-1})	v_{dom} (m hr^{-1})	v_{mean} (m hr^{-1})	v_{min} (m hr^{-1})
12/06/2004	Wet Pit at L	4.00	14:04	-	4.29	-	-
13/06/2004	Wet Pit at L	4.00	12:00	23.81	16.14	15.58	11.66
15/06/2004	Pit A at L	4.00	13:50	16.00	-	-	-
18/06/2004	Pit A at L	4.00	14:40	24.00	9.60	-	2.64
19/06/2004	Pit B at L	4.00	12:49	6.23	3.52	-	-
21/06/2004	Pit A at L	4.00	14:25	6.10	1.35	-	-
19/07/2004	M2	4.00	13:28	17.34	9.29	6.58	2.00
21/07/2004	M2	4.00	11:51	1.80	1.39	1.36	-
21/07/2004	M2	4.00	15:31	19.27	10.45	2.61	-
26/07/2004	M5	4.00	12:30	5.40	2.74	2.27	-

The peaked form of return curves from basal injections indicates that little dispersal of the dye pulse occurred during flow through the saturated layer. Calculated values for the dispersion coefficient D and dispersivity d are shown in Table 5.10. Values for D ranged between 2.29×10^{-6} and 2.61×10^{-3} m^2 s^{-1} in 2003 and between 5.15×10^{-5} and 1.00×10^{-3} m^2 s^{-1} in 2004. Values for d ranged between 3.25×10^{-3} and 5.08×10^{-1} m in 2003 and between 0.0115 and 0.749 m in 2004. Values of both D and d largely overlap with those found for surface dye injections in sections 5.2.4 and 5.2.9.

Table 5.10: *D* and *d* values for basal dye injections in a) 2003 and b) 2004, together with flow velocities used in their calculation.

a) Date	v net (m hr^{-1})	D (m^2 s^{-1})	d (m)
25/05/2003	8.09	4.50E-05	2.00E-02
02/06/2003	3.77	6.99E-05	6.68E-02
06/06/2003	9.66	3.48E-04	1.30E-01
10/06/2003	11.17	2.58E-04	8.33E-02
20/06/2003	2.53	2.29E-06	3.25E-03
22/06/2003	6.90	9.17E-06	4.78E-03
10/07/2003	18.48	2.61E-03	5.08E-01

b) Date	v net (m hr^{-1})	D (m^2 s^{-1})	d (m)
13/06/2004	16.14	5.15E-05	1.15E-02
19/06/2004	3.52	2.01E-04	2.06E-01
21/06/2004	1.35	2.81E-04	7.49E-01
19/07/2004	9.29	1.00E-03	3.89E-01

5.4.2 Summary

Results from quantitative dye tracing in the basal saturated layer confirm that water flow at the snowpack base takes place much faster (typically by one to two orders of magnitude) than vertical percolation through the snowpack. Flow in the saturated layer will therefore cause less change to the timing and magnitude of the runoff hydrograph.

5.5 SPATIALLY INTEGRATED EFFECT OF SNOWPACK HYDROLOGY

Results presented in sections 5.2 to 5.4 provide valuable information about the nature and evolution of water flow both vertically through the snowpack depth and laterally in the basal saturated layer. However, if the snowpack's effect on discharge into the englacial and subglacial drainage systems (and subsequently on ice dynamics) is to be considered, it is necessary to examine how these essentially 'point' processes influence runoff across a wider area of the supraglacial drainage system. This section analyses records of basal saturated layer depth as a measure of water discharge across the glacier surface. This data shows the runoff pattern that results from snowpack effects across the supraglacial catchment upglacier from the measurement site. Basal water table records were analysed to examine the change in runoff timing and magnitude caused by flow through the snow-covered supraglacial drainage system, and any change in this effect through time (section 5.5.2). Modelling and observation of saturated layer distribution across the glacier surface were used to consider the importance for runoff of spatial variations in water table depth (section 5.5.3).

5.5.1 Principles of basal water table monitoring

At the outset, it is necessary to outline several assumptions made during analysis of basal water table records, and the principles that are used during interpretation of this data. Firstly, water level in the basal saturated layer is assumed to correspond to discharge through this part of the drainage system. Changing water level as measured using pressure transducers therefore enables investigation of discharge patterns across the glacier surface. Although pressure transducers were not located close to exit points from the supraglacial drainage system (moulins or crevasses), patterns of water level change observed at pressure transducer locations are assumed to represent changing water discharge equivalent to that across a supraglacial catchment of unknown size. Local spatial variations in water table trends (particularly the difference between water level change in supraglacial channels of different sizes) are unknown, but pressure transducer data is presumed to usefully indicate runoff trends.

The pattern of water flow at the snowpack base is the product of spatial and temporal variations in meltwater generation at the snow surface and the way in which water is subsequently routed through the snowpack. Basal water table records were analysed to investigate their relationship to meltwater inputs at the snow surface, from which the net modifying role of the supraglacial snowpack could be inferred. The arrival of water at the pressure transducer location is a function of delaying and dispersive effects during percolation through the snowpack depth and lateral flow in the saturated layer. Evidence for the magnitude of such effects was sought in the timing and form of any diurnal cycles

present in the basal water table record. If the transit time through the snow system is large, any short-period variation of input flux will be damped out (as noted by Colbeck (1974) in his analysis of water flow in the basal saturated layer). Conversely, if transit time is small compared to the period of input flux variations (in this case one day), the cyclic character of flow at the snow surface will be preserved (Colbeck, 1974). Dispersion of the hydrograph form between the snow surface and measurement location in the basal saturated layer is attributed to dispersive processes during percolation and to a lesser degree during basal saturated flow, *plus* the differing timing of hydrograph delivery to the measurement point due to water transit across a catchment of varying shape, slope, and snowpack depth. Any evidence of these dispersive effects was also sought during analysis of basal water depth records.

5.5.2 Basal water depths

2003

Pressure transducers records at L in 2003 were obtained from 13th May until logger failure on 6th June. Decreasing snow depths shortly thereafter would have made further pressure transducer positioning impossible. Records were obtained at U from 16th May until 6th July, although the final few days of data may not be reliable due to shallow snow depths and instrument instability.

2004

A pressure transducer at U provided data throughout summer 2004 from 20th May onwards and a pressure transducer at M provided data from 14th June until the end of the season. For unknown reasons, the pressure transducer placed in the basal saturated layer at L produced erroneous data throughout the 2004 field season.

Basal water depth records from the 2003 and 2004 field seasons are presented in Figures 5.26 and 5.27 respectively.

5.5.2.1 Description of basal water depths

There is considerable variation between the four basal water depth records obtained. In 2003, the record from L shows water depths rising during the early melt season and the onset of marked diurnal hydrograph cycles (amplitude c.2 to 4 cm) around 28th May (Figure 5.26a). Water depths at U in 2003 were consistently above 14 cm, although this may be attributed to an error in pressure transducer calibration. There was a gradual increase in water depth at U from the start of the record with diurnal cycles also becoming visible around 28th May and becoming more pronounced over the following three weeks (Figure 5.26b). The form of these diurnal cycles was more subdued than those at L, with amplitude less than 0.5 cm. On 23rd June there was a sudden rise in water depth at U and diurnal cycles become more marked, with a somewhat asymmetric shape.

a)
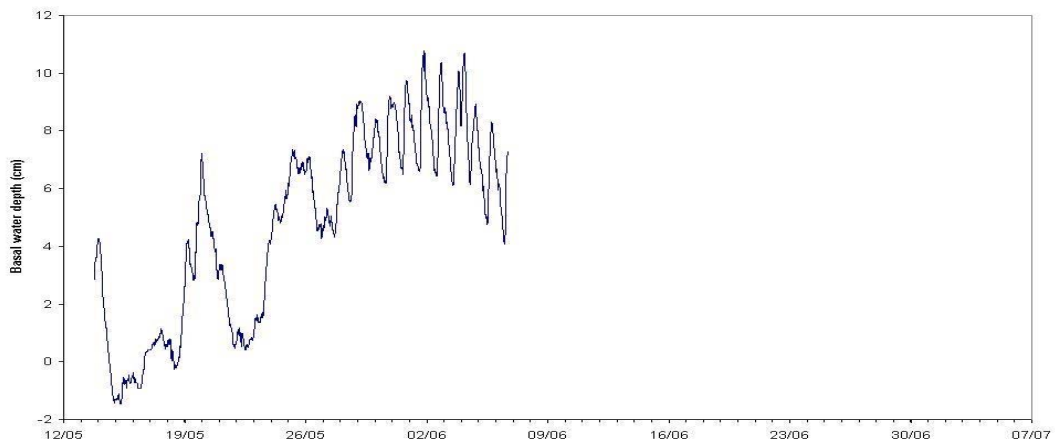
b)
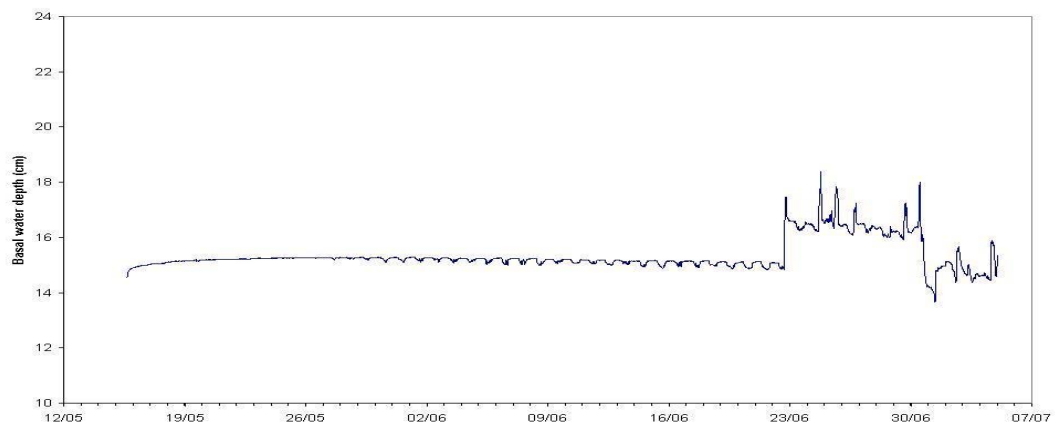
Figure 5.26: Basal water table records from a) L and b) U in 2003, both showing evidence of increasing water table depth and more pronounced diurnal cyclicity through time.

The water table record from M in 2004 showed marked diurnal cycles (Figure 5.27a), although of a slightly different form from those seen at L in 2003 and greater amplitude (up to 10 cm water level variation). The 2004 U record initially bears some similarity to that from U in 2003 as it rises gradually with poorly-developed diurnal cycling, before it develops clear, though low amplitude (3-4 cm), diurnal cycles on 8th June (Figure 5.27b). Although the depths of basal water at M and U were very different, a plot of both data series with y-axes adjusted to enable comparison (Figure 5.28) reveals a very good match between the two data series in terms of the timing of daily hydrographs and some of the major increasing or decreasing trends of hydrograph magnitude. This suggests a general similarity in the pattern of runoff at the base of the snowpack, presumably due to similar snow depths (Figure 4.5) and snowpack hydraulics in the catchments above M and U.
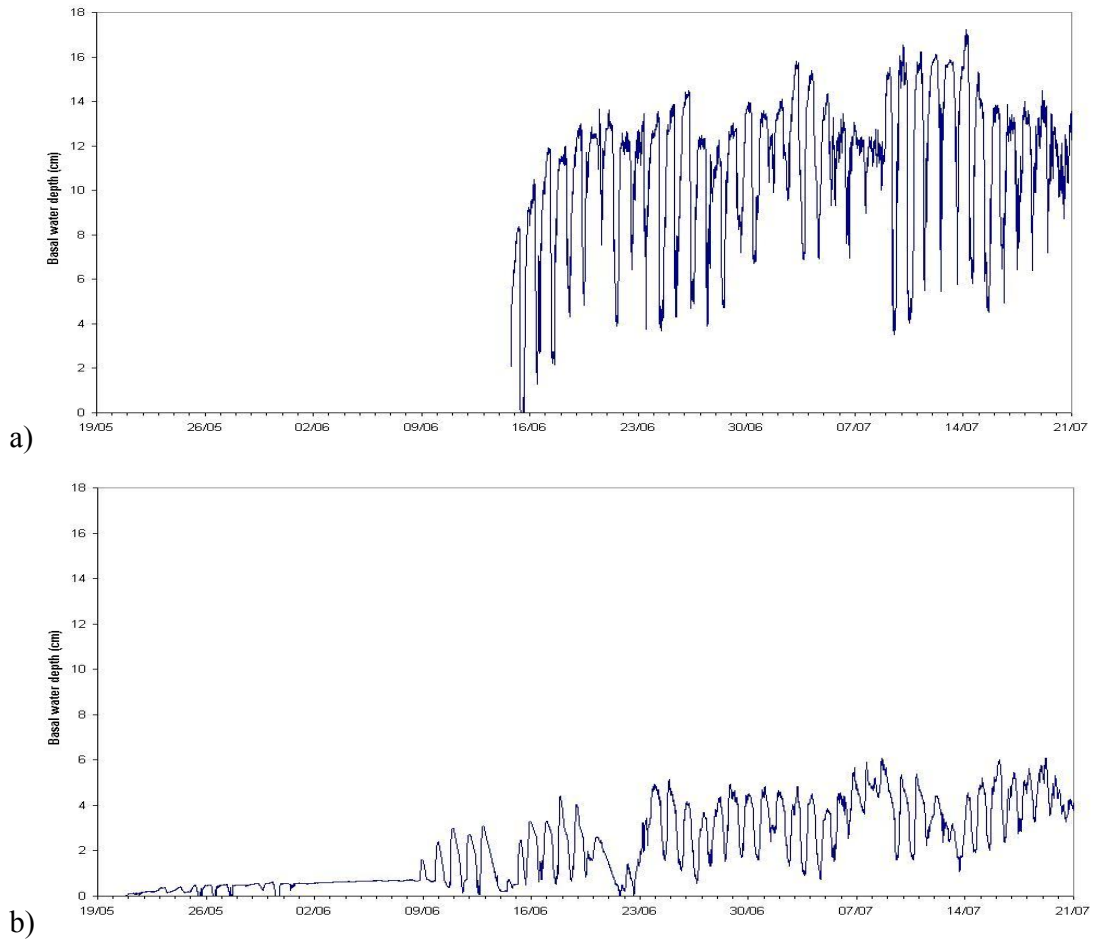
Figure 5.27: Basal water table records from a) M and b) U in 2004. Marked diurnal cycles can be seen at M. The record from U shows poorly-developed diurnal cycles initially, becoming clear on 8th June.
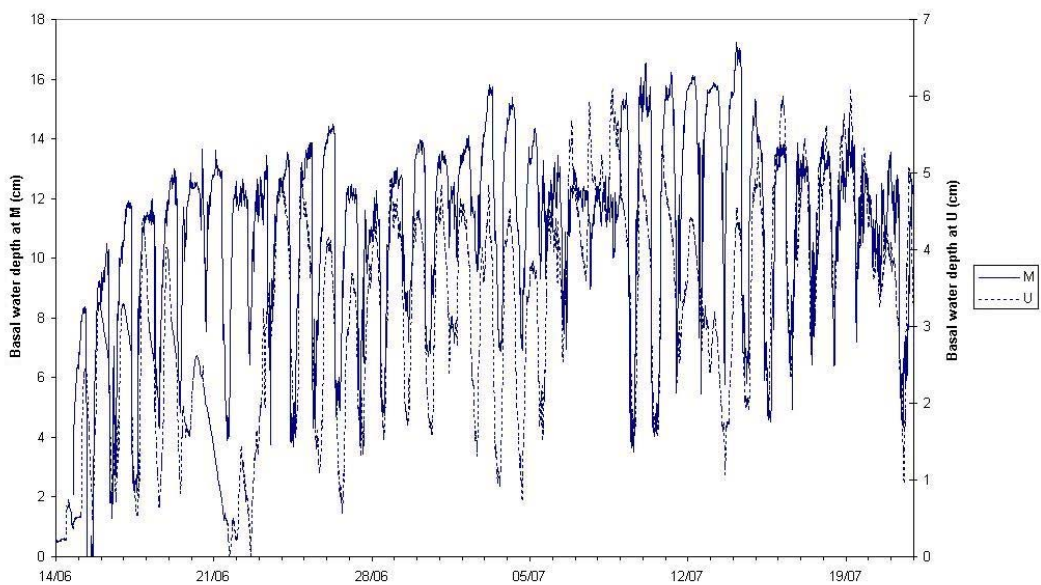
Figure 5.28: Comparison of basal water table records from M and U in 2004, showing a very good match between the two data series in terms of the timing of daily hydrographs and some of the major increasing or decreasing trends of hydrograph magnitude.

5.5.2.2 Analysis of basal water depth records

The presence of clear diurnal cycles in all basal water table records indicates that much of the surface meltwater is moving through the supraglacial catchment in much less than one day, allowing preservation of hydrograph form. The snowpack therefore does not store water for long time periods, although a large volume of water may be in transient storage in the snowpack at any one time.

Comparison of basal water depth series to air temperature series (Figures 5.29-5.32) yielded more information about the effect on runoff of water transit through the snow-covered supraglacial catchment. Air temperature was used in place of modelled surface melt flux as data was available at a higher temporal resolution and for the complete period of basal water table data in both 2003 and 2004. Air temperature is a commonly used index of melt input but generally lags melt production; in a previous study at Haut Glacier d'Arolla, Swift et al. (2005) found this lag to be around two hours.

In two of the data sets (L 2003 and U 2004; Figures 5.29 and 5.32), the changing depth of the basal saturated layer can clearly be seen to follow the pattern of changing air temperature. This is particularly clear in the case of 2003 L data, when the depth of the basal water table closely responds to varying inputs even in May. This correspondence, as with the preservation of diurnal hydrograph cycles discussed above, suggests that flow through the snowpack is sufficiently efficient as to preserve the pattern of melt input from the snowpack surface.

For all days on which diurnal variation was clear in both the air temperature and basal water depth records, the lag time between peak air temperature and peak water depth was calculated. This lag time represents the net delay imparted on runoff by flow through the supraglacial snowpack across a distributed area. Lag times for each suitable day are marked on Figures 5.29 and 5.30 for 2003 and plotted separately in Figure 5.33 for 2004. Considering all 2003 and 2004 data, the delay to runoff caused by flow through a snow-covered supraglacial catchment was between 2 and 20 hours.

Isolated, pronounced rainfall inputs on the evenings of 30th May and 3rd June 2003 triggered secondary peaks in basal water table depth, and these were used to calculate an independent estimate of lag time for short-term water inputs. This yielded lags of 6.25 and 7.25 hours respectively, in comparison with values of 7.25 and 5.25 hours derived by the method above on the same days. A close match between values cannot be expected due to differences in flux conditions; the general range of time lags is however corroborated.

_____

In 2003 L data, there is clear ($p < 0.05$) evidence of the lag time between peak input and peak runoff decreasing through time during the three weeks for which data is available, from around 15 to 5 hours (Figure 5.29). This decrease is most pronounced between the 29th and 30th of May, when lag time decreases from 15 to 7 hours between consecutive days. Two periods can therefore be identified in this data: 18th to 29th May, when lag ranges between 10 and 19 hours, and 30th May to 9th June, when lag ranges between 3 and 7 hours. This marked decrease in lag time suggests that water was being routed through the snowpack more efficiently in the latter period, and this is likely to have generated a more peaked input of meltwater to the englacial system. UDG records (Figure 4.6) indicate that snow depth at L on 30th May was around 1.7 m. Examination of records of snowpack stratigraphy (Figure 4.15a) at L shows that four significant ice layers were located just above this depth (between 1.7 and 1.9 m above the glacier ice surface), therefore suggesting that this sudden decrease in runoff lag time may have been related to the melt out of these ice layers. That such a sudden decrease in runoff lag took place while snow depth decreased only gradually points to the limited role that changing snow depth alone plays in influencing changes in runoff. Instead, information about ice layer position would be required in order to understand this change in runoff. Increasing surface melt flux may also have contributed to this change, possibly in combination with the evolution of other snowpack properties (including permeability and preferential flow organisation) that could cause water transmission to change over a short time period.

Data for U in 2003 appears to show a similar decrease in peak-to-peak lag time with date (Figure 5.30), from around 20 hours in early June to around 2 hours in late June. However,
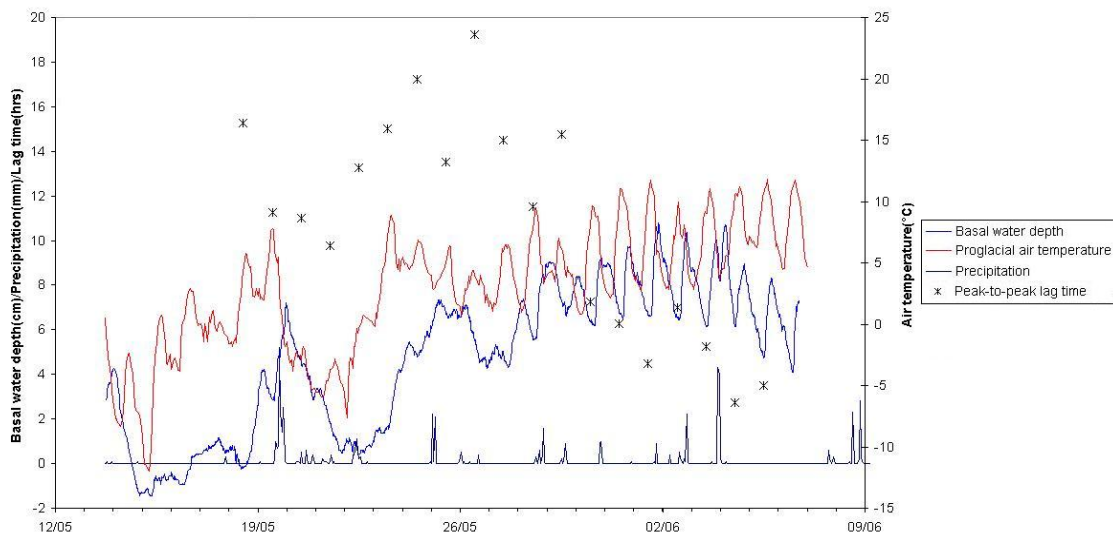
Figure 5.29: Comparison of diurnal cycles of air temperature and basal water table depth at L in 2003, with peak-to-peak lag time indicated. There is clear evidence of the lag decreasing through time, most markedly between the 29th and 30th of May. As snow depth at L on 30th May was around 1.7 m (from UDG data, Figure 4.6), examination of records of snowpack stratigraphy (Figure 4.15a) suggests that this sudden decrease in runoff lag time may have been related to the melt out of the four significant ice layers that were between 1.7 and 1.9 m above the glacier ice surface.

due to the rounded form of diurnal water depth variations prior to 23rd June less confidence is placed in the accurate identification of peak basal water depth and this decrease in lag time may not be reliable. Neither location in 2004 showed evidence of a significant decrease in lag through time (Figure 5.33). This may reflect a real lack of temporal trend in runoff time, but could also be attributed to uncertainty in the analysis: mixed weather conditions and irregular diurnal melt patterns during 2004 likely mean that the time of peak air temperature is a poor index of peak melt input.
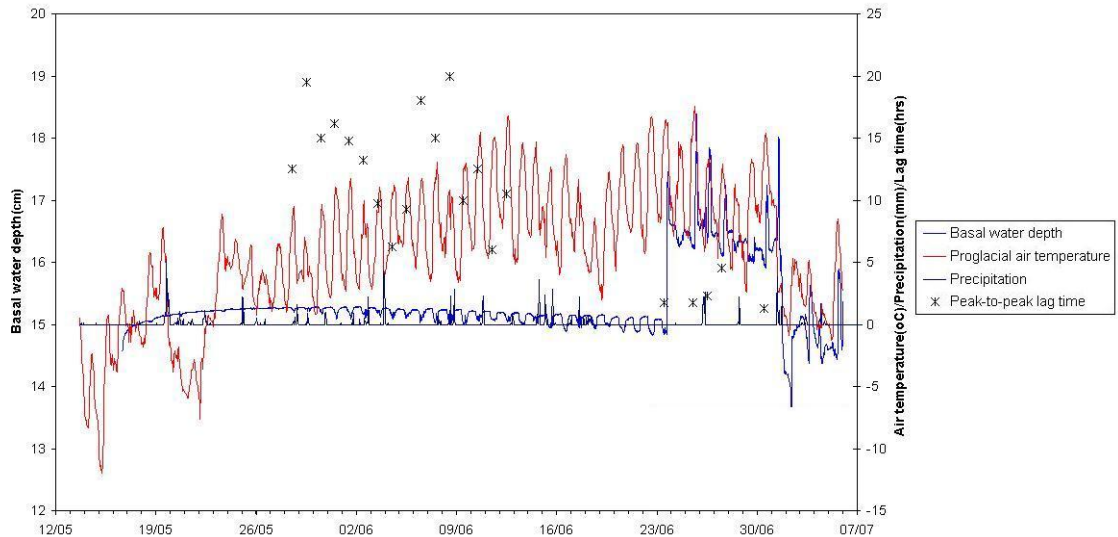
Figure 5.30: Comparison of diurnal cycles of air temperature and basal water table depth at U in 2003, with peak-to-peak lag time indicated. As at L (Figure 5.31), there appears to be a decrease in lag time with date, although less confidence is placed in this trend due to the rounded form of diurnal water depth variations prior to 23rd June and the resulting difficulty in accurately identifying peak basal water depth.
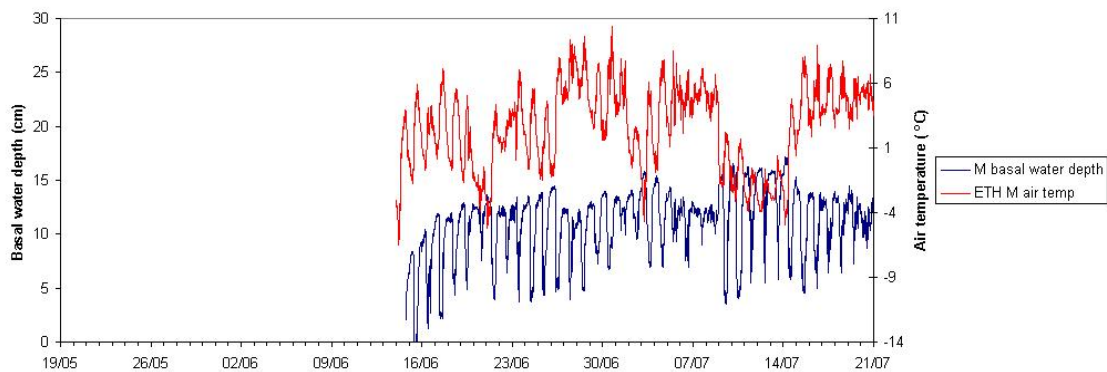
Figure 5.31: Comparison of diurnal cycles of air temperature and basal water table depth at M in 2004.
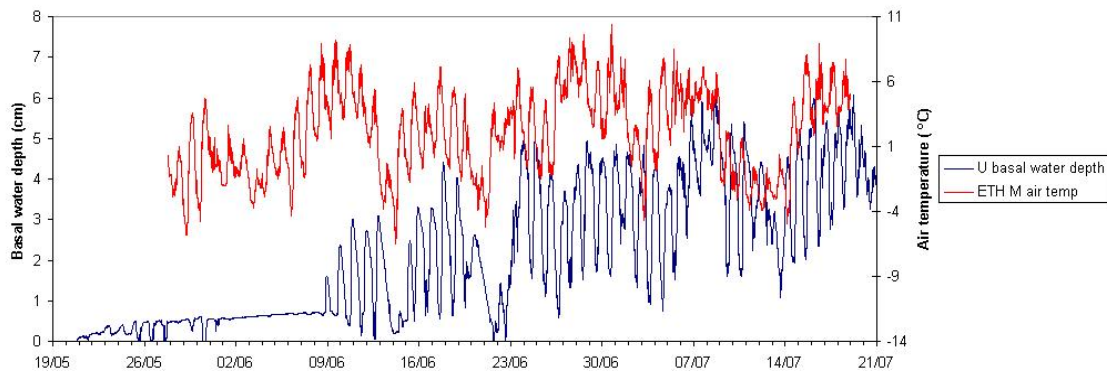
Figure 5.32: Comparison of diurnal cycles of air temperature and basal water table depth at U in 2004.
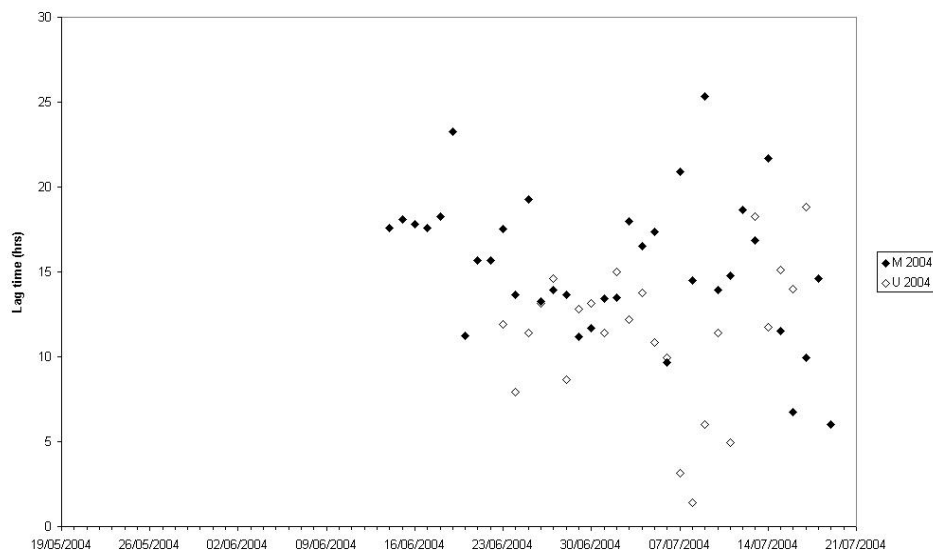
Figure 5.33: Lag time between peak air temperature and peak basal water table depth for M and U in 2004. Neither location shows evidence of a significant decrease in lag through time.

5.5.3 Spatial variation in water table depth

Spatial variation in the depth of the water table may influence runoff at the base of the snowpack. The spatial pattern of water depth on the glacier surface was estimated using a Topographic Wetness Index (TWI) in which wetness is calculated as ln(specific flow accumulation from upslope/tan(slope)) (Schmidt and Persson, 2003; Sørensen et al., 2006). A 20 m digital elevation model (DEM) of the glacier ice surface provided the basis for TWI calculation (DEM provided by A. Sole). The predicted distribution of water across the ice surface is shown in Figure 5.34. This predicted pattern of supraglacial drainage is not a perfect match for that observed in the field, as a result of the expected large errors in ice surface topography in the DEM. However, it illustrates well the general pattern of drainage channels which will be expected on a glacier such as this.

Water flow at the base of the snowpack will also be routed by the topography of the ice surface into channels and catchments similar to those shown in Figure 5.34. On the bare ice surface after snowpack removal many smaller channels, not reproduced in Figure 5.34 due

to the resolution of the DEM, were also observed (Figure 5.35). Observations at the base of snowpits dug throughout both field seasons revealed huge spatial variation in wetness, with the ice surface completely dry in some locations and a water table some 30 cm deep in others. Two transects probed transverse to the ice surface slope at M in July 2004 showed the distribution of basal water in more detail (Figure 5.36). In both, water can be seen attaining a maximum depth of 50 cm in a topographic depression linked to a large supraglacial channel downslope, and is more thinly spread on sloping surfaces.

It is suggested that the efficiency with which water is transferred across the glacier ice surface will be limited where water depths are very low. The injection of dye onto comparatively 'dry' areas of the ice surface during quantitative dye experiments in the basal saturated layer is therefore suggested as a factor contributing to some of the slower flow velocities presented in section 5.4. Conversely, where water is concentrated into channels runoff will be more efficient. The spatial pattern of channels on the ice surface will therefore be an important control on runoff timing and magnitude.
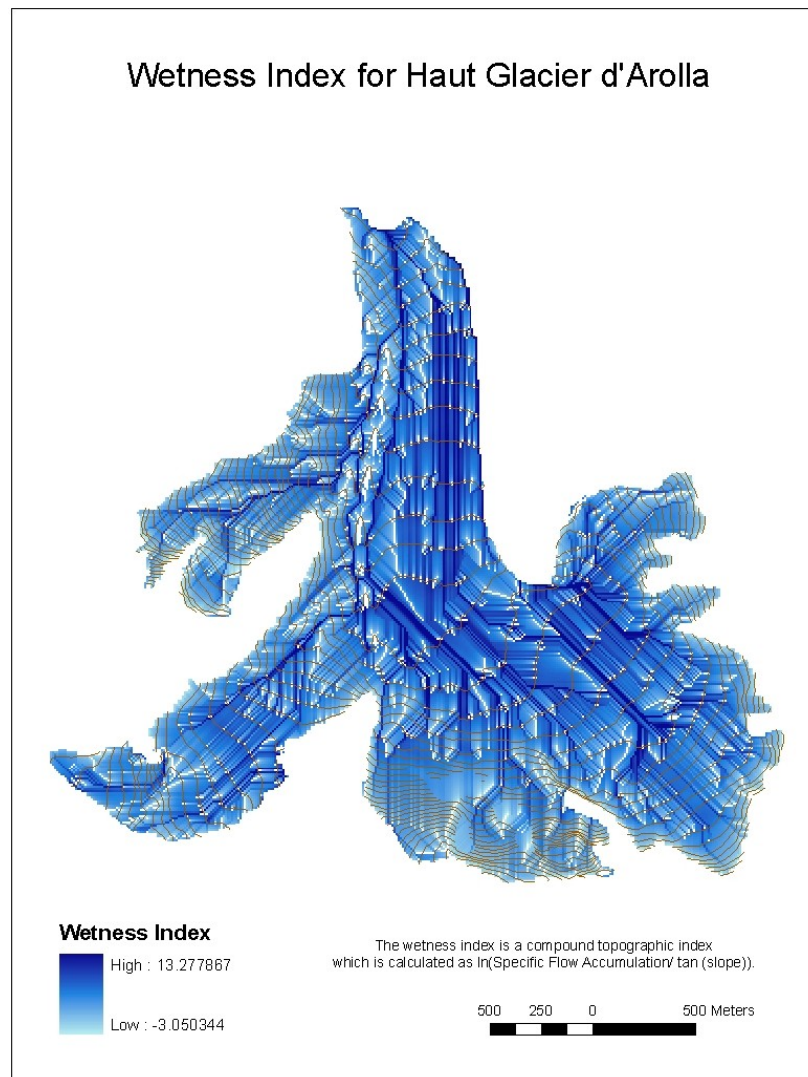
Figure 5.34: Ice surface wetness distribution at Haut Glacier d'Arolla as predicted by TWI.

_____
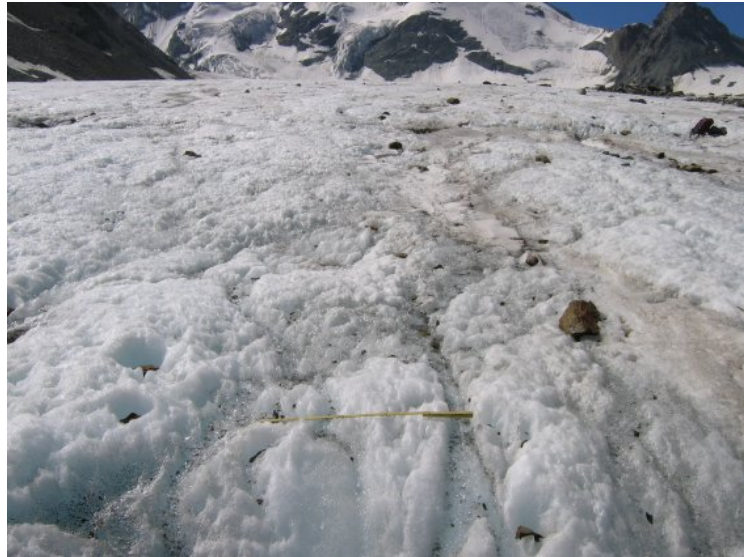
Figure 5.35: Supraglacial drainage at L in late 2004, showing small-scale channel pattern. Rule = 2 m.
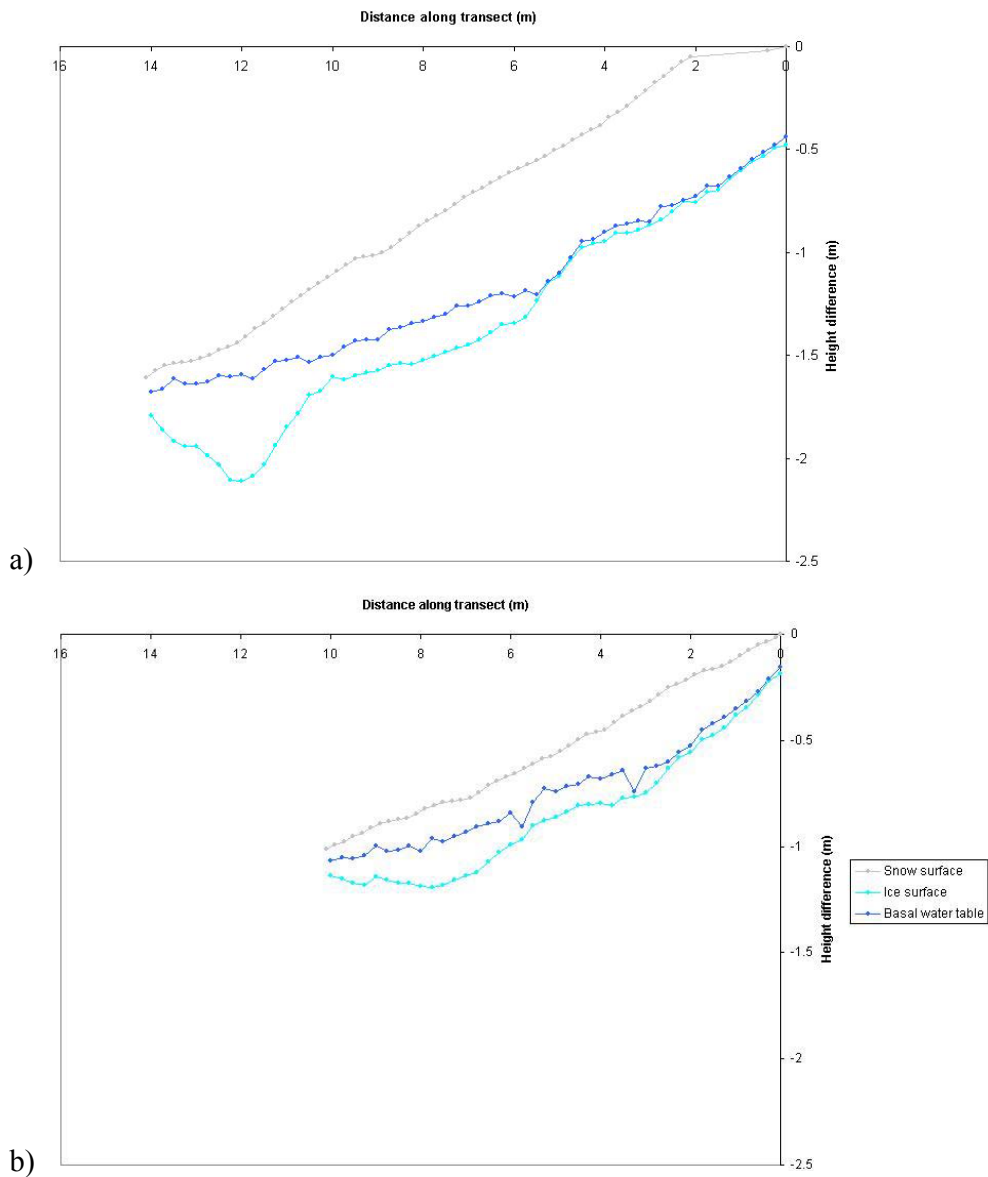
Figure 5.36: Distribution of the water table at the snowpack base at M, on a) 21st and b) 25th July 2004.

5.5.4 Summary: spatially integrated effect of snowpack hydrology

The delay imparted to runoff by flow through the snowpack, as shown by lag times between peak surface melt and peak runoff in the basal saturated layer, may be as much as 20 hours early in the melt season. Early in 2003, runoff through the snowpack at L, despite being delayed by over 10 hours, was sufficiently efficient as to preserve the pattern of input surface flux in runoff (Figure 5.29). On other occasions (e.g. at U in 2004; Figure 5.32), diurnal runoff cycles were dampened early in the melt season, becoming more pronounced later.

With the exception of those from M in 2004, all basal water table records showed clear evidence of evolution through time. More pronounced diurnal cyclicity in runoff records (Figures 5.30 and 5.32) and decreasing lag times between input and output peak fluxes (Figures 5.29 and 5.30) indicate that water transfer through the snowpack became more efficient and that the net delay imparted on runoff into the rest of the glacier system decreased with date through the melt season. In 2003, data from L showed a particularly marked decrease in lag time occurring suddenly around 30th May (Figure 5.29), which must have resulted in more peaked inputs of meltwater to the englacial system. The relative importance of increasing surface melt flux, decreasing snow depth, and increasing snow permeability (due to ice layer and preferential flow changes) in driving this change is considered more fully in the next chapter.

This section has shown that the influence of the supraglacial snowpack can be clearly seen in patterns of discharge across the glacier surface, and that this influence changes through time. The implications of this for subglacial hydrology and ice dynamics will be considered in Chapter 7.

5.6 CONCLUSIONS: SUPRAGLACIAL SNOWPACK HYDROLOGY AT HAUT GLACIER D'AROLLA

In this chapter, a variety of qualitative and quantitative methods have been used to investigate supraglacial snowpack hydrology. Here, these data are drawn together to present conclusions about the nature of and controls on water flow through and beneath the supraglacial snowpack at Haut Glacier d'Arolla, and the evolution of this through the melt season. These conclusions are organised around two themes through which these issues can be clearly considered: firstly, a comparison between water flow in the unsaturated (percolation) and saturated (basal flow) regimes and the importance of each in influencing runoff patterns (section 5.6.1), and secondly, a comparison of data from the 2003 and 2004 field seasons through which the relative importance of factors controlling snowpack runoff can be elucidated (section 5.6.2).

5.6.1 Role of the unsaturated vs. saturated regimes in influencing runoff

It is clear from the field data presented above that the presence of a supraglacial snowpack can have a significant delaying and attenuating effect on runoff. Information about the velocity and dispersion of flow through the snowpack from all quantitative dye experiments on both the snowpack surface and in the basal saturated layer is brought together in Figure 5.37, superimposed upon the velocity and dispersion ranges presented by Brugman (unpublished) for a range of hydrological systems. Data for both flow regimes is notably removed from the range expected for flow in surface channels, indicating the marked difference in runoff that will occur across a snow-covered as opposed to bare-ice glacier surface. The low values found for dominant percolation velocity, ranging between 0.08 and 0.49 m hr^{-1}, indicate the delay that flow in this part of the snowpack will cause. Flow velocities in the basal saturated layer were found to be one to two orders of magnitude higher, ranging between 1.35 and 18.48 m hr^{-1}. Flow in the basal saturated layer therefore plays a lesser role in altering the timing of runoff than the lag caused by percolation, but remains much slower than supraglacial flow when no snowpack is present. The delaying and attenuating effect of the snowpack on runoff was confirmed by basal water table records, which revealed lag times of up to 20 hours between peak surface melt input and peak runoff in the basal saturated layer and almost total dampening of diurnal runoff cycles in early-season records.

Permeability values derived from dye tracing results and confirmed by lysimeter data were in all cases significantly lower than those used in previous studies of supraglacial snow hydrology (Figure 5.38). Values from this study are also among the lower range of those
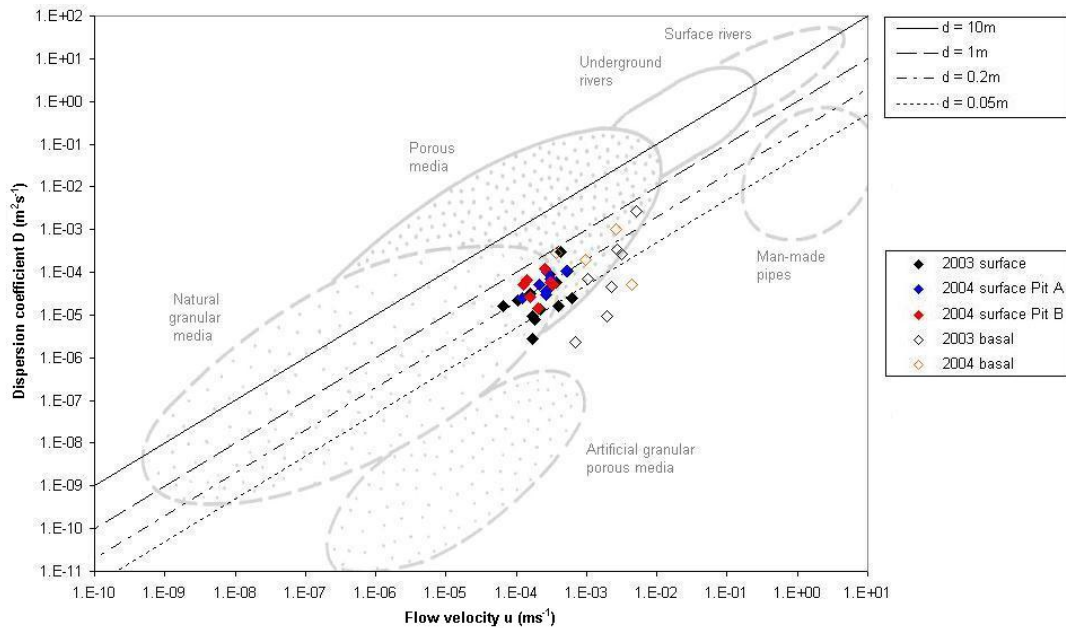
Figure 5.37: Comparison of all velocity and dispersion information from quantitative dye injections at Haut Glacier d'Arolla to values expected in other media (Brugman, unpublished). Measurements are in the range expected for flow through porous media and are notably removed from the range expected for flow in surface channels, indicating the marked difference in runoff that will occur across a snow-covered as opposed to bare-ice glacier surface.

measured in previous field and laboratory studies, comparable only to values reported by Fox et al. (1999) (Figure 5.38). As these previous measurements were carried out in a variety of snow types (some in firn (Colbeck, 1972; Denoth et al., 1979) and others in cold snowpacks (Hardy and Albert, 1993; Albert et al., 2000)), considerable variability in permeability values is of course expected. That values reported in this study are among the lowest, even in comparison to permeability values measured in cold snow, is notable. Inhibition of downward flow by ice layers is suggested as the primary cause of net snowpack permeability values being lower than that predicted for homogeneous snow. This indicates a need for future studies of snow and glacier hydrology to be better informed by field-derived measurements of snow permeability, in which the effect of heterogeneous flow features such as ice layers and preferential flow zones are incorporated.

Percolation patterns in the snowpack were in general highly heterogeneous (section 4.4). This heterogeneity primarily took the form of the interaction of percolating meltwater with ice layers and the formation of preferential flow zones. Both of these heterogeneous flow features will influence the rate of water percolation and the dispersion of the meltwater wave, and are therefore important factors controlling the percolation rates and dispersivity values reported in section 5.2. Ice layers, while clearly impeding the downward movement of meltwater and therefore imparting a delay on meltwater runoff, exhibited a spatial variability in their permeability which resulted in concentration of further downward flow
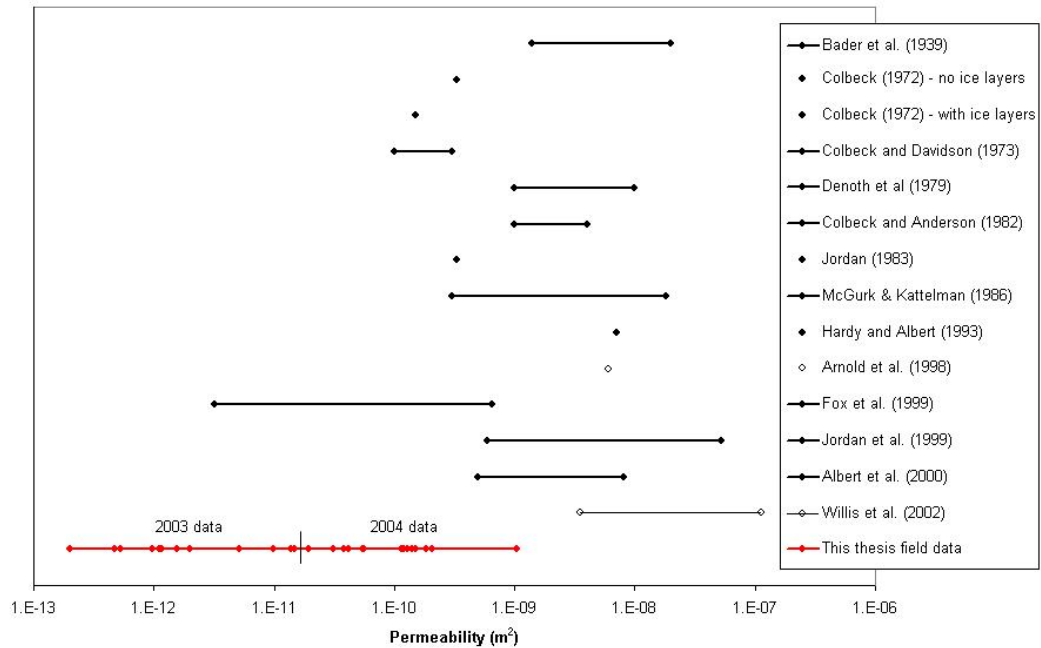
Figure 5.38: Comparison of snow permeability values derived from dye tracing studies at Haut Glacier d'Arolla (red circles) to values used in previous studies of supraglacial snow hydrology (open circles/thin lines) and found in previous field and laboratory studies (solid circles/thick lines). Values found here are notably lower than most others. Note permeability axis has a logarithmic scale.

within flow zones of varying size, and in this way may also increase runoff efficiency. Preferential flow zones may also be linked to the topography of the snowpack surface (Figure 4.34); on other occasions, no obvious control on their formation could be observed. The way in which ice layer and preferential flow effects interact to influence the net character of runoff from the snowpack is very difficult to identify. Their effects must be better understood in order for snowpack runoff to be more reliably predicted.

Field data presented here has further shown that the snowpack's mediating influence on runoff will change through time. In 2004, dye return curve form, percolation velocities, and net snowpack permeability values were all observed to show an evolution through time that indicates increasing hydrological efficiency of the snowpack. No clear increase in snow grain size nor change in snow density was observed that could explain the increase in snow permeability (section 4.3). Instead, changes in the role of ice layers in inhibiting percolation are suggested as an important factor. Meltwater retention by ice layers will decrease over the course of a melt season firstly as the permeability of individual ice layers increases and secondly as ice layers melt out at the snowpack surface in the course of ablation. As ice layers were concentrated at the top of the snowpack (section 4.3), this second mechanism in particular may have caused the snowpack's effect on runoff to change rapidly during the early melt season. The development of preferential flow zones may also have driven an increase in runoff efficiency, but little information is available to fully determine this effect.

The presence of a supraglacial snowpack therefore not only has a significant delaying and attenuating effect on runoff, but this effect is dynamic through time. Information about both snow depth and net snowpack permeability, and their evolution through time, is therefore required in order to understand changing runoff patterns.

5.6.2 Comparison of snow conditions in 2003 and 2004: factors controlling snow hydrology

Comparison of snowpack hydrological behaviour in 2003 and 2004 aids in identification of the factors that play the most important role in runoff modification. Although snowpack ablation and retreat took place much later in 2004 (section 4.3.1), the delaying effect of the snowpack on runoff was very similar at equivalent dates during both melt seasons (Figure 5.39). In mid to late June for example, snow depth in 2004 was over 1m deeper at L than it had been in 2003, yet the time lag for dye flow through the snowpack is similar at around 5 to 6 hours. From this fact it is clear that snow depth alone does not control the delay imparted on runoff. Comparison of the relationship between snowpack depth and dye transit time (Figure 5.40) confirms this: a given snow depth was generally associated with longer (by around 2 hours) lags in 2003 than in 2004. Factors other than snow depth are therefore playing a vital role in controlling runoff timing.

This difference in dye transit time was reflected in the lower percolation velocities (Figure 5.41) and lower snowpack permeability values (sections 5.2.5 and 5.2.10) found in 2003 compared to 2004. Given the markedly higher melt rates and generally more advanced metamorphic state of the snowpack in 2003 (section 4.2 and 4.3), this pattern is the opposite
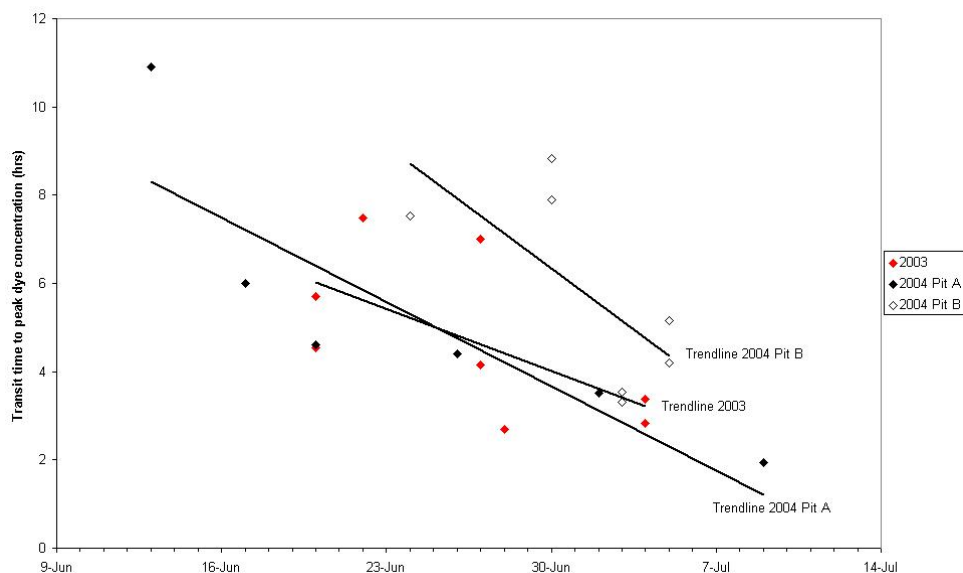
Figure 5.39: Comparison of the evolution of dye transit time with date in both field seasons, revealing that the snowpack had a very similar delaying effect on runoff at equivalent dates during both melt seasons despite the very different timing of snowpack ablation and retreat in the two years.

of that expected. Although the magnitude of flux values is expected to be a key factor controlling runoff timing via Equation 2.12 (Colbeck, 1978a), the higher melt inputs in 2003 were clearly not sufficient to create higher percolation velocities in that year, and other factors must be invoked to explain the difference observed. It is possible that differences in ice layer and preferential flow effects were the cause of differing snowpack hydraulic efficiency between the study years. Some difference was observed between the more homogeneous dye percolation patterns and suncup-controlled flow zones observed in 2003 and the generally smaller scale heterogeneity seen in 2004, but more detailed consideration of the role that this may have played is not possible using the data collected in this project. The incorporation of ice layer and preferential flow effects must be a priority for future studies if snowpack runoff is to be more fully understood.
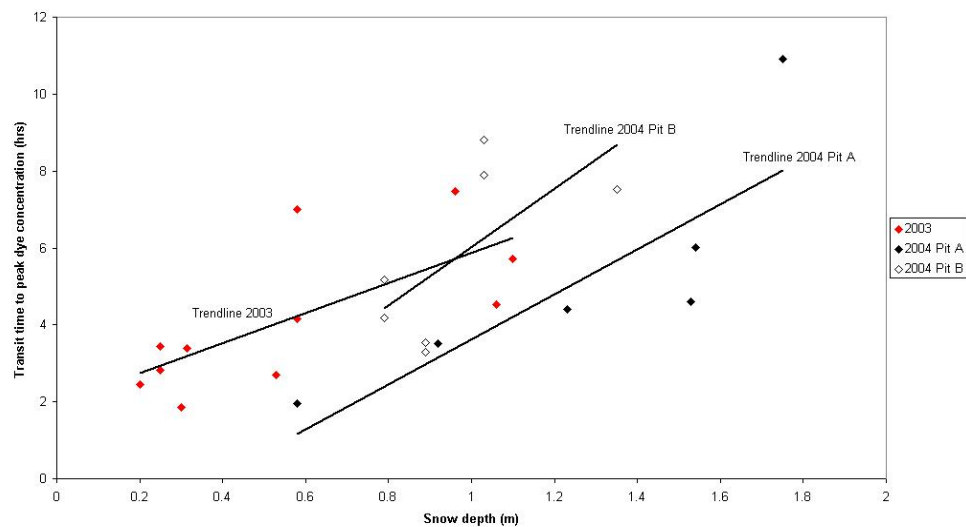
Figure 5.40: Comparison of the relationship between snow depth and dye transit time in both field seasons. It can be seen that a given snow depth was generally associated with longer (by around 2 hours) lags in 2003 than in 2004.
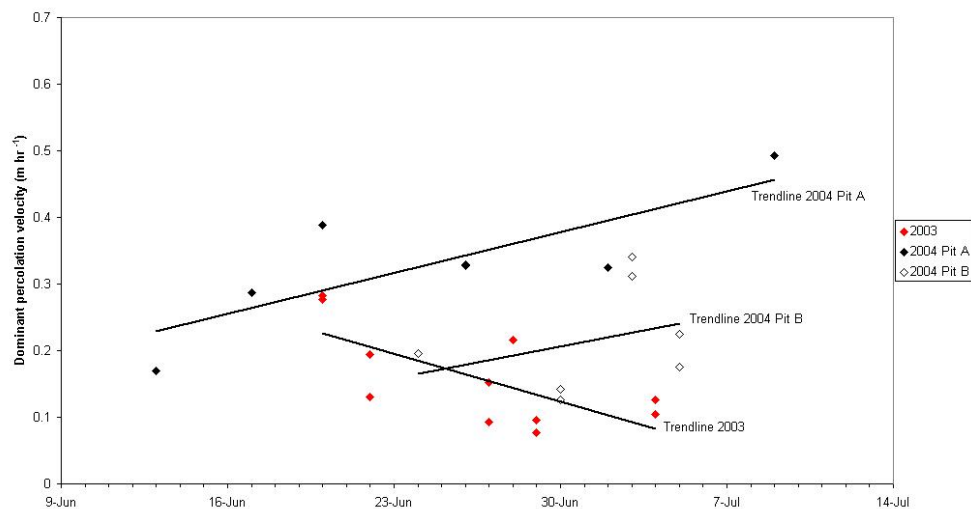
Figure 5.41: Comparison of the evolution of dye percolation velocities with date in both field seasons. Percolation velocities from 2003 are markedly lower than those from 2004 in spite of the higher melt rates and generally more advanced metamorphic state of the snowpack in 2003. Percolation velocities also decreased through time in 2003 (discussed in section 5.2.3).

Chapter 6. Modelling supraglacial snowpack hydrology

6.1 INTRODUCTION

While the field observations presented and discussed in Chapters 4 and 5 have allowed us to significantly advance our understanding of the nature of, and factors controlling, water flow through the supraglacial snowpack and the resulting impact on runoff, our analysis of these relationships can be made more thorough by considering physically-based modelling representations of snow hydrology. Established theoretical understanding of the physical processes controlling water movement through snow is expressed in equations and models that relate flow though snow to a number of controlling factors. These can therefore be used to investigate the importance of these controlling factors and their influence on snowpack runoff under a range of conditions.

A review of modelling work in snow hydrology was presented in section 2.2.3, introducing important modelling tools including the gravity flow theory for vertical percolation through unsaturated snow (Colbeck, 1972; 1978a; Equations 2.11 and 2.12), an expression for lateral, saturated flow over an impermeable boundary (Colbeck, 1974; Equation 2.14), and comprehensive snow process models such as SNTHERM (Jordan, 1991), SNOWPACK (Lehning et al., 1999; 2002a, b; Bartelt and Lehning, 2002), and CROCUS (Brun et al., 1989; 1992). In this chapter, the model used in this study to represent water percolation through snow – the US Army's SNTHERM model – is described in more detail (section 6.2). This model was used to address three questions. Firstly, the factors controlling water percolation through snow and their relative importance in influencing runoff patterns were investigated in a full sensitivity analysis (section 6.3). A second sensitivity analysis used Colbeck's (1974) equation for water flow in the basal saturated layer to investigate controls on flow rate in that part of the snow hydrological system (section 6.4). The SNTHERM model was then run for an extended time period in order to examine the expected evolution of runoff from the snowpack base as snow properties evolve naturally during the melt season (section 6.6). Thirdly, data collected in the field was compared with model output in order to consider weaknesses and possible improvements to this method of modelling water percolation through snow (section 6.7).

Finally, runoff through the snow-covered supraglacial drainage system as modelled using conditions observed at Haut Glacier d'Arolla was used to calibrate a linear reservoir model

of glacier hydrology (section 6.8). This enables possible improvements to the representation of the snow reservoir in linear reservoir modelling to be considered.

6.2 THE SNTHERM MODEL

SNTHERM (Jordan, 1991) is a comprehensive one-dimensional mass and energy balance model that represents the temperature evolution, metamorphosis, densification, depth change and water transport in a multi-layered seasonal snowpack. Developed at the US Army Corps of Engineers Cold Regions Research and Engineering Laboratory (CRREL), SNTHERM has been widely used in investigations of snowpack temperature (Jordan, 1991; Jordan et al., 1999b), energy balance (Cline, 1997; Hardy et al., 1997; Melloh et al., 1997; Jordan et al., 1999a) and internal evolution (Rowe et al., 1995). Its treatment of water percolation through the snowpack is based on the work of Colbeck (1972, 1978a), with the driving equations solved numerically across a grid representing multiple snow layers. A full description of the driving equations and numeral methods used can be found in Jordan (1991) and Fox (2003). SNTHERM is one of the most detailed physical models currently available in terms of simulation of water percolation through snow.

The version of SNTHERM used in this project was adapted by Fox (2003) to incorporate an empirically derived albedo scheme developed at Haut Glacier d'Arolla by Brock et al. (2000a). A layer of glacier ice was also added to the model in place of the soil layers originally used when running SNTHERM in non-glacial settings, with a drain immediately above the ice surface capturing runoff from the snowpack base for output and examination (Fox, 2003). When validated against records of lysimeter outflow from Haut Glacier d'Arolla, the model was found to estimate the timing of daily runoff hydrographs very well and the magnitude of daily runoff minima well, although peak runoff values were generally underestimated (Fox, 2003). Fox suggests underestimation of snow density or lysimeter over-catch as possible factors to explain this underestimation.

6.2.1 SNTHERM input variables

Water flux into the modelled snowpack is driven by the meteorological variables shown in Table 6.1 together with the snow albedo (specified at the start of the model run and evolving through time according to either the original SNTHERM albedo scheme or that of Brock et al. (2000a)). The temperature (K), bulk water density (kg m^{-3}), average grain diameter (m) and thickness (m) of each layer within the snowpack are specified at the start of the model run. In the absence of field measurements of snowpack irreducible water saturation at Arolla, a value of 0.04 was used in accordance with Fox (2003). In a warm snowpack which experiences refreezing only in surface layers overnight, as is believed to

be the case here, the irreducible water content will be satisfied the vast majority of the time and the choice of value will therefore play little role in controlling runoff.

Table 6.1: Meteorological variables driving SNTHERM input melt flux.

Variable	Unit
Ambient air temperature	K
Relative humidity	-
Wind speed	$m\ s^{-1}$
Incident shortwave radiation	$W\ m^{-2}$
Reflected shortwave radiation	$W\ m^{-2}$
Incident longwave radiation	$W\ m^{-2}$
Precipitation amount	$m\ hr^{-1}$
Precipitation type	type code
Cloud type	type code
Cloud fractional coverage	-

6.2.2 Modelling issues – representing heterogeneous flow

As a one-dimensional model, SNTHERM is unable to represent the heterogeneous flow patterns that have been widely observed in natural snowpacks including the supraglacial snowpack at Haut Glacier d'Arolla (section 4.4). Model output is therefore representative of that from a snowpack in which flow is laterally homogeneous, and the likely divergence of such results from a heterogeneous case must be kept in mind when considering the validity of model output. However, homogeneous flow remains the simplest case for which to consider the operation of the snow hydrology system. Moreover, the role of heterogeneous flow patterns can be investigated quite simply by considering the change in effective flux volume through different areas of the snowpack that is brought about by heterogeneous flow (following Wankiewicz (1979) (section 2.2.2.3, Equation 2.2)), and this is considered later in this chapter (section 6.3.4).

6.3 SENSITIVITY ANALYSIS OF FACTORS CONTROLLING SNOWPACK RUNOFF - PERCOLATION

Adjustment of the meteorological parameters and snowpack properties in SNTHERM runs enables us to investigate in detail the role of various factors in controlling runoff from the snowpack base and to consider what influence the changes in snowpack properties observed in the field would have had on runoff. These investigations are described here.

A full sensitivity analysis was carried out using SNTHERM to investigate the way in which changes in snowpack depth, snow permeability, and input melt flux control discharge from the base of the snowpack. The aims of this sensitivity analysis can be summarised as:

i)   to investigate the importance of snowpack depth, snow permeability, and input melt flux in controlling the timing and magnitude of the discharge hydrograph emerging at the snowpack base after percolation through the snowpack depth,

ii)   to quantify the influence of snowpack and flux properties on runoff by considering changes in hydrograph timing and discharge magnitude between the snowpack surface and base,

iii)   to discover how this influence on runoff changes as snowpack properties and input melt flux change through time, and across what range of the controlling variables we expect runoff to change most quickly, and

iv)   to consider the implications of the findings from i to iii for input requirements for future modelling studies of water percolation in supraglacial snowpacks.

6.3.1 Description of model runs

Multiple runs of SNTHERM were carried out with snowpack depth, snow permeability and input melt flux varied across ranges guided by field observations and the literature (Table 6.2). As one parameter was varied others were kept constant at an intermediate value, allowing examination of the change in output that is due to a known change in that driving variable. The availability of field-measured values is particularly valuable in the case of snowpack permeability, as values obtained from dye tracing at Haut Glacier d'Arolla are significantly lower than those used in previous modelling studies (Figure 5.38) and the effect of permeability values in this lower range has therefore not previously been considered.

Table 6.2: Ranges of values used in sensitivity analysis of factors controlling percolation through snow.

Variable	Lower limit	Upper limit	Unit
Snow depth	0	3	m
Snowpack net permeability	1.67×10^{-10}	3.19×10^{-8}	m^2
Peak input melt flux	0	0.007	$m\ hr^{-1}$

Due to spin-up time required for the model to initialise, runs were for a five day period, with identical meteorological data on days 1 to 3 to allow the snowpack to reach equilibrium condition before output on the third day was used for further examination. Each run continued for fourth and fifth days of no surface melt in order to allow examination of

the trailing limb of the runoff hydrograph from day 3 without interference from the next day's melt.

Snow depth was controlled directly by altering the number and thickness of layers in the snowpack at the start of the model run, although subsequent ablation decreased the snow depth before output was examined on the third day. Input melt flux was controlled by varying incoming shortwave radiation while keeping other meteorological variables (Table 6.1) constant, and a mean albedo value (0.60) from field measurements in 2004 was used to initiate all runs. The resulting melt flux into the model could be read from output files.

SNTHERM uses Shimizu's (1970) formula (Equation 2.1) to estimate snow permeability from grain size and dry snow density. Grain size and bulk water density (subsequently adjusted to dry snow density by the model) were therefore varied across the ranges shown in Table 6.3 and combined to create a range of snowpack permeability values for which the model could be run. Although the values for grain size and density were chosen to approximately cover the ranges observed in the field (section 4.3.3 - 4.3.4), the intention here was not to reproduce real combinations of grain size and density observed in the field but simply to use these variables to force changes in snow permeability. The lower limit of snow grain size was taken as 0.2 mm so that by the third day of the model run grain growth processes had increased grain sizes to around 0.5 mm, a realistic minimum value for grain size observed during stratigraphic investigations in the snowpack at Haut Glacier d'Arolla (section 4.3.3). The range of permeability values created corresponds approximately with that used in previous studies but could not be extended to cover the low permeability values found during fieldwork at Haut Glacier d'Arolla (Chapter 5) and by Fox et al. (2003). Any attempt to artificially force snow permeability to lower values by increasing snow density above 600 kg m^{-3} had the opposite effect, in fact increasing effective saturation and therefore unsaturated permeability. As the low permeability values observed in the field are attributed to the delaying effect of ice layers within the snowpack, it is not surprising that similarly low values cannot be reproduced in homogeneous snow.

Table 6.3: Range of snow grain size and bulk water density values used in SNTHERM sensitivity studies and resulting range of snow permeability values produced.

Variable	Lower limit of range	Upper limit of range	Unit
Snow grain size	0.2	2.0	mm
Bulk water density	300	600	kg m^{-3}
Permeability	1.67×10^{-10}	3.19×10^{-8}	m^2

6.3.2 Modification of the runoff hydrograph

Visual examination of the changing form of the runoff hydrograph when snowpack depth, permeability, or input melt flux is varied provides a first impression of the significance of these controls. Figure 6.1 shows the marked attenuation of flux magnitude caused by percolation through the snowpack if it is over about 1 m thick. For shallower snowpacks (0.5 m) the runoff hydrograph quite closely resembles that input at the surface, with only a slight decrease in peak flux value and a lag of about 3 hours. For snowpacks deeper than about 2m, there is little further attenuation of peak flux value, though hydrographs continue to be increasingly delayed. It is clear that the changing depth of the snowpack has the potential to drastically alter the form of the runoff hydrograph. Although the general nature of this effect is expected, hydrograph comparison is valuable in providing a clear illustration of the significance of snow depth in altering the timing and magnitude of runoff.

Figure 6.2 shows the changing form of the runoff hydrograph when flow takes place through snow having different permeabilities. Again, there is a marked difference in the form of the runoff hydrographs, showing that changing snowpack permeability also has the potential to drastically alter runoff from the snowpack base. For the highest permeability considered, peak flux is in fact increased, indicating the formation of a shock front as the water percolates. As permeability decreases, output flux is increasingly attenuated until the peak output flux is only one third of the peak input flux. There is also an increasing lag imparted to the runoff hydrograph, though this is less than the effect of snow depth seen in Figure 6.1. It must be remembered, however, that the low permeability values observed in the field could not be reproduced in the model. If they had been, the observed impact on runoff would be even greater than illustrated here. The changing permeability of a supraglacial snowpack has not previously been considered, but this analysis shows clearly that its effect can be as significant as that of changing snow depth, and must be taken into consideration in order for the snowpack's effect on runoff to be properly appreciated.

In Figure 6.3 we see the runoff hydrographs produced at the snowpack base by different magnitudes of input flux at the surface. Although the most peaked input hydrograph (peak flux value 0.007 m hr^{-1}) is transmitted to the base of the snowpack with around two-thirds of its magnitude preserved, at the other end of the range a hydrograph with peak input melt flux of only 0.002 m hr^{-1} is completely attenuated by the time it arrives at the base. The magnitude of the input melt flux is clearly vital in controlling runoff magnitude, and as the delaying and attenuating effect of the snowpack acts most strongly on input fluxes which are small to begin with, the effect of passage through the snowpack is to amplify day-to-day variations in input flux.
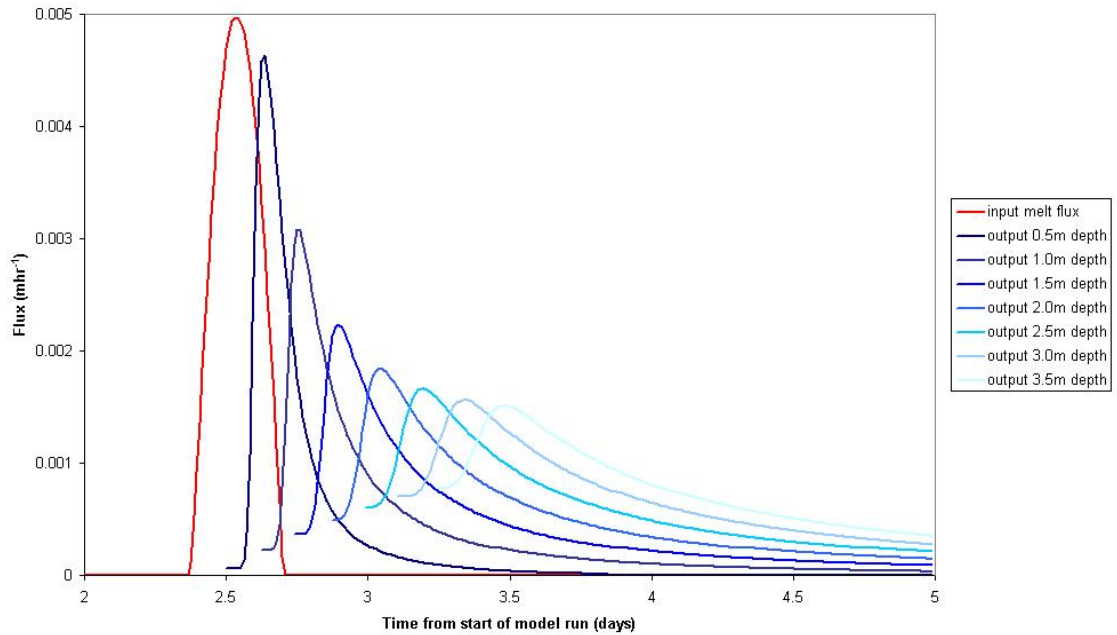
Figure 6.1: Change in hydrograph form and timing caused by percolation through snowpacks of different depths, showing the considerable hydrograph delay and attenuation of peak runoff magnitude that is caused by flow through an increasing depth of snow. The trailing limb of all runoff hydrographs from the previous day have been removed for clarity. As snowpack depth was varied between runs, snow permeability was kept constant at a value of 1.67×10^{-10} m^2, the lowest which could be represented in the model and within the range of permeability values found during fieldwork (Chapter 5).
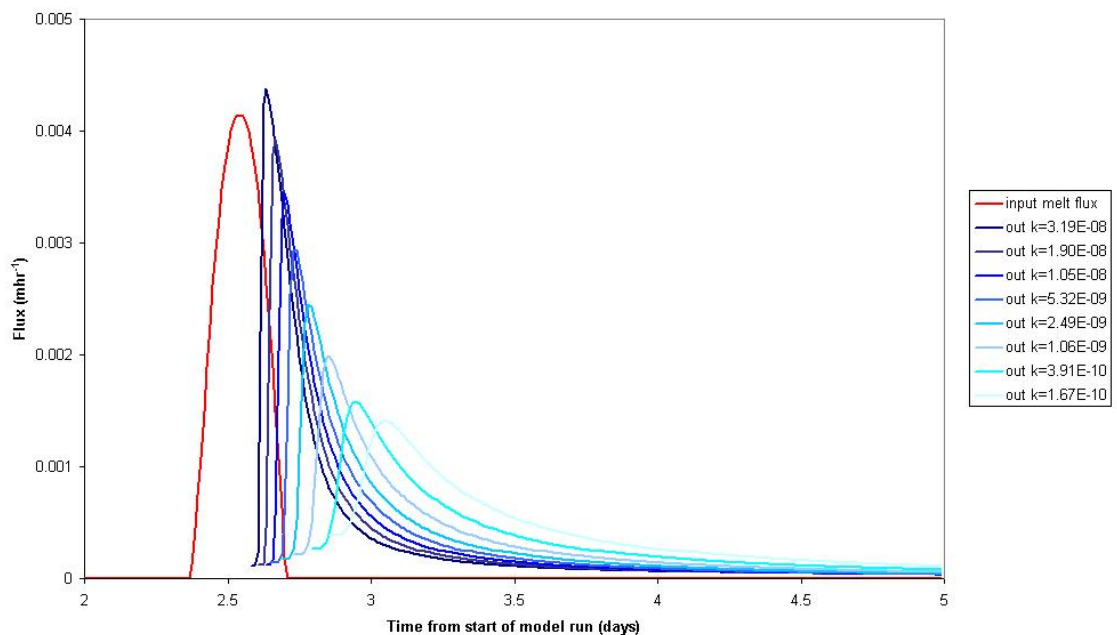
Figure 6.2: Change in hydrograph form and timing caused by percolation through snowpacks of different permeability, showing attenuation and delay of runoff comparable to that caused by snow depth in Figure 6.1. The trailing limb of all runoff hydrographs from the previous day have again been removed for clarity. As snow permeability was varied between runs, snowpack depth remained at 1.5 m, an intermediate value for the snowpack at Haut Glacier d'Arolla. NB values of k are not spread evenly, as they could not be directly controlled in the model, but do cover most of the possible range. The range of k values across which hydrograph form and timing are most altered will be investigated in section 6.3.3.

_____
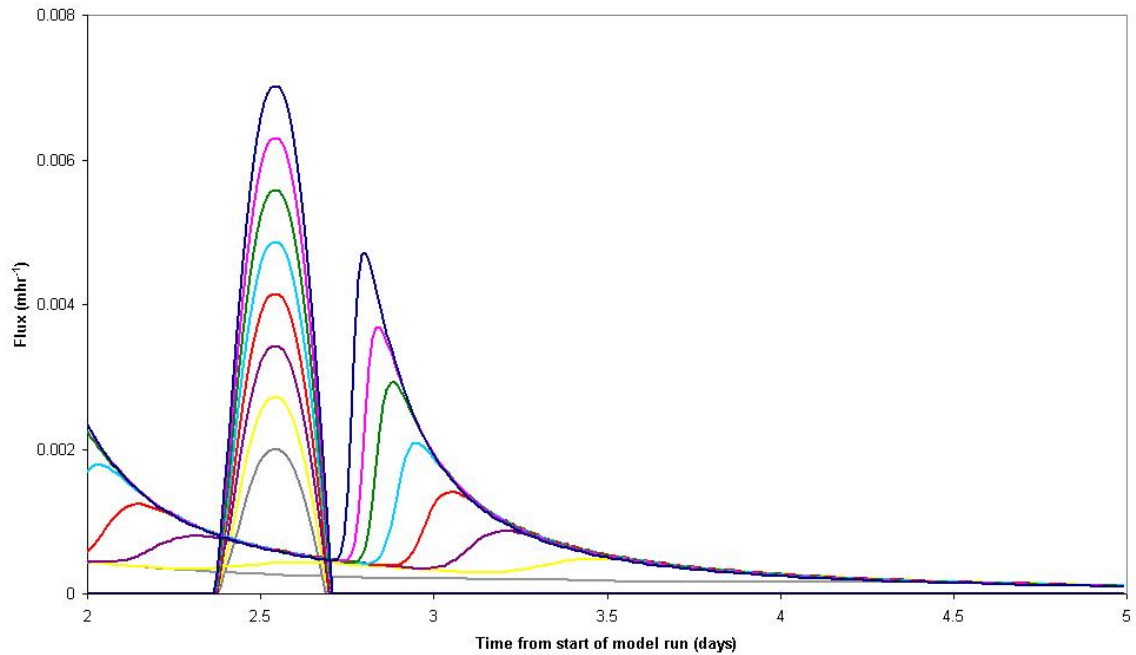
Figure 6.3: Change in hydrograph form and timing imparted on different input melt fluxes by percolation through the snowpack. Corresponding input and output hydrographs are shown in the same colour (curve on left is the surface input flux, curve on right is discharge at a depth of 1.5 m beneath the snowpack surface).

6.3.3 Quantifying the snowpack's effect on runoff

In order to quantitatively examine the snowpack's influence on runoff, two parameters were extracted from the input and output hydrographs on day 3 of each run. These were:

1)   lag time (hours) between peak input and peak output flux, and

2)   ratio of peak output flux value to peak input flux value ((peak out/peak in)*100).

Correlation of these parameters against changing snowpack depth, permeability and input melt flux allows consideration of how the influence of these variables on runoff is expected to change through time, and across what range of the controlling variables we expect runoff to change most quickly.

Figures 6.4 and 6.5 show the variation of parameters 1 and 2 respectively caused by variation of the three driving variables. The variation in each driving variable is expressed as a fraction of the total range stated in Table 6.2, such that they can be plotted on the same graph and their roles in controlling runoff compared; additional x-axes beneath each graph show the real values of each variable.

From Figure 6.4 it can be seen that the lag time for water percolation through the snowpack decreases fairly linearly as snow depth decreases, from around 20 to just 1 or 2 hours. As

snowpack depth decreases (and if all other factors remain constant), the lag time for water to percolate is therefore expected to decrease at a constant rate.

Both changing input flux and snow permeability, in contrast, exhibit non-linearity in their effect on peak-to-peak lag time. In particular, as permeability increases across the lowest values in the likely range (from around 2.0×10^{-11} to 2.5×10^{-9} m^2), there is a rapid decrease in lag time; across higher permeability values this decrease is much more gradual. It is across this lowest part of the possible range that net snowpack permeability values measured at Haut Glacier d'Arolla were observed to increase during the course of the 2004 melt season (Figure 5.19). It is therefore likely that this change in permeability will have played an important role in driving a change in runoff delay.

Changes in snowpack depth, permeability, or input melt flux also change the snowpack's attenuating effect on runoff magnitude (Figure 6.5). The increase in flux magnitude preservation as input flux increases is approximately linear, while decreasing snow depth leads to a more rapid increase in the preservation of peak flux magnitude at snow depths below about 1.5 metres. As the depth of the supraglacial snowpack decreases over the course of the melt season, there will therefore be a point at which any large melt fluxes which are input at the snowpack surface are transmitted to the base with little attenuation, increasing the magnitude of runoff into the englacial system.

Snowpack permeability again exhibits a markedly non-linear relationship, with its attenuating influence on hydrograph peak flux decreasing quickly as permeability increases over very low values (again between approximately 2.0×10^{-11} and 2.5×10^{-9} m^2). Again, the change in snow permeability across this range, indicated by field dye tracing experiments to have taken place in the snowpack at Haut Glacier d'Arolla in 2004 (Figure 5.19), seems likely to have played a key role in controlling runoff from the snowpack.
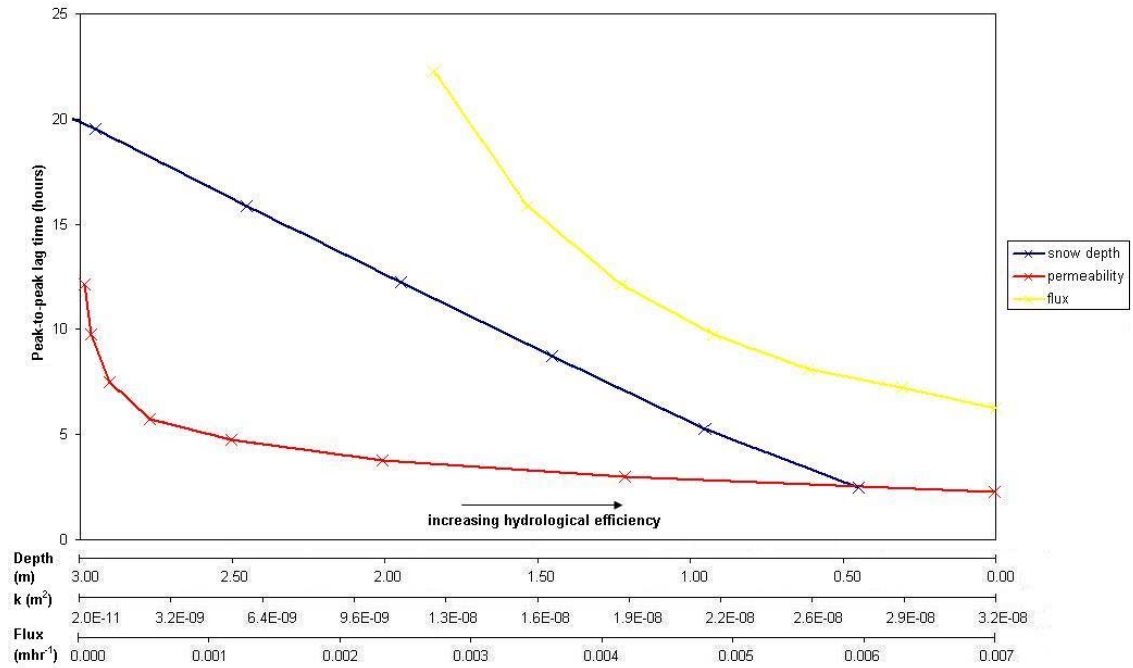
Figure 6.4: Change in peak-to-peak lag time caused by flow through the snowpack as each driving variable changes between least hydrologically efficient (maximum snow depth, minimum snow permeability, or low input melt flux – far left of plot) and most hydrologically efficient (minimum snow depth, maximum snow permeability, or high input melt flux – far right of plot) conditions. The x-axis scales for snowpack depth, snow permeability, and peak input melt flux are shown on three separate x-axes.
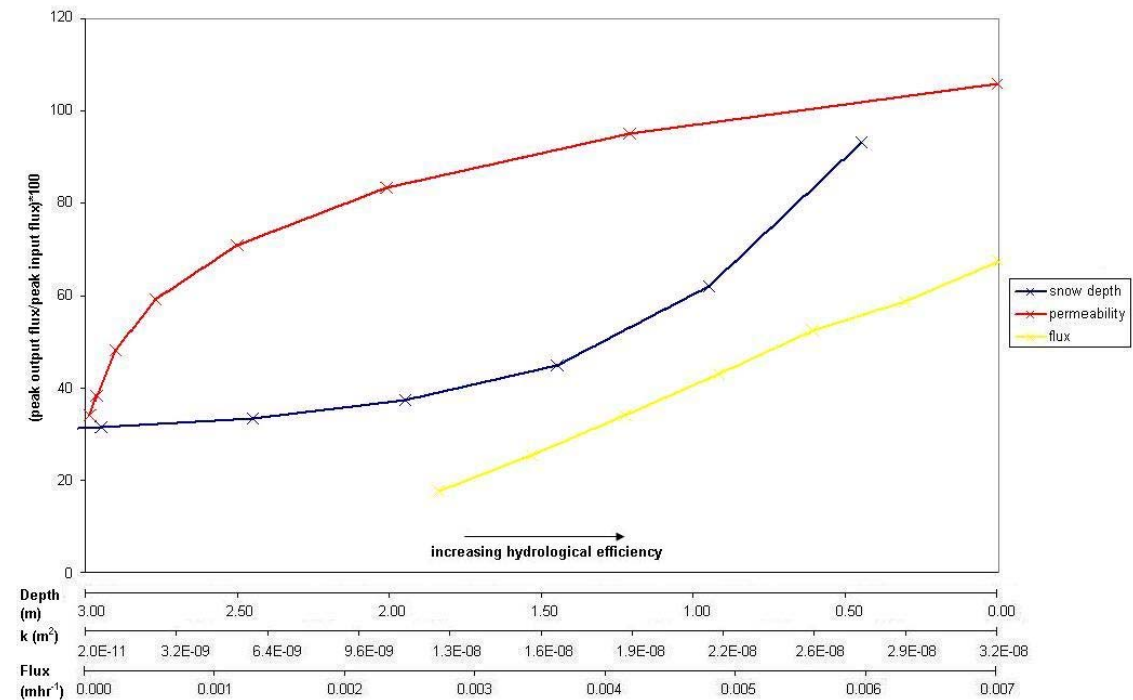
Figure 6.5: Change in preservation of flux magnitude allowed by flow through the snowpack as driving variables change from least hydrologically efficient (maximum snow depth, minimum snow permeability, or low input melt flux) and most hydrologically efficient (minimum snow depth, maximum snow permeability, or high input melt flux) conditions. The x-axis scales for snowpack depth, snow permeability, and peak input melt flux are shown on three separate x-axes.

6.3.4 Role of heterogeneous flow patterns

Although SNTHERM, as a one-dimensional model, is unable to represent the heterogeneous flow patterns that have been widely observed in natural snowpacks, the role of such features can be investigated quite simply by considering the change in effective flux volume brought about when water flows through only a fraction of the snowpack volume. As described by Wankiewicz (1979), when flow is concentrated within vertical zones of the snowpack the flux in each preferential flow finger is amplified relative to uniform flow by a factor f, the inverse of the fraction of the snowpack occupied by flow fingers (Equation 2.2, section 2.2.2.3). As flux is increased within preferential flow zones, so too is liquid water saturation and unsaturated permeability, therefore increasing the efficiency with which water is able to propagate to the snowpack base. The presence of preferential flow zones is therefore expected to allow quicker and less attenuated runoff. The precise form of this control could be explored using a three-dimensional snow model such as that developed by Marsh and Woo (1985), in which water is routed between the snowpack surface and base via multiple flowpaths, each of which may carry a different proportion of the surface flux.

More simply, reference to the flux magnitude sensitivity analysis carried out using SNTHERM in section 6.3.2 above allows initial consideration and illustration of the importance of the preferential flow effect. In Figure 6.6, Figure 6.3 is redrawn omitting all lines except those for flux values of 0.0035 and 0.0070 m hr^{-1}. In effect, this shows the increase in effective flux magnitude which would occur if a surface melt flux of 0.0035 m hr^{-1} travelled through a snowpack in which only 50% of the volume was occupied by flow fingers - not a unlikely situation, as demonstrated by dye flow observations at Haut Glacier d'Arolla (section 4.4.3) and previous studies of heterogeneous flow patters (section 2.2.2.3). The decrease in lag time and increase in runoff magnitude are clear, with peak runoff magnitude actually greater than the 0.0035 m hr^{-1} surface flux. Figure 6.6 also indicates the range of other runoff hydrographs which would be expected if the percentage of snowpack volume occupied by preferential flow fingers was less than or greater than 50%; analysis of dye flow patterns in section 4.4.3 indicated that preferential flow zones frequently occupied as little as 15 to 30 percent of the snowpit cross-section.

Although a very general indication (and in particular, overly simplified in its assumption that flux will be evenly spread between preferential flow zones), Figure 6.6 is useful in illustrating the marked change in runoff timing and magnitude that will result if the snowpack's hydrological efficiency is increased by the concentration of flow within preferential flow channels. There is therefore a need for better field-based information about the preferential flow patterns that can be expected in snowpacks of different types under
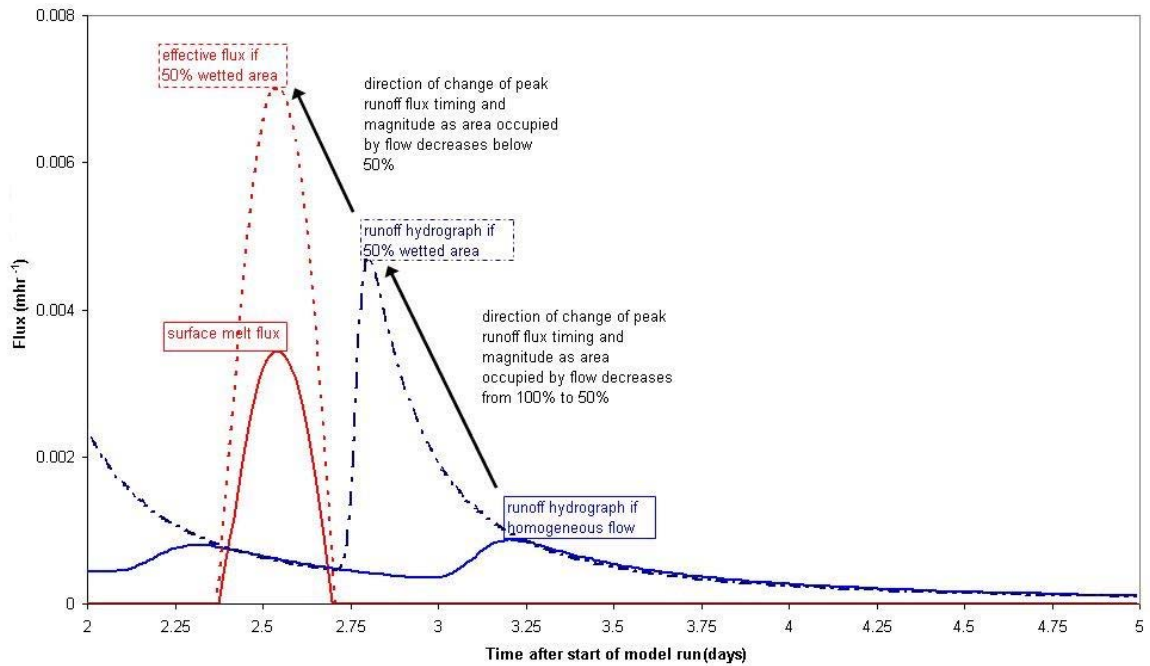
Figure 6.6: Change in effective input flux magnitude (red lines) when percolation takes place through just 50% of the snowpack volume, and range of output fluxes which will result.

different melt conditions, to be incorporated in future studies of snow hydrology. The difficulty of extracting general principals from the huge natural variability in snowpack conditions and behaviour will, however, continue to pose a serious challenge to efforts in this area.

6.3.5 Summary – snowpack effect on runoff

This examination of the factors controlling water percolation through snow has shown that although a change in any of the driving variables (snowpack depth, permeability, or input flux magnitude) will lead to a change in runoff, increasing snowpack permeability may cause the most pronounced change. As snowpack permeability changes, it shows the most pronounced non-linearity in its changing effect on both the delay and attenuation of runoff (Figures 6.4 and 6.5), and this change occurs across the low range of permeability values that field observations have shown to exist in the supraglacial snowpack at Haut Glacier d'Arolla. It has also been shown that the organisation of percolating meltwater into preferential flow channels has the potential to further influence the timing and magnitude of the runoff hydrograph. The understanding provided by this sensitivity analysis of the way in which snowpack depth, snow permeability, and input melt flux magnitude control runoff can be used to inform variable choice in future modelling studies of snow hydrology.

6.3.6 Implications for modelling water percolation in supraglacial snow

In previous studies which have modelled water percolation in supraglacial snowpacks, it has been common to incorporate information about changing meteorological data and snowpack depth through time but to use a constant value for permeability throughout the melt season (e.g. Arnold et al., 1998; Willis et al., 2002). The analysis above has shown that changing snowpack permeability has the potential to significantly alter the timing and magnitude of runoff from the snowpack, and it is therefore clear that reliable information about snowpack permeability and its evolution through time must be taken into account if snowpack runoff is to be correctly estimated. This is particularly important where permeability values are low; notably, it is across this low range of values that permeability derived from field dye tracing experiments was observed to change (Figure 5.19), and previous modelling studies of glacier hydrology have assumed much higher k values (Figure 5.38). The role of snowpack permeability in controlling water discharge into the rest of the glacier hydrological system is more important than has been previously appreciated in modelling studies, and recognition of this fact reinforces the need - first identified from field data analysis (section 5.6) - for reliable field evidence of natural snowpack permeability and its evolution during the melt season. In addition, modelling studies have rarely included preferential flow patterns as a factor capable of influencing the timing and magnitude of runoff, and both the collection of increased field data to capture likely preferential flow patterns and the development of modelling work which incorporates this influence are areas for future research. The implications of inadequate treatment of snowpack hydrology in studies of glacier hydrology and dynamics will be discussed in the final chapter of this thesis.

6.4 SENSITIVITY ANALYSIS OF FACTORS CONTROLLING SNOWPACK RUNOFF – BASAL SATURATED FLOW

A second sensitivity analysis was carried out using Equation 2.14 (Colbeck, 1974; reproduced below as Equation 6.1) to investigate the controls on runoff rate in the basal saturated layer. The role of saturated layer permeability is of particular interest, as this variable is likely to evolve during the melt season.

$$c_s = \alpha k_s \theta \phi^{-1} \tag{6.1}$$

where c_s is the rate of water flow in basal saturated layer, k_s is snow saturated permeability, θ is slope, ϕ is snow porosity, and α is the constant defined in Equation 2.8.

This analysis aimed to:

i)   investigate the role of different factors in controlling the rate of runoff in the basal saturated layer and therefore the lag induced by flow in this part of the snowpack hydrological system,

ii)   discover how this influence on runoff timing changes as the properties of the basal layer change through time, and across what range of the controlling variables we expect runoff timing to change most quickly, and

iii)   consider the implications of the findings from i and ii for future modelling studies of water movement in the basal saturated layer.

6.4.1 Description of sensitivity analysis

Colbeck's (1974) expression for the rate of water flow in the basal saturated layer (Equation 6.1) is easily solved due to its linearity. Each of the driving variables (snow permeability and surface slope) was varied in turn while other variables were held constant (changing snow porosity is not considered, as its effect will be similar to that of changing permeability). As in the percolation analysis above, a range of saturated permeabilities was produced based on the assumption that snow grain size varies between 0.5 and 2 mm and bulk snow density between 300 and 600 kg m^{-3} (Table 6.3). A constant value of 0.5095 was used for porosity during all runs. Surface slope was varied between 1 and 15° (converted to radians for use in the equation): although slope angles on Haut Glacier d'Arolla are generally low (<10°) (Fox, 2003), other glaciers have steeper slopes. The variable ranges used are summarised in Table 6.4.

The form of the relationships examined is linear in each case, and the change in runoff rate caused by a change in any driving variable is therefore independent of the range across which the driving variable is changing. Although the varying rate of runoff change is therefore not of the interest that it was in the case of percolation (section 6.3.3), this sensitivity analysis is of use in illustrating the range across which runoff rate is expected to vary due to changes in the controlling factors. This information will indicate the importance of correctly representing each driving variable and any change it experiences through time.

Table 6.4: Ranges of values used in sensitivity analysis of factors controlling runoff rate in the basal saturated layer.

Variable	Lower limit	Upper limit	Unit
Snow permeability	1.17×10^{-10}	2.40×10^{-8}	m^2
Surface slope	1	15	$^\circ$

6.4.2 Controls on runoff rate

Figure 6.7 shows flow velocity c_s increasing linearly as permeability k_s increases, potentially reaching almost 70 m hr^{-1} if slope θ is also high. If slope angles remain below 10°, as at Haut Glacier d'Arolla, maximum basal flow velocity is more likely to be around 45 m hr^{-1}. When slope is small (5° or less) there is less variation in flow velocity as permeability increases, with velocities remaining below 25 m hr^{-1}. Varying surface slope has a similar influence on flow rate, depending on the concurrent value of snow permeability (Figure 6.8).
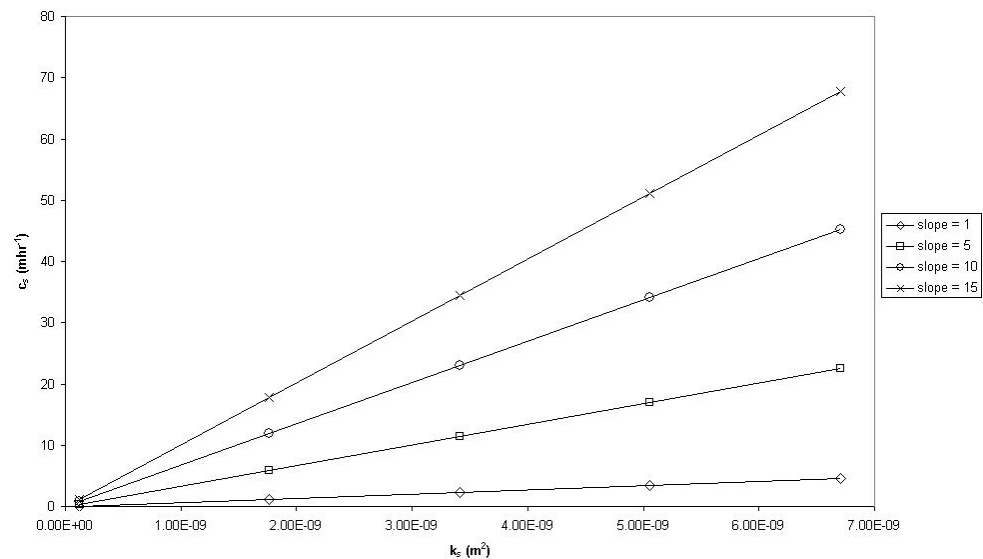
Figure 6.7: Change in flow velocity c_s in the basal saturated layer as snow permeability k_s varies. Lines are shown for a range of possible ice surface slopes.
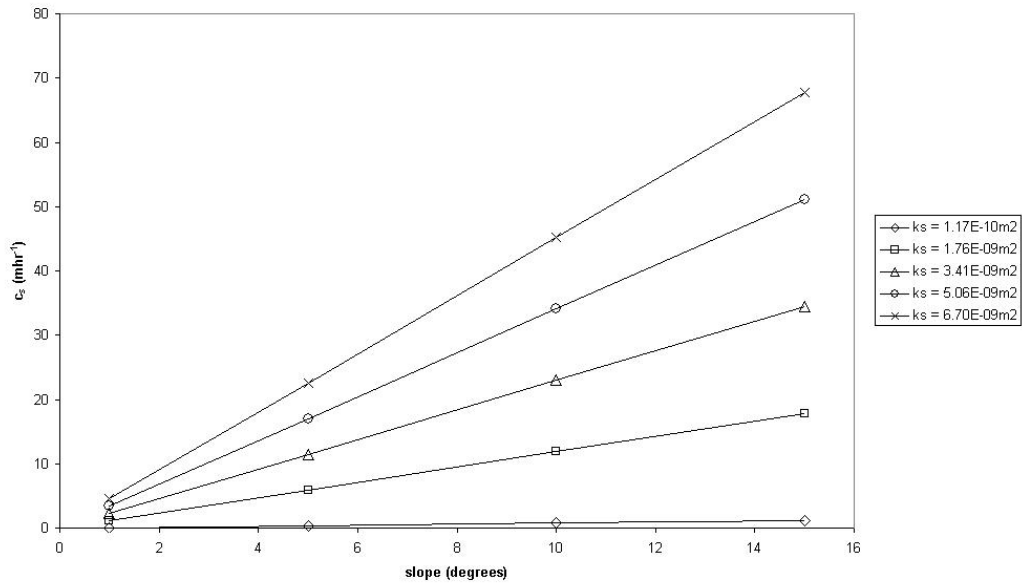
Figure 6.8: Change in flow velocity c_s in the basal saturated layer as ice surface slope varies. Lines are shown for a range of possible values of snow permeability.

6.4.3 Change in runoff rate as driving variables change

In contrast to percolation, where we expect snowpack depth, grain size and density to change over the course of the melt season, it remains unclear how the factors driving flow in the basal saturated layer might be expected to evolve through time. Results from dye tracing in the basal saturated layer at Haut Glacier d'Arolla showed no conclusive change in flow velocities over the course of the melt season (section 5.4). The topography of the ice surface, and therefore slope θ, will remain approximately constant while snow covered. An increase in snow permeability through time might be expected, as saturation of the basal snow layer encourages increased grain growth, but this effect may be offset by increasing density. There remain no field observations of changing basal layer properties during the melt season that could be used to consider this effect. This sensitivity analysis is not therefore intended to explain possible changes in runoff with time through the melt season, but to illustrate the importance of the various driving variables and the range across which runoff rates may vary, and to demonstrate the importance of accurate input data.

6.4.4 Implications for modelling of water flow in the basal saturated layer

The sensitivity analysis above shows that reliable information about snow permeability in the basal saturated layer as well as ice surface slope along the flow path is required if flow rates in this part of the snow hydrology system are to be accurately modelled, as variation in both k_s and θ can lead to large changes in flow rate c_s (Figures 6.7 and 6.8). Unfortunately, snow permeability data of the detail required is not readily available for the saturated layer and is not easily measured in the field. As observations at Haut Glacier d'Arolla have shown (section 5.5.3), water flow on the ice surface beneath the snowpack frequently takes place via a network of 'channels' (or areas where the saturated layer is deeper) similar to those on a snow-free ice surface. Continuous saturation within these 'channels' may lead to increased permeability and therefore efficiency of runoff. Improved information is needed about permeability within these channels and the way in which runoff at the base of the snowpack is organised into them. Lateral flow paths in distributed modelling of supraglacial hydrology are generally derived from ice surface slope information taken from large-scale digital elevation models (DEMs), with flow assumed to take place down the steepest slope. At the local scale, slopes may be considerably different from the average values derived from DEMs. In this respect, LIDAR data and other high resolution DEM sources have the potential to be of great use. Incorrect parameterisation of either ice surface slope or basal snow permeability along the water flowpath will lead to errors in modelled runoff.

6.5 SENSITIVITY ANALYSES - SUMMARY

The sensitivity analyses presented in the previous two sections have illustrated the significant effect that variations in snow depth, permeability (both in the unsaturated and saturated regimes), input melt flux magnitude and glacier surface slope can have on runoff from the snowpack. Changing snowpack permeability in the unsaturated regime in particular has a markedly non-linear effect on hydrograph delay and attenuation, with runoff becoming rapidly more efficient as permeability increases across low values. As it is across this lowest part of the possible range that net snowpack permeability values measured at Haut Glacier d'Arolla were observed to increase during the course of the melt season (section 5.2), it is likely that this change in permeability will have played an important role in driving a change in runoff. That these factors have the potential to significantly alter runoff indicates a need for high quality, ideally field-derived, input data for modelling studies if runoff from the snowpack, and its evolution through time, is to be reliably modelled.

A key point which the analysis of basal flow rates has reinforced is the marked difference between flow rates in the unsaturated and saturated regimes, with flow in the basal saturated

layer frequently reaching over 20 m hr^{-1} compared with percolation rates in general around 2 orders of magnitude lower (modelled time lags of between 2 and 20 hours for percolation through a snow depth of around 1.5 metres correspond to percolation velocities ranging between 0.07 and 0.75 m hr^{-1}). Percolation and saturated flow velocities derived from dye tracing experiments in the field agree well with the magnitude of these modelled flow rates. Because percolation is much slower than flow at the snowpack base, it will act as the more important control on runoff, with variations in flow rate in the saturated layer having comparatively little effect, as identified by Colbeck (1974). Consequently, despite the significant changes in basal runoff rate identified above as resulting from varying snow permeability and ice surface slope, the precise identification of these parameters for modelling studies remains of less concern than the need to correctly capture the factors controlling percolation.

Although the gravity flow theory and Colbeck's (1974) equation for water flow rate in the basal saturated layer give a valuable indication of the controls on flow rate in the unsaturated and saturated regimes, this does not directly help us to understand patterns of discharge into the rest of the glacier system. The net lag and magnitude of runoff into the englacial system can only be determined by distributed modelling that takes into account the varying depths of snow through which water has percolated, the distance it travels in the basal layer before reaching an englacial entry point, and the area across which each supraglacial catchment collects percolating meltwater. For this to be possible, accurate information about the location of moulins and crevasses and the delineation of supraglacial catchments is required. Previous studies have briefly noted the influence on runoff patterns of supraglacial catchments of different geometries (Arnold et al., 1998), but more detailed consideration of such effects remains a subject for future research.

6.6 EVOLUTION OF SNOWPACK RUNOFF DURING THE MELT SEASON

A longer run of SNTHERM was undertaken in order to examine the simulated change in runoff from the base of the snowpack as snow properties evolve through time, and therefore to consider the importance of changing snowpack properties in driving changing discharge into the englacial system. An initial run in which surface melt was driven by observed meteorological data proved to be of little use in examining the role of snowpack properties, as significant day-to-day variations in melt input in summer 2004 masked the influence of changing snow depth and permeability. Instead, the model was run using one set of idealised daily meteorological data repeated for a period of 50 days in order to isolate the effect of changing snowpack properties. Initial conditions were taken from field observations of snowpack depth, density, grain size and albedo at the lower snow study station around Julian Day 155, the date after which there was no significant new snowfall.

6.6.1 Evolution of snowpack properties

Although daily meteorological inputs did not change throughout the run, modelled input flux to the snowpack surface increased slightly over time as snow surface albedo decreased. Snowpack depth, density, grain size and albedo were allowed to evolve according to the driving schemes in the model, and examination of their values throughout the period (Figures 6.9 a to c and 6.10) showed that this evolution was in good agreement with that expected in a natural snowpack during the melt season.

The input values of snow density and grain size generated values of snowpack permeability which increased from 5.00×10^{-10} m^2 at the start of the run to around 4.00×10^{-9} m^2 at the end (Figure 6.9d). These values are, as before, significantly higher than those derived from dye tracing experiments in the field, as the very low real world permeability values attributed to the presence of ice layers cannot be represented in SNTHERM. The range does, however, fall within that shown in the percolation sensitivity analysis presented previously (section 6.3.3) to cause the most pronounced change in peak-to-peak lag time (Figure 6.4) and flux magnitude preservation (Figure 6.5). The delaying and attenuating effect of the snowpack may therefore be more severe than it appears here, but this model run should give an indication of the change in runoff that can be caused by snowpack evolution.

6.6.2 Evolution of snowpack effect on runoff

The modelled surface melt input and basal outflow hydrographs between Julian Day 155 and 205 are shown in Figures 6.10 a and b. The transformation of the hydrograph caused by percolation through the snowpack is clear, with a delay in the timing of peak values and attenuation of peak flux value very obvious early in the run. This effect decreased through time, with the total value of peak flux transmitted through the snowpack from around Julian Day 195 onwards. The snowpack's effect on runoff was quantified as in section 6.3.3 using the indices 'peak-to-peak lag time' and 'percentage preservation of peak flux magnitude'. Figure 6.11 shows the significant decrease in peak-to-peak lag time, from 19 hours to less than 1 hour, and increase in preservation of flux magnitude, from around 25% to over 100% (due to shock front formation), that resulted as snow depth decreased and permeability increased over the course of the model run.

The liquid water content of the snowpack at any point in time can be viewed as temporary storage due to the time taken for flow between the surface and base, and its evolution throughout the run is shown in Figure 6.12. The amount of water held in the snowpack is controlled by the melt input, the snowpack depth, and the rate of percolation. Despite the slight increase in melt input as the model run progressed, liquid water content decreased from around 0.08 m to around 0.02 m water equivalent due to the decreasing snowpack depth and more efficient transfer of meltwater between the snowpack surface and base.

Decreasing peak-to-peak lag times, increasing preservation of input flux magnitude in runoff, and decreasing water storage within the snowpack all indicate an important reduction in the snowpack's delaying and attenuating effect on runoff, caused by decreasing snowpack depth and increasing permeability. This more efficient transmission of input melt flux will play a role in increasing runoff into the subglacial drainage system.
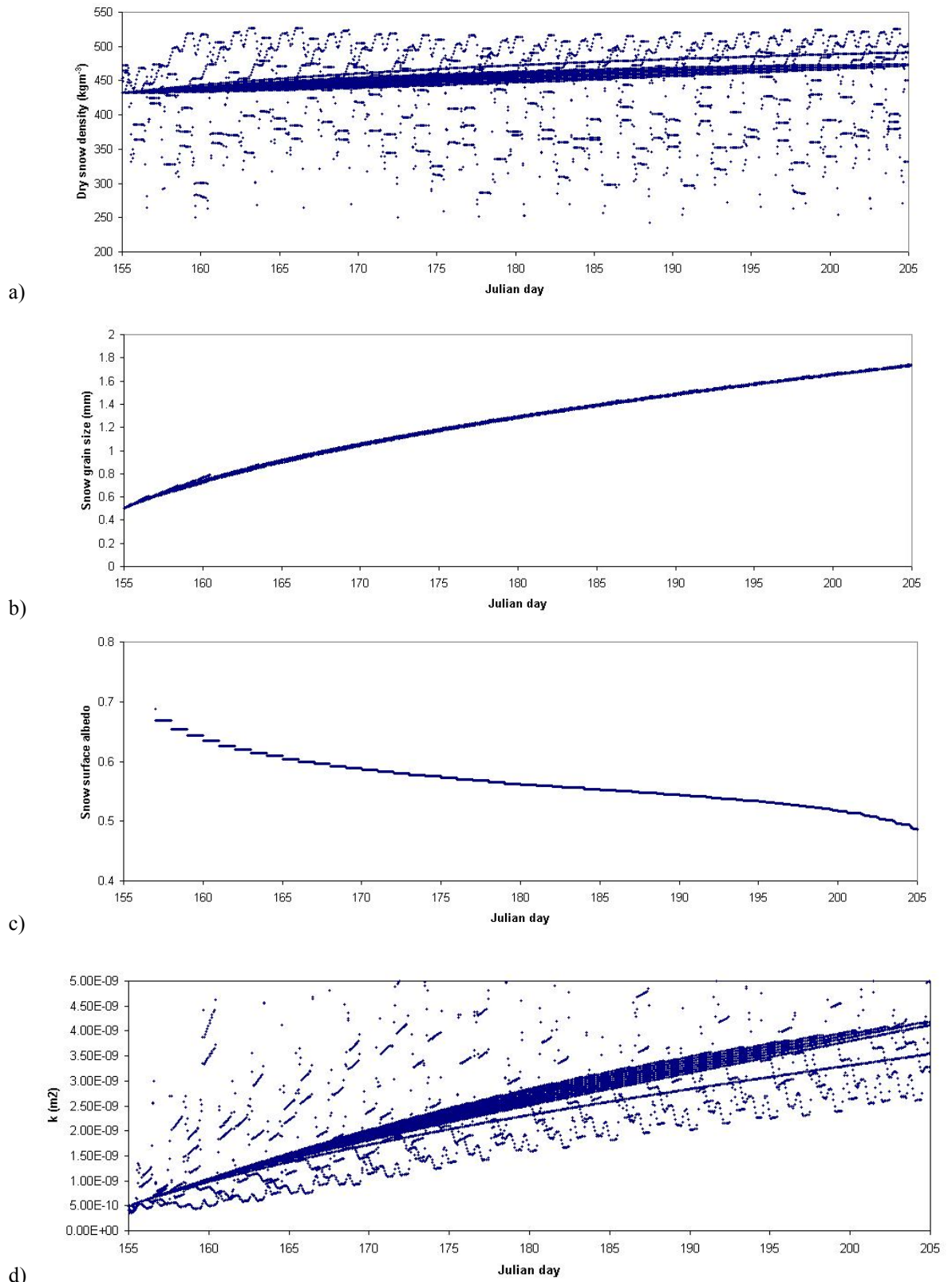
Figure 6.9: Evolution of a) dry snow density, b) snow grain size, c) surface snow albedo and d) snow permeability k during the model run. The large scatter in points on a) and d) is due to the difference in snow density and permeability with depth through the snowpack. Density, grain size and albedo all evolve through the melt season in a manner that is in good agreement with that expected in a natural snowpack. As discussed previously, modelled *k* values are higher than those derived from dye experiments in the field, but do fall within the range shown in sensitivity analyses (section 6.3.3) to cause a pronounced change in runoff timing and magnitude.

a)

b)
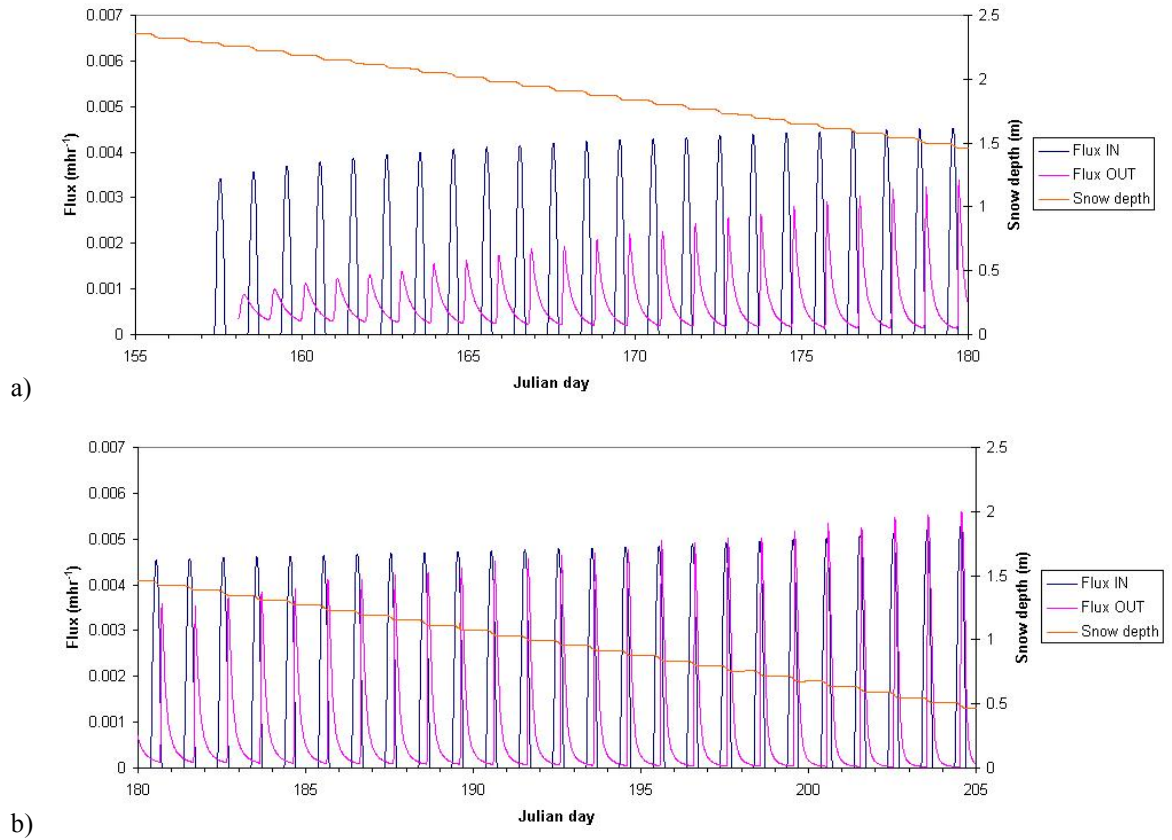
Figure 6.10: Evolution of the input and output hydrograph and snow depth during a) the first half and b) the second half of the model run, showing delay and attenuation of the hydrograph at the start of the run and a decrease in this effect through time.
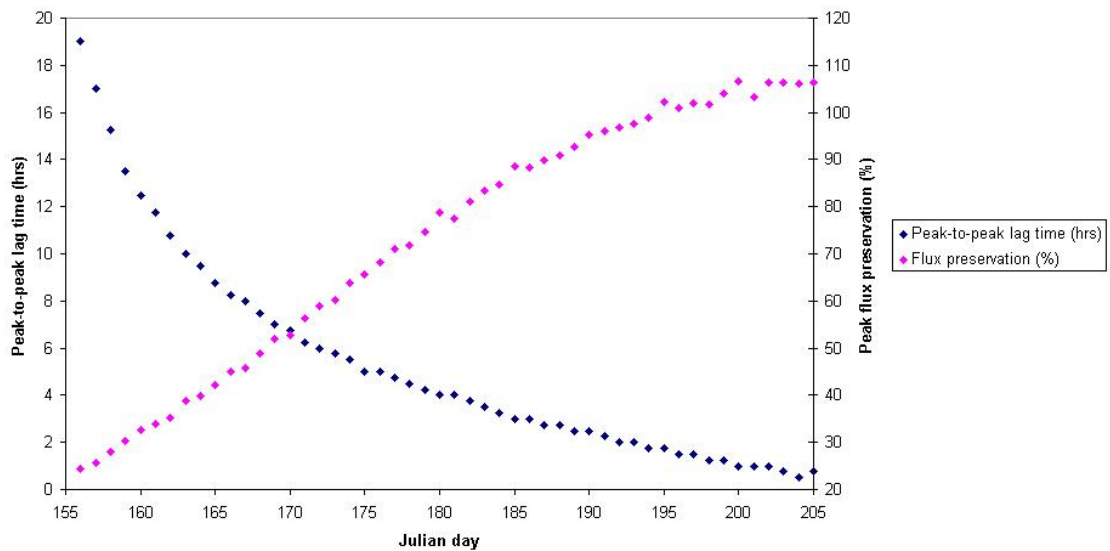
Figure 6.11: Change in lag time and attenuation imparted on runoff hydrograph as snow properties evolve during model run. At the start of the model run, runoff is delayed by over 19 hours and attenuated to only ~25% of its surface magnitude. As the snowpack evolves, this effect decreases until the full surface flux magnitude is transmitted to the snowpack base with less than 1 hour delay.
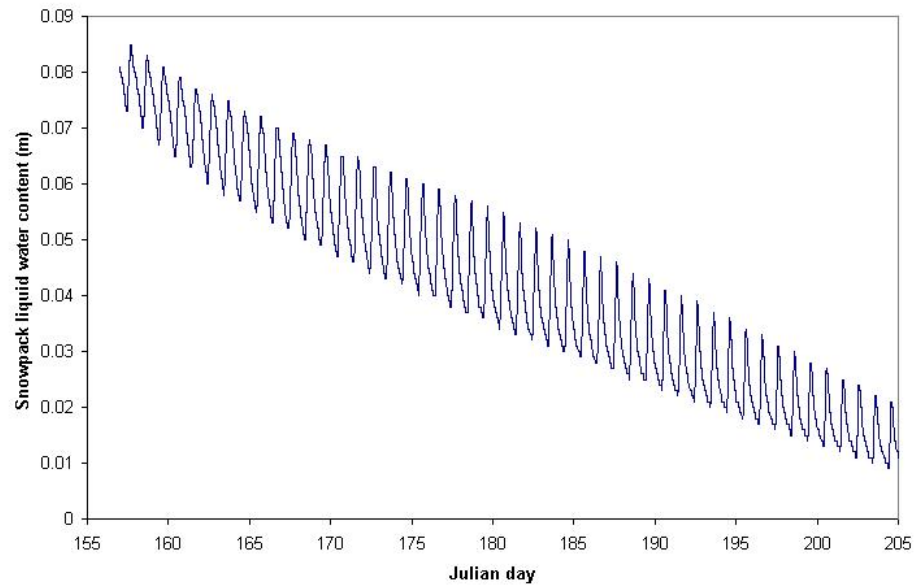
Figure 6.12: Decrease in water storage in the snowpack during the course of the model run.

6.7 COMPARISON OF MODEL OUTPUT WITH FIELD DATA

Although SNTHERM is one of the best tools available for modelling snow percolation, there remain questions as to whether any currently available physical model can accurately represent runoff from natural, highly inhomogeneous, snowpacks. In particular, the percolation of water via preferential flow paths is expected to cause significant deviation of actual discharge values from the results predicted by models assuming homogeneous flow (c.f. Marsh and Woo, 1985; section 6.3.4), and there remains little information about the controls on and patterns of preferential flow that could be used in modelling studies. Snowpack discharge data collected using lysimeters during the 2004 field season was useful in allowing verification of SNTHERM model output and consideration of its reliability despite these concerns.

6.7.1 Lysimeter data

Due to installation difficulties together with logger failure in mid-July (section 3.7.1), lysimeter data was only collected between Julian days 183 and 194. From this period, days 184 to 186 were selected for use in verification due to their well-defined melt input and absence of rainfall. During days 184 and 185 a single drainpipe lysimeter (Lysimeter C) was located close to the snowpack surface and provides some verification of input flux. Early on day 186 it was moved to the snowpack base, 65cm from the snow surface, and provided verification of the hydrograph measured by Lysimeter A, already installed at that depth. During this period snow depth at this site was just under one metre, with a decrease in snow depth of around 10cm between JD 184 and 186 (Figure 4.5).

6.7.2 Description of model run

The SNTHERM run was started on Julian day 182 in order to allow the model to 'spin up' before the days of interest. Initial snow depth was taken from measurements adjacent to lysimeter location and meteorological data from the nearby AWS_M used to drive surface melt. Starting values of 650 kg m^{-3} and 0.3 mm (quickly becoming 0.5 mm due to grain growth processes) were used for snow density and grain size respectively in order to create snow permeability as close as possible to that measured in dye tracing experiments.

6.7.3 Comparison of modelled and measured discharge

Measured lysimeter discharges along with SNTHERM modelled input and output flux are shown in Figure 6.13. Modelled discharge is notably overly delayed compared with that measured by the lysimeter; on JD 184 the lysimeter registers runoff 3.7 hours after the start of surface melt but modelled runoff does not begin until 2.8 hours after that (a 75% increase in delay). On JD 185 the lysimeter registers runoff 4.15 hours after the start of surface melt but modelled runoff does not begin until 2.1 hours after that (a 50% increase in delay). On JD186 the match is better. The shape of the modelled discharge hydrograph is generally quite accurate, exhibiting approximately the correct degree of dispersion. The magnitude of flux values is not expected to match well due to the small size of the lysimeters (which if flow patterns are heterogeneous will lead to either over- or under-estimation of mean discharge), and the resulting coarseness of the data. Peak discharge values do however to reasonably well. Modelled discharge, in agreement with lysimeter data, shows almost no attenuation of the input flux, which is to be expected given the fairly shallow snow depth (falling from around 80 to 65 cm during this period; the degree of attenuation expected for this snow depth can be seen in Figure 6.5). It would be more informative to verify model performance when the snowpack is more hydrologically inefficient, but lysimeter data for earlier in the melt season is unfortunately not available.

The improved match between modelled and measured discharge on JD 186 results from significantly earlier modelled runoff. Modelled runoff takes place only 5.25 hours after surface melt input on JD 186 compared to 6.25 hours on JD 185. By examining the results of the sensitivity analysis presented earlier (section 6.3; Figure 6.4), it can be seen that a decrease in runoff lag such as this - of approximately 1 hour – is similar to that expected to be caused by a decrease in snow depth of around 5 cm, though somewhat greater. The higher melt flux on JD 186, however, would also contribute to earlier runoff (although this applies more to the timing of peak runoff that the start of runoff). Examination of snow permeability values used by the model show an increase from on average 1.30 to 1.93 x 10^{-10} m^2 during this two-day period, within the range shown likely to cause a rapid increase in

runoff efficiency (Figure 6.5). The change in modelled hydrograph timing on JD 186 can therefore easily be explained by changing snow depth, permeability, and input melt flux. At the same time, the difference between measured and modelled runoff on days 184 and 185 could also clearly arise from slight divergence of these model parameters from those in the real snowpack. With this in mind, the match of modelled hydrographs to measured hydrographs is in fact encouraging, in particular with respect to hydrograph form. A longer record of lysimeter runoff, together with high quality information about the properties of the snowpack above lysimeters and input melt fluxes, is required before further conclusions can be drawn regarding the reliability of water percolation modelling in the SNTHERM model.
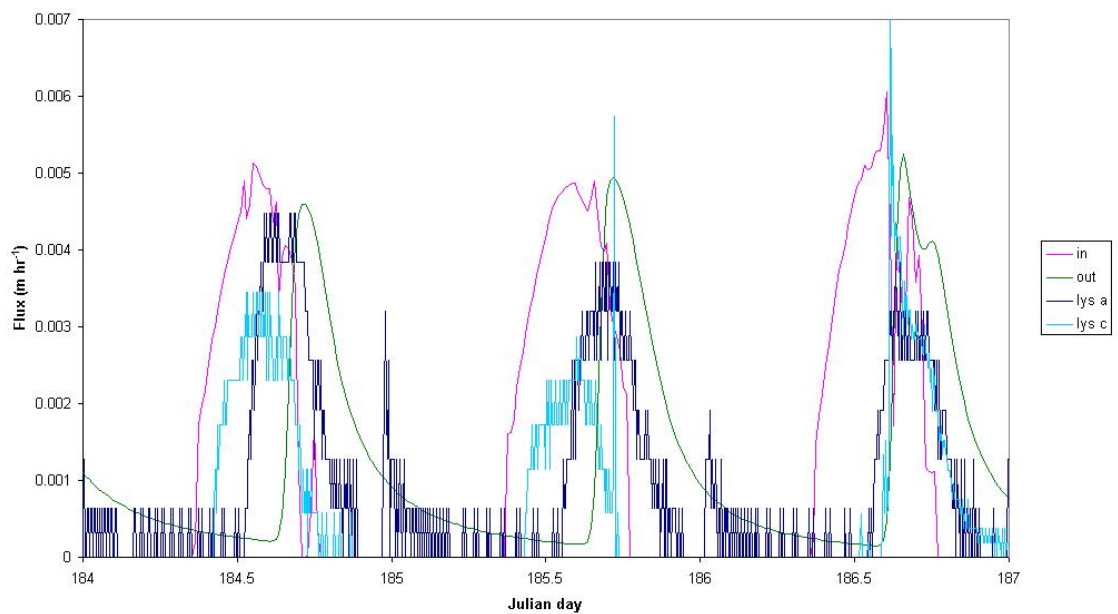
Figure 6.13: Modelled surface melt flux (pink), measured discharge through Lysimeters A (dark blue) and C (pale blue), and modelled runoff at the depth of Lysimeter A (decreasing from ~80 to ~65 cm during this period) (green). Lysimeter C is close to the snowpack surface on days 184 and 185, and at the same depth as Lysimeter A on JD 186.

6.8 LINEAR RESERVOIR MODELLING OF GLACIER HYDROLOGY

Linear reservoir modelling has been widely used as a method of estimating glacier runoff that does not have the heavy data and processing requirements of fully distributed modelling yet still takes some account of the physical processes operating in the glacier system, albeit in a simplified manner (e.g Oerter et al., 1981; Baker et al., 1982; Hock and Noetzli, 1997; Verbunt et al., 2003; Schaefli et al., 2005; Hock and Jansson, 2005). Such modelling is therefore *conceptual*, in that physical processes *within* the glacier are represented instead of simply statistical relationships between the input and out variables sought, and is generally *lumped*, dealing only with the mean properties of different parts of the glacier system.

In linear reservoir modelling, water inputs are routed through a number of reservoirs representing different parts of the hydrological system. The discharge of water Q_t from a reservoir at any point in time is controlled by surface input m_t, discharge at the previous timestep Q_{t-1}, and storage within the reservoir via the storage coefficient K, the average delay time imposed on the inflow by the reservoir:

$$Q_t = Q_{t-1}e^{-1/K} + m_t(1 - e^{-1/K})$$
(6.2)

This section examines the reliability of linear reservoir modelling for accurately representing runoff from supraglacial snowpacks and considers possible improvements to this method.

6.8.1 The snow reservoir

Previous linear reservoir models have used between one (Collins, 1982) and four (Baker et al., 1982; Gurnell, 1993) reservoirs to represent the glacier hydrological system, but generally agree on the existence of a 'slow' reservoir representing the drainage of water through the supraglacial snowpack. Values of K_{snow} used previously are summarised in Table 6.5 and show considerable variation, likely due to differences in glacier size and specific hydrological features. In these studies the value of K_{snow} was most frequently determined by tuning to produce the best match between modelled and observed discharge. Only Collins (1982), Gurnell (1993) and Hannah and Gurnell (2001) calculate K_{snow} directly from field data, by analysis of hydrograph recession limbs. In many previous studies the routing of water through the snow reservoir has therefore had little basis in physical understanding of water flow through snow, and the calculation of K_{snow} values more closely tied to processes in the snowpack is desirable. The relationship between surface input

hydrographs and runoff at the snowpack base as modelled using established physical principles is used here to suggest values of K_{snow} for use in linear reservoir modelling of snowpack runoff, and in particular to consider the likely change in K_{snow} through time.

Table 6.5: Values of the storage coefficient K used for the snow reservoir in previous linear reservoir modelling of glacier hydrology.

Study location	K_{snow} (hours)	Method of calculation of K_{snow}	Reference
Vernagtferner	30	Optimized to produce best fit between measured and modelled discharge	Baker et al. (1982)
Gornergletscher	11.5	Hydrograph recession limb analysis	Collins (1982)
Haut Glacier d'Arolla	8/24	Hydrograph recession limb analysis (separated K values)	Gurnell (1993)
Storglaciären	30	Optimized to produce best fit between measured and modelled discharge	Hock and Noetzli (1997)
Rhone Glacier	120	Optimized to produce best fit between measured and modelled discharge	Escher-Vetter (2000)
Taillin Glacier, French Pyrénées	45.0-17.75 (decreasing through time)	Hydrograph recession limb analysis	Hannah and Gurnell (2001)
Rhone Glacier catchment, central Switzerland	120	Optimized to produce best fit between measured and modelled discharge	Klok et al. (2001)
Three Swiss high-alpine catchments (Rhone, Massa and Dischmabach)	120	Optimized to produce best fit between measured and modelled discharge for all three catchments combined.	Verbunt et al. (2003)
Three Swiss high-alpine catchments (Rhone, Lonza and Drance)	4.0-5.9	Optimized to produce best fit between measured and modelled discharge	Schaefli et al. (2005)

6.8.2 K_{snow} derived from modelled snowpack runoff data

Rearrangement of Equation 6.2 gives an expression relating the storage efficient K to input and output flux values:

$$K = \frac{-1}{\ln\left(\dfrac{Q_t - m_t}{Q_{t-1} - m_t}\right)} \qquad (6.3)$$

The input and output flux series produced by a season-long run of SNTHERM therefore present an opportunity to examine the storage coefficient for flow through the snowpack as predicted by the physical principles driving water percolation in SNTHERM, and in particular to consider how the value of K_{snow} may be expected to change through time. Using the input flux and modelled runoff series presented in section 6.6, K_{snow} was calculated using Equation 6.3 for each time step where output flux values were on the

falling limb of the hydrograph (K is defined only for recession flows when discharge is controlled by the storage characteristics of the reservoir and not by the rate of input). As would be expected, K_{snow} values vary within each day, with lower values corresponding to the more efficient transmission of peak discharge values and higher K_{snow} values formed by the more slowly draining fluxes on the trailing limb. The K_{snow} values (Figure 6.14) show a clear decrease through the season, falling from around 50 hours at the start of the run to less than 10 hours at the end. The best fit exponential trendline $y = 17945e^{-0.0375x}$ ($r^2 = 0.67$) gives a useful impression of the mean value of K on each day and the decreasing trend through time. Hannah and Gurnell (2001), from hydrograph recession limb analysis at a small Pyrénéan glacier, also observed a decrease through time in the storage coefficient for the slow reservoir, falling from 45.00 to 17.75 hours between the early and mid melt season. This temporal decrease in K_{snow} is in agreement with the increase in snowpack hydrological efficiency observed through time in both the field (Chapter 5) and in modelling of snow percolation (section 6.5). Hannah and Gurnell (2001) suggested the development of flow paths within the snowpack as the cause of this decrease, but no observations of water movement in the snowpack were available to support this. That K values derived from the SNTHERM run show a similar decrease indicates that a significant change in K_{snow} can be driven simply by snowpack ablation, increasing permeability, and albedo decrease. The development of preferential flow paths would cause an even greater decrease in K_{snow}.
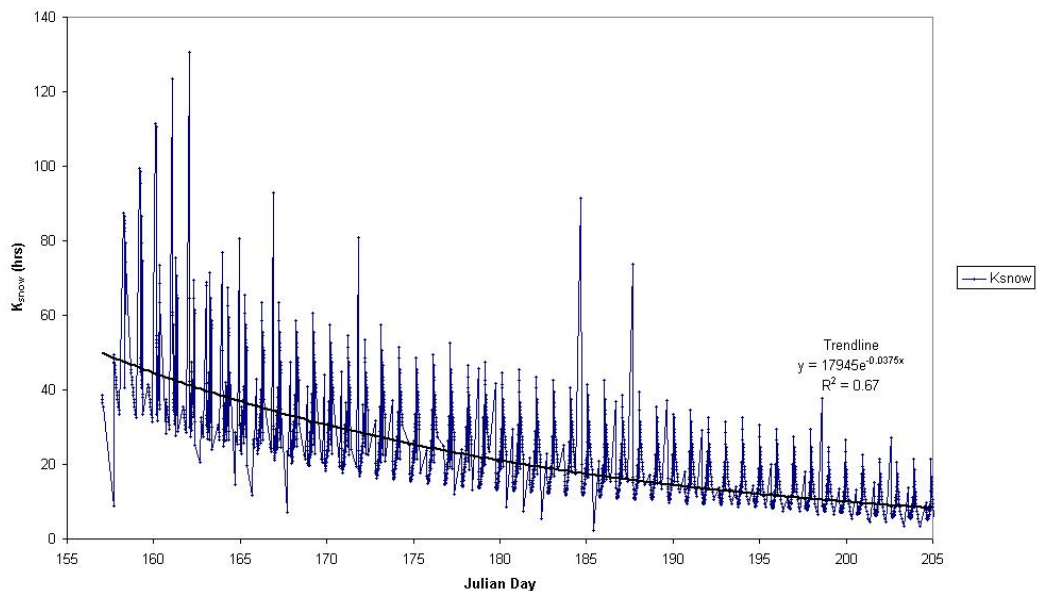
Figure 6.14: Decrease in the storage coefficient K_{snow} with date through the melt season, as derived from SNTHERM input and output flux series.

_____

Figure 6.15 shows K_{snow} values throughout the model run alongside values of the two indices of hydrograph delay and attenuation, 'peak-to-peak lag time' and 'preservation of peak flux'. This enables consideration of what effect on runoff different values of K_{snow} represent. A storage coefficient of 50 hours, for example, corresponds with a delay in the timing of peak flux of around 17 hours and almost complete attenuation of peak flux magnitude (peak output flux being less than 30% of the input peak flux value). K_{snow} of 10 hours corresponds to a lag in peak runoff timing of just one hour and complete preservation of peak flux magnitude.
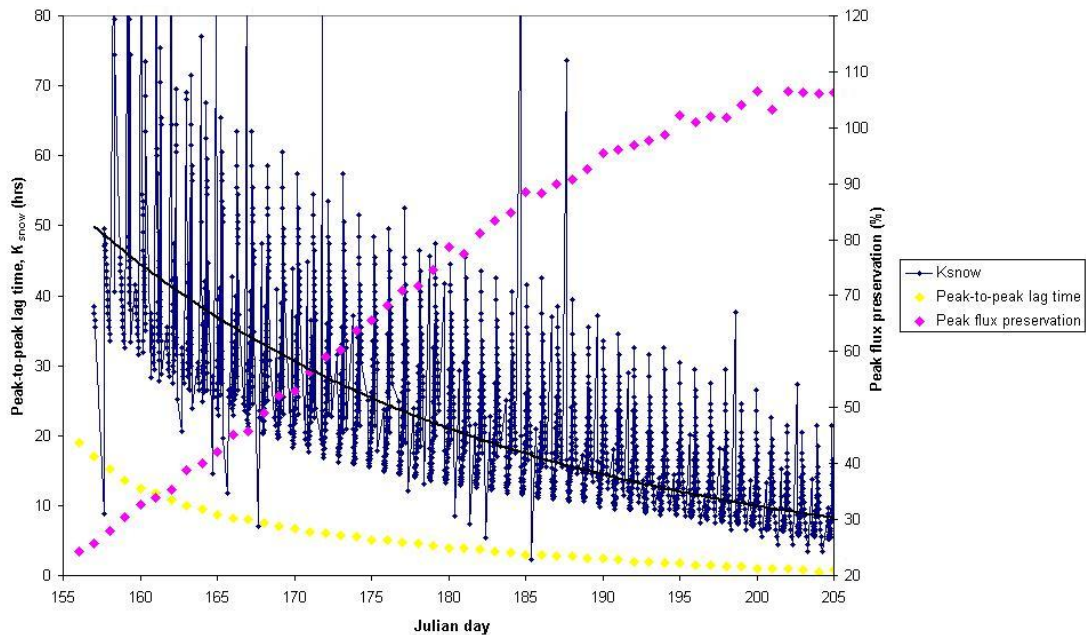
Figure 6.15: Comparison of the value of the storage coefficient K_{snow} with peak-to-peak lag time and peak flux preservation for each day of the model run, indicating the modification of hydrograph timing and magnitude with which values of K_{snow} correspond. For example, a storage coefficient of 50 hours corresponds with a delay in the timing of peak flux of around 17 hours and almost complete attenuation of peak flux magnitude (peak output flux being less than 30% of the input peak flux value).

Figure 6.16 illustrates the difference in modelled runoff that results when a value of 10 rather than 50 hours (the decrease in K_{snow} seen in the season-long SNTHERM run; Figure 6.14) is used for K_{snow}. The amplitude of the runoff hydrograph is markedly higher when K_{snow} is 10 hours, indicating the significant error in modelled runoff magnitude that will result at the end of the melt season if the value of K_{snow} is not lowered through time. A further discrepancy is apparent: hydrograph rising limbs when runoff is modelled by the linear reservoir method using both 10 and 50 hours for K_{snow} are seen to rise at the same time as meltwater input at the snowpack surface begins, while the onset of runoff as modelled by SNTHERM exhibits a ~4 hour lag. The linear reservoir approach, as essentially a storage model, is clearly not adequately representing the delay in runoff timing that is expected due to percolation through snow. To improve model estimation of runoff

_____
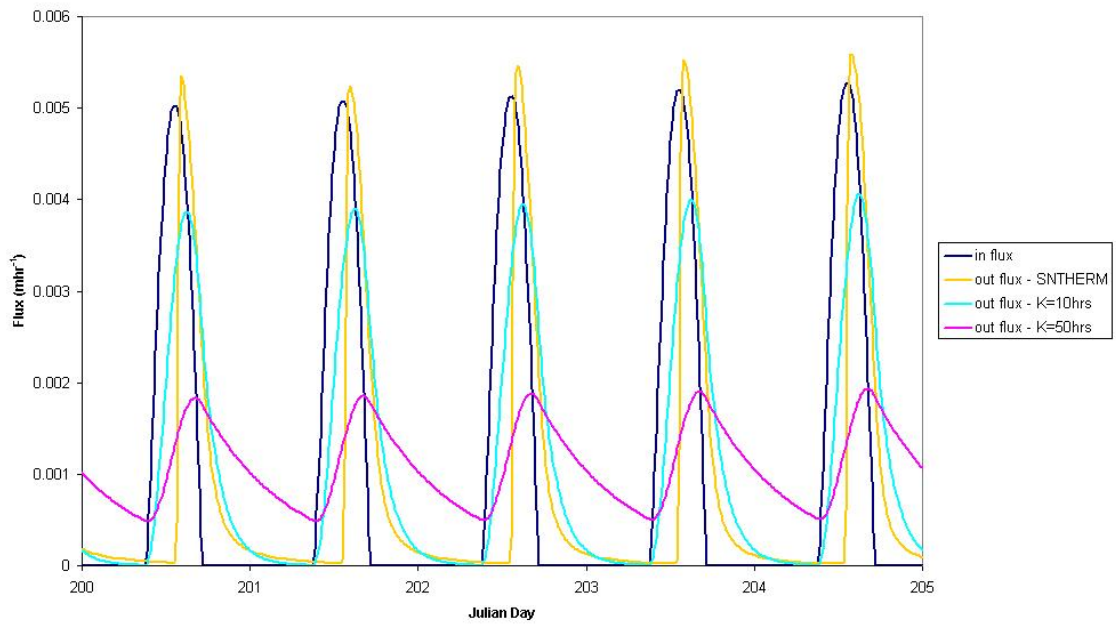
Figure 6.16: Runoff hydrographs modelled by the linear reservoir method, illustrating the difference in modelled runoff that results when a value of 10 rather than 50 hours (the decrease in K_{snow} seen in the season-long SNTHERM run; Figure 6.14) is used for K_{snow}, and therefore the need for K_{snow} to be dynamic through time. Comparison to runoff modelled by SNTHERM shows that linear reservoir modelling is not correctly predicting the delay before runoff begins.

timing, the linear reservoir approach may need to be adapted to include both a lag and a storage influence.

Values of K_{snow} calculated from SNTHERM input and output flux series are point values, representing only percolation through one section of the snowpack. The storage coefficient for the snowpack reservoir as a whole will be higher than the K_{snow} values shown in Figure 6.14, to incorporate the time taken for water from across each supraglacial catchment to flow laterally in the saturated layer before reaching an englacial entry point. Hydrograph recession limb analysis remains the most feasible method of obtaining the storage coefficient for the snowpack reservoir as a whole.

Given the marked evolution of K_{snow} in time (Figure 6.14), it is clear that for glacier runoff to be reliably modelled, the behaviour of the snowpack reservoir should be represented as dynamic and not as static, as has been the case in most previous studies. In this, the findings here support the earlier work of Moore (1993) and Hannah and Gurnell (2001) on linear reservoir modelling and the conclusions of field investigations of snowpack hydrological behaviour presented earlier in this thesis (section 5.6).

When larger glaciers are being modelled, there is likely to be considerable variability in snowpack depth and permeability, and perhaps melt conditions, with altitude along the glacier centre-line. As a result, K_{snow} will also vary in space, making the use of a single storage coefficient to represent the entire snowpack seem unrealistic. The division of the snowpack into multiple reservoirs by altitude, with K_{snow} increasing upglacier, might improve runoff prediction, and should be investigated.

6.9   CONCLUSIONS: MODELLING   SUPRAGLACIAL   SNOWPACK HYDROLOGY

This chapter has considered physically-based modelling representations of snow hydrology in order to add to our understanding of the factors controlling water discharge from the supraglacial snowpack and the way in which this discharge can be expected to change through time as the snowpack evolves. It has been shown that changes in snow depth, permeability and input melt flux magnitude can have significant effects on the form and timing of the runoff hydrograph. Changing snowpack permeability in particular has a markedly non-linear effect on hydrograph delay and attenuation, with runoff becoming rapidly more efficient as permeability increases across low values. As it is across this lowest part of the possible range that net snowpack permeability values measured at Haut Glacier d'Arolla were observed to increase during the course of the melt season (section 5.2.10), it is likely that this change in permeability will have played an important role in driving an increase in the efficiency of runoff. A longer run of SNTHERM (section 6.6) showed the marked change in runoff that is expected to occur during the course of the melt season as snowpack properties (primarily snow depth and snowpack permeability) evolve. That changing snowpack permeability has the potential to drastically alter runoff has particular implications for future modelling studies. Previous studies have often assumed a constant value for permeability throughout the melt season, but improved parameterisation of snow permeability values and the way in which they change through time, ideally based on field observations, is clearly necessary if runoff is to be more reliably modelled. This should be a focus for future research.

The slope of the glacier ice surface over which basal saturated flow takes place and the permeability of basal snow can also significantly affect runoff timing (section 6.4), and these factors must be correctly represented in runoff modelling. However, as flow rates in the basal saturated layer are an order of magnitude or more higher than those in the unsaturated regime, it is percolation through the snowpack depth that acts as the most important control on runoff.

In accordance with the observations of increasing snow hydrological efficiency presented in Chapter 5 and section 6.6, it has been shown that the behaviour of the snow reservoir when runoff is modelled by a linear reservoir model must be treated as dynamic rather than unchanging through time (section 6.8). Most previous studies have had K_{snow} unchanging through time. Other possible improvements to linear reservoir modelling of snow runoff might include variation of K_{snow} in space and the additional of a lag term to better represent the delay of runoff.

Although linear reservoir modelling as presented in section 6.8 provides a useful method of modelling glacier runoff, the role of the supraglacial snowpack in controlling discharge could be more thoroughly investigated using a physical model of snow percolation, such as SNTHERM, combined with basal flow routing in a distributed model of supraglacial snowpack hydrology. The development of such a model is, however, beyond the scope of this project. Snowpack hydrology has been represented in a distributed manner previously in models developed by Fox (2003) and Arnold et al. (1998). Although these models routed water flow through the snowpack in a sophisticated manner according to physical principles, both assumed homogeneous percolation and lacked information about snowpack properties other than depth, and temporal variability of snowpack permeability was therefore not considered. The use of a distributed model in association with the information on snowpack hydrological behaviour collected in this project would enable the point information on snowpack properties described in Chapter 5 to be distributed across the glacier and the importance of variation of snowpack properties both in time and space to be investigated. In addition, a distributed model would allow investigation of the way in which different values of snow permeability in the saturated layer and different configurations of flow across the ice surface influence runoff. These were identified by the sensitivity analysis of basal saturated flow (section 6.4) as factors of potential importance to the rate of runoff, but their role has received little attention. The size and shape of supraglacial catchments, defined by ice surface topography and the locations of crevasses and moulins, will be important controls on runoff into the subglacial drainage system. The way in which snowpack properties vary across supraglacial catchments and the pattern of snowline retreat will have implications for runoff which have yet to be fully considered. This could be investigated with a distributed model.

Chapter 7. Supraglacial snow hydrology: links to glacier hydrology and dynamics

7.1 INTRODUCTION

As outlined in the introduction to this thesis, the principal driving force for improving our understanding of supraglacial snow hydrology is the potential that this offers for better understanding the controls on hydrological processes in the subglacial environment, glacier runoff, and ice dynamics. In this chapter, data on proglacial runoff, water EC and turbidity, and ice dynamics are presented in turn and analysed to identify the timing of any temporal evolution that they show (sections 7.2 to 7.4). This information is then used to infer conditions in the subglacial drainage system and any associated response of ice dynamics (section 7.5). By comparing the timing of changes in subglacial conditions and ice dynamics with the observations of supraglacial snowpack hydrological behaviour presented in Chapters 4 to 6, the role of the snowpack in influencing subglacial drainage system evolution and the timing and magnitude of ice dynamic events can be considered (section 7.6). It is beyond the scope of this project to rigorously establish the links between water discharge through the snowpack and events in the rest of the glacier system; hence there is no modelling of water movement beyond the glacier surface nor of ice dynamics. Instead, the coincidence in time between changes in the hydrological behaviour of the snowpack and the evolution of bulk meltwater parameters or ice dynamics is used to suggest likely links between snowpack hydrology and events in the rest of the glacier system.

7.2 PROGLACIAL RUNOFF

Discharge records obtained from Hydro Exploitation SA hydroelectric company show runoff from the Haut Glacier d'Arolla catchment (at the gauging station approximately 1km downstream from the glacier snout; Figure 2.1) during the 2003 and 2004 field seasons (Figure 7.1). Discharge series from both years exhibit the well documented Northern Hemisphere ablation season trend (Collins and Young, 1981; Hannah et al., 1999), with runoff rising gradually during the early melt season and peaking in mid summer. However, the effect of the difference in melt conditions between 2003 and 2004 (section 4.2) is very apparent, with proglacial runoff beginning to show a consistent and prolonged rise earlier in 2003 (on around 22nd May, compared to around 5th June in 2004) and runoff magnitude consistently higher in 2003 than in 2004. The 2003 runoff series also exhibits high amplitude diurnal variation from early June onwards, but diurnal cyclicity remains less well developed throughout 2004.
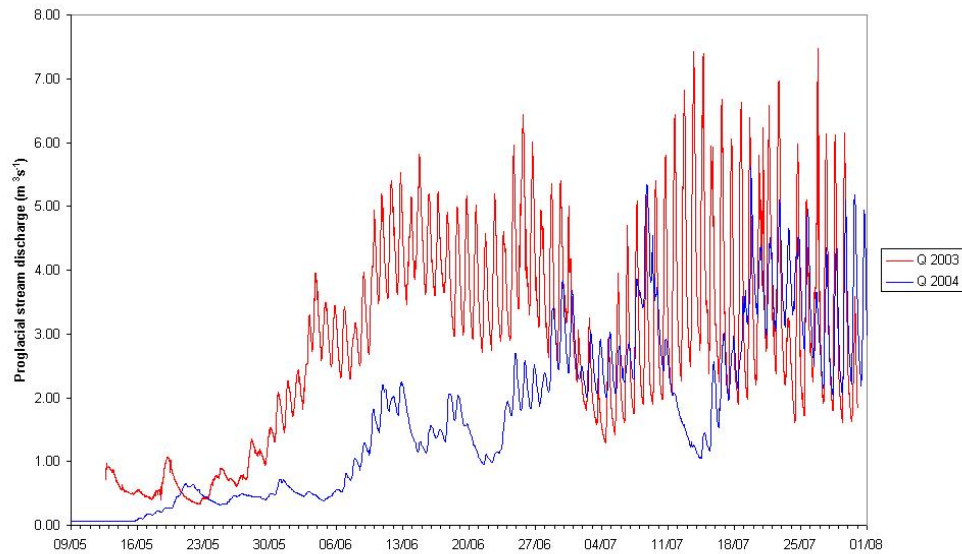
Figure 7.1: Proglacial discharge from the Haut Arolla catchment during the 2003 and 2004 melt seasons. Discharge rises gradually during the early melt season and peaks in mid summer. In 2004 this rise is delayed compared to 2003 and peak discharge values are lower and diurnal cyclicity less well developed.

7.2.1 Hydrograph evolution

The proglacial discharge record was analysed to identify its evolution through time, for later comparison to hydrological conditions in the supraglacial snowpack. Analysis of proglacial hydrograph development drew on the statistical methodologies proposed by Hannah et al. (1999, 2000) and Swift et al. (2005), which enable rigorous objective description of hydrograph form and timing for use in further analysis. Seven indices describing hydrograph magnitude and timing were calculated for each peaked diurnal hydrograph, giving information about hydrograph bulk flow, baseflow and diurnal flow components as follows:

- *Mean runoff* (Q_{mean}), the mean of all runoff derived from ice melt, snow melt and long residence time meltwater/groundwater
- *Minimum runoff* (or baseflow; Q_b), the lowest runoff between 07:00h and the runoff peak, and representing the magnitude of long residence time meltwater/groundwater and meltwater released from storage
- *Maximum (or peak) runoff* (Q_p), the peak runoff from all meltwater sources combined
- *Runoff amplitude* (Q_{amp}), the difference between diurnal maximum (Q_p) and diurnal minimum (Q_b) flows (that is, the magnitude of the superimposed diurnal signal created by rapidly routed snow and ice melt)
- *Standardised runoff amplitude* (Q_{stdamp}), the diurnal runoff amplitude expressed as a proportion of the diurnal minimum flow (i.e. the approximate ratio of rapidly routed to long residence time meltwater):

$$Q_{stdamp} = (Q_p - Q_b)/Q_b$$

- *Time of maximum runoff* (t_{max}), the time of day at which maximum runoff occurs
- *Peak-to-peak lag time* (t_{lag}), the lag between the time of peak meltwater production at the snowpack or glacier surface and the time of peak proglacial runoff.

Figures 7.2 to 7.8 present the values of these indices through both field seasons. The values for Q_{mean} presented in Figure 7.2 clearly show the difference in bulk discharge between the two study years. The values of Q_b and Q_p shown in Figures 7.3 and 7.4 for 2003 and 2004 respectively clarify the discharge trends in Figure 7.1, showing the slow variation of the baseflow component of runoff and the more rapid response of peak flow values to variations in melt input. In both years, peak flux Q_p generally became greater later in the melt season.
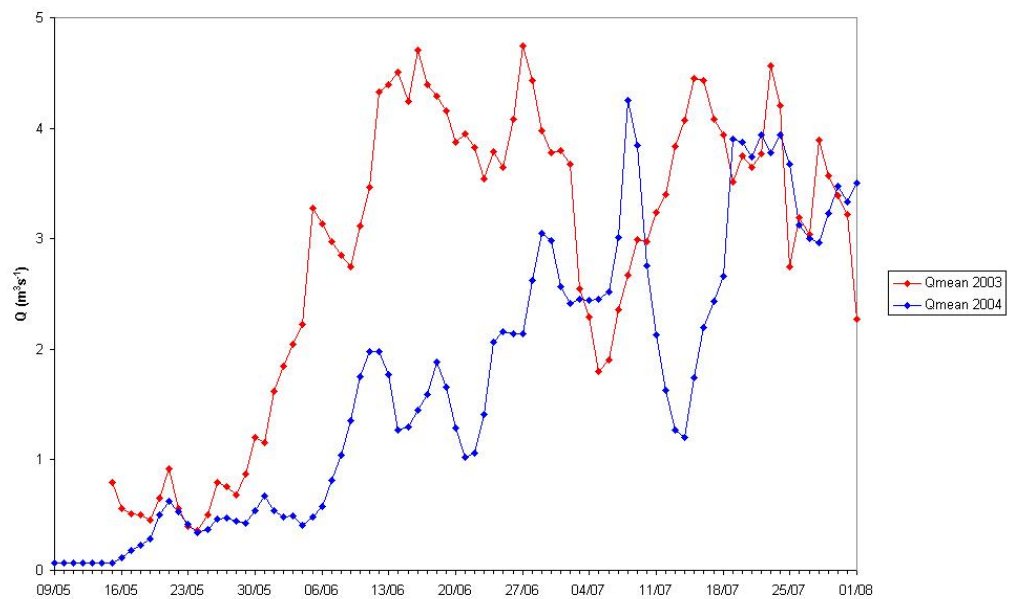
Figure 7.2: Daily Q_{mean} for 2003 and 2004 proglacial discharge, clearly showing the difference in bulk discharge between the study years.
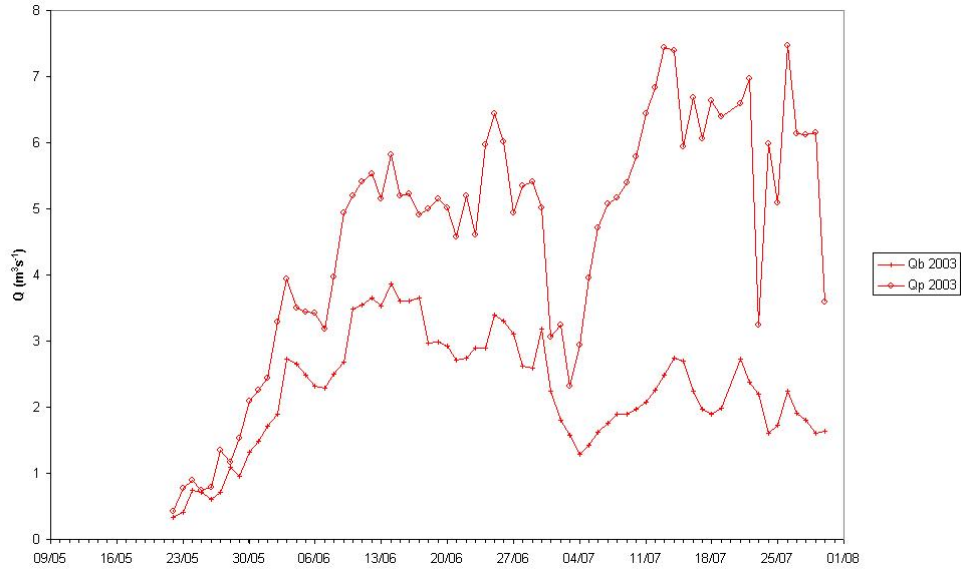
Figure 7.3: Daily maximum (Q_p) and minimum (Q_b) proglacial discharge in summer 2003. The value of peak flux Q_p, which responds to variations in melt input, generally becomes greater later in the melt season.
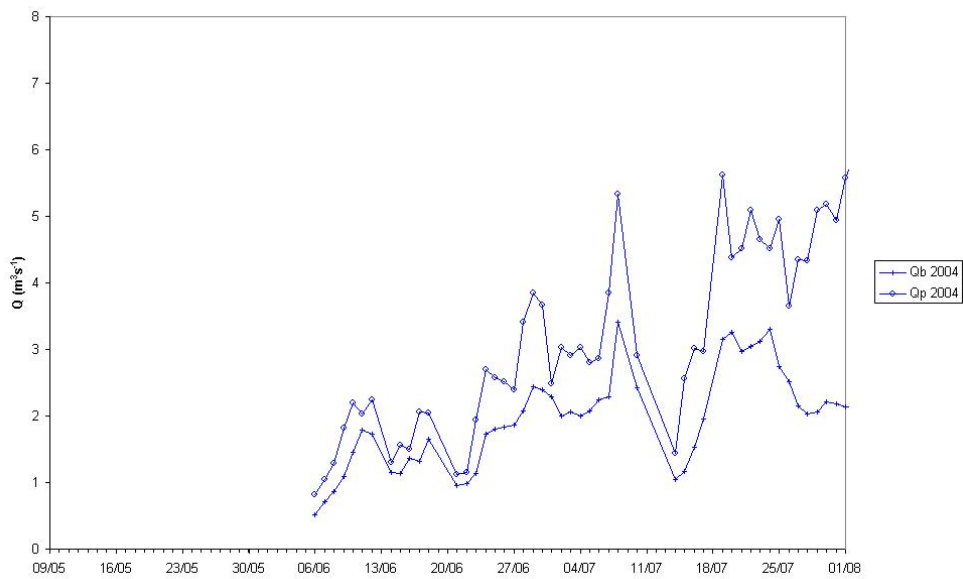
Figure 7.4: Daily maximum (Q_p) and minimum (Q_b) proglacial discharge in summer 2004. The value of peak flux Q_p, which responds to variations in melt input, generally becomes greater later in the melt season.

In both 2003 and 2004 there was strong evidence of an increase in runoff amplitude Q_{amp} with time (p < 0.01 in both years; Figures 7.5 and 7.6). Standardised runoff amplitude Q_{stdamp} also increased through time, though less strongly in 2004 (p < 0.01 in both years).
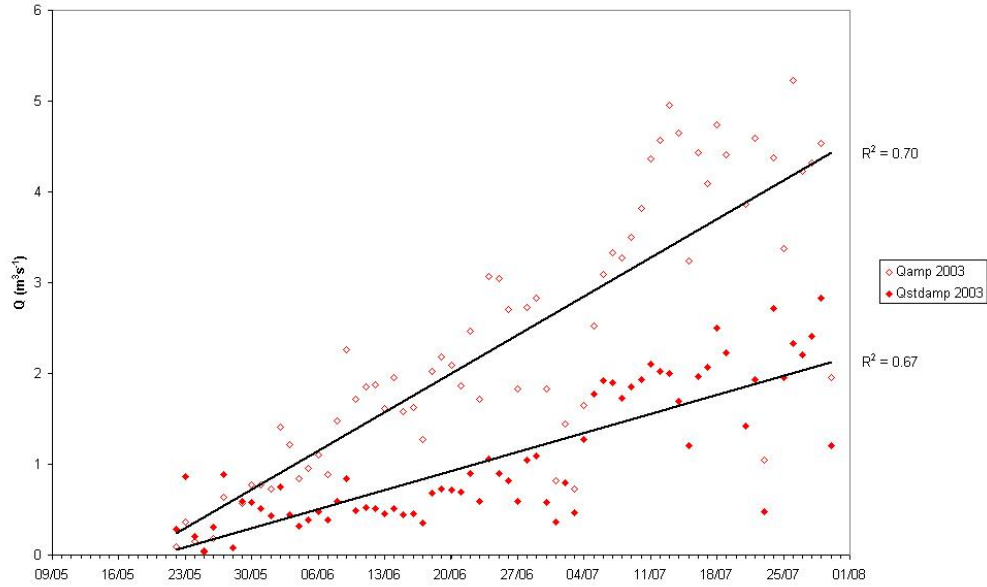
Figure 7.5: Daily runoff amplitude (Q_{amp}) and standardised amplitude (Q_{stdamp}) of proglacial discharge in summer 2003, showing strong evidence of an increase in both runoff amplitude Q_{amp} and standardised runoff amplitude Q_{stdamp} with time (p < 0.01 for both).
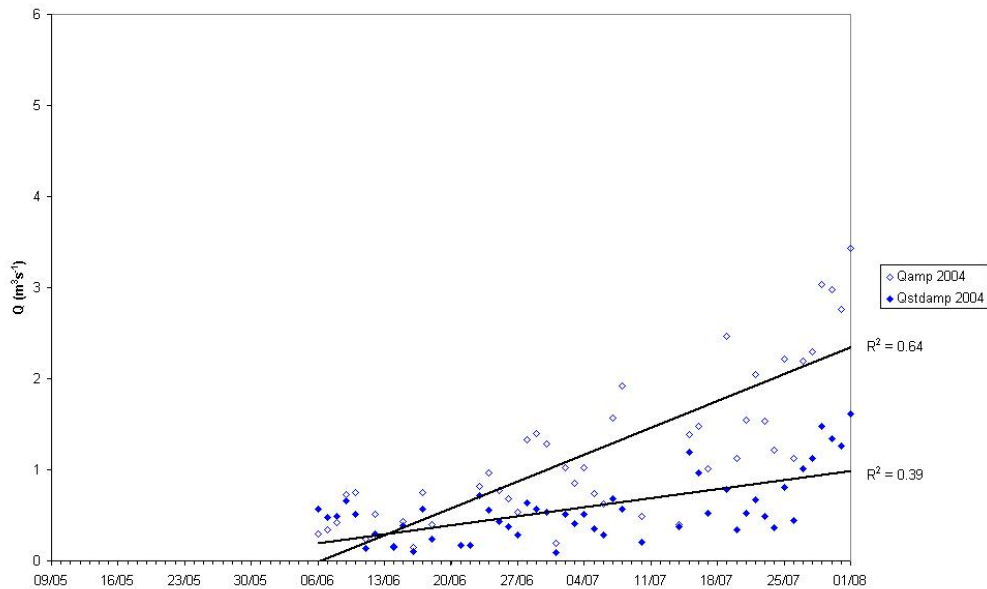
Figure 7.6: Daily runoff amplitude (Q_{amp}) and standardised amplitude (Q_{stdamp}) of proglacial discharge in summer 2004, showing strong evidence of an increase in both runoff amplitude Q_{amp} and standardised runoff amplitude Q_{stdamp} with time (p < 0.01 for both).

As expected, there was a significant change in the timing of peak diurnal runoff during both summers, becoming earlier through time (Figure 7.7; p < 0.01 for both years). Maximum discharge frequently occurred around midnight, if not later, in the early melt season, and as early as 3:00pm in July. Throughout 2004, the time of peak runoff was consistently several hours later than at the equivalent date in 2003. As transit times for water percolation through the snowpack were shown by dye tracing experiments to be fairly similar with date in both field seasons (section 5.6.2), this difference in overall lag is likely due to the lower melt inputs and resulting inefficiency of the subglacial drainage system (Nienow et al., 1998) in 2004.
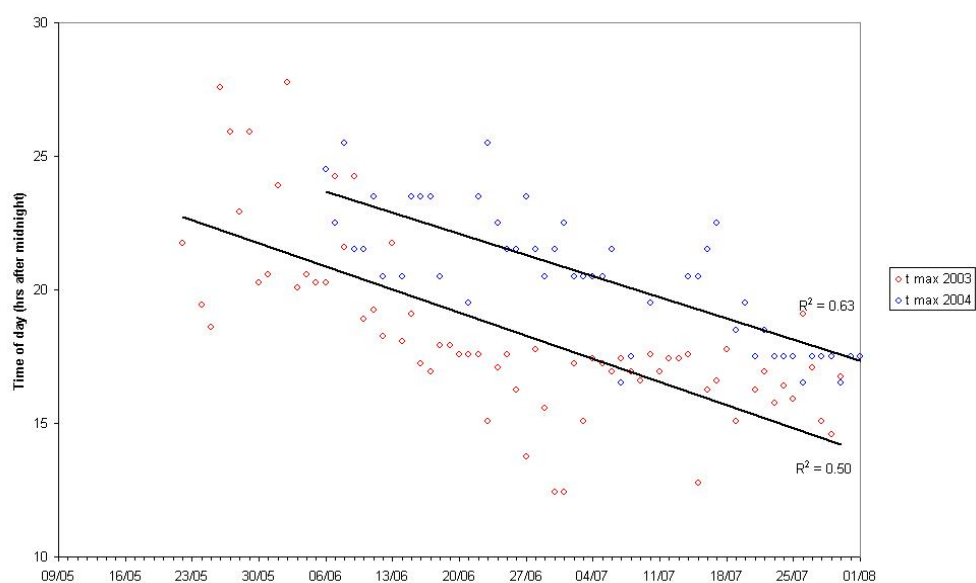
Figure 7.7: Time of maximum diurnal discharge (t_{max}) in summers 2003 and 2004, showing significant evidence of a runoff occurring earlier with time through both summers (p < 0.01 for both years).

Peak-to-peak lag time, an important index for considering the effect of the snowpack (and other parts of the glacier hydrological system) in delaying the timing of runoff arrival at the proglacial stream, showed some evidence (p < 0.01) of decrease through time during the 2003 melt season, but a poor trend in 2004 (Figure 7.8). In the absence of detailed information about meltwater inputs to the glacier surface throughout both field seasons, the time of peak diurnal air temperature was used as a proxy for the time of peak melt. As incident radiation (and therefore melt flux) generally leads air temperature by a couple of hours (Swift et al., 2005), the time lag between peak melt input and peak runoff is assumed to be approximately two hours greater than that indicated in Figure 7.8. The lack of trend in the 2004 data may reflect a real absence of any temporal decrease in meltwater transit time through the glacial system, likely due to limited development of hydraulic efficiency in the subglacial drainage system, but might also be attributed to a less well defined relationship between temperature and melt input under the variable meteorological conditions of 2004.
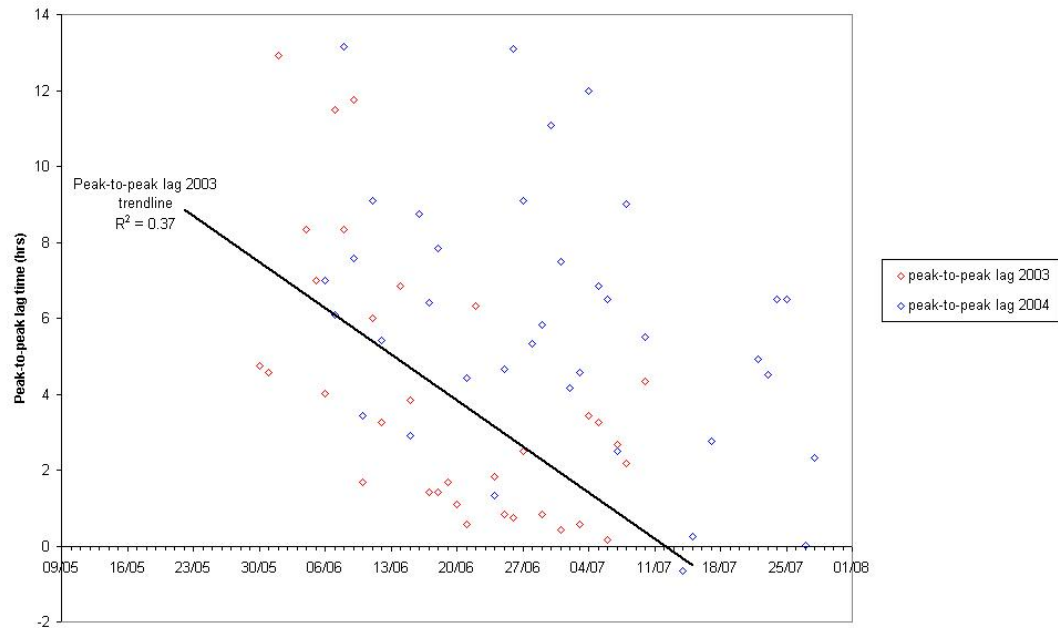
Figure 7.8: Lag time between peak diurnal air temperature and peak diurnal proglacial discharge throughout summers 2003 and 2004. There is evidence of a decrease in runoff lag with time during the 2003 melt season (p < 0.01), but a poor trend in 2004 (although this may be due to the less well defined relationship between temperature and melt input under the variable meteorological conditions of 2004).

The analysis above has shown evidence for evolution of proglacial hydrograph shape, magnitude and timing during the course of both the 2003 and 2004 melt seasons, all indicative of more efficient meltwater transfer through the glacier system. The cause of these changes, and in particular any role that the supraglacial snowpack might play, is considered in section 7.6.

Although data from the two field seasons have this trend of increasing hydrological efficiency in common, the indices presented here otherwise highlight the significant difference in runoff conditions between 2003 and 2004. This year-to-year variability is much more dramatic than usually observed at Haut Glacier d'Arolla. Due to the unusually warm temperatures during summer 2003, snow and ice melt and therefore runoff were abnormally high in that year (Haeberli et al., 2006). In comparison to the values presented by Swift et al. (2005, Figure 2d and Table 4) for a more representative melt year at Haut Glacier d'Arolla (1998), average Q_{mean} for the late melt season in 2003 was over 1 m^3 s^{-1} higher. 2004, in contrast, saw unusually low melt and runoff for most of the summer. The extreme nature of the melt conditions under which data for this project was collected must be kept in mind during data analysis and interpretation.

7.3 PROGLACIAL STREAM ELECTRICAL CONDUCTIVITY AND TURBIDITY

Time series of proglacial stream electrical conductivity and turbidity are presented in Figure 7.9. Variations in electrical conductivity (EC) provide a proxy for variations in solute load in the subglacial drainage system (Collins, 1979, 1995; Fenn, 1987), while turbidity provides a measure of meltwater suspended sediment concentration (SSC). Records were obtained between 12th May and 6th July in 2003 and 29th May and 26th July in 2004. The monitoring site was moved twice during the 2003 season (on 17th and 30th June) and once in 2004 (on 25th June), as changing channel positions in the braided proglacial channel made its position unstable. In 2004, this move appears to have exposed the sensors to water of very different characteristics, with a sudden rise in EC and to a lesser extent turbidity. Moves in 2003 do not appear to have had such an effect. The 2003 EC record, however, shows a sudden increase on 11th June, although no change in conditions at the monitoring site was observed. As the EC of glacial runoff is generally expected to decrease through the melt season, this increase is likely due to some unobserved shift in the channel upstream from the sensors or change in the degree of mixing between the main and tributary channels.

7.3.1 Turbidity and EC trends

Disregarding the discontinuities mentioned above, the general trend in both seasons was of high EC (30 to 50 μS cm^{-1}) in the early melt season, falling rapidly over a period of about 10 days before the establishment of diurnal cycles around 10 μS cm^{-1}. Turbidity values were initially low and rose in parallel with the fall in EC before displaying diurnal cyclicity. These EC values agree in general with those previously observed at Haut Glacier d'Arolla: Gurnell et al. (1992; data for 1989) report early-season values of 30 to 40 μS cm^{-1} falling to around 20 μS cm^{-1}, while Richards et al. (1996; data for 1990) report early-season values of 20 to 30 μScm^{-1} falling to around 15 μS cm^{-1}. That the data presented here falls to values lower than reported in these studies can possibly be attributed to greater dilution of subglacial runoff by other water sources. The general pattern shown by EC and turbidity data remains similar to that previously found.

The use of proglacial stream turbidity and EC to infer conditions in the subglacial drainage system and assist in the interpretation of subglacial flow pathways and storage mechanisms has been established by Collins (1979b), Clifford et al. (1995), Willis et al. (1996), and Swift et al. (2002) among others. More detailed meltwater chemistry data in terms of individual cations and anions is desirable in order to draw more firm inferences about the hydrological system (Richards et al., 1996), but to collect such data was beyond the scope

of this project. In previous studies at Haut Glacier d'Arolla, the simultaneous decrease in EC and increase in turbidity observed in the early melt season has been shown to correspond with destabilisation of the distributed winter subglacial drainage system by increasing meltwater inputs, the occurrence of the spring dynamic event, and the establishment of a more efficient channelised subglacial drainage system (Tranter et al., 1996; Swift et al., 2002). That these typical EC and turbidity trends were seen in 2003 and 2004 (Figure 7.9) is therefore taken as evidence of similar perturbation and reorganisation of the subglacial drainage system, with the corresponding occurrence of any glacier dynamic event to be further investigated using survey data (section 7.4).

a)

b)
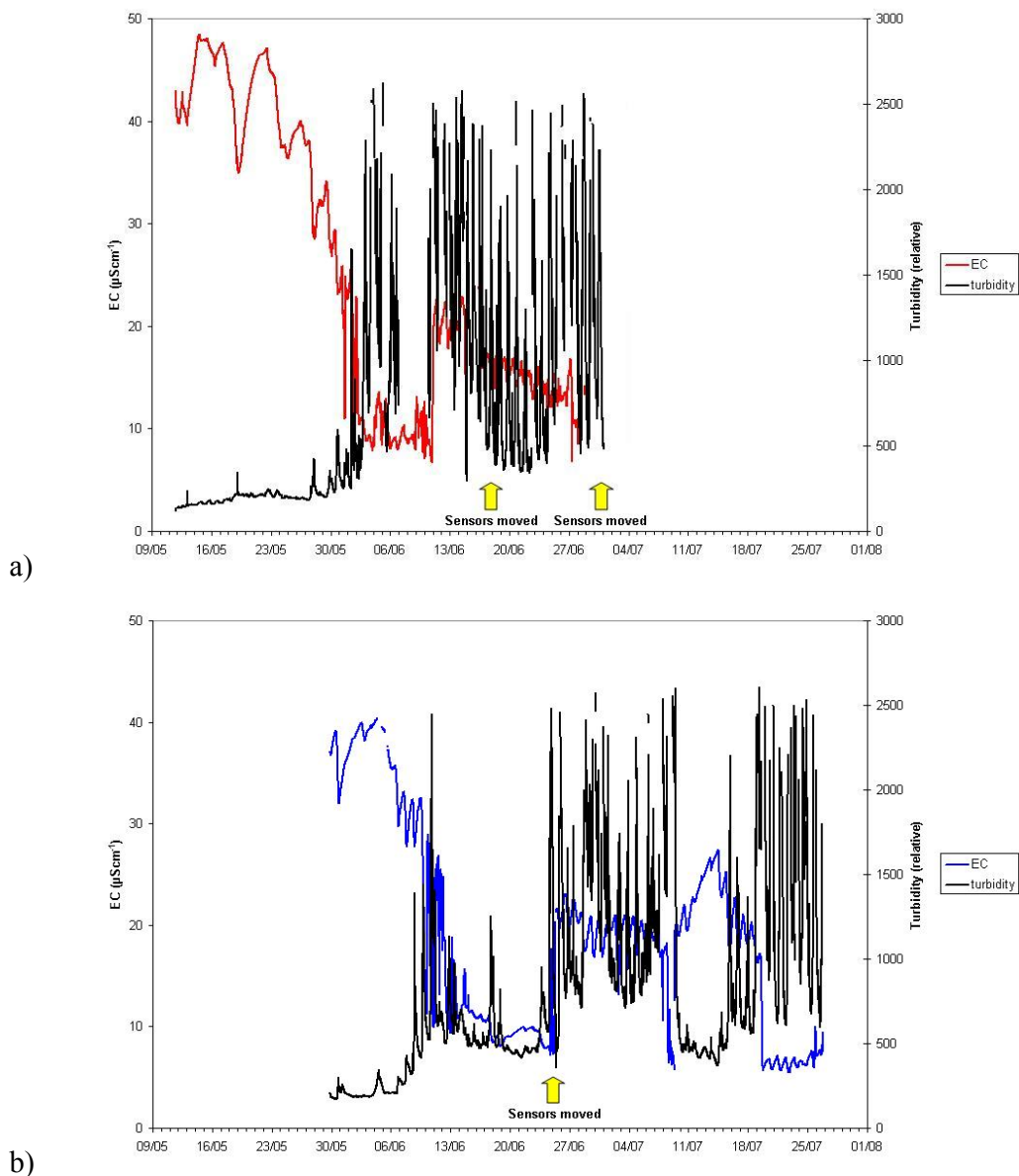
Figure 7.9: Proglacial runoff EC and turbidity data series for a) 2003 and b) 2004. The general trend in both seasons is of high EC (30 to 50 μS cm^{-1}) in the early melt season, falling rapidly over a period of about 10 days before the establishment of diurnal cycles around 10 μS cm^{-1}. Turbidity values are initially low and rise in parallel with the fall in EC before displaying diurnal cyclicity.

7.4 INTRA-SEASONAL FLOW DYNAMICS OF HAUT GLACIER D'AROLLA

Previous studies have established the spatial and temporal patterns of ice dynamics typically seen at Haut Glacier d'Arolla (Harbor et al., 1997; Hubbard et al., 1998; Mair et al., 2001, 2002b, 2003). In common with many other glaciers (e.g Iken et al., 1983; Hooke et al., 1983; Harper et al., 2002), Haut Glacier d'Arolla is observed to exhibit increased flow velocities during the summer months, when surface velocity averages around 4 cm day^{-1} compared to around 2 cm day^{-1} during winter months (Harbor et al., 1997). Peak ice surface velocities, reaching 10 to 12 cm day^{-1}, are typically observed over the course of a few days early in the melt season (Harbor et al., 1997; Mair et al., 2003), a phenomenon termed the 'spring event'. Observations of subglacial conditions using dye-tracer tests (Nienow et al., 1998) and down-borehole pressure sensors (Hubbard et al., 1995) have indicated that this speed-up event corresponds with increased melt inputs to an inefficient distributed drainage system not yet adapted to increased flux, high subglacial water pressures, and often a change in subglacial drainage system structure.

Due to the importance of high subglacial discharges in driving glacier dynamic events, the influence of water flow through a supraglacial snowpack on runoff magnitudes into the rest of the glacier system may have important implications for ice dynamics. This section presents field data collected in order to identify ice dynamic events at Haut Glacier d'Arolla during the summer melt seasons of 2003 and 2004. In section 7.6 this data will be considered alongside snowpack information in order to assess what effect supraglacial snowpack hydrology may have had on ice dynamics. From our existing understanding of snowpack hydrology, a number of conceptual hypotheses can be constructed to suggest the way in which water flow through a supraglacial snowpack hydrology will influence ice dynamics, and these are illustrated in Figure 7.10. These hypotheses indicate which properties should be of interest during analysis of glacier velocity data.

As discussed previously in section 2.3.2, the dampening effect that flow through the supraglacial snowpack has on runoff magnitudes into the englacial and subglacial drainage systems will mean that the magnitude of discharge through the subglacial drainage system resulting from a given surface melt flux will be lower if there is a significant and inefficient supraglacial snowpack than if the ice surface is snow-free. In Figure 7.10, which presents idealised subglacial discharge and subglacial water pressure trends through a melt season for glaciers with either a snow-covered or bare ice surface, it can be seen that subglacial discharge when there is a snowpack present does not rise as soon as melt begins. The thick, hydrologically inefficient snowpack at the start of the melt season attenuates the runoff hydrograph completely such that there is no increase in subglacial discharge. If no
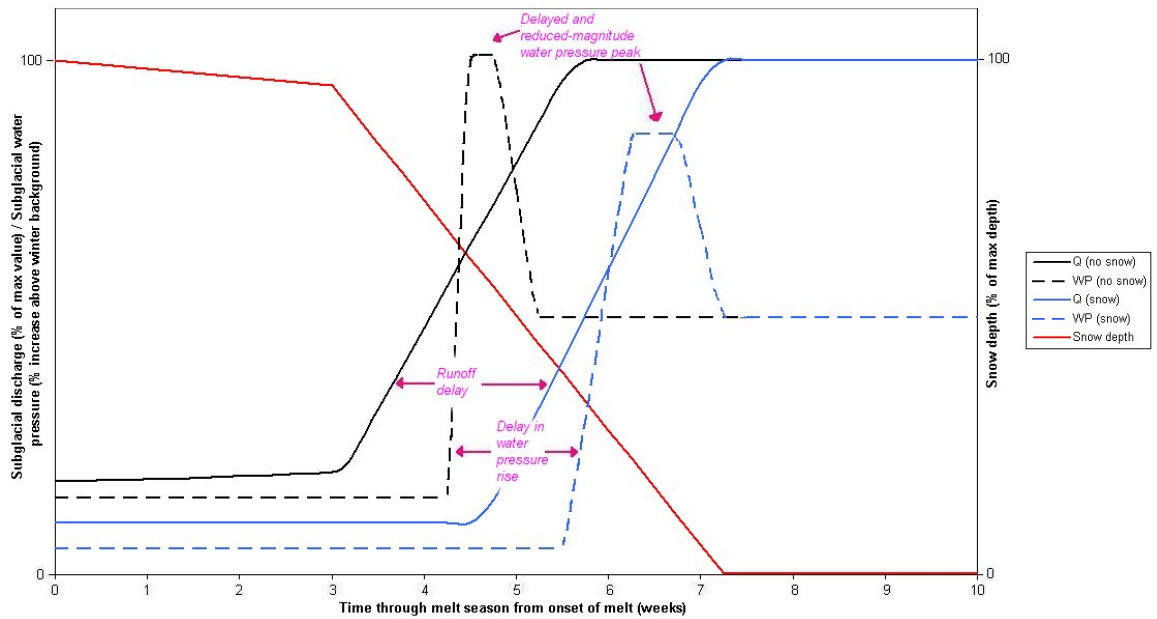
Figure 7.10: Idealised subglacial discharge (solid lines) and subglacial water pressure (dashed lines) trends through a melt season for glaciers with either a snow-covered (blue lines) or bare ice (black lines) surface. Snowpack depth is also shown (red line). This example is intended to illustrate the most likely impacts that flow through a supraglacial snowpack will have on subglacial discharge and water pressure, and therefore the occurrence of the spring dynamic event. The timescale on the x-axis is approximate and intended to reflect the approximate timing of hydrograph and water pressure evolution that might be observed at Haut Glacier d'Arolla when melt is driven only by solar radiation and not by unique föhn and rainfall events. It can be seen that the increases in subglacial discharge and water pressure are delayed, and maximum water pressure reduced, when the glacier surface is covered with snow.

snowpack is present, subglacial discharge will begin to rise immediately in response to surface melt – in Figure 7.10 this is shown by the gradual rise of the solid black line from the start of the melt season and the steeper rise after three weeks when melt increases. When a snowpack is present, subglacial discharge (solid blue line) only begins to rise after around 4½ weeks of melt, once the surface melt flux is greater (and therefore percolates more efficiently through the snowpack resulting in higher runoff) and/or decreasing snowpack depth and increasing snow hydrological efficiency allow runoff to be transmitted to the englacial system with less attenuation. There is therefore a delay in the timing of increasing subglacial discharge when the snowpack is present (Figure 7.10). Correspondingly, if there is a snowpack present then the increase in subglacial water pressure (dashed blue line) will also be delayed relative to the 'no snow' case (dashed black line) (Figure 7.10), as water pressure increases are driven by increased subglacial discharge. There is therefore also likely to be a delay in the attainment of subglacial water pressure sufficient to trigger a speed-up event, i.e. spring event occurrence will be delayed by the supraglacial snowpack. Furthermore, when a speed-up event does occur, attenuation of the hydrograph by flow through the snowpack may result in this event having a lower magnitude (i.e. slower velocity) than it would were the snowpack absent (Figure 7.10).

The phenomena described above (delay of rises in subglacial discharge and water pressure, delay in occurrence of the spring event, and reduction of speed-up magnitude caused by the supraglacial snowpack) will be enhanced in a upglacier direction, as the snowpack remains deeper and less hydrologically efficient for longer. This is the mechanism suggested by Nienow (1997) as causing the lag in the timing of the spring event and lower peak ice velocities with distance upglacier that have been observed previously at Haut Glacier d'Arolla.

The discussion above has suggested three ways in which supraglacial snowpack hydrology is expected to influence glacier dynamics, namely delaying spring event occurrence, reducing speed-up magnitude, and causing an upglacier lag in the timing of the spring event and upglacier decrease in peak ice velocities. A lack of information about the hydrological behaviour of the supraglacial snowpack has to date prevented further consideration of these links between snow hydrology and ice dynamics, and this thesis aims to aid in the clarification of this relationship.

Surveying of glacier dynamics was carried out during both field seasons as described in section 3.8.4, with the aim of obtaining a data set with which the following aims could be investigated:

   i)   to determine the timing and magnitude of any glacier velocity events;
   ii)   to identify whether there is any longitudinal spatial pattern in the occurrence of velocity events; and
   iii)   to assess the correspondence between supraglacial snowpack hydrological behaviour and ice dynamics.

Survey data was collected between 16th May and 19th June in 2003 and between 25th May and 28th June in 2004. Stake positions were surveyed on average every 2 days during these periods, as weather conditions, the demands of experimental work in the snowpack, and the presence of field assistants permitted. Ice surface velocities were calculated from measurements of distance to survey stakes following the method outlined in section 3.8.4.1, and the resulting time series of ice velocity data is presented in section 7.4.1. Conclusions regarding the occurrence and timing of any velocity event comparable to the 'spring event' are drawn in section 7.4.2.

7.4.1 Short-term variations in ice surface velocity

Time series of velocity for each survey stake are presented in Figures 7.11 and 7.12 for the 2003 and 2004 field seasons respectively. Stake locations are shown in Figure 3.16.

In 2003, downglacier stake velocities ranged between 0.004 and 0.083 m day^{-1}. For all four stakes considered, velocities were generally below mean values for the first half of the survey period, and rose above mean values during the second half (Figure 7.11). This increase in stake velocity occurred around 6th June for stake 101 and around 3rd June for stakes 201, 401 and 501 (Figure 7.11). Mean velocity after these dates increased by between 78 and 218 % compared to mean values in the early season (Table 7.1).

Table 7.1: Comparison of ice surface velocities before and after the observed speed-up in 2003.

Stake	Date of velocity increase	Mean velocity period 1 (m day^{-1})	Mean velocity period 2 (m day^{-1})	Percentage increase
101	6th June	0.0090	0.0286	218
201	3rd June	0.0127	0.0359	182
401	3rd June	0.0204	0.0513	152
501	3rd June	0.0246	0.0438	78

In 2004, downglacier stake velocities ranged between 0.002 and 0.062 m day^{-1}. Stake 101 showed little evidence of any temporal change in velocity. Stakes 401 and 501 exhibited velocities rising above mean values between 10th and 14th June (Figure 7.12). A second increase in velocity can be seen on 24th or 25th June in records for stakes 201, 401, 501 and 601. During the earlier speed-up event, velocity rose only by around 25% (Table 7.2). The second speed-up event was more pronounced, representing an increase of 50 to 180 % over mean values for the survey period (Table 7.2).

Table 7.2: Comparison of ice surface velocities during speed-up events in 2004 to mean values for the whole survey period.

Stake	Date of velocity increase(s)	Mean velocity for survey period (m day^{-1})	Mean velocity - speed-up 1 (m day^{-1})	Mean velocity - speed-up 2 (m day^{-1})	Percentage increase - speed-up 1	Percentage increase - speed-up 2
201	25th June	0.0158	-	0.0442	-	180
401	10th and 24th June	0.0299	0.0372	0.0624	24	109
501	10th and 24th June	0.0301	0.0375	0.0513	25	70
601	24th June	0.0411	-	0.0615	-	50
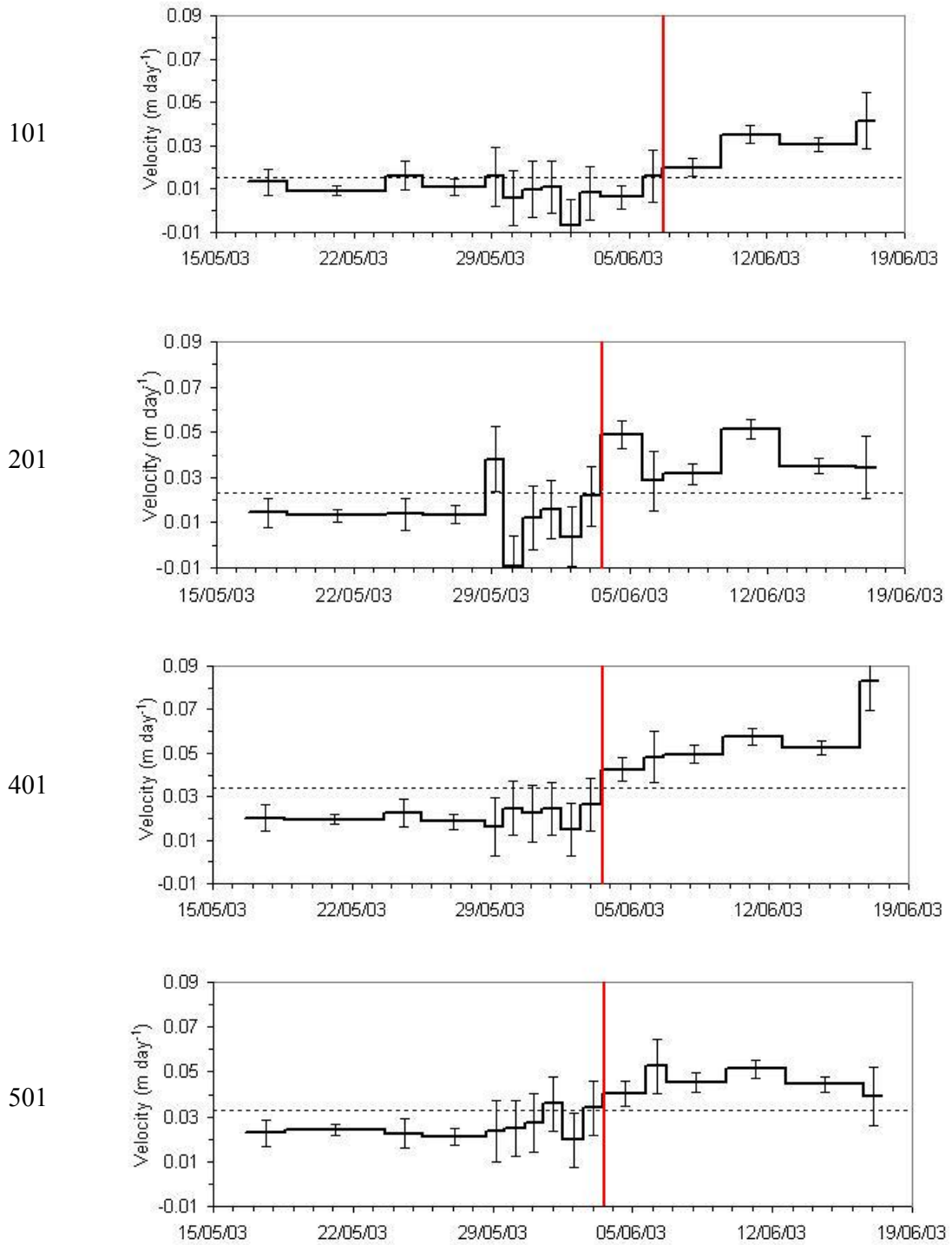
Figure 7.11: Stake velocities during the 2003 field season. Dashed lines indicate mean velocities for each stake during the survey period. Red vertical lines mark the beginning of inferred speed-up events.
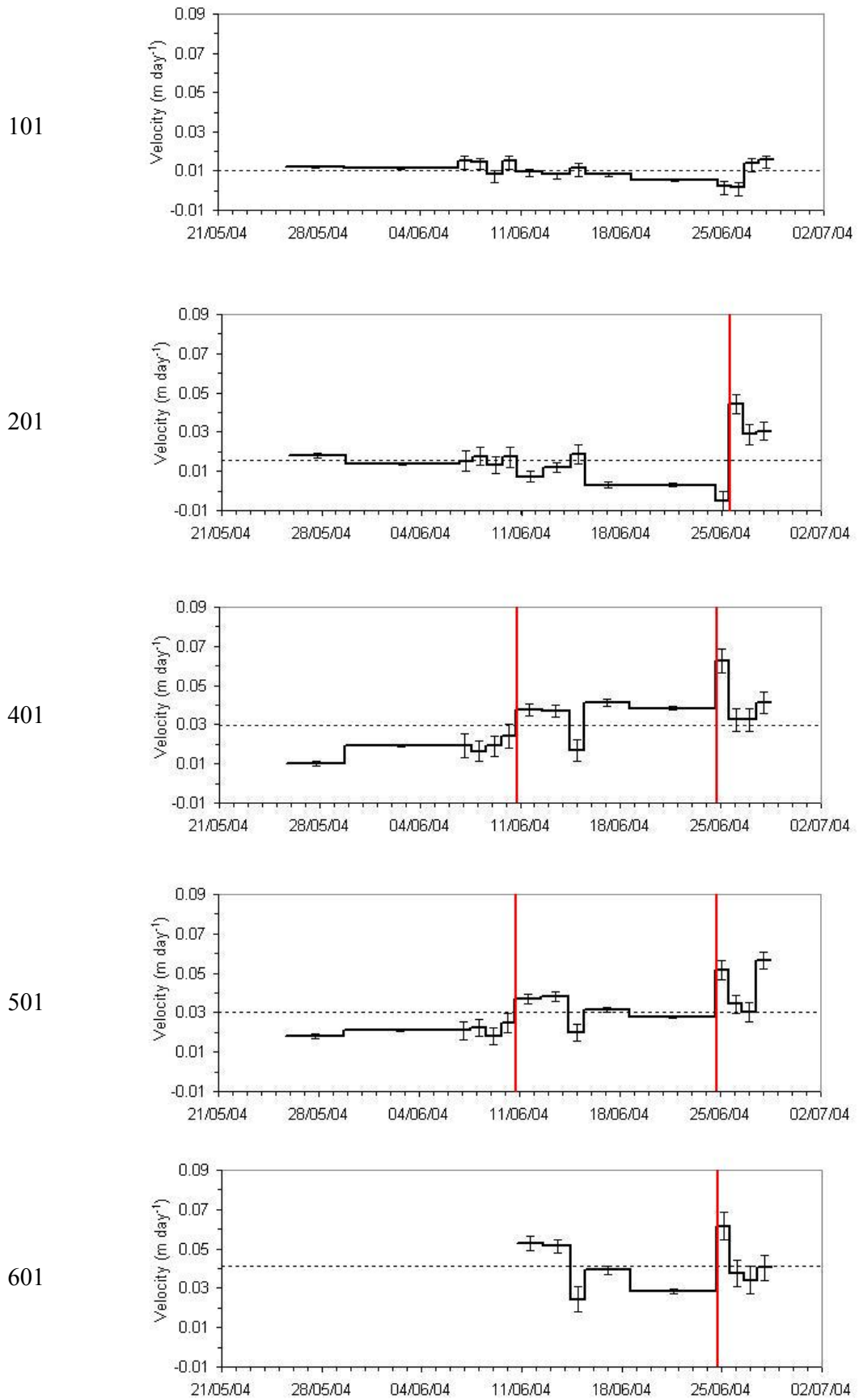
Figure 7.12: Stake velocities during the 2004 field season. Red vertical lines mark the beginning of inferred speed-up events.

No spatial trend in the timing of speed-up events was seen in either 2003 or 2004. In both years, however, the amplitude of the velocity increase becomes greater in the downglacier direction (Tables 7.1 and 7.2).

Data concerning the timing and magnitude of spring events previously observed at Haut Glacier d'Arolla is compiled in Table 7.3. In previous years, the glacier has been observed to flow at a background velocity of between 0.01 and 0.05 m day^{-1}, with velocities increasing to ~0.10 to 0.12 m day^{-1} during speed-up events (Harbor et al., 1997; Mair et al., 2003). These speed-up events have occurred at varying times between early June and mid July and there may be one or two events per summer (Table 7.3). In comparison to these previous observations, ice surface velocities measured in 2003 and 2004 were lower, reaching at most 0.05 or 0.06 m day^{-1} during the speed-up events identified in Tables 7.1 and 7.2. As in 1995 and 1998, there is evidence of two speed-up events occurring in 2004.

Table 7.3: Previous speed-up events observed at Haut Glacier d'Arolla.

Year	Date of speed-up event(s)	Peak daily velocity (m day^{-1})	Source
1994	22nd – 28th June	0.18	Nienow (1997), Mair et al. (2001)
1995	2nd – 4th July; 10th – 14th July	0.12; 0.09	Mair et al. (2002b)
1998	4th – 7th June; 21st – 26th June	0.12; 0.10	Mair et al. (2003)
1999	1st – 9th July	0.10	Mair et al. (2003)

7.5 INTERPRETATION OF PROGLACIAL HYDROLOGY AND ICE DYNAMIC DATA

This section draws together the data on proglacial discharge, water EC and turbidity and ice surface velocities (sections 7.2 to 7.4) in order to reach conclusions about conditions in the subglacial drainage system and possible response of ice dynamics during the field seasons at Haut Glacier d'Arolla. The timing of changes in subglacial hydrology and ice dynamics will then be considered against the changing hydrological behaviour of the supraglacial snowpack (as revealed in Chapters 4 to 6), and the possible role of the snowpack in driving changes elsewhere in the glacier system will be considered (section 7.6).

Plots of the temporal variation in proglacial discharge, water EC and turbidity, and ice surface velocity are brought together for comparison in Figures 7.13 and 7.14 for summers 2003 and 2004 respectively. Together these records can reveal conditions in the subglacial drainage system throughout the melt season (sections 7.5.1 and 7.5.2) and the timing of hydrological and ice dynamic events (section 7.5.3).

7.5.1 Early-season subglacial hydrological conditions

At the onset of records in both field seasons, both proglacial meltwater discharge and turbidity were low and slowly varying, while electrical conductivity was high and slowly varying (Figures 7.13 and 7.14). Such conditions result from low meltwater inputs to the glacier system, long contact times with subglacial sediment and/or bedrock, and water flow velocities insufficient to mobilize subglacial sediment (Richards et al., 1996; Swift et al., 2002; 2005). From this, the existence of an inefficient distributed subglacial drainage system is inferred.

7.5.2 Evidence for subglacial drainage evolution

Both 2003 and 2004 data sets show a correspondence between falling EC, rising turbidity, rising proglacial meltwater discharge, and the onset of diurnally-varying hydrographs in the discharge record, taking place around 31st May in 2003 and 7th June in 2004 (Figures 7.13 and 7.14). Such conditions result from increased meltwater inputs to the subglacial environment, transmitted through the drainage system sufficiently quickly that diurnal cycles are retained, little EC signature is picked up by contact with subglacial sediment, and subglacial sediment can be entrained and evacuated (Richards, 1996; Swift et al., 2002; 2005). This evolution of hydrological parameters therefore provides evidence of a change in subglacial drainage system structure from the inefficient distributed system in place during winter to a more efficient channelised system required to deal with larger summer melt inputs. In 2004, after the initial rise around 7th June, turbidity values returned to lower, slowly varying values for a further two weeks (Figure 7.14). It therefore appears that complete evolution of the subglacial drainage system did not take place at that time. Turbidity rose again on 24th June 2004 and thereafter exhibited the high and diurnally varying values typical of runoff through an efficient subglacial drainage system.

7.5.3 Evidence for the occurrence of a 'spring event'

Data for both 2003 and 2004 shows a close temporal correspondence between the changes in proglacial discharge, water EC and turbidity described in section 7.5.2 and the speed-up events on ~3rd June 2003 and ~10th June 2004 proposed in section 7.4.2 (Figures 7.13 and 7.14). It therefore appears that these speed-up events were triggered, as expected, by increased meltwater flux into a distributed subglacial drainage system. As the event on 10th June 2004 did not trigger the formation of an efficient subglacial drainage system (section 7.5.2), the subsequent rise in discharge on 24th June appears to have triggered a second speed-up event (Figure 7.14). Detailed studies of ice dynamics and subglacial drainage system characteristics during previous melt seasons at Haut Glacier d'Arolla have identified high subglacial water pressure caused by rapidly increasing discharge as the cause of spring events in previous years (Nienow, 1997; Mair et al., 2002b; 2003). It is therefore proposed
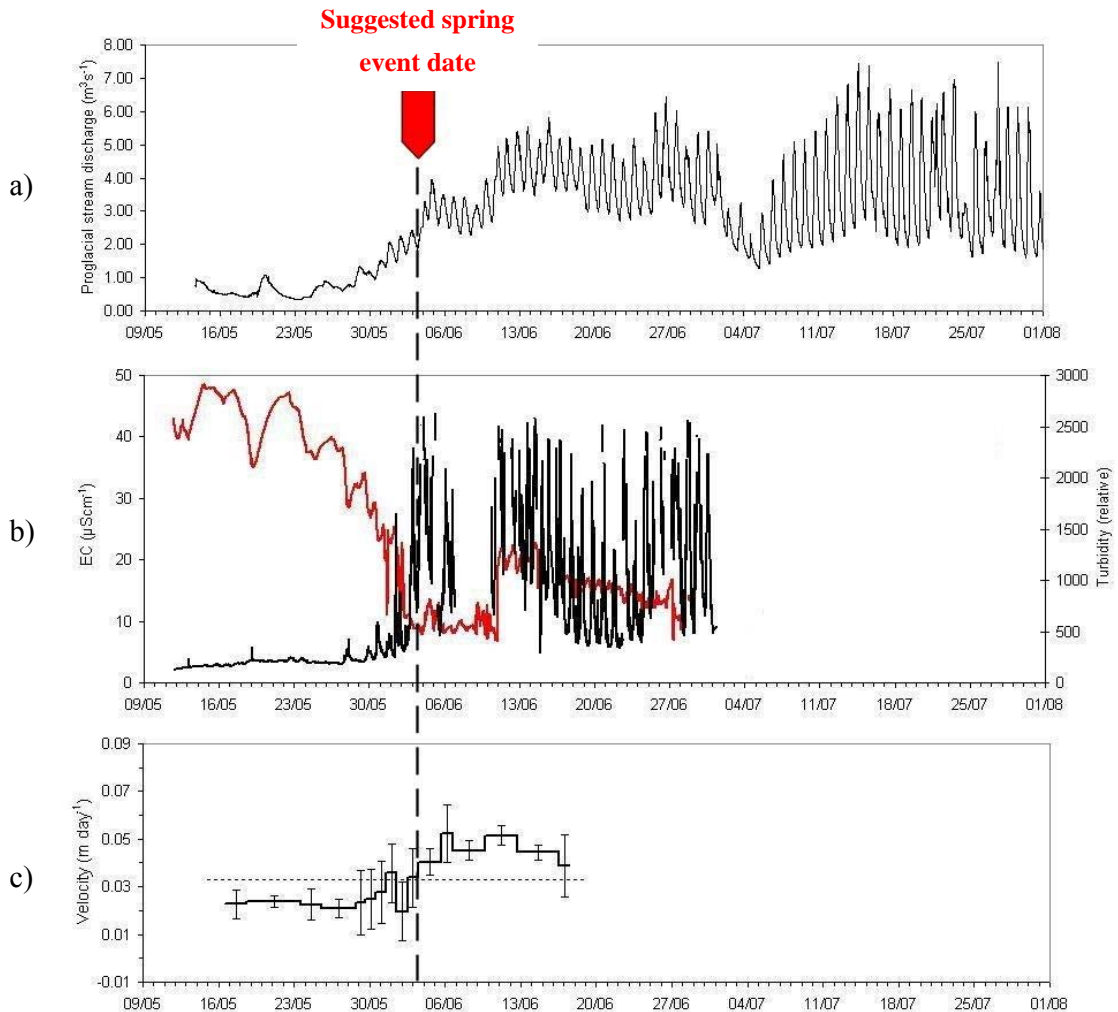
Figure 7.13: Evolution of hydrological and ice dynamic parameters during the 2003 melt season: a) proglacial stream discharge, b) proglacial stream EC (red line) and turbidity, and c) ice surface velocity measured at stake 501. The dashed line indicates the proposed date of spring event onset, when there is a close temporal correspondence between changes in proglacial discharge, water EC and turbidity, and ice velocity.

that these increases in ice surface velocity in 2003 and 2004 were 'spring events' comparable to those previously documented at Haut Glacier d'Arolla (by Nienow (1997) and Mair et al. (2001; 2002; 2003) among others). Both high melt volumes and heavy rainfall have been identified as the trigger for past spring events (Mair et al., 2003). The speed-up events in 2004 did not coincide with any rainfall events (see Figure 4.2h); rather, increased melt was the sole cause of high water discharges into the glacier system. In 2003, there was fairly heavy rain for 30 minutes at 8.30pm on the evening before the inferred spring event (field notes). Although this rainfall was only measured as attaining a maximum flux of 2.2 mm hr^{-1} (Figure 4.2d) and its timing does not directly match that of the observed dynamic speed up, it may have contributed to the onset of the event. If this rainfall resulted in increased water content within the snowpack on the following day, this could also have been important in increasing the efficiency with which meltwater was transmitted through the snowpack, increasing the magnitude of discharge through the subglacial drainage

system. Particularly noticeable prior to 3rd June 2003 was the onset of warmer weather in the preceding days and the warm overnight temperature the night before, which suggest that an increase in melt was an important factor in driving spring event occurrence.
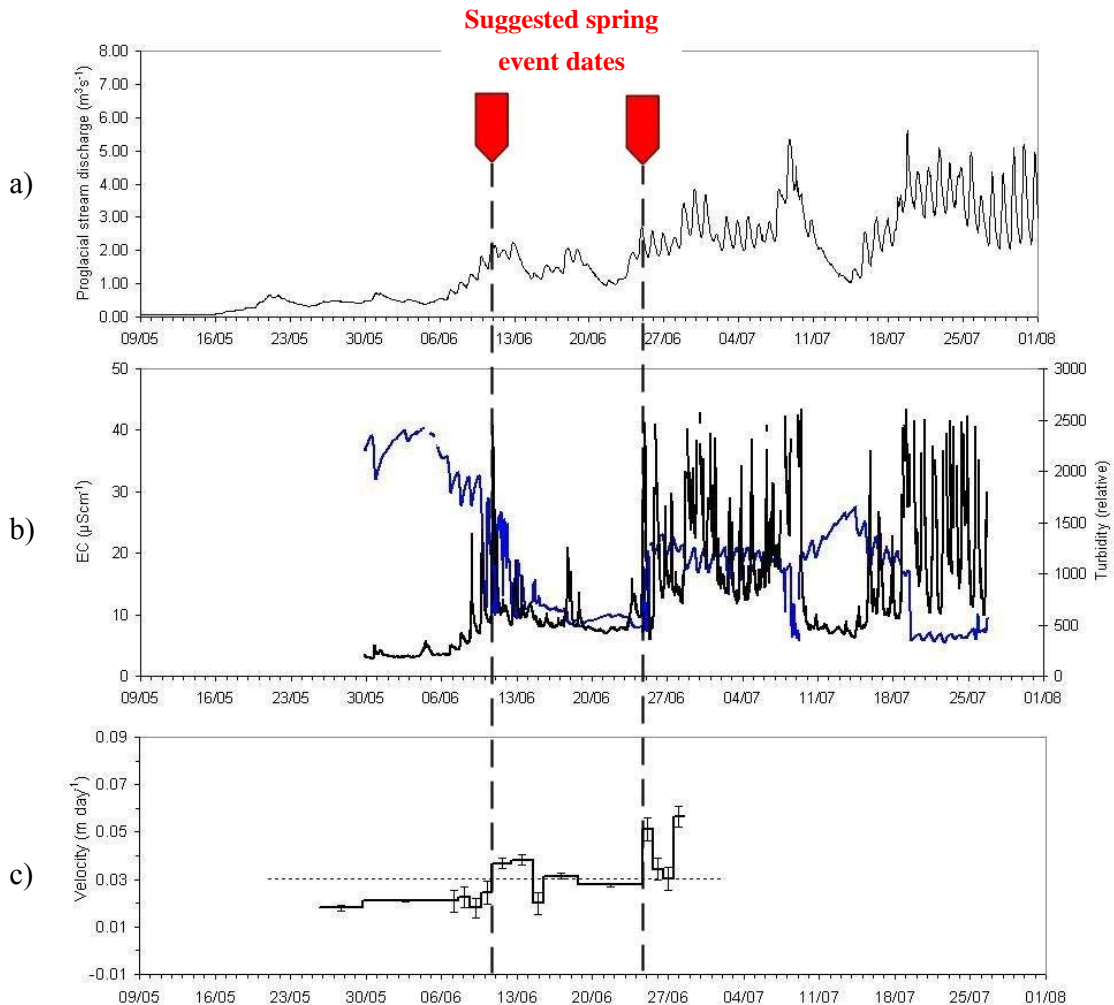
Figure 7.14: Evolution of hydrological and ice dynamic parameters during the 2004 melt season: a) proglacial stream discharge, b) proglacial stream EC (blue line) and turbidity, and c) ice surface velocity measured at stake 501. The dashed lines indicate the dates of the suggested spring events; as in Figure 7.13, a temporal correspondence between changes in proglacial discharge, water EC and turbidity, and ice velocity can be seen.

In previous years, the rapid rise in proglacial stream discharge which has accompanied the spring event at Haut Glacier d'Arolla has been an increase of between 3 and 4 m^3 s^{-1}, from early season values of 1-2 m^3 s^{-1} to around 4-5m^3 s^{-1} (Mair et al. 2002b; 2003). The increase in proglacial discharge at the time of the proposed spring event in 2003 was similar to this (Figure 7.13a), with the continuing increase in discharge until ~16th June possibly explaining the continuation of the above-average velocities throughout the second half of the survey period (Figure 7.13c). The increase in proglacial discharge around 10th June 2004 was of lower magnitude (reaching only 2.2 m^3 s^{-1}; Figure 7.14a), and this may explain the

low amplitude of this speed-up event (reaching ~0.04 m day^{-1} at most; Figure 7.12). In addition, as discharges were particularly high during summer 2003 it is possible that drainage channels beneath the lower glacier remained open during the subsequent winter, aided by low over-winter closure rates where ice above is thin (Nienow, 1993; Nienow et al., 1998). This would help explain the low magnitude of the first speed-up event in 2004, and in particular the absence of this early season speed-up at stakes 101 and 201.

Following the speed-up event on 10th June 2004, proglacial discharge dropped below 2m^{3}s^{-1} again (Figure 7.14a) and water turbidity, while not returning to early season values, did not exhibit the high values and marked diurnal variability characteristic of high runoff through an efficient channelised subglacial drainage system (Figure 7.14b; Richards et al., 1996; Swift et al., 2005). It therefore appears that the increase in discharge through the subglacial drainage system around 10th June was not sufficient to trigger the development of a channelised system, but instead that the subglacial drainage system (at least above stake 201) retained a relatively inefficient configuration. Proglacial discharge rose above 2 m^3 s^{-1} again on 24th June 2004 (Figure 7.14a), and it appears that this increase in runoff triggered a second, more pronounced, speed-up event (Figure 7.14c). The increase in runoff turbidity at this time suggests that the subglacial drainage system became channelised after this time, although this data may also have been influenced by movement of the turbidity sensor to a different location on the proglacial channel (section 7.3).

The occurrence of a second speed-up event has been previously documented at Haut Glacier d'Arolla during the 1995 and 1998 melt seasons (Table 7.3; Mair et al., 2002b; 2003). As discussed by Mair et al. (2002b, 2003), the antecedent conditions of the subglacial drainage system are a crucial control on spring event occurrence in addition to the requirement for high surface water inputs. Hydrology will only cause a velocity response when discharge is rising and when the drainage system is not fully channelised (Mair et al., 2002b). If a channelised drainage system is established following an initial spring event, subsequent high water inputs will be unlikely to trigger a second speed-up event. However, likely due in part to the low discharge values at the time of the first speed-up event in 2004, both high water inputs and an inefficient subglacial drainage system appear to have combined around 24th June 2004, resulting in the second speed-up event of the season.

The availability of concurrent data on proglacial discharge, water EC and turbidity, and ice surface velocity has enabled conclusions about subglacial drainage system evolution and spring event occurrence to be made with confidence despite difficulties in the analysis of ice dynamics data due to survey station movement. Although peak ice flow velocities observed in 2003 and 2004 reached only ~50% of the magnitude of peak values measured

in previous years (Table 7.3), time series of ice surface velocities did show evidence of periodic increase above background values (Figures 7.11 and 7.12). That the timing of these increases in ice surface velocity coincided with increases in proglacial discharge, drops in water EC and increases in turbidity suggests that these speed-ups are 'spring events' comparable to those previously documented at Haut Glacier d'Arolla by Nienow (1997) and Mair et al. (2001; 2002b; 2003) among others and triggered by high water fluxes into an inefficient subglacial drainage system. The spring event began around 3rd June in 2003, though may have built up gradually from ~31st May when discharge began to rise and increased ice surface velocity was first observed at stake 501 (Figure 7.13 a and c). In 2004 there were two events, beginning around ~10th and ~24th June.

7.6 RELATIONSHIP BETWEEN SNOWPACK HYDROLOGICAL CONDITIONS, DRAINAGE SYSTEM EVOLUTION, AND ICE DYNAMICS

This section aims to identify the role, if any, that supraglacial snowpack hydrological behaviour played in influencing hydrological conditions and dynamics in the wider glacier system at Haut Glacier d'Arolla. The effects which snowpack hydrology may be expected to have on ice dynamics were discussed at the start of section 7.4 (Figure 7.10), and evidence of these effects was sought in the analysis presented here; namely, analysis aimed to investigate whether flow through the supraglacial snowpack had i) delayed the timing of the spring event, ii) reduced its magnitude, and/or iii) caused an upglacier lag in the timing of the spring event and upglacier decrease in peak ice velocities. However, no evidence of an upglacier propagation of spring event occurrence or upglacier decrease in spring event magnitude was seen in survey data (section 7.4.1), so this effect is not considered further. First, the character and hydrological behaviour of the supraglacial snowpack (as identified in chapters 4 and 5) at the time of subglacial drainage system evolution and the 'spring event' is considered, in order to identify any snowpack change that may have played a role in altering meltwater inputs to the subglacial system and thereby triggering the drainage system evolution and ice velocity events identified in section 7.5 (section 7.6.1). The importance of the snowpack role in driving these events compared to that of changing surface melt inputs is then considered in section 7.6.2.

7.6.1 Supraglacial snowpack condition at the time of subglacial drainage system evolution and spring events

7.6.1.1 Snowpack depth/bare-ice effect
In both 2003 and 2004, increased proglacial runoff and associated spring events in ice velocity took place while a significant depth of snow (~1.4 m in 2003 and ~2 m in 2004) remained at L (and therefore across much of the rest of the glacier surface) (Figure 7.15). In 2003, patches of bare glacier ice were first revealed by snowpack ablation two days before

the spring event (Figure 7.15a); in 2004, the glacier remained entirely snow-covered for three weeks after the date of the first spring event (Figure 7.15b).

Spring events in the 1994, 1995, 1998 and 1999 melt seasons also occurred while the glacier was still snow-covered (Mair et al., 2001; 2002b; 2003). Earlier studies based on data from the 1990 and 1991 melt seasons, in contrast, found that the evolution of the channelised subglacial drainage system (and therefore the increase in discharge that
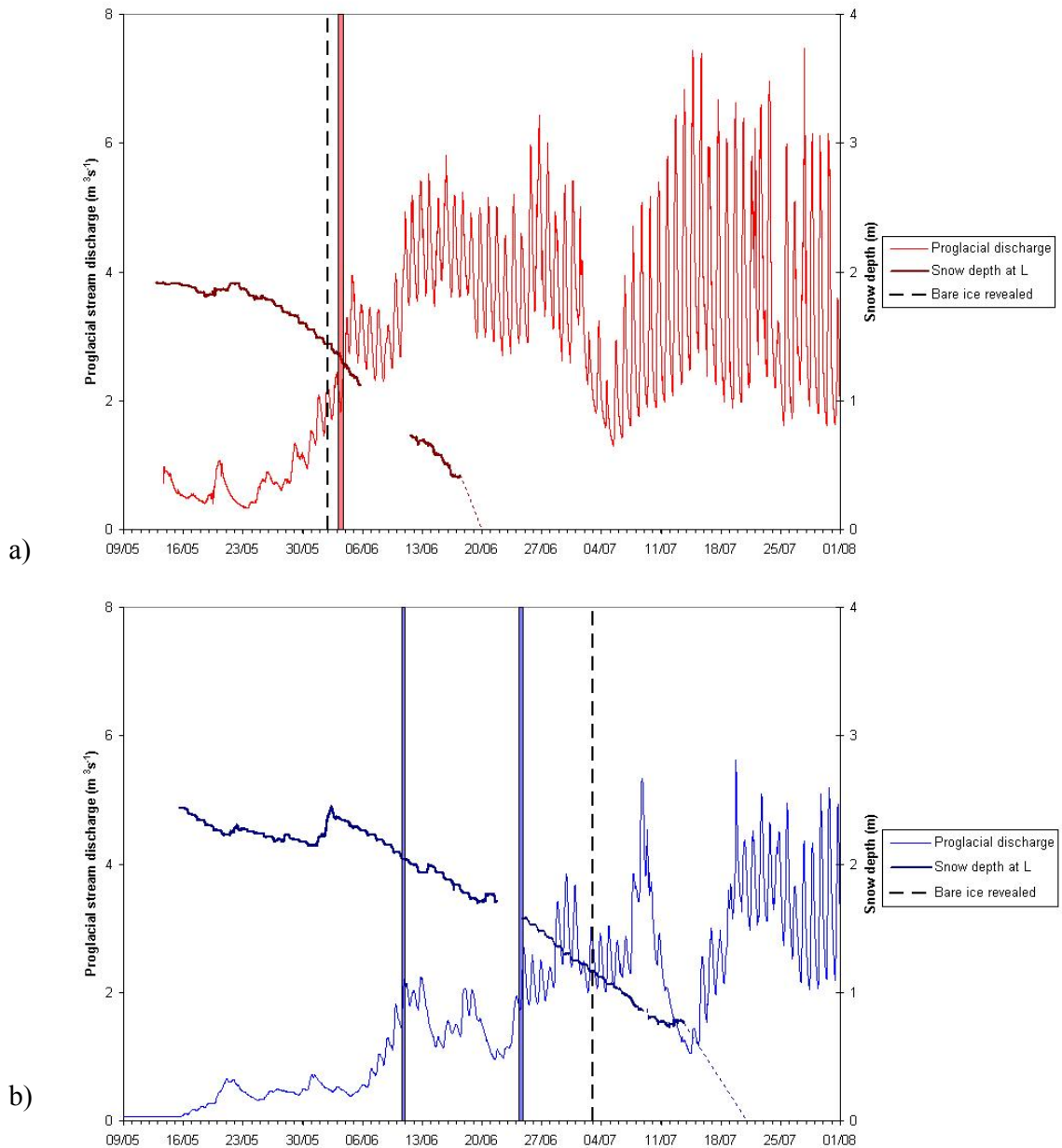
Figure 7.15: Snowpack depth at L at the time of proglacial discharge evolution and spring events in a) 2003 and b) 2004. Dates of spring event onset as established in section 7.5 are indicated by coloured vertical lines. Dashed vertical lines show the date on which bare ice was first exposed on the glacier surface for both field seasons. In both years bare ice was first revealed near the western margin of the main glacier snout and snow remained at L for a further 2 to 3 weeks (see Figures 4.7 and 4.8).

triggered it) was closely tied to the upglacier migration of the snowline (Richards et al., 1996; Nienow et al., 1998), therefore suggesting that it is exposure of the impermeable, low-albedo ice surface and the resulting onset of increased melt and rapid supraglacial runoff that plays a critical role in triggering drainage system evolution (Arnold et al., 1998). The results of the present study therefore support the work of Mair et al. (2001, 2002b, 2003) in showing that runoff into the subglacial system can be sufficiently high as to trigger drainage system evolution and ice dynamic response even while the glacier remains extensively and thickly snow-covered.

7.6.1.2 Snowpack hydrological behaviour

It appears from section 7.6.1.1 that a significant change in water transmission through the glacier hydrological system, sufficient to trigger the spring event, can take place while the glacier surface is still entirely snow-covered. In order to more fully understand the controls on spring event occurrence, therefore, it is now necessary to consider what role the changing hydrological behaviour of the supraglacial snowpack may have played in influencing water discharge into the subglacial drainage system.

Unfortunately, in both 2003 and 2004 no results from quantitative dye tracing on the snowpack surface were obtained until after the date of the spring velocity event. That snowpack hydrological conditions were sufficiently inefficient as to make dye tracing impossible - with percolating dye so diverted by ice layers that it could not be measured by the borehole fluorometer in the basal saturated layer 3 metres downslope from the injection point (Figure 4.35) - is indication of the significant delaying and dispersive effect that the snowpack was having on runoff in the early melt season. Successful quantitative detection of surface dye injections was achieved shortly after the spring event in both years (on 6th June in 2003 and 14th June in 2004), reflecting an increase in snowpack hydrological efficiency that allowed more direct percolation of dye between the surface and base.

In 2003, the first successful surface dye injections at L on the 6th and 10th June showed peaked return curve form and fairly rapid dye recovery (peak dye concentration after ~2 hours) (Figure 5.1), indicating efficient transport of water through the snowpack. Basal water table records from L showed the onset of marked diurnal cyclicity in runoff through the basal saturated layer around 28th May (Figure 5.26a), indicating that the delivery of water from the supraglacial drainage system became more efficient shortly before the spring event. There was also a marked decrease in lag time between peak surface melt input and peak runoff in the basal saturated layer (from over 10 to around 6 hours) around 29th May (Figure 5.29), and it is likely that this will have generated more peaked inputs of meltwater

to the englacial system. There is therefore evidence of an increase in the efficiency of runoff through the snowpack around the time of the spring event in 2003 which is likely related to spring event occurrence.

The first successful quantitative dye injection in 2004, on 14th June, showed water percolation through the snowpack to be greatly delayed, taking over 6 hours before dye was first detected at the fluorometer and over 10 hours before peak dye concentration was detected (Figure 5.13). Calculated percolation velocity and snowpack permeability were correspondingly low, with v_{dom} equal to 0.17 m hr^{-1} and k equal to 3.77x10^{-11} m^2. The wide, dispersed form of the dye return curve for 14th June (Figure 5.13) was also indicative of hydrological inefficiency and the attenuation of flux values during passage through the snowpack. The lag between surface melt inputs and runoff in the basal saturated layer could not be derived until mid-June, at which time it remained high (up to 20 hours) (Figure 5.33). Earlier in the season it is assumed that this lag would be greater. The first speed-up event on 10th June 2004 therefore took place while the supraglacial snowpack was still having a significant delaying and attenuating effect on runoff. The onset of diurnal cyclicity in saturated layer depth at U on 8th June 2004 (Figure 5.27b) did however show that water was transmitted through the snowpack more efficiently from this date onwards, and this is likely linked to spring event occurrence. Unfortunately, the lack of quantitative dye tracing data obtained before the occurrence of the spring event makes it difficult to comment on how snowpack hydrological behaviour may have changed around this time.

7.6.1.3 Changes in snowpack properties

Although no dye tracing data is available to directly show a change in snowpack hydrological behaviour around the time of spring events, observations of temporal changes in snowpack properties suggest factors that are likely to have contributed to increased runoff.

The primary difficulty in obtaining successful quantitative dye tracing results in the early melt season could clearly be attributed to the effect of multiple ice layers preventing percolating meltwater reaching the base of the snowpack (Figure 4.35). The subsequent success of the dye tracing technique relied at least in part on reduced ice layer effect on runoff, allowing dye to reach the basal saturated layer within the ~3 m distance between the injection area and borehole fluorometer. That the onset of successful dye tracing experiments in both years corresponded in time with the spring event makes it tempting to suggest that this reduction in the retaining effect of ice layers on percolating meltwater also contributed to the occurrence of the spring event. Decreasing ice layer effect would result

from either a reduction in the number of ice layers present in the snowpack as those at the surface melt out, or from increasing permeability of individual layers; here, a combination of both factors is possible. As discussed in section 4.3.3, a large number of ice layers were present near the top of the snowpack at the start of both field seasons, many of which melted out in late May/early June. Decay of individual ice layers is also expected under increased water fluxes, following Langham (1979a, b; section 2.2.2.3), thereby increasing their permeability.

The organisation of percolating meltwater into preferential flow zones is another factor which can influence the efficiency of water flow through the snowpack (section 2.2.2.3); the sensitivity analysis in section 6.3.4 clearly illustrated the marked change in runoff timing and magnitude that will result if the snowpack's hydrological efficiency is increased by the concentration of flow within preferential flow channels. In 2003, concentration of percolating meltwater below depressions on the newly suncupped surface was first observed soon after the spring event (Figure 4.34), in contrast to the very homogeneous percolation pattern observed immediately before (Figure 4.33). Although it is tempting to suggest that this may have played a role in increasing the efficiency of snowpack runoff, the limited number of observations made in 2003 would make such a suggestion premature. No clear evolution of preferential flow organisation was observed in 2004 that could help explain changing snowpack runoff. Further investigation of the role that preferential flow patterns play in influencing snowpack runoff remains a topic for future research.

The sensitivity analysis presented in section 6.3 showed that decreasing snowpack depth, as expected, can be another important control on runoff efficiency. In particular, the attenuation of input flux magnitude by flow through the snowpack can decrease non-linearly as snow depth decreases (Figure 6.5). This would cause runoff to become suddenly more efficient at a certain point in time. Thresholds in the factors influencing snowpack behaviour can therefore be important in driving sudden runoff change, even when these controlling factors evolve gradually over time.

Similarly, sensitivity analyses (section 6.3) showed that an increase in net snowpack permeability can trigger significantly more peaked (Figure 6.5) and more rapid (Figure 6.4) runoff. Notably, this increase in runoff efficiency is most marked as snowpack permeability increases across the lower range of values measured in dye tracing experiments. The temporal increase of k values during the 2004 melt season (section 5.2.10) is therefore likely to have led to significantly more efficient runoff and higher discharges into the subglacial drainage system. Reduced retention of percolating water by ice layers was

suggested as an important cause of increasing snowpack permeability. A change in the distribution of flux through preferential flow zones and any increase in snow grain size may also have contributed to increasing effective snow permeability, but no evidence of these was observed.

7.6.1.4 Summary

Data collected for this thesis provides further evidence that the spring event can take place while the glacier is thickly and extensively snow-covered. The delivery of meltwater through the supraglacial snowpack, despite having a significant delaying and attenuating effect on runoff, can therefore be sufficiently efficient as to trigger speed-up events via increased water inputs to the subglacial environment. Due to the lack of quantitative dye tracing data collected prior to the occurrence of spring events in 2003 and 2004, it is difficult to identify how snowpack hydrological behaviour may have changed around the time of the spring event, altering runoff into the subglacial drainage system. Basal water table records do however show that runoff through the snowpack became more efficient around the time of the spring event in both study years. Decreasing snow depth, the development of preferential flow patterns, and in particular a reduction in the retaining effect of ice layers on percolating meltwater and increased net snowpack permeability have been identified as factors which are likely to have contributed towards increased meltwater discharge from the snow-covered supraglacial environment into the subglacial drainage systems and potentially therefore the occurrence of spring events.

7.7 CONCLUSIONS: SNOWPACK INFLUENCE ON SPRING EVENT TIMING AND MAGNITUDE

Any change in runoff through the subglacial drainage system, which may then be linked to an ice dynamic response, will primarily be driven by changing surface melt inputs, which are then mediated by passage through the supraglacial snowpack. Evidence considering the relative importance of the snowpack's effect compared to that of increased melt inputs to the snowpack surface is presented in this section. The key question is whether the hydrological influence of the snowpack on runoff can be sufficient to influence either the timing or magnitude of the glacier's dynamic response to high melt inputs.

In both 2003 and 2004, early June saw higher temperatures and increased snow melt following generally cold conditions in May, and this will have been the principal driving force for spring event occurrence. The influence of high input fluxes is enhanced by their more rapid percolation through the snowpack and limited attenuation (section 6.3.2). In addition, as surface melt increases, the efficiency of runoff will be enhanced by the

increasing permeability of ice layers as they are exposed to large amounts of water (following Langham, 1979a, b) and potentially by the development of preferential flow channels as undulating melt forms develop on the snowpack surface. Snowpack processes can therefore trigger further positive feedbacks between increased input flux and increased output flux.

It is notable that runoff into the subglacial drainage system in early June 2004 was sufficiently efficient as to cause a rise in proglacial discharge and the spring event on 10th June, even after flow through a snowpack over 2 m deep and containing around 15 ice layers (Figures 4.6 and 4.16). It is therefore clear that even this significant depth of hydrologically poorly developed snow can allow the transmission of runoff volumes capable of triggering a speed-up event. In light of the significant delaying and dispersive effect that the snowpack has on runoff, as demonstrated by both field data (Chapters 4 and 5) and physically-based modelling (Chapter 6), this is surprising. It appears that the magnitude of input melt flux at this time was sufficiently high as to dominate over the mediating effect of the snowpack. As melt rates in summer 2004 were lower than usual (section 4.2.2), it is likely that the role of rising input melt flux will dominate over the mediating effect of the snowpack in controlling spring event timing in most years. As discharge through the glacier system was only ~2 $m^3 s^{-1}$ around the time of the spring event on 10th June 2004, compared to values of 4 to 5 $m^3 s^{-1}$ at the time of spring events in other years (Mair et al., 2002; 2003), it is clear that the subglacial drainage system is sensitive to relatively small increases in melt volume in spring. Even this fairly low increase in discharge was sufficient to raise water pressures in the subglacial drainage system across a large enough area to induce enhanced motion at stakes 401 and 501.

While input melt pattern has therefore been the main control on spring event timing, the question of whether the snowpack can affect the way in which the spring event manifests itself once melt increases remains. Dye tracing results showed that differences in flow within the snowpack, possibly different ice layer and preferential flow effects, were able to increase snowpack hydrological efficiency in 2004 compared to 2003, despite lower melt rates in 2004 (section 5.6.2). These features of snowpack hydrology therefore have the potential to significantly influence runoff volumes into the subglacial drainage system.

It remains very likely, therefore, that the mediating effect of the supraglacial snowpack will influence the magnitude of the glacier's dynamic response to melt inputs. Survey data (section 7.4) showed that the spring event on 10th June 2004 was of low magnitude, but this could be attributed to the combination of low melt rates at that time plus the possible survival of a more efficient subglacial drainage system over the previous winter (section

7.5.3). The second spring event in 2004 took place under similar melt inputs (Figure 4.3b) but the snowpack had ablated a further ~50 cm (Figure 4.6) and been exposed to water flow for a further 2 weeks. The greater magnitude of this speed-up event (Figure 7.12) may have been a function of a reduction in the snowpack's attenuating effect on runoff. The spring event on 3rd June 2003 took place when discharge was fairly high (reaching 4 m^3 s^{-1}; Figure 7.13a), but the velocity increase (Figure 7.11) was of low magnitude compared to that measured during past spring events at Haut Glacier d'Arolla (Table 7.3). Despite warm temperatures as early as April in 2003 (section 4.2.1), the snowpack in early June may have limited the magnitude of the glacier's dynamic response to high surface melt fluxes.

It is impossible, given the information available here, to further unravel the balance between the effect of input flux magnitude and the mediating effect of the snowpack in controlling the magnitude of ice dynamic events. Longer records of field data (showing the evolution of supraglacial snowpack hydrology, subglacial drainage system structure and ice dynamics through the entire melt season, and in other years), combined with detailed modelling of water fluxes through the whole glacier system (supraglacially and subglacially), would be required to further address this issue. In the meantime, this study supports the work of Mair et al. (2002) in showing that the development of more hydraulically efficient water movement through the snowpack can allow spring events to occur while a glacier is snow covered, but has also showed that the mediating effect of the snowpack can limit the magnitude of velocity increase (as has been suggested was the case in 2003 and during the first speed-up event of 2004).

On a snow covered glacier, meltwater input patterns at the snowpack surface therefore remain the first order control on discharge patterns into the subglacial drainage system and the timing of dynamic events. However, both field investigations (Chapters 4 and 5) and physically-based modelling (Chapter 6) have shown clearly that hydrological processes operating within the supraglacial snowpack can influence both the timing and magnitude of the runoff hydrograph. These snowpack processes therefore have the potential to mediate the magnitude of the glacier's dynamic response to melt inputs. Much remains to be clarified about the processes at work in controlling the snowpack's influence on runoff, and the snowpack's hydrological effect must be incorporated in future studies of glacier hydrology. With this improved understanding of supraglacial snowpack hydrology, our ability to predict runoff timing and magnitude will be enhanced. This will not only enhance understanding of glacier hydrological system development and ice dynamic response to melt inputs, but will feed into improved management and use of water resources from glaciated catchments.

Chapter 8. Contributions, implications and outlook

8.1 INTRODUCTION

This thesis has investigated the role that supraglacial snowpack hydrology plays in mediating meltwater delivery to glacier systems, and considered the implications of this effect for the timing and magnitude of ice dynamic events. Specifically, field data was collected to address the following research aims (laid out in section 1.2):

i)   to determine the nature of water flow through the supraglacial snowpack of the studied glacier;

ii)   in particular, to explore and develop the use of dye tracing techniques to obtain quantitative information about water flow through snow;

iii)   to determine if, and in what way, the nature of water flow through the snowpack evolves over the course of the melt season;

iv)   to establish what are the factors controlling water movement through the snowpack, and the importance of their roles;

v)   to obtain season-long records of glacier dynamics, proglacial meltwater discharge, and water quality parameters indicating subglacial conditions; and

vi)   to assess the possible links between the changing hydrological behaviour of the snowpack (as determined from i) to iv)) and the factors listed in v).

Examination of physically-based modelling representations of water flow through snow supplemented field data in consideration of aims i), iii) and iv), and through comparison with field data enabled one further research aim to be addressed, namely:

vii)   to identify any weaknesses in, and suggest possible improvements to, existing approaches to modelling supraglacial snow hydrology.

Field investigations at Haut Glacier d'Arolla during the 2003 and 2004 melt seasons provided the data upon which this thesis is primarily based. Dye tracing experiments were used as the primary method of obtaining information about water flow through the snowpack. Dye was used both qualitatively, to give a visual impression of flow patterns through the snowpack (section 4.4), and quantitatively, with return curves detected by a fluorometer providing detailed information about rates of dye movement and dispersion through the snowpack (sections 5.2 and 5.4). Lysimeter measurements of water discharge

through the snowpack (section 5.3) and pressure transducer records of water levels in the basal saturated layer (section 5.5) provided additional information about snowpack hydrology. Supplementary information about snowpack properties and surface melt inputs was collected to inform consideration of the factors controlling runoff characteristics. Data from the concurrent monitoring of proglacial runoff characteristics (sections 7.2 and 7.3) and ice surface velocities (section 7.4) enabled consideration of the wider role of supraglacial snowpack hydrology in influencing conditions in the subglacial drainage system and glacier dynamic events (section 7.6).

This chapter first summarizes the contributions which this thesis has made to understanding supraglacial snowpack hydrology and its links to ice dynamic events, assessing how successfully the research aims listed above have been achieved (section 8.2). It then discusses the implications of the research findings for our wider understanding of issues in glacier hydrology, ice dynamics, mass balance and runoff (section 8.3). Finally, the outlook for research in snow hydrology and ice dynamics is assessed by reflecting upon the limitations of the work presented here and areas of future research which would further our understanding of the issues identified in this thesis (section 8.4).

8.2 CONTRIBUTIONS OF THIS RESEARCH

8.2.1 Nature of water flow through the supraglacial snowpack

Dye tracing and associated experiments carried out at Haut Glacier d'Arolla during the 2003 and 2004 melt seasons yielded a substantial amount of information revealing the nature of water flow through the supraglacial snowpack (research aim (i)). Dye tracing data from the 2004 field season has been published in Campbell et al. (2006). Percolation was shown to take place in a highly heterogeneous manner, influenced by ice layers and preferential flow zones. Ice layers restricted downwards water movement (e.g. Figures 4.20 and 4.25) and deflected flow for considerable lateral distances before percolation could continue (Figure 4.29). This ice layer effect continued throughout each melt season (see Figure 4.27 for dye retention above an ice layer on 25th July), therefore contradicting the suggestion of some earlier work (e.g. Gerdel, 1954) that ice layers in wet snow disintegrate quickly and have little effect on water flow. Ice layers may also enhance runoff efficiency by concentrating water flux beneath gaps or more permeable areas of the ice layer structure, resulting in faster percolation. The location and size of preferential flow zones also appeared to be influenced on occasion by the topography of the snow surface, with concentration of percolating meltwater beneath suncup depressions in June 2003 (Figure 4.34). Preferential flow patterns were highly variable, with dye flow paths occupying between 15 and 52 % of the snowpack cross-section (derived by image analysis, section

4.4.3). Based on these observations of percolation patterns, it was suggested that heterogeneous flow patterns can significantly affect the rate of water flow through the snowpack and the degree to which meltwater waves are attenuated during percolation. However, it is difficult to unravel the precise effect of ice layers and preferential flow zones, and doing so remains an important aim for future research in order that the factors controlling water movement though snow and their relative importance can be more fully (ideally quantitatively) understood.

A reliable technique was developed to obtain quantitative information about water flow through the snowpack using fluorometric techniques (research aim (ii); section 3.6). This technique provided valuable information about the velocity and dispersion of flow, such that the nature of water flow (research aim (i)) could be assessed in quantitative terms. Quantitative dye tracing techniques as developed here could make a useful contribution to future hydrological investigations in snow. Dominant velocities for water percolation through the snowpack were found to range between 0.08 and 0.49 m hr^{-1} (sections 5.2.3 and 5.2.8), confirming that percolation through the snowpack will impart a significant delay to runoff. The dispersed form of dye return curves together with calculated dispersivity values showed that the dye wave can be significantly spread out during passage through the snowpack, implying that peak values of flux will be attenuated. Net snowpack permeability values were found to be significantly lower than those used in most previous studies; values found here range between 2.02×10^{-13} and 1.05×10^{-9} m^2 (section 5.2.5 and 5.2.10) in comparison to values of 6×10^{-9} m^2 and (on average) 5.8×10^{-8} m^2 used by Arnold et al. (1998) and Willis et al. (2002) respectively in previous modelling of supraglacial snow hydrology (Figure 5.38). Based on observations of dye percolation patterns, it was suggested that water retention by ice layers is an important factor in lowering net snowpack permeability. It is therefore argued that future modelling studies should not rely on the calculation of snow permeability based simply on snow density and grain size (following Shimizu (1970)), but must be informed by field measurements of net snowpack permeability that take into account the influence of ice layers and preferential flow zones.

Water flow rates through the basal saturated layer were found to be one to two orders of magnitude greater than those for percolation, ranging between 1.35 and 18.48 mhr^{-1} (section 5.4). These results therefore confirm that percolation in the unsaturated regime will play the primary role in controlling the form and magnitude of runoff from the snowpack, with transfer through the saturated layer (and across the largely impermeable glacier surface) having less effect, except where supraglacial catchments are very large.

Flow velocities and dispersion values for dye transit through both the unsaturated and saturated regimes, however, were very different from those expected in open-channel hydrological systems such as surpraglacial channels (Figure 5.37). Both components of snowpack flow will therefore contribute to a marked difference between runoff through a snow-covered supraglacial catchment and that across the bare-ice glacier surface later in the melt season. The net delaying and attenuating effect of the snowpack on runoff was confirmed by basal water table records (section 5.5.2), which revealed lag times of up to 20 hours between peak surface melt input and peak runoff in the basal saturated layer and almost total dampening of diurnal runoff cycles in early-season records (e.g. Figure 5.30).

8.2.2 Temporal evolution of snowpack runoff

The collection of field data about snowpack hydrological behaviour between May and July in both study years enabled the temporal evolution of water flow through the snowpack to be studied (research aim (iii)). Evidence of temporal evolution of snowpack hydrology at Haut Glacier d'Arolla was published in Campbell et al. (2006). In 2004, percolation velocities (Figure 5.17) and net snowpack permeability values (Figure 5.19) evolved through time indicating increasing hydrological efficiency of the snowpack, in addition to the reduction in its mediating effect as snow depth decreased. The formation of marked diurnal cyclicity in basal water table records (e.g. Figure 5.27b) also indicated an increase in net snowpack hydrological efficiency with time. No clear increase in snow grain size (section 4.3.3) nor change in snow density (section 4.3.4) was observed that would explain this increase in snow permeability. Instead, ice layers are suggested as an important factor in this respect. The net delaying influence of ice layers on runoff will decrease through time both as their individual permeability increases and as layers close to the surface melt out. The distribution of ice layers through the snowpack depth is suggested as an important factor causing the mediating influence of the snowpack to change non-linearly through time.

Investigations using a physical model of water percolation through snow (the US Army's SNTHERM model; sections 6.2 and 6.6) also highlighted the marked change in runoff that is expected to occur over the course of the melt season as snowpack properties (primarily snow depth and snowpack permeability) evolve. The temporal evolution of snowpack hydrological behaviour has been largely neglected by previous studies (including Arnold et al. (1998), Willis et al. (2002) and Fox (2003)), but its effect on runoff has been shown here to be significant.

8.2.3 Factors controlling water movement through snow

From both field and modelling investigations, conclusions can be drawn regarding the factors controlling water movement through the snowpack (research aim (iv)). The magnitude of input melt flux is a primary control on runoff, with the influence of high input fluxes enhanced by their more rapid percolation through the snowpack and limited attenuation (see Figure 6.3). In addition, as surface melt increases, the efficiency of runoff will be enhanced by the increasing permeability of ice layers as they are exposed to large amounts of water (following Langham, 1979a, b) and potentially by the development of preferential flow channels as undulating melt forms develop on the snowpack surface (the increase in runoff efficiency due to preferential flow is illustrated in Figure 6.6). Snowpack processes can therefore trigger positive feedbacks between increasing input flux and increased output flux.

The depth of the snowpack has been widely recognised as a factor influencing runoff, and SNTHERM sensitivity analyses here confirmed its significant effect on the timing and magnitude of runoff (see Figure 6.1). An important further outcome of sensitivity analyses was their illustration of the equally significant role which snowpack permeability can play in controlling runoff timing and magnitude (Figure 6.2). Moreover, changing snowpack permeability was shown to have a markedly non-linear effect on hydrograph delay and attenuation (Figures 6.4 and 6.5), with runoff becoming rapidly more efficient as permeability increases across low values (between approximately 2.0×10^{-11} and 2.5×10^{-9} m^2 in the example in section 6.3.3). As it is across this low range that net snowpack permeability values measured at Haut Glacier d'Arolla were observed to increase during the course of the 2004 melt season (Figure 5.19), it is suggested that this change in permeability will have been an important factor driving an increase in the efficiency of runoff.

As discussed above, it has been argued here that ice layers and preferential flow patterns can significantly affect net snowpack permeability and therefore the rate of water flow through the snowpack and the degree to which meltwater waves are attenuated during percolation. Information about these internal snowpack processes is therefore required in order for snowpack runoff to be fully understood. The importance of these factors was argued in particular with respect to the surprisingly low dye percolation velocities measured in 2003 (see section 5.6.2). As melt fluxes were generally larger and snowpack melt stage more advanced throughout that year (see data in sections 4.2 and 4.3), the fact that measured percolation velocities were in fact lower than in 2004 suggests that runoff cannot be easily understood simply as a function of snow depth nor even input flux, but requires understanding of processes operating *within* the snowpack, including the influence of ice layers and preferential flow zones.

The speed of water flow through the basal saturated layer was shown to be faster than percolation (dye tracing results presented in section 5.4), but the slope across which water flows and the permeability of basal snow will influence runoff timing (see Figures 6.7 and 6.8 for modelled sensitivity of basal runoff rate to slope and permeability), and must be correctly represented in models of glacier hydrology. In addition, the size and shape of supraglacial catchments will control the net effect of this flow regime on the timing of runoff.

8.2.4 Links between snow hydrology, drainage system evolution, and ice dynamics

Ice surface velocities indicated the occurrence of speed-up events beginning around 3rd June 2003 (Figure 7.10) and 10th and 24th June 2004 (Figure 7.11). These are believed to have been 'spring events' comparable to those previously documented at Haut Glacier d'Arolla and triggered by high water fluxes into an inefficient subglacial drainage system. The glacier remained extensively and thickly snow-covered on these dates (Figure 7.14), therefore confirming the work of Mair et al. (2001, 2002, 2003) in showing that runoff through the supraglacial snowpack can be sufficiently high as to trigger ice dynamic response. Changing runoff into the subglacial drainage system is therefore not necessarily the result of faster water transfer across the bare ice surface as the snowline retreats, as has been previously suggested.

It is therefore suggested that temporal changes in the hydrological behaviour of the supraglacial snowpack could play a role in driving ice dynamic events. Although no quantitative dye tracing data was obtained prior to the spring event in either year, the onset of diurnal cyclicity in basal water table records around the spring event dates does indicate that runoff through the snowpack became more efficient at this time. The lag times between peak surface melt input and peak runoff in the basal saturated layer showed a particularly marked decrease corresponding with the spring event in 2003 (Figure 5.29). That quantitative dye tracing techniques became successful around the time of the first spring event in both years makes it tempting to suggest that changes in the effect of ice layers played a role in altering runoff and thereby contributed to the occurrence of these spring events (retention of percolating meltwater by ice layers was observed to be a key problem inhibiting the success of quantitative dye tracing early in the melt season). For 2003, it is tentatively suggested that the concentration of percolating meltwater in preferential flow zones below depressions on the newly suncupped surface (see Figure 4.34) might also have played a role in enhancing runoff efficiency, but further research is required to investigate the role that preferential flow patterns play in influencing snowpack runoff. Decreasing snow depth and increasing net snowpack permeability (the result of grain growth) would also have contributed to greater runoff efficiency.

In both 2003 and 2004, early June saw higher temperatures and increased snow melt following generally cold conditions in May, and this will have been the principal driving force for spring event occurrence. However, it remains very likely that the mediating effect of the supraglacial snowpack can influence the magnitude of the glacier's dynamic response to high melt inputs. In particular, it was suggested here that the higher velocities observed during the second spring event in 2004 (Figure 7.11) may be attributed to snowpack ablation and maturation in the two weeks following the first event. Conversely, the snowpack in early June 2003 appears to have limited the magnitude of the glacier's dynamic response to high surface melt fluxes (Figure 7.10). It is impossible, given the information available here, to further unravel the balance between the effect of input flux magnitude and the mediating effect of the snowpack in controlling the magnitude of ice dynamic events, but better information about processes operating within the snowpack is clearly required for this issue to be further investigated.

8.2.5 Synthesis

Meltwater input patterns remain the primary control on discharge patterns into the subglacial drainage system and the occurrence of ice velocity events, with the macro-permeability of the ice mass (the distribution of crevasses and moulins linking the supraglacial and subglacial drainage system) playing a further important role in controlling discharge magnitude and input location. However, both field investigations (Chapters 4 and 5) and physically-based modelling (Chapter 6) presented in this thesis have shown clearly that hydrological processes operating within the supraglacial snowpack can influence both the timing and magnitude of the runoff hydrograph, such that they have the potential to mediate the magnitude of the glacier's dynamic response to melt inputs. The hydrological influence of the supraglacial snowpack, including ice layer and preferential flow effects and informed by field measurements of snowpack permeability, should be incorporated in studies of glacier hydrology in order that the delay and attenuation of runoff is properly appreciated.

8.3 IMPLICATIONS OF THIS RESEARCH

The findings of this research project have a number of significant implications for research in glacier hydrology and dynamics. Specifically, field observations at Haut Glacier d'Arolla have shown that the passage of water through the supraglacial snowpack causes significant delay and attenuation of runoff. A correct understanding of the way in which the snowpack modifies runoff is essential if subsequent glacier hydrology, ice dynamics, and catchment runoff are to be properly understood. The implications of incorrect representation of the snowpack's effect fall under two themes: implications for the understanding of glacier

hydrology and dynamics in the present day (section 8.3.1), and those for understanding changes in hydrology and mass balance in a future changing climate (section 8.3.2).

8.3.1 Understanding of current glacier hydrology and dynamics processes

As shown by both field data and modelling studies presented in this thesis, snowpack hydrology can alter both the timing and magnitude of meltwater runoff, and this will be the case in both glaciated and non-glaciated catchments. Snowpack conditions therefore impact on the management of water resources for drinking water, industrial, irrigation and hydroelectric use, and have considerable commercial implications in Switzerland and other Alpine countries. Numerous models have investigated and successfully reproduced meltwater production across catchments and spatial patterns of snowpack removal (e.g. Blöschl et al., 1991; Luce et al., 1998; Daly et al., 2000; and Motoya et al., 2001), but the simulation of subsequent water flow through the snowpack has received much less attention. The findings of this study urge that hydrological processes operating *within* the snowpack must also be considered in order for runoff to be fully understood.

The need for improved academic understanding of the glacier hydrology/dynamics relationship and subglacial and proglacial geomorphic processes provides a further important impetus for improving understanding of supraglacial snow hydrology. Failure to acknowledge the delaying and attenuating effect of the snowpack on runoff patterns, and the likely change in these effects through time as the snowpack evolves, will result in erroneous predictions of glacier runoff and of conditions in the subglacial drainage system and beyond. If water flow through the snowpack is modelled using erroneously high permeability values, as the low values measured here suggest has been the case in most previous studies (including Arnold et al (1998) and Willis et al. (2002)), predicted water flow into the rest of the glacier hydrological system will be higher and more varying than the real case. This may have important implications for conclusions drawn from such studies. As verification of model performance is generally by reference to water discharge from the whole glacier system, it is difficult to assess in which component of the glacial system any errors may lie. Correspondingly, errors in the representation of one part of the glacier system may be compensated for by errors in another subpart, with net model output giving the impression of correctness yet incorrect conclusions being drawn about important issues.

Arnold et al. (1998), for example, presented an distributed hydrological model of Haut Glacier d'Arolla in which a time-invariant value, significantly higher than those reported in this study (6×10^{-9} m^2 compared with values between 2.02×10^{-13} and 1.05×10^{-9} m^2 found here (sections 5.2.5 and 5.2.10)), was used for the permeability of the snowpack. The authors

reasonably state that the modelling of snowpack evolution at a micro-scale was beyond the scope of that particular project. As a result of this overestimation of snowpack permeability, it is expected that runoff from the supraglacial drainage system would in reality be slower and more attenuated than their model predicts, particularly in the early part of the melt season. Indeed, at the start of each model run presented, proglacial discharge modelled by Arnold et al. (1998) is significantly higher than that measured at the Hydro Exploitation water intake during the same period. The work presented in this thesis provides a clear explanation for this mismatch and suggests the improvements necessary to the representation of supraglacial snowpack hydrology in order to improve runoff modelling.

As modelled snowpack runoff is transferred to the rest of the glacial drainage system, errors in it may lead to incorrect conclusions about the nature and evolution of the subglacial drainage system, the main focus of Arnold et al.'s (1998) study. Net glacial runoff as predicted by the model was found to be in fact generally lower than measured. As the effect of the snowpack would be to further lower modelled runoff, it appears that some other part of the modelled glacial drainage system must be overly attenuating predicted runoff. If this error is in the subglacial drainage system, it has implications for drainage system structure including the size and roughness of conduits, which are key controls on runoff amplitude (Richards et al., 1996).

8.3.2 Snow and glacier hydrology under climate change

The role of the snowpack in mediating water discharge renders changing snowpack conditions of great interest when considering the change in runoff from both glaciated and non-glaciated catchments which will occur under climate change. However, there remains much difficulty in predicting likely changes in snow conditions that will result from climate change. Snowfall is principally controlled by temperature and precipitation conditions; as climate changes, the associated changes in temperature distributions and precipitation patterns will correspondingly impact on the amount and duration of snowfall (Beniston et al., 2003). Regional studies of climatic change in Switzerland (Marinucci et al., 1995; Beniston et al., 1996; Rotach et al., 1997; Maisch, 1998) have predicted that Alpine temperatures could rise by as much as 3°C by 2050. The predicted 400m rise in snowline altitude which would result would equal a decrease from 18,000km^2 currently covered by the winter snowpack across the Swiss Alps (Baumgartner and Apfl, 1994) to less than 14,000km^2 by 2050 (Haeberli and Beniston, 1998; Beniston et al., 2003).

However, a rise in temperature will lead to increased snowfall in some locations. A tendency towards increased snowfall at high elevations and increased liquid precipitation at low to medium elevations has been identified by several studies (Beniston et al., 1996;

Martin and Durand, 1998; Parry, 2000). Beniston et al. (2003) calculate that the "cross over" altitude at which snow becomes more abundant under milder conditions will be located between 1700 and 2000m a.s.l.. Other studies have confirmed that it is low altitude areas which are most susceptible to decreasing snowfall as temperatures increase (Bultot et al., 1994; Laternser, 2002).

More reliable predictions of snowfall changes at high altitude under climate change remain lacking, exacerbated by limited data collection in remote high locations. Moreover, that data which *is* available is restricted primarily, for obvious reasons, to measurements of snowpack depth. As demonstrated by the observations of snowpack hydrological behaviour discussed in this thesis, more detailed information about the stratigraphic properties of the snowpack (in particular, information about snow properties at the grain scale, the presence of ice layers, and the resulting permeability of the snowpack) is needed in order to understand its effect on runoff. The expected change in these properties under climate change will be difficult to ascertain. Due to the important role that ice layers play in influencing the permeability of the snowcover, it may in fact be the variability of winter temperature conditions between periods of melting and refreezing that is very important for subsequent hydrology. Increased frequency of rain-on-snow events may also be important in this respect.

Clearly, there remains much that cannot be reliably identified about the changes to snow conditions that would be expected under climate change, and information at the level of detail that this thesis has suggested is necessary for prediction of runoff patterns will be difficult to obtain. However, it is clear that the mediating effect of water flow through snow and its evolution under changing climate conditions should be incorporated in studies of future runoff from mountain catchments.

In a future warming climate, the health of alpine glaciers will primarily be controlled by the temperature increase, with changes in accumulation due to changing snowfall amounts also contributing. In polythermal and cold ice masses, however, the way in which a supraglacial snowpack can influence water movement and potentially ice dynamics may have important implications for future ice mass health. Pfeffer and Meier (1991) showed that the retention of runoff by refreezing in the snowpack is crucial to the mass balance of the Greenland Ice Sheet and could mediate future sea level change, but little work has since investigated this issue (with the exception of Janssens and Huybrechts (2000)). Similarly, Wright et al. (2005) have recently shown that the refreezing of meltwater in the snowpack and in particular the formation of superimposed ice make an important positive contribution to the

mass balance of a High Arctic glacier (Midre Lovénbreen, Svalbard) under present conditions and will play a vital future role in slowing down the response of glacier mass balance to climate change. Hydrological processes in the snowpack, similar to those identified in this thesis, therefore have important implications for the future mass balance of these ice masses. Preferential flow, in bringing percolating meltwater to depth in the snowpack while the surrounding snow remains cold (Illangasekare et al., 1990), is an important mechanism leading to ice formation in arctic snowpacks.

In addition, by mediating the relationship between surface melt inputs and the downslope (and often seawards) movement of ice masses, snowpack hydrology potentially has further implications for the mass balance response of ice masses to changing climatic conditions. Recent findings from Greenland have demonstrated surface melt-induced acceleration of ice sheet flow as a result of enhanced basal sliding (Zwally et al., 2002; Rignot and Kanagaratnam, 2006). Such a coupling between surface melt and ice dynamics provides a mechanism for the rapid response of ice sheets to climate change and may be responsible for the recently observed rapid thinning of parts of the Greenland Ice Sheet (Krabill et al., 1999). The extent of refreezing and the nature of flow (particularly the influence of ice layers and preferential flow features) within the snowpack will impact on meltwater discharge into crevasses and thus the likely dynamic response of the ice mass. The future of the Greenland Ice Sheet may therefore depend critically on hydrological processes operating within the snowpack.

Snowpack hydrology therefore has implications not only for future runoff patterns under climate change, but also for the mass balance of ice masses in colder climates. The observations of flow patterns and discussions of factors controlling snowpack runoff that have been presented in this thesis therefore serve as a reminder of factors which must be taken into account in future studies. The hydrological effect of the supraglacial snowpack and its evolution under changing climate conditions should be taken into consideration in studies of glacier hydrology, dynamics, and mass balance response to climate change.

8.4 OUTLOOK

This thesis has identified several important shortcomings in the current treatment of water flow through the supraglacial snowpack. Specifically, it has been shown that percolation through snow is considerably more complex than has often been assumed in glacial studies, and is influenced by ice layers and preferential flow patterns that make the net permeability of the snowpack difficult to predict *a priori*. While the research presented here has made significant advances towards an improved treatment of supraglacial snow hydrology in studies of glacier hydrology and dynamics, there remains much potential for further

research in this field. Here, directions for further research in supraglacial snow hydrology are proposed under two headings: firstly, improvements to the work presented in this thesis are suggested (section 8.4.1), before future areas of work in the wider field of snow hydrology are proposed (section 8.4.2).

8.4.1 Improvements to work carried out in this project

Possible improvements to the work carried out in this project relate primarily to the instrumentation used for field data collection. While the availability of the down-borehole fluorometer presented valuable opportunities for the collection of quantitative information about rates of dye movement and dispersion through the snowpack, the fact that it was originally designed for use in channelised water flow led to difficulties when it was used in snow. Redesign of the fluorometer head to locate the sensing apparatus closer to the base would enable the concentration of dye flowing through the basal saturated layer to be measured without the need to place the fluorometer in a "detection pool" as in this study (section 3.6.4.2, Figure 3.6). The fluorometer could then be relocated more quickly if dye emerged at an unexpected location, and more data would be retrieved. In addition, the availability of a second fluorometer would be invaluable in enabling dye tracing investigations to be carried out simultaneously in the snowpack at different altitudes on the glacier. The spatial variability of snow hydrology could then be assessed and distributed modelling better informed.

The simple drainpipe lysimeters used at Haut Glacier d'Arolla during the 2004 melt season (section 3.7.1) provided useful information about water discharge through the snowpack, albeit for a very limited time period. Larger lysimeters will remain difficult to install in a glacial setting where access during early winter snowfalls is unlikely to be viable and lysimeters therefore cannot be allowed to 'snow in'. However, smaller lysimeter structures such as the drainpipes used here, ideally connected together to create a larger net collection area, could be installed directly into the snowpack in the early melt season and would provide season-long information about runoff. Now that a successful lysimeter design and method of installation has been established, the use of lysimeters to monitor snowpack runoff for the full duration of the melt season at multiple locations across the altitudinal range of the glacier would be easy and relatively low cost. This would provide direct information about the form and timing of the runoff hydrograph after percolation through the snowpack (something that is not provided by dye tracing studies), for use in considering the snowpack's role in modifying runoff. Most importantly, lysimeters may allow information about water flow through the snowpack to be collected in the early melt season before quantitative dye tracing is possible, and therefore would inform consideration of changing snowpack behaviour at the time of the spring event.

A limitation of the research presented here is the lack of detailed information about subglacial hydrology and ice dynamics, which restricts the extent to which the wider implications of observed snow hydrological changes can be considered. Although previous work establishing links between runoff patterns in the subglacial environment and glacier dynamic events at Haut Glacier d'Arolla has enabled some consideration of the snowpack's role here, the collection of more detailed concurrent information about subglacial hydrology and ice dynamics while snowpack hydrology is monitored would enable these relationships to be more fully considered. In particular, dye tracing in the subglacial drainage system would confirm the nature and timing of its evolution in response to changing supraglacial water inputs, and the role of the snowpack in this could be more clearly identified. Data on subglacial water pressures would also more directly show the way in which water inputs trigger increased ice flow velocities, for comparison to snowpack hydrological behaviour. Furthermore, as the study years covered by this project were respectively warmer (2003) and cooler (2004) than average, the collection of a comprehensive hydrology/dynamics data set during a melt season more typical of those usually experienced at Haut Glacier d'Arolla would enable better consideration of the temporal evolution of conditions under average melt inputs.

8.4.2 Future areas of research in supraglacial snow hydrology

Following the conclusions outlined in section 8.2, one of the primary messages of this thesis is the need for improved information about the factors influencing the passage of water through the supraglacial snowpack, for use in more reliably representing the role of the snowpack in mediating runoff into the glacier system. As discussed in section 3.2, the heterogeneous nature and inherent natural variability of water flow through snow means that this information can only be gathered through field studies. At the same time, results must be taken beyond each individual study location, and the significant site-to-site variability expected, in order to contribute to a wider understanding of issues in glacier hydrology and dynamics. There is therefore a need for more field studies, together with associated laboratory and modelling work, to search for general principles governing the influence of the snowpack on runoff, in particular the roles of ice layers and preferential flow patterns. This may draw on work in other porous media that addresses similar issues of flow heterogeneity, and on work in non-glacial snowpacks. Representative values for snowpack permeability and hydrological influence should be sought for snowpacks of different physical characteristics in order to facilitate representation of snowpack hydrological effect without the need for hydrological investigations at every site.

This improved information about ice layer and preferential flow effects and snowpack permeability, and their evolution through time, must then be incorporated in future

modelling studies of glacier hydrology. The correct representation of flow in the basal saturated layer (encompassing the effects of saturated layer permeability and supraglacial catchment size, shape and topography) should also be an aim for future modelling studies. A key issue for future modelling of snowpack hydrology is the need to balance reliable runoff modelling with realistic input data requirements. Observations here have shown that many interacting and temporally-evolving factors influence snowpack runoff, but detailed incorporation of these would hinder the applicability of models across multiple sites and their value for operational use. Ultimately, modelling must aim to predict snowpack runoff using input meteorological data plus a minimum of snowpack information required to ensure useful output. Snowpack depth can be incorporated relatively simply in distributed modelling, but the work presented here argues that some measure of snowpack permeability must also be included. Whether this requires knowledge of individual snow and ice layer permeability or can average their net effect remains to be investigated. As mentioned above (and similar to the suggestion of Colbeck (1978) that typical values of the parameter $k^{1/3}/\varphi_e$ for snow at various stages of maturing should be sought), it may be possible to find representative values for snowpack permeability and hydrological influence for snowpacks of different physical characteristics, thereby facilitating representation of the snowpack's hydrological effect without the need for hydrological investigations at every site.

This thesis has presented an integrated study of supraglacial snow hydrology, glacier hydrology, and ice dynamics at one alpine glacier in order to explore the possible links between these parts of the glacier system. In order to further investigate these links, there is a need for similar integrated studies at other glaciers, ideally with different thermal characteristics, which will indicate the extent to which the supraglacial snowpack plays an important role in influencing runoff patterns at locations other than Arolla. It is clear that supraglacial hydrology, including water flow through the snowpack, will be important in influencing water discharge and associated ice dynamic events, but the extent of this importance and the degree to which observations at Haut Glacier d'Arolla are representative of the snowpack's role in general, are key questions still to be answered.

References

Albert, M. R., & Hardy, J. P. (1995). Ventilation experiments in a seasonal snow cover. In K. A. Tonnessen & M. W. Williams & M. Tranter (Eds.), *Biochemistry of Seasonally Snow-Covered Catchments* (Vol. 228, pp. 41-49). Wallingford: IAHS.

Albert, M., Koh, G., & Perron, F. (1999). Radar investigations of melt pathways in a natural snowpack. *Hydrological Processes, 13*, 2991-3000.

Albert, M. R., & Perron, J., F.E. (2000). Ice layer and surface crust permeability in a seasonal snowpack. *Hydrological Processes, 14*, 3207-3214.

Albert, M. R., Shultz, E. F., & Perron, F. E., Jr. (2000). Snow and firn permeability at Siple Dome, Antarctica. *Annals of Glaciology, 31*, 353-356.

Ambach, W., Blumthaler, M., & Kirchlechner, P. (1981). Application of the gravity flow theory to the percolation of melt water through snow. *Journal of Glaciology, 29*(95), 67-75.

Arnold, N. S., Willis, I. C., Sharp, M. J., Richards, K. S., & Lawson, W. J. (1996). A distributed surface energy balance model for a small valley glacier: I. Development and testing for Haut Glacier d'Arolla, Valais, Switzerland. *Journal of Glaciology, 42*, 77-89.

Arnold, N., Richards, K., Willis, I., & Sharp, M. (1998). Initial results from a distibuted, physically based model of glacier hydrology. In M. Sharp & K. S. Richards & M. Tranter (Eds.), *Glacier Hydrology and Hydrochemistry* (pp. 299-327). Chichester: John Wiley and Sons Ltd.

Bader, H. R., Haefeli, E., Bucher, E., Neher, I., Eckel, O., & Thams, C. (1939). Der Schnee und seine Metamorphose (Snow and its Metamorphism). *Beit Geol. Schweiz., Geotech. Ser., Hydrol., Lief 3, Bern. [English translation by US Army Snow, Ice, Permafrost Res. Estab., Transl. 14], 3*.

Baker, D., Escher-Vetter, H., Moser, H., Oerter, H., & Reinwarth, O. (1982). *A glacier discharge model based on results from field studies of energy balance, water storage and flow*. Paper presented at the Hydrological Aspects of Mountain Areas, Exeter.

Bales, R. C., & Harrington, R. F. (1995). Recent progress in snow hydrology. *Reviews of Geophysics, Supplement*, 1011-1020.

Bartelt, P., & Lehning, M. (2002). A physical SNOWPACK model for the Swiss avalanche warning. Part I: numerical model. *Cold Regions Science and Technology, 35*, 123-145.

Baumgartner, M. F., & Apfl, G. (1994). Monitoring snow cover variations in the Alps using the Alpine Snow Cover Analysis System (ASCAS). In M. Beniston (Ed.), *Mountain Environments in Changing Climates* (pp. 108-120). London, New York: Routledge.

Bear, J. (1972). *Dynamics of Fluids in Porous Media*. New York: American Elsevier Publishing Co.

Bengtsson, L. (1981). Snowmelt generated run-off from small areas as a daily transcient process. *Geophysica, 17*, 109-121.

Beniston, M., Fox, D. G., Adhikary, S., Andressen, R., Guisan, A., Holten, J., Innes, I., Maitima, J., Price, M., & Tessier, L. (1996). *The impacts of climate change on mountain regions. Second Assessment Report of the Intergovernmental Panel on Climate Change (IPCC)*: Cambridge University Press.

Beniston, M., Keller, F., & Goyette, S. (2003). Snow pack in the Swiss Alps under changing climatic conditions: an empirical approach for climate impacts studies. *Theoretical and Applied Climatology, 74*, 19-31.

Bergman, J. A. (1987). *Accuracy and repeatability of in situ snow wetness measurements using the newly-developed twin-disk capacitance.* Paper presented at the 55th Western Snow Conference, Vancouver.

Betterton, M. D. (2001). Formation of Structure in Snowfields: Penitentes, Suncups, and Dirt Cones. *Physical Review E, 63*, 656129-656121 to -656112.

Bingham, R. G. (2003). *The Hydrology and Dynamics of a High Arctic Glacier.* Unpublished PhD, University of Glasgow, Glasgow.

Blöschl, G., Kirnbauer, R., & Gutknecht, D. (1991). Distributed Snowmelt Simulations in an Alpine Catchment 1. Model Evaluation on the Basis of Snow Cover Patterns. *Water Resources Research, 27*(12), 3171-3179.

Braithwaite, R.J. & Olesen, O.B. (1990). A simple energy-balance model to calculate ice ablation at the margin of the Greenland Ice Sheet. *Journal of Glaciology*, 36(123), 222-229.

Brock, B.W. (1997). *Seasonal and spatial variations in the surface energy-balance of valley glaciers*. Unpublished PhD., University of Cambridge.

Brock, B. W., & Arnold, N. S. (2000). A spreadsheet-based (Microsoft Excel) point surface energy balance model for glacier and snow melt studies. *Earth Surface Processes and Landforms, 25*, 649-658.

Brock, B. W., Willis, I. C., & Sharp, M. J. (2000a). Measurement and parameterisation of albedo variations at Haut Glacier d'Arolla, Switzerland. *Journal of Glaciology, 46*(155), 675-688.

Brock, B. W., Willis, I. C., Sharp, M. J., & Arnold, N. S. (2000b). Modelling spatial and seasonal variations in the surface energy balance of Haut Glacier d'Arolla, Switzerland. *Annals of Glaciology, 31*, 53-62.

Brown, R. D., & Goodison, B. E. (1996). Interannual variability in reconstructed Canadian snow cover, 1915-1992. *Journal of Climate, 9*, 1299-1318.

Brugman, M. M. (1986). *Water flow at the base of a surging glacier.* Unpublished PhD, California Institute of Technology, Pasadena.

Brun, E., Martin, E., Simon, V., Gendre, C., & Coleou, C. (1989). An energy and mass model of snow cover suitable for operational avalanche forecasting. *Journal of Glaciology, 35*(121), 333-342.

Brun, E., David, P., Sudul, M., & Brunot, G. (1992). A numerical model to simulate snow-cover stratigraphy for operational avalanche forecasting. *Journal of Glaciology, 38*(128), 13-22.

Bultot, F., Gellens, D., Schadler, B., & Spreafico, M. (1994). Effects of climate change on snow accumulation and melting in the Broye catchment (Switzerland). *Climatic Change, 28*(4), 339-363.

Campbell, F. M. A., Nienow, P. W., & Purves, R. S. (2006). Role of the supraglacial snowpack in mediating meltwater delivery to the glacier system as inferred from dye tracing investigations. *Hydrological Processes, 20*, 969-985.

Carman, P. C. (1937). Fluid flow through a granular bed. *Transactions of the Institute of Chemical Engineers, London, 15*, 150-156.

Chandler, D. (2005). *Measuring and modelling glacier sliding.* Unpublished Ph.D., University of Wales, Aberystwyth.

Clarke, A. S. (2005). *Ice layers and their influence on snowpack hydrology at Haut Glacier d'Arolla, Switzerland.* Unpublished Undergraduate, University of Bristol, Bristol.

Clarke, G. K. C., Collins, S. G., & Thompson, D. E. (1984). Flow, thermal structure, and subglacial conditions of a surge-type glacier. *Canadian Journal of Earth Sciences, 21*(2), 232-240.

Clifford, N. J., Richards, K. S., Brown, R. A., & Lane, S. N. (1995). Scales of variation of suspended sediment concentraton and turbidity in a glacial meltwater stream. *Geografiska Annaler, 77 A*(1-2), 45-65.

Cline, D. W. (1997). Snow surface exchanges and snowmelt at a continental, mid-latitude alpine site. *Water Resources Research, 33*(4), 689-701.

Colbeck, S. C. (1972). A theory of water percolation in snow. *Journal of Glaciology, 11*(63), 369-385.

Colbeck, S. C. (1973). *Theory of metamorphism of wet snow* (311). Hanover, New Hampshire: US Army Corps of Engineers Cold Regions Research and Engineering Laboratory.

Colbeck, S. C. (1974). Water flow through snow overlying an impermeable boundary. *Water Resources Research, 10*(1), 119-123.

Colbeck, S. C. (1975a). A theory for water flow through a layered snowpack. *Water Resources Research, 11*(2), 261-266.

Colbeck, S. C. (1975b). Grain and bond growth in wet snow, *Snow Mechanics: Proceedings of a symposium held at Grindelwald, April 1974* (Vol. 114, pp. 51-61): IAHS Publication.

Colbeck, S. C. (1976). An analysis of water flow in dry snow. *Water Resources Research, 12*(3), 523-527.

Colbeck, S. C. (1977). Short-term forecasting of water run-off from snow and ice. *Journal of Glaciology, 19*(81), 571-588.

Colbeck, S. C. (1978a). The physical aspects of water flow through snow. *Advances in Hydroscience, 11*, 165-206.

Colbeck, S. C. (1978b). The difficulties of measuring the water saturation and porosity of snow. *Journal of Glaciology, 20*(82), 189-201.

Colbeck, S. C. (1979). Water flow through heterogeneous snow. *Cold Regions Science and Technology, 1*, 37-45.

Colbeck, S. C., & Davidson, G. (1973). *Water percolation through homogeneous snow.* Paper presented at the Role of Snow and Ice in Hydrology, Banff.

Colbeck, S. C., & Anderson, E. A. (1982). The Permeability of a Melting Snow Cover. *Water Resources Research, 18*(4), 904-908.

Colbeck, S., Akitaya, E., Armstrong, R., Gubler, H., Lafeuille, J., Lied, K., McClung, D., & Morris, E. (1990). *The International Classification for Seasonal Snow on the Ground*: The International Commission on Snow and Ice of the International Association of Scientific Hydrology.

Coleou, C., & Lesaffre, B. (1998). Irreducible water saturation in snow: experimental results in a cold laboratory. *Annals of Glaciology, 26*, 64-68.

Collins, D. N. (1979a). Sediment concentration in meltwaters as an indicator of erosion processes beneath an alpine glacier. *Journal of Glaciology, 23*, 247-257.

Collins, D. N. (1979b). Quantitative determination of the subglacial hydrology of two Alpine glaciers. *Journal of Glaciology, 23*, 347-362.

Collins, D. N. (1982). *Water storage in an alpine glacier.* Paper presented at the Hydrological Aspects of Mountain Areas, Exeter.

Collins, D. N. (1995). Dissolution kinetics, transit times through subglacial hydrological pathways and diurnal variations of solute content of meltwaters draining from an Alpine glacier. *Hydrological Processes, 9*(8), 897-910.

Collins, D. N., & Young, G. J. (1981). Meltwater hydrology and hydrochemistry in snow and ice covered catchments. *Nordic Hydrology, 12*, 319-334.

Conway, H., & Abrahamson, J. (1984). Air permeability as a textural indicator of snow. *Journal of Glaciology, 30*, 328-333.

Conway, H., & Raymond, C. F. (1993). Snow stability during rain. *Journal of Glaciology, 39*(133), 635-642.

Conway, H., & Benedict, R. (1994). Infiltration of water into snow. *Water Resources Research, 30*(3), 641-649.

Daly, S. F., Davis, R., Ochs, E., & Pangburn, T. (2000). An approach to spatially distributed snow modelling of the Sacramento and San Joaquin basins, California. *Hydrological Processes, 14*, 3257-3271.

Davie, T. (2003). *Fundamentals of Hydrology*. New York: Routledge.

de Quervain, M. R. (1972). *Snow structure, heat and mass flux through snow.* Paper presented at the International Symposium on Properties and Processes in Snow, UNESCO, Banff.

Denoth, A., Seidenbusch, W., Blumthaler, P., Kirchlechner, P., & Colbeck, S. C. (1979). *Study of water drainage from columns of snow* (79-1). Hanover, NH: Cold Rehions Research and Engineering Laboratory.

Denoth, A. (1980). The pendular-funicular liquid transition in snow. *Journal of Glaciology, 25*(91), 93-97.

Denoth, A. (1982). The pendular-funicular liquid transition and snow metamorphism. *Journal of Glaciology, 28*(99), 357-363.

Denoth, A. (1994). An electronic device for long-term snow wetness recording. *Annals of Glaciology, 19*, 104-106.

Denoth, A. (1997). The Monopole-Antenna: a practical snow and soil wetness sensor. *IEEE Transactions on Geoscience and Remote Sensing, 35*(5), 1371-1375.

Dole, R. B. (1906). Use of fluorescein in the study of underground waters. In M. C. Fuller (Ed.), *U.S. Geological Survey Water Supply Papers 160*.

Dullien, F. A. L. (1992). *Porous Media: Fluid Transport and Pore Structure* (2nd ed.). San Diego: Academic Press Inc.

Dunne, T., Price, A. G., & Colbeck, S. C. (1976). The Generation of Runoff From Subarctic Snowpacks. *Water Resources Research, 12*(4), 677-685.

Ebaugh, W. P., & De Walle, D. R. (1977). *Retension and transmission of liquid water in fresh snow.* Paper presented at the 2nd Conference of Hydrometeorology, Toronto.

Elliston, G. R. (1973). *Water movement through the Gornergletscher.* Paper presented at the Int. Symp. Hydrology of Glaciers.

Erickson, T. A., Williams, M. W., & Sommerfeld, R. A. (2000). Spatial statistics of snowmelt. In Bentley, L.R. et al. (Eds.), *Computational Methods in Water Resources XIII*. Rotterdam: Balkema.

Escher-Vetter, H. (2000). Modelling meltwater production with a distributed energy balance method and runoff using a linear reservoir approach - results from Vernagtferner, Oetztal Alps, for the ablation seasons 1992 to 1995. *Zeitschrift fur Gletscherkunde und Glazialgeologie, 36*, 119-150.

Etchevers, Martin, Brown, Fierz, Lejeune, Bazile, Boone, Dai, Essery, Fernandez, Gusev, Jordan, Koren, Kowalczyk, Nasonova, Pyles, Schlosser, Shmakin, Smirnova, Strasser, Verseghy, Yamazaki, & Yang. (2004). Validation of the surface energy budget simulated by several snow models. *Annals of Glaciology, 39*, 150-158.

Fenn, C. R. (1987). Electrical Conductivity. In A. M. Gurnell & M. J. Clark (Eds.), *Glacio-fluvial Sediment Transfer* (pp. 337-414). Chichester, UK: Wiley.

Fischer, H. B. (1968). Methods for predicting dispersion coefficients in natural stream, with applications to lower reaches of the Green and Duwamish Rivers, Washington. *United States Geological Survey Professional Paper*, 528-A.

Fliri, F. (1992). *Der Schnee in Nord- und Osttirol 1895 - 1991: Ein Graphik-Atlas [Snow in North and East Tirol 1895 - 1991: a graphical atlas].* (Vol. 2). Innsbruck: Wagner.

Fortin, G., Jones, G. H., Bernier, M., & Schneebeli, M. (2002). *Changes in the structure and permeability of artificial ice layers containing fluorescent tracer in cold and wet snow cover.* Paper presented at the 59th Eastern Snow Conference, Stowe, Vermont USA.

Fortin, G. (2003). *Conceptualisation des processus de formation, d'evolution et de desagregation des couches de glace dans un couvert nival saisonnier (Conceptualisation of the processes of formation, evolution and decay of ice layers in a seasonal snow cover).* Unpublished PhD., Universite du Quebec, Quebec.

Fountain, A. G. (1989). The storage of water in, and hydraulic characteristics of, the firn of South Cascade Glacier, Washington State, U.S.A. *Annals of Glaciology, 13*, 69-76.

Fountain, A. G. (1992). Subglacial water flow inferred from stream measurements at South Cascade Glacier, Washington, U.S.A. *Journal of Glaciology, 38*(128), 51-64.

Fountain, A. G. (1996). Effect of snow and firn hydrology on the physical and chemical characteristics of glacial runoff. *Hydrological Processes, 10*, 509-521.

Fountain, A. G., & Walder, J. S. (1998). Water flow through temperate glaciers. *Reviews of Geophysics, 36*(3), 299-328.

Fox, A. M. (2003). *A distributed, physically based snow melt and runoff model for alpine glaciers.* Unpublished PhD., University of Cambridge, Cambridge.

Fox, A. M., Williams, M. W., & Caine, N. (1999). Equivalent permeability of a continental, alpine snowpack in the Colorado Front Range, USA. *http://snobear.colorado.edu/Markw/Research/Fox_paper.html*.

Fujino, K. (1971). Measurement of flow down speed of meltwater in snow cover, 2: Flow of meltwater in snow cover on a slope. *Low Temperature Science Series A, 29*, 151-158.

Furbish, D. J. (1988). The influence of ice layers on the travel time of meltwater flow through a snowpack. *Arctic and Alpine Research, 20*, 265-272.

Gerdel, R. W. (1954). The transmission of water through snow. *Transactions, American Geophysical Union, 35*(3), 475-485.

GGUN-FL Fluorometer User Manual, Geomagnetism Group, University of Neuchâtel (http://www-geol.unine.ch/GEOMAGNETISME/HomePage.html).

Glass, R. J., Parlange, J.-Y., & Steenhuis, T. S. (1989a). Wetting Front Instability 1. Theoretical Discusion and Dimensional Analysis. *Water Resources Research, 25*(6), 1187-1194.

Glass, R. J., Steenhuis, T. S., & Parlange, J.-Y. (1989b). Wetting Front Instability 2. Experimental Determination of Relationships Between System Parameters and Two-Dimensional Unstable Flow Field Behaviour in Initially Dry Porous Media. *Water Resources Research, 25*(6), 1195-1207.

Granger, R.J., Male, D.H., & Gray, D.M. (1978) *Prairie Snowmelt.* Proc. Appl. Prairie Hydrology. Symp., Seventh Symp. Water Stud. Inst., Saskatoon, Saskatchewan.

Greuell, W., & Konzelmann, T. (1994). Numerical modelling of the energy balance and the englacial temperature of the Greenland Ice Sheet. Calculation for the ETH-Camp location (West Greenland, 1155 m a.s.l.). *Global and Planetary Change, 9*, 91-114.

Greuell, W., & Smeets, C. J. J. P. (2001). Variations with elevation in the surface energy balance on the Pasterze (Austria). *Journal of Geophysical Research, 106 (D23)*, 31,717-731,727.

Grust, K. (2004). *The hydrology and dynamics of a glacier overlying a linked-cavity drainage system.* Unpublished PhD., University of Glasgow, Glasgow.

Gurnell, A. M. (1993). How many reservoirs? An analysis of flow recessions from a glacier basin. *Journal of Glaciology, 39*(132), 409-414.

Gurnell, A. M., & Fenn, C. R. (1985). Spatial and temporal variations in electrical conductivity in a pro-glacial stream system. *Journal of Glaciology, 31*(108), 108-114.

Gurnell, A. M., Clark, M. J., & Hill, C. T. (1992). Analysis and interpretation of patterns within and between hydroclimatological time series in an alpine glacier. *Earth Surface Processes and Landforms, 17*, 821-839.

Gustafsson, D., Waldner, P. A., & Stahli, M. (2004). Factors governing the formation and persistence of layers in a subalpine snowpack. *Hydrological Processes, 18*(7), 1165-1183.

Haeberli, W., & Beniston, M. (1998). Climate change and its impacts on glaciers and permafrost in the Alps. *Ambio, 27*, 258-265.

Haeberli, W., Hoelzle, M., Paul, F., & Zemp, M. (2006). *Integrated monitoring of mountain glaciers as key indicators of global climate change: the example of the European Alps.* Paper presented at the International Symposium on Cryospheric Indicators of Global Climate Change, Cambridge, UK.

Hannah, D. M., & Gurnell, A. M. (2001). A conceptual, linear reservoir runoff model to investigate melt season changes in cirque glacier hydrology. *Journal of Hydrology, 246*, 123-141.

Hannah, D. M., Gurnell, A. M., & McGregor, G. R. (1999). A methodology for investigation of the seasonal evolution in proglacial hydrograph form. *Hydrological Processes, 13*, 2603-2621.

Hannah, D. M., Smith, B. P. G., Gurnell, A. M., & McGregor, G. R. (2000). An approach to hydrograph classification. *Hydrological Processes, 14*, 317-338.

Harbor, J., Sharp, M., Copland, L., Hubbard, B., Nienow, P., & Mair, D. (1997). Influence of subglacial drainage conditions on the velocity conditions within a glacier cross section. *Geology, 25*(8), 739-742.

Hardy, J. P., & Albert, D. G. (1993). *The permeability of temperate snow: preliminary links to microstructure.* Paper presented at the 50th Eastern Snow Conference, Quebec City.

Hardy, J., Davis, R. E., Jordan, R., Ni, W., & Woodcock, C. (1997). *Snow ablation modelling in conifer and deciduous stands of the boreal forest.* Paper presented at the Eastern Snow Conference, Banff, Alberta, Canada.

Harper, J. T., & Bradford, J. H. (2003). Snow stratigraphy over a uniform depositional surface: spatial variability and measurement tools. *Cold Regions Science and Technology, 37*, 289-298.

Harper, J. T., Humphrey, N. F., & Greenwood, M. C. (2002). Basal conditions and glacier motion during the winter/spring transition, Worthington Glacier, Alaska, USA. *Journal of Glaciology, 48*(160), 42-50.

Harrington, R., & Bales, R. C. (1998). Interannual, seasonal, and spatial patterns of meltwater and solute fluxes in a seasonal snowpack. *Water Resources Research, 34*(4), 823-831.

Haupt, H. F. (1969). A simple snowmelt lysimeter. *Water Resources Research, 5*(3), 714-718.

Hay, J.E & Fitzharris, B.B. (1988). A comparison of the energy-balance and bulk-aerodynamic approaches for estimating glacier melt. *Journal of Glaciology*, 34(117), 145-153.

Herzfeld, U. C., Mayer, H., Caine, N., Losleben, M., & Erbrecht, T. (2003). Morphogenesis of typical winter and summer snow surface patterns in a continental alpine environment. *Hydrological Processes, 17*, 619-649.

Hill, D. E., & Parlange, J.-Y. (1972). Wetting front instability in layered soils. *Soild Science Society of America Proceedings, 36*, 697–702.

Hock, R. (2005). Glacier melt: a review of processes and their modelling. *Progress in Physical Geography, 29*(3), 362-391.

Hock, R., & Hooke, R. L. (1993). Evolution of the internal drainage system in the lower part of the ablation area of Storglacären, Sweden. *Geological Society of America Bulletin, 105*, 537-546.

Hock, R., & Noetzli, C. (1997). Areal melt and discharge modelling of Storglaciaren, Sweden. *Annals of Glaciology, 24*, 211-216.

Hock, R., & Jansson, P. (2005). Modeling Glacier Hydrology. In M. G. Anderson (Ed.), *Encyclopedia of Hydrological Sciences*: John Wiley & Sons.

Hooke, R. L. (1984). On the role of mechanical energy in maintaining subglacial water conduits at atmospheric pressure. *Journal of Glaciology, 30*(105), 180-187.

Hooke, R. L. (1989). Englacial and subglacial hydrology: a qualitative review. *Arctic and Alpine Research, 21*(3), 221-233.

Hooke, R. L., Brzozowski, J., & Bronge, C. (1983). Seasonal variations in surface velocity, Storglaciären, Sweden. *Geografiska Annaler, 65 A*(3-4), 263-277.

Hooke, R. L., Laumann, T., & Kohler, J. (1990). Subglacial water pressures and the shape of subglacial conduits. *Journal of Glaciology, 36*, 67-71.

Hubbard, B., & Nienow, P. (1997). Alpine subglacial hydrology. *Quaternary Science Reviews, 16*(9), 939-955.

Hubbard, B. P., Sharp, M. J., Willis, I. C., Nielsen, M. K., & Smart, C. C. (1995). Borehole water-level variations and the structure of the subglacial hydrological system of Haut Glacier d'Arolla, Valais, Switzerland. *Journal of Glaciology, 41*(139), 572-584.

Hubbard, A., Blatter, H., Nienow, P. W., Mair, D., & Hubbard, B. (1998). Comparison of a three-dimensional model for glacier flow with field data from Haut Glacier d'Arolla, Switzerland. *Journal of Glaciology, 44*(147), 368-378.

Hughes, M. G., & Robinson, D. A. (1996). Historical snow cover variability in the Great Plains region of the USA: 1910 through 1993. *International Journal of Climatology, 16*, 1005-1018.

Iken, A., Röthlisberger, H., Flotron, A., & Haeberli, W. (1983). The uplift of Unteraargletscher at the beginning of the melt season - a consequence of water storage at the bed? *Journal of Glaciology, 29*(101), 28-47.

Illangasekare, T. H., Walter, J., R.J., Meier, M. F., & Pfeffer, W. T. (1990). Modeling of Meltwater Infiltration in Subfreezing Snow. *Water Resources Research, 26*(5), 1001-1012.

Jaagus, J. (1997). The impact of climate change on the snow cover pattern in Estonia. *Climatic Change, 36*, 65-77.

Janssens, I., & Huybrechts, P. (2000). The treatment of meltwatre retention in mass-balance parameterisations of the Greenland Ice Sheet. *Annals of Glaciology, 31*, 133-140.

Jordan, P. (1983a). Meltwater Movement in a Deep Snowpack 1. Field Observations. *Water Resources Research, 19*(4), 971-978.

Jordan, P. (1983b). Meltwater Movement in a Deep Snowpack 2. Simulation Model. *Water Resources Research, 19*(4), 979-985.

Jordan, R. (1991). *A one-dimensional temperature model for a snow cover* (91-16). Hanover, New Hampshire: US Army Corps of Engineers Cold Regions Research and Engineering Laboratory.

Jordan, R. E., Andreas, E. L., & Makshtas, A. P. (1999a). Heat budget of snow-covered sea ice at North Pole 4. *Journal of Geophysical Research, 104*(C4), 7785-7806.

Jordan, R. E., Hardy, J. P., Perron, F. E., Jr., & Fisk, D. J. (1999b). Air permeability and capillary rise as measures of the pore structure of snow: an experimental and theoretical study. *Hydrological Processes, 13*, 1733-1753.

Kamb, B. (1987). Glacier surge mechanism based on linked cavity configuration of the basal water conduit system. *Journal of Glaciology 9, 2*(B9), 9083-9100.

Kass, W. (1998). *Tracer Technique in Geohydrology*. Rotterdam, Netherlands: Balkema.

Kattelman, R. C. (1985). Macropores in snowpack of Sierra Nevada. *Annals of Glaciology, 6*, 272-273.

Kattelman, R. C. (1989). Spatial variability of snow-pack outflow at a site in the Sierra Nevada. *Annals of Glaciology, 13*, 124-128.

Kattelmann, R., & Dozier, J. (1999). Observations of snowpack ripening in the Sierra Nevada, California, U.S.A. *Journal of Glaciology, 45*(151), 409-416.

Kawashima, K., Endo, T., & Takeuchi, Y. (1998). A portable calorimeter for measuring liquid-water content of wet snow. *Annals of Glaciology, 26*, 103-106.

Klok, E. J., Jasper, K., Roelofsma, K. P., Gurtz, J., & Badoux, A. (2001). Distributed hydrological modelling of a heavily glaciated Alpine river basin. *Hydrological Sciences Journal, 46*(4), 553-570.

Kozeny, J. S. (1927). Capillary conduction of water in the ground. *Berlin Wiener Akademy, 136a*, 271-306.

Krabill, W., Frederick, E., Manizade, S., Martin, C., Sonntag, J., Swift, R., Thomas, R., Wright, W., & Yungel, J. (1999). Rapid Thinning of Parts of the Southern Greenland Ice Sheet. *Science, 283*, 1522-1524.

Kronholm, K., Schneebeli, M., & Schweizer, J. (2004). Spatial variability of micropenetration resistance in snow layers on a small slope. *Annals of Glaciology, 38*(1), 202-208.

Lane, S. N. (2000). Hydraulic modelling in hydrology and geomorphology: a review of high resolution approaches. In P. D. Bates & S. N. Lane (Eds.), *High Resolution Flow Modelling in Hydrology and Geomorphology* (pp. 15-34). Chichester: Wiley.

Langham, E. J. (1971). *A new method of using dye in the study of meltwater movement in the snowpack.* Paper presented at the 8th National Hydrology Symposium, Ottawa.

Langham, E. J. (1974a). Network Geometry of Veins in Polycrystalline Ice. *Canadian Journal of Earth Science, 11*, 1274-1279.

Langham, E. J. (1974b). Phase Equilibria of Veins in Polycrystalline Ice. *Canadian Journal of Earth Science, 11*, 1280-1287.

Langham, E. J. (1974c). The occurrence and movement of liquid water in the snowpack. In H. S. Santeford & J. L. Smith (Eds.), *Advanced Concepts and Techniques in the Study of Snow and Ice Resources* (pp. 67-75). Washington, D.C.: National Academy of Sciences.

Laternser, M. (2002). *Snow and Avalanche Climatology of Switzerland.* Unpublished PhD, ETH, Zurich.

Laternser, M., & Schneebeli, M. (2003). Long-term snow climate trends of the Swiss Alps (1931-1999). *International Journal of Climatology, 23*, 733-750.

Lehning, M., Bartelt, P., Brown, B., Russi, T., Stockli, U., & Zimmerli, M. (1999). SNOWPACK model calculations for avalanche warning based upon a new network of weather and snow stations. *Cold Regions Science and Technology, 30*, 145-157.

Lehning, M., Bartelt, P., Brown, B., Fierz, C., & Satyawali, P. (2002a). A physical SNOWPACK model for the Swiss avalanche warning. Part II: snow microstructure. *Cold Regions Science and Technology, 35*, 147-167.

Lehning, M., Bartelt, P., Brown, B., & Fierz, C. (2002b). A physical SNOWPACK model for the Swiss avalanche warning. Part III: meteorological forcing, thin layer formation and evaluation. *Cold Regions Science and Technology, 35*, 169-184.

Leibundgut, C. (1995). *Tracer Technologies for Hydrological Systems (Proceedings of a Boulder Symposium)*, Boulder, USA.

Lillesand, T. M., Kiefer, R. W., & Chipman, J. W. (2004). *Remote Sensing and Image Interpretation* (5th ed.). New York: John Wiley and Sons Inc.

Lliboutry, L. (1968). General theory of subglacial cavitation and sliding of temperate glaciers. *Journal of Glaciology, 7*(49), 21-58.

Luce, C. H., Tarboton, D. G., & Cooley, K. R. (1998). The influence of the spatial distribution of snow on basin-averaged snowmelt. *Hydrological Processes, 12*, 1671-1683.

Lundberg, A. (1997). Laboratory calibration of TDR-probes for snow wetness measurements. *Cold Regions Science and Technology, 25*, 197-205.

Mair, D., Nienow, P., Willis, I., & Sharp, M. (2001). Spatial patterns of glacier motion during a high-velocity event: Haut Glacier d'Arolla, Switzerland. *Journal of Glaciology, 47*(156), 9-20.

Mair, D., Sharp, M., & Willis, I. (2002a). Evidence of basal cavity opening from analysis of surface uplift during a high-velocity event: Haut Glacier d'Arolla, Switzerland. *Journal of Glaciology, 48*(161), 208-216.

Mair, D., Nienow, P., Sharp, M., Wohlleben, T., & Willis, I. (2002b). Influence of subglacial drainage system evolution on glacier surface motion: Haut Glacier d'Arolla, Switzerland. *Journal of Geophysical Research, 107*(B8), 1-13.

Mair, D., Willis, I., Fischer, U., Hubbard, B., Nienow, P., & Hubbard, A. (2003). Hydrological controls on patterns of surface, internal and basal motion during three "spring events": Haut Glacier d'Arolla, Switzerland. *Journal of Glaciology, 49*(167), 555-567.

Maisch, M. (1998). *Die Gletscher der Schweizer Alpen*. Zurich: VdF Publishers.

Male, D. H. (1980). The Seasonal Snowcover. In S. C. Colbeck (Ed.), *Dynamics of Snow and Ice Masses* (pp. 305-395). New York: Academic Press.

Male, D. H., & Gray, D. M. (1981). Snowcover Ablation and Runoff. In D. M. Gray & D. H. Male (Eds.), *Handbook of Snow: Principles, Processes, Management and Use.* Toronto: Pergamon Press.

Marcus, M.G., Moore, R.D., Owens, I.F. (1985). Short-term estimates of surface energy balance transfers and ablation on the lower Franz Josef Glacier, South Westland, New Zealand. *New Zealand Journal of Geology and Geophysics*, 28, 559-567.

Marinucci, M. R., Giorgi, F., Beniston, M., Wild, M., Tschuck, P., & Bernasconi, A. (1995). High resolution simulations of January and July climate over the Western Alpine region with a nested regional modelling system. *Theoretical and Applied Climatology, 51*, 119-138.

Marsh, P., & Woo, M.-K. (1984a). Wetting Front Advance and Freezing of Meltwater Within a Snow Cover 1. Observations in the Canadian Arctic. *Water Resources Research, 20*(12), 1853-1864.

Marsh, P., & Woo, M.-K. (1984b). Wetting Front Advance and Freezing of Meltwater Within a Snow Cover 2. A Simulation Model. *Water Resources Research, 20*(12), 1865-1874.

Marsh, P., & Woo, M.-K. (1985). Meltwater Movement in Natural Heterogeneous Snow Covers. *Water Resources Research, 21*(11), 1710-1716.

Marsh, P. (1991). Water flux in melting snow covers. In M. Y. Corapcioglu (Ed.), *Advances in porous media* (Vol. 1, pp. 61-124). Amsterdam: Elsevier.

Marsh, P. (1999). Snowcover formation and melt: recent advances and future prospects. *Hydrological Processes, 13*, 2117-2134.

Martin, E., & Durand, Y. (1998). Precipitation and snow cover variability in the French Alps. In M. Beniston & J. L. Innes (Eds.), *The Impacts of Climate Change in Forests* (pp. 81-92). Heidelberg, New York: Springer.

McGurk, B. J., & Kattelman, R. C. (1986). Water flow rates, porosity and permeability in snowpacks in the Central Sierra Nevada. In D. L. Kane (Ed.), *Cold Regions Hydrology Symposium.* Bethesda, MD: American Water Resources Association.

McGurk, B. J., & Kattelman, R. C. (1988). *Transport of liquid water: flow finger evidence from thick-section photography.* Paper presented at the International Snow Science Workshop, Whistler, BC, Canada.

McGurk, B. J., & Marsh, P. (1995). Flow-finger continuity in serial thick-sections in a melting Sierra snowpack. In K. A. Tonnessen & M. W. Williams & M. Tranter (Eds.), *Biogeochemistry of Seasonally Snow-Covered Catchments* (Vol. 228, pp. 81-88). Wallingford, Oxfordshire: I.A.H.S. Press.

Melloh, R., Daly, S., Davis, R., Jordan, R., & Koenig, G. (1997). *An operational snow dynamics model for the Sava River, Bosnia.* Paper presented at the Eastern Snow Conference, Banff, Alberta, Canada.

Moore, R. D. (1993). Application of a conceptual streamflow model in a glacierized drainage basin. *Journal of Hydrology, 150*, 151-168.

Motoya, K., Yamazaki, T., & Yasuda, N. (2001). Evaluating the spatial and temporal distribution of snow accumulation, snowmelts and discharge in a multi basin scale: an application to the Tohoku Region, Japan. *Hydrological Processes, 15*, 2101-2129.

Nakawo, M., & Hayakawa, N. (1998). *Snow and Ice in Hydrology*. Nagoya: Institute for Hydrospheric-Atmospheric Sciences, Nagoya University, and United Nations Educational Scientific Organization.

Nienow, P. W. (1993). *Dye tracer investigations of glacier hydrological systems.* Unpublished PhD thesis, Cambridge University.

Nienow, P. (1997). *Hydrological influences on basal flow dynamics in valley glaciers.* Glasgow: NERC Research Fellowship Final Report.

Nienow, P., Sharp, M., & Willis, I. C. (1996a). Velocity-discharge relationships derived from dye tracer experiments in glacial meltwaters: implications for subglacial flow conditions. *Hydrological Processes, 10*(10), 1411-1426.

Nienow, P., Sharp, M., & Willis, I. (1996b). Temporal switching between englacial and subglacial drainage pathways: dye tracer evidence from the Haut Glacier d'Arolla, Switzerland. *Geografiska Annaler, 78 A*(1), 51-60.

Nienow, P., Sharp, M., & Willis, I. (1998). Seasonal changes in the morphology of the subglacial drainage system, Haut Glacier d'Arolla, Switzerland. *Earth Surface Processes and Landforms, 23*, 825-843.

Nye, N. F. (1973). *Water at the bed of a glacier.* Paper presented at the Symposium on the Hydrology of Glaciers, Cambridge, 7-13 September, 1969.

Nye, J. F., & Frank, F. C. (1973). *Hydrology of intergranular veins in a temperate glacier.* Paper presented at the Symposium on the Hydrology of Glaciers, Cambridge, 7-13 September, 1969.

Oerter, H., Baker, D., Moser, H., & Reinwarth, O. (1981). Glacial-hydrological investigations at the Vernagtferner Glacier as a basis for a discharge model. *Nordic Hydrology, 12*(4/5), 335-348.

Ottera, O. H., Drange, H., Bentsen, M., Kvamsto, N. G., & Jiang, D. (2003). The sensitivity of the present-day Atlantic meridional overturning circulation to freshwater forcing. *Geophysical Research Letters, 30*(17), art. no. 1898.

Parry, M. L. (2000). *Assessment of potential effects and adaptations for climate change in Europe: The ACACIA Report*: Jackson Environmental Institute Publications, Norwich, and European Commission Publications, Brussels.

Paterson, W. S. B. (1994). *The Physics of Glaciers* (3rd ed.). Oxford: Butterworth Heinemann.

Pellicciotti, F., Brock, B., Strasser, U., Burlando, P., Funk, M., & Corripio, J. (2005). An enhanced temperature-index glacier melt model including the shortwave radiation balance: development and testing for Haut Glacier d'Arolla, Switzerland. *Journal of Glaciology, 51*(175), 573-587.

Pfeffer, W. T., & Meier, M. F. (1991). Retention of Greenland runoff by refreezing: Implications for projected future sea level change. *Journal of Geophysical Research, 96*(C12), 22,117-122,124.

Pfeffer, W. T., Illangasekare, T. H., & Meier, M. F. (1990). Analysis and modelling of melt-water refreezing in dry snow. *Journal of Glaciology, 36*, 143-151.

Price, A.G. (1986). Modelling of snowmelt rates in a deciduous forest. In H.G. Jones & W.J. Orville-Thomas (Eds.) *Seasonal Snowcovers: Physics, Chemistry, Hydrology Symposium, Les Arcs, France, 13-25 July 1986.* NATO ASI Series C, Mathematical and Physical Sciences, Volume 211: 151-165.

Raudkivi, A. J. (1979). *Hydrology*. Oxford: Pergamon.

Ream, D. (2000) *Pit_instructions*, Excel file for drawing snow pit profiles, presented at the International Snow Science Workshop in 2000 and available at http://www.avalanchemapping.org/gpscollect.htm.

Richards, K., Sharp, M., Arnold, N., Gurnell, A., Clark, M., Tranter, M., Nienow, P., Brown, G., Willis, I., & Lawson, W. (1996). An integrated approach to modelling hydrology and water quality in glacierized catchments. *Hydrological Processes, 10*, 479-508.

Rignot, E., & Kanagaratnam, P. (2006). Changes in the Velocity Structure of the Greenland Ice Sheet. *Science, 311*, 986-990.

Rotach, M., Wild, M., Tschuck, P., Beniston, M., & Marinucci, M. R. (1996). A double CO_2 experiment over the Alpine region with a nested GCM-LAM modelling approach. *Theoretical and Applied Climatology, 57*, 209-227.

Röthlisberger, H. (1972). Water pressure in intra- and subglacial channels. *Journal of Glaciology, 11*(62), 177-203.

Röthlisberger, H., & Lang, H. (1987). Glacial Hydrology. In A. M. Gurnell & M. J. Clark (Eds.), *Glacio-fluvial Sediment Transfer* (pp. 207-284). Chichester: John Wiley and Sons Ltd.

Rowe, C. M., Kuivinen, K. C., & Jordan, R. (1995). Simulation of summer snowmelt on the Greenland ice sheet using a one-dimensional model. *Journal of Geophysical Research, 100*(D8), 16265-16273.

Schaefli, B., Hingray, B., Niggli, M., & Musy, A. (2005). A conceptual glacio-hydrological model for high mountainous catchments. *Hydrology and Earth System Sciences, 9*, 95-109.

Schmidt, F., & Persson, A. (2003). Comparison of DEM Data Capture and Topographic Wetness Indices. *Precision Agriculture, 4*(2), 179-192.

Schneebeli, M. (1995). Development and stability of preferential flow paths in a layered snowpack. In K. A. Tonnessen & M. W. Williams & M. Tranter (Eds.), *Biogeochemistry of Seasonally Snow-Covered Catchments* (Vol. 228, pp. 89-95). Wallingford, Oxfordshire: I.A.H.S. Press.

Schneebeli, M., Coleou, C., Touvier, F., & Lesaffre, B. (1998). Measurement of density and wetness in snow using time-domain reflectometry. *Annals of Glaciology, 26*, 69-72.

Schneider, T. (1999). Water movement in the firn of Storglaciaren, Sweden. *Journal of Glaciology, 45*(150), 286-294.

Schneider, T. (2000). Hydrological processes in the wet-snow zone of the glacier - a review. *Zeitschrift fur Gletscherkunde und Glazialgeologie, 36*, 89-105.

Schneider, T. (2001). *Hydrological processes in firn on Storglaciaren, Sweden.* Unpublished Collection of 4 papers, Stockholm University, Stockholm.

Seaberg, S. Z., Seaberg, J. Z., Hooke, R. L., & Wieberg, D. W. (1988). Character of the englacial and subglacial drainage system in the lower part of the ablation area of Storglaciären, Sweded, as revealed by dye-trace studies. *Journal of Glaciology, 34*(117), 217-227.

Sellers, S. (2000). Theory of water transport in melting snow with a moving surface. *Cold Regions Science and Technology, 31*, 47-57.

Sharp, R. P. (1952). Meltwater behaviour in firn on upper Seward Glacier, St. Elias Mountains, Canada. *Union Geodesique et GeophysiqueInternationale, Association Internationale d'Hydrologie Scientifique, Assemblee generale de Bruxelles, 1*, 246-253.

Sharp, M., Gemmell, J. C., & Tison, J.-L. (1989). Structure and stability of the former subglacial drainage system of the Glacier de Tsanfleuron, Switzerland. *Earth Surface Processes and Landforms, 14*, 119-134.

Sharp, M., Richards, K., Willis, I., Arnold, N., Nienow, P., Lawson, W., & Tison, J.-L. (1993). Geometry, bed topography and drainage system structure of the Haut Glacier d'Arolla, Switzerland. *Earth Surface Processes and Landforms, 18*, 557-571.

Sharp, M., Richards, K. S., & Tranter, M. (1998). *Glacier Hydrology and Hydrochemistry.* Chichester: John Wiley and Sons Ltd.

Shimizu, H. (1970). Air permeability of deposited snow. *Low Temperature Science Series A, 22*, 1-32.

Shoemaker, E. M. (1986). Subglacial hydrology for an ice-sheet resting on a deformable aquifer. *Journal of Glaciology, 32*(110), 20-30.

Sihvola, A., & Tiuri, M. (1986). Snow fork for field determination of the density and wetness profiles of a snow pack. *IEEE Transactions on Geoscience and Remote Sensing, GE-24*(5), 717-721.

Singh, P., Spitzbart, G., Hubl, H., & Weinmeister, H. W. (1997). Hydrological response of a snowpack under rain-on-snow events: a field study. *Journal of Hydrology, 202*, 1-20.

Singh, P., Spitzbart, G., Huebl, H., & Weinmeister, H. W. (1999). Importance of ice layers on liquid water storage within a snowpack. *Hydrological Processes, 13*, 1799-1805.

Singh, V. P., Bengtsson, L., & Westerstrom, G. (2000a). Kinematic wave modelling of vertical movement of snowmelt water through a snowpack. In P. D. Bates & S. N. Lane (Eds.), *High Resolution Flow Modelling in Hydrology and Geomorphology* (pp. 263-281). Chichester: Wiley.

Singh, V. P., Bengtsson, L., & Westerstrom, G. (2000b). Kinematic wave modelling of saturated basal flow in a snowpack. In P. D. Bates & S. N. Lane (Eds.), *High Resolution Flow Modelling in Hydrology and Geomorphology* (pp. 283-293). Chichester: Wiley.

SLF (2003). *WinterAktuell 2002/2003*, [Web page]. Available: http://www.slf.ch/ winteraktuell/welcome2003-de.html [2006, 18/05/2006].

SLF (2004). *WinterAktuell 2003/2004*, [Web page]. Available: http://wa.slf.ch/ [2006, 18/05/2006].

Smart, P. L., & Laidlaw, I. M. S. (1977). An evaluation of some fluorescent dyes for water tracing. *Water Resources Research, 13*(1), 15-33.

Smart, P. L., Atkinson, T. C., Laidlaw, I. M. S., Newson, M. D., & Trudgill, S. T. (1986). Comparison of the results of quantitative and non-quantitative tracer tests for determination of karst conduit networks: an example from the Traligill Basin, Scotland. *Earth Surface Processes and Landforms, 11*, 249-261.

Sommerfeld, R. A., & LaChappelle, E. (1970). The classification of snow metamorphism. *Journal of Glaciology, 9*(55), 3-17.

Sommerfeld, R. A., Bales, R. C., & Mast, A. (1994). Spatial Statistics of Snowmelt Flow: Data from Lysimeters and Aerial Photos. *Geophysical Research Letters, 21*(25), 2821-2824.

Sørensen, R., Zinko, U., & Seibert, J. (2006). On the calculation of the topographic wetness index: evaluation of different methods based on field observations. *Hydrology and Earth System Sciences, 10*, 101-112.

Stadler, D., Stahli, M., Aeby, P., & Fluhler, H. (2000). Dye tracing and image analysis for quantifying water infiltration into frozen soils. *Soil Science Society of America Journal, 64*, 505-516.

Stein, J., Laberge, G., & Levesque, D. (1997). Monitoring the dry density and the liquid water content of snow using time domain reflectometry. *Cold Regions Science and Technology, 25*, 123-136.

Stenborg, T. (1969). Studies of the internal drainage of glaciers. *Geografiska Annaler, 51 A*(1-2), 13-41.

Stenborg, T. (1973). *Some viewpoints on the internal drainage of glacier.* Paper presented at the Symposium on the Hydrology of Glaciers, Cambridge.

Strasser, U., Corripio, J., Pellicciotti, F., Burlando, P., Brock, B., & Funk, M. (2004). Spatial and temporal variability of meteorological variables at Haut Glacier d'Arolla (Switzerland) during the ablation period 2001: measurements and simulations. *Journal of Geophysical Research, D03103.*

Sturm, M., & Holmgren, J. (1993). Rain-Induced Water Percolation in Snow as Detected Using Heat Flux Transducers. *Water Resources Research, 29*(7), 2323-2334.

Swift, D. A., Nienow, P. W., Spedding, N., & Hoey, T. B. (2002). Geomorphic implications of subglacial drainage configuration: rates of basal sediment evacuation controlled by seasonal drainage system evolution. *Sedimentary Geology, 149*(1-3), 5-19.

Swift, D. A., Nienow, P. W., Hoey, T. B., & Mair, D. W. F. (2005). Seasonal evolution of runoff from Haut Glacier d'Arolla, Switzerland and implications for glacial geomorphic processes. *Journal of Hydrology, 309*, 133-148.

Taylor, G. I. (1954). Dispersion of matter in turbulent flow through a pipe. *Proceedings of the Royal Society of London, 223A*(1155), 446-468.

Tranter, M., Brown, G. H., Hodson, A., & Gurnell, A. M. (1996). Hydrochemistry as an indicator of the nature of subglacial drainage system structure: a comparison of Arctic and Alpine environments. *Hydrological Processes, 10*, 541-556.

Tseng, P.-H., Illangasekare, T. H., & Meier, M. F. (1994). Modeling of snow melting and uniform wetting front migration in a layered subfreezing snowpack. *Water Resources Research, 30*(8), 2363-2376.

van der Veen, C. J. (1999). *Fundamentals of Glacier Dynamics*. Rotterdam: Balkema.

Verbunt, M., Gurtz, J., Jasper, K., Lang, H., Warmerdam, P., & Zappa, M. (2003). The hydrological role of snow and glaciers in alpine river basins and their distributed modelling. *Journal of Hydrology, 282*, 36-55.

Wakahama, G. (1968). *The metamorphism of wet snow.* Paper presented at the Comm. on Snow and Ice, Int. Union Geodesy Geophys., Int. Assoc. Sci. Hydro., Gen. Assembly, Sept.-Oct. 1967, Bern.

Walder, J. S. (1986). Hydraulics of subglacial cavities. *Journal of Glaciology, 32*(112), 439-445.

Walder, J. S., & Fowler, A. (1994). Channelised subglacial drainage over a deformable bed. *Journal of Glaciology, 40*, 3-15.

Waldner, P. A., Schneebeli, M., Schultze-Zimmermann, U., & Fluhler, H. (2004). Effect of snow structure on water flow and solute transport. *Hydrological Processes, 18*(7), 1271-1290.

Wankiewicz, A. (1979). *A review of water movement in snow.* Paper presented at the Modeling of snow cover runoff, US Army Cold Regions Research and Engineering Laboratory, Hanover, New Hampshire.

Weertman, J. (1969). Water lubrication mechanism of glacier surges. *Canadian Journal of Earth Sciences, 6*(4), 929-942.

Weertman, J. (1972). General theory of water flow at the base of a glacier or ice sheet. *Reviews of Geophysics and Space Physics, 10*(1), 287-333.

Williams, M. W., Sommerfeld, R., Massman, S., & Rikkers, M. (1999). Correlation lengths of meltwater flow through ripe snowpacks, Colorado Front Range, USA. *Hydrological Processes, 13*, 1807-1826.

Williams, M. W., Rikkers, M., & Pfeffer, W. T. (2000). Ice columns and frozen rills in a warm snowpack, Green Lakes Valley, Colorado, USA. *Nordic Hydrology, 31*(3), 169-186.

Willis, I. C. (1995). Intra-annual variations in glacier motion: a review. *Progress in Physical Geography, 19*(1), 61-106.

Willis, I. C., Sharp, M. J., & Richards, K. S. (1990). Configuration of the drainage system of Midtdalsbreen, Norway, as indicated by dye-tracing experiments. *Journal of Glaciology, 36*, 89-101.

Willis, I. C., Richards, K. S., & Sharp, M. J. (1996). Links between proglacial stream suspended sediment dynamics, glacier hydrology and glacier motion at Midtdalsbreen, Norway. *Hydrological Processes, 10*(4), 629-648.

Willis, I. C., Arnold, N. S., & Brock, B. W. (2002). Effect of snowpack removal on energy balance, melt and runoff in a small supraglacial catchment. *Hydrological Processes, 16*, 2721-2749.

Wright, A., Wadham, J., Siegert, M., Luckman, A., & Kohler, J. (2005). Modelling the Impact of Superimposed Ice on the Mass Balance of an Arctic Glacier under Scenarios of Future Climate Change. *Annals of Glaciology, 42*(1), 277-283.

Ye, H. (2001). Increases in snow season length due to earlier first snow and later last snow dates over North Central and Northwest Asia during 1973-94. *Geophysical Research Letters, 28*, 551-554.

Yosida, Z. (1973). Infiltration of thaw water into a dry snow cover. *Low Temperature Science Series A, 31*.

Zwally, J. H., Abdalati, W., Herring, T., Larson, K., Saba, J., & Steffen, K. (2002). Surface Melt-Induced Acceleration of Greenland Ice-Sheet Flow. *Science, 297*, 218-222.

Appendix A. ICSI Classification for Seasonal Snow on the Ground (Colbeck et al., 1990).

ICSI Classification for Seasonal Snow on the Ground

Basic Classification	Code	Subclass	Abbrev	Shape	Place of Formation	Classification	Physical Process	Dependence on Most Important Parameters	Common Effect on Strength
		Morphological Classification			Process-Oriented Classification			Additional Information on Physical and Strength	
Precipitation Particles	1		PP		Cloud				
	a	Columns	cl	Short prismatic crystal, solid or hollow			Growth at high supersaturation at –3° to –8°C and below –22°C		
	b	Needles	nd	Needle-like approximately cylindrical			Growth at high supersaturation at –3°C to –5°C		
	c	Plates	pl	Plate-like mostly hexagonal			Growth at high supersaturation at 0° to –3°C and –8° to –25°C		
	d	Stellars (dendrites)	sd	Six-fold star-like planar or spacial			Growth at high supersaturation at temperatures between –12° to –16°C		
	e	Irregular crystals	ir	Clusters of very small crystals			Polycrystals growing at varying environmental conditions		
	f	Graupel	gp	Heavily rimed particles			Heavy riming of particles by accretion of supercooled water		
	g	Hail	hl	Laminar internal structure, translucent or milky glazed surface			Growth by accretion of supercooled water		
	h	Ice pellets	ip	Transparent, mostly small spheroids			Frozen rain		

Basic Classification	Morphological Classification				Process-Oriented Classification			Additional Information on Physical and Strength	
	Code	Subclass	Abbrev	Shape	Place of Formation	Classification	Physical Process	Dependence on Most Important Parameters	Common Effect on Strength
Decomposing and fragmented precipitation particles	2		DF						
	a	Partly decomposed precipitation particles	dc	Partly rounded particles, characteristic shapes of precipitation particles still recognizable	Recently deposited layer	Initial rounding and separation	Decrease of surface area to reduce surface free energy at low temperature gradients	Speed of decomposition decreases with decreasing snow temperatures and decreasing temperature gradients	Strength decreases with time; felt-like arrangement of dendrites has modest initial strength
	b	Highly broken particles	bk	Packed, shards or rounded fragments of precipitation particles	Saltation layer	Wind-broken particles; initially fractured then rapid rounding due to small size	Fragmented particles are closely packed by wind; fragmentation followed by rounding and growth	Fragmentation and packing increase with wind speed	Quick sintering results in rapid strength increase
Rounded grains (Monocrystals)	3		RG		Dry snow				
	a	Small rounded particles	sr	Well rounded particles of size <0.5 mm often well bonded		Small equilibrium form	Decrease of specific surface area by slow decrease of number of grains and increase of mean grain diameter; equilibrium form may be partly faceted at lower temperatures	Growth rate increases with increasing temperature and temperature gradient; growth slower in high density snow with smaller pores	Strength increases with time, density and decreasing grain size
	b	Large rounded particles	lr	Well-rounded particles of size >0.5 mm		Large equilibrium form	Grain-to-grain vapor diffusion due to low to medium temperature gradients; mean excess vapor density remains below critical value for kinetic growth	Same as above	Strength increases with time and density and decreasing grain size
	c	Mixed forms	mx	Rounded particles with few facets which are developing		Transitional form as temperature gradient increases	Growth regime changes if temperature gradient increases above critical value of about 10°C/m	Grains are changing in response to an increasing temperature gradient	De-sintering could decrease strength

Basic Classification	Code	Morphological Classification			Process-Oriented Classification			Additional Information on Physical and Strength		
		Subclass	Abbrev	Shape	Place of Formation	Classification	Physical Process	Dependence on Most Important Parameters	Common Effect on Strength
Faceted crystals	4		FC		Dry snow				
	a	Solid faceted particles ☐	fa	Solid faceted crystals; usually hexagonal prisms		Solid kinetic growth form	Strong grain-to-grain vapor diffusion driven by large temperature gradient; excess vapor density above critical value for kinetic growth	Growth rate increases with temperature, temperature gradient, and decreasing density, may not occur in high density snow because of small pores	Strength decreases with increasing growth rate and grain size
	b	Small faceted particles ▨	sf	Small faceted crystals in surface layer; <0.5 mm in size	Near surface	Kinetic growth form at early stage of development	May develop directly from 1 or 2a due to large, near-surface temperature gradients	Temperature gradient may periodically change sign but remains at a high absolute value	Low strength snow
	c	Mixed-forms ◨	mx	Faceted crystals with recent rounding of facets		Transitional form as temperature gradient decreases	Faceted grains are rounding due to decrease in temperature gradient		

Basic Classification	Code	Morphological Classification			Process-Oriented Classification			Additional Information on Physical and Strength	
		Subclass	Abbrev	Shape	Place of Formation	Classification	Physical Process	Dependence on Most Important Parameters	Common Effect on Strength
Cup-shaped crystals: Depth hoar	5		DH		Dry snow				
	a	Cup crystal	cp	Cup-shaped, striated crystal; usually hollow		Hollow or partly solid cup-shaped kinetic growth crystals	Very fast growth at large temperature gradient	Formation increases with increasing vapor flux	Usually fragile but strength increases with density
	b	Columns of depth hoar	dh	Large cup-shaped striated hollow crystals arranged in columns (< 10 mm)		Large cup-shaped kinetic growth forms arranged in columns	Intergranular arrangement in columns; most of the lateral bonds between columns have disappeared during crystal growth	Snow has almost completely recrystallized; high recrystallization rate for long period and at low snow density and high external temperature gradient facilitates formation	Very fragile snow
	c	Columnar crystals	cl	Very large, columnar crystals with c-axis horizontal (10–20 mm)		Final growth stage of depth hoar at high temperature gradient in low density snow	Evolves from earlier stage described above; some bonding occurs and new crystals are initiated	Longer time required than for any other snow crystal	Some strength returns
Wet grains	6		WG		Wet snow				
	a	Clustered rounded grains	cl	Clustered rounded crystals held by large ice-to-ice bonds; water in internal veins among three crystals or two grain boundaries		Grain clusters without melt-freeze cycles	Wet snow at low water content pendular regime; clusters form to minimize surface free energy	Meltwater can drain; too much water leads to slush; freezing leads to melt-freeze particles	Ice-to-ice bonds give strength
	b	Rounded poly crystals	mf	Individual crystals are frozen into a solid polycrystalline grain; may be seen either wet or refrozen		Melt-freeze polycrystals	Wet snow at low water content, melt-freeze cycles form polycrystals when water in veins freezes	Particle size increases with number of melt-freeze cycles; radiation penetration over time restores 6a; excess water leads to 6c	High strength in the frozen state; lower strength in the wet state; strength increases with number of melt-freeze cycles

Basic Classification	Code	Morphological Classification			Process-Oriented Classification		Additional Information on Physical and Strength		
		Subclass	Abbrev	Shape	Place of Formation	Classification	Physical Process	Dependence on Most Important Parameters	Common Effect on Strength
	c	Slush ∞	sl	Separated rounded crystals completely immersed in water		Poorly bonded rounded single crystals	High liquid content equilibrium form of ice in water	Water drainage blocked by impermeable layer or ground; high energy input to snow cover by solar radiation, high air temperature or water input	Little strength due to decaying bonds
Feathery crystals 7 ∨		SH							
	a	Surface hoar crystals ∨	sh	Striated, usually feathery crystal; aligned; usually flat, sometimes needle-like	Cold snow surface	Kinetic growth form in air	Rapid kinetic growth of crystals at the snow surface by rapid transfer of vapor toward the snow surface; snow surface cooled to below ambient temperature by radiational cooling	Increasing growth rate with increased cooling of the snow surface below air temperature and increasing relative humidity of the air	Fragile, extremely low shear strength; strength may remain low for extended periods when buried in cold snow
	b	Cavity hoar ∨	ch	Striated, planar or feathery crystals grown in cavities; random orientation	Cavities in snow; same form might grow in very low density snow with extreme temperature gradient	Kinetic growth form in cavities	Plate or feathery crystals may grow in high-temperature gradient fields in large voids in the snow, e.g. in the vicinity of tree trunks, buried bushes or below sun crusts		

	Morphological Classification				Process-Oriented Classification			Additional Information on Physical and Strength	
Basic Classification	Code	Subclass	Abbrev	Shape	Place of Formation	Classification	Physical Process	Dependence on Most Important Parameters	Common Effect on Strength
Ice masses	8		IM						
	a	Ice layer	il	Horizontal ice layer	Buried layers in snow becoming melted and refrozen	Ice layer from refreezing of draining meltwater; usually some degree of permeability	Rain or meltwater from the surface percolates into cold snow where it refreezes; water may be preferentially held by fine-grain layer such as a buried wind crust	Depends on timing of percolating water and cycles of melting and refreezing; more likely to occur if snow is highly stratified	Ice layers are strong but strength decays once snow is completely wetted
	b	Ice column	ic	Vertical ice body	Within layers	Ice column from refreezing of draining meltwater	Water within flow fingers freezes due to heat conduction into surrounding snow at $T<0°C$	Flow fingers more likely to occur if snow is highly stratified; freezing greater if snow is very cold	
	c	Basal ice	bi	Basal ice layer	Base of snow cover	Ice forms from freezing of ponded meltwater	Water ponds above substrate and freezes by heat conduction into cold substrate	Formation enhanced if substrate is impermeable and very cold (e.g. permafrost)	Weak slush layer may form on top
Surface deposits and crust	9		CR						
	a	Rime	rm	Soft rime: irregular deposit; Hard rime: small supercooled water droplets frozen in place	Surface	Surface rime	Accretion of supercooled fog droplets onto surface grains	Increases with fog density and exposure to wind	Thin breakable crust forms if process continues long enough
	b	Rain Crust	rc	Thin, transparent glaze or clear ice surface layer	Surface	Frozen rain water at snow surface	Result from freezing rain on snow, forms a surface glaze	Droplets have to be supercooled but coalesce before freezing	Thin breakable crust

264

Basic Classification	Morphological Classification				Process-Oriented Classification			Additional Information on Physical and Strength		
	Code	Subclass	Abbrev	Shape	Place of Formation	Classification	Physical Process	Dependence on Most Important Parameters	Common Effect on Strength
	c	Sun crust, firnspiegel	sc	Thin, transparent glaze or surface film	Surface	Refrozen meltwater at snow surface	Refrozen surface layer partially melted by solar radiation; shortwave absorption in the glaze is decreased; cooling of the glaze by longwave radiation and evaporation; greenhouse effect for the underlying snow; water vapor condenses below the glaze; may develop into smooth, shiny layer of clear ice at surface	Builds during clear weather (longwave cooling), air temperatures below freezing and strong irradiation (not to be confused with melt-freeze crust); melting can occur below the crust in clean snow	Thin, often breakable crust
	d	Wind crust	wc	Small, broken or abraded, closely-packed particles; well sintered	Surface	Wind crust	Fragmentation and packing of wind transported snow particles; high number of contact points and small size causes rapid strength increase through sintering	Hardness of crust increases with wind speed, decreasing particle size and moderate temperature	Hard, sometimes breakable crust
	e	Melt-freeze crust	mfc	Crust of recognizable melt-freeze polycrystals	Near surface	Crust of melt-freeze particles	Refrozen layer (e.g. wind crust) which was wetted with water at least once	Particle size and density increases with number of melt-freeze cycles	Hardness increases with number of melt-freeze cycles

265

Appendix B. The Brock and Arnold (2000) energy balance model: key components, uncertainties in input data, and implication of errors in modelled melt.

The energy balance model used in this project was developed by Brock and Arnold (2000) with the aim of enabling accurate melt modelling while remaining widely accessible and easily adaptable to different sites and surface conditions. The model achieves these aims by running in the widely-used Microsoft Excel spreadsheet package and allowing site-specific information including latitude, longitude, slope angle, aspect, elevation, local temperature lapse rate, albedo and surface roughness to be easily specified by the user. It incorporates energy balance work established by many previous studies and has been found to yield accurate melt estimates when compared to measured surface rates at Haut Glacier d'Arolla (Brock and Arnold, 2000); the authors report a root mean square error of 2.0 mm day^{-1} water equivalent melt for measured melt rates in the range 23 to 42 mm day^{-1} water equivalent melt. This appendix details the key components of the Brock and Arnold (2000) model and critically discusses the appropriateness of its use in this study and the implications of any errors in modelled melt.

The model calculates the surface energy balance and surface melt rate for a point on a melting snow or ice surface. Following previous research which has shown energy inputs from shortwave radiation and the turbulent transfer of latent and sensible heat to dominate the energy balance on such surfaces (e.g. Price, 1986; Röthlisberger and Lang, 1987; Hay and Fitzharris, 1988; Braithwaite and Olesen, 1990; Paterson, 1994; Arnold et al., 1996), these components are treated in the greatest detail. Longwave radiation is generally believed to contribute a relatively small net loss of energy and so is found indirectly, and the energy contribution from rainfall is not included as it is argued to be important only in exceptional circumstances (Marcus et al., 1985; Röthlisberger and Lang, 1987).

The model therefore requires measurements of incoming shortwave radiation, air temperature, vapour pressure and wind speed as meteorological input data, together with the Julian day and hour at which they were recorded. Surface albedo is specified by the user and used to calculate the net shortwave radiation flux. The energy balance equations used in the model are described fully in Brock and Arnold (2000), and only the important issues regarding the application of the model in this project are summarised here.

Energy balance equation

The surface melt rate, *MLT*, is found as the residual in the surface energy balance equation:

$$MLT = SWR + LWR + SHF + LHF \tag{B.1}$$

in which *SWR* and *LWR* are the net shortwave and longwave radiation fluxes respectively and *SHF* and *LHF* are the sensible and latent heat fluxes respectively.

Net shortwave radiation flux SWR

- Shading

The model assumes that the incoming shortwave radiation measured in a horizontal plane at the automatic weather station is representative of that at the point for which energy balance calculations are being made. Differences in shading between these two sites, due to either cloud cover or surrounding topography, may therefore introduce error into the calculated melt. When the model was used to illustrate the magnitude and pattern of melt through both field seasons and differences between them, as presented in Figure 4.3, it was melt at the site of AWS_M that was considered and this is therefore not an issue. When melt flux was calculated for use in calculating permeability values from dye tracing data (sections 5.2.5 and 5.2.10) or for comparison to lysimeter discharge data (section 5.3.1) – both of which data sets were collected at L – there may be a discrepancy between calculated and actual melt due to shading differences. Differential shading due to cloud cover cannot be known but is expected to have only a minor and brief effect as L and AWS_M were located only c.400m apart. Shading difference due to topography will be minimal, again as L and AWS_M were only c.400m apart and because both were on the main snout of the glacier where shading is governed by the same topographic features. Furthermore, shading by surrounding topography will only occur first thing in the morning and last thing in the evening, and would not be important at the time of dye experiments. The tails of the diurnal melt curves used for comparison to lysimeter data may be slightly incorrect, but this will not cause significant error in analysis of lysimeter data.

- Surface albedo

The model uses the surface albedo value input by the user to calculate the net shortwave radiation flux *SWR* from measurements of incoming shortwave radiation. The AWSs on Haut Glacier d'Arolla measured both incoming and outgoing shortwave radiation (Table 3.3) and the net shortwave radiation flux could therefore have been known directly. The model therefore did not make full use of the data available, and editing the way in which it calculated net shortwave radiation flux (using the difference between measured incoming and outgoing shortwave radiation directly) would have been advisable. Instead, the known values of incoming and outgoing shortwave radiation were used to calculate surface albedo at every time interval (Figure B1) and these field-derived albedo values were used to select

average albedo values for use in model runs. When melt for a whole field season was calculated for Figure 4.3, the input meteorological data was split into multiple model runs by identifying periods during which albedo did not vary greatly (sub-division of the season-long runs was also necessary to ensure model stability). The most pronounced change in albedo takes place when glacier ice is revealed by snowpack removal (around 12th July in Figure B1a for example), and so the use of averaged albedo values is therefore of less concern earlier in the season when dye and lysimeter data was collected.

a)

b)
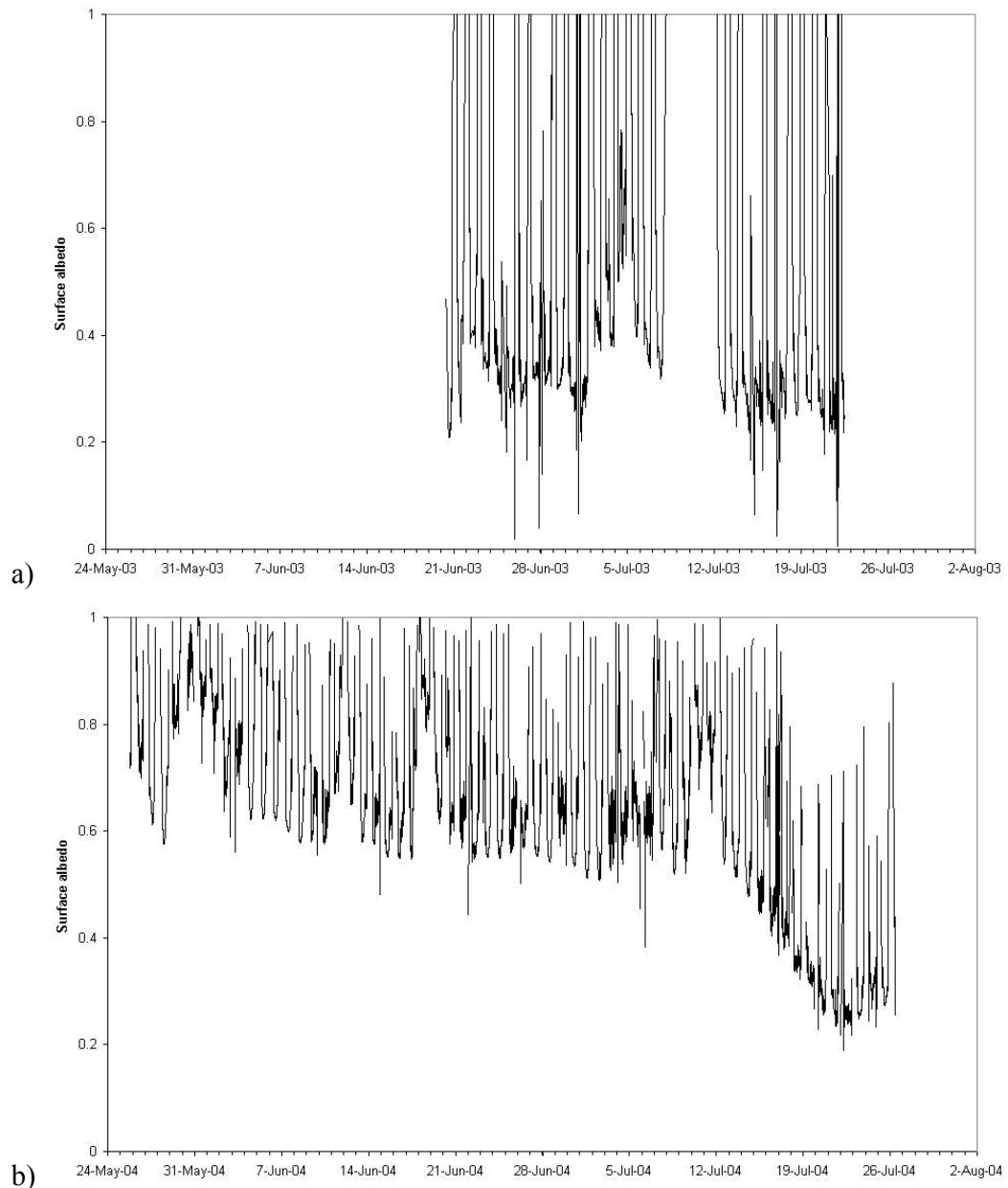
Figure B1: Time series of albedo values for the glacier surface at Haut Glacier d'Arolla during a) 2003 and b) 2004, calculated from incoming and outgoing shortwave radiation measurements made at ETH_M. In 2003, meteorological data was not available until late June, when glacier ice was already exposed at the site of ETH_M, and albedo measurements therefore reflect glacier ice throughout the data set (albedo values ≈ 0.3). Data was available from late May in 2004, and reveals the higher albedo values (0.6 – 0.8) of a snow surface, with some slight decreasing trend, until mid July, when glacier ice began to be revealed and albedo fell.

Other imperfectly known input data

Other values which require to be input to the model were also imperfectly known, with the resulting possibility of errors in calculated melt. Small errors in the measured angle and aspect of slope at the site where melt was to be calculated will lead to errors in the calculated net shortwave radiation flux, but these are likely to be small. No direct field data was collected about surface roughness z_0, but the turbulent fluxes are known to be very sensitive to changes in this parameter. However, the observations of snow surface topography which were presented in section 4.3.2 allowed values for z_0 to be selected from those measured previously at Haut Glacier d'Arolla by Brock (1997) and to be varied with time through the melt seasons as necessary.

Implications of errors in modelled melt

As mentioned above, the performance of the model has been verified at Haut Glacier d'Arolla in the past and found to give good results (Brock and Arnold, 2000). However, uncertainties in the model input values used in this work, as described above, will have resulted in slight deviation of modelled melt from actual values. This is of minimal importance when model output is used only to illustrate the magnitude and pattern of melt through both field seasons and differences between them, as was the case in Figure 4.3. When model output was used in the analysis of lysimeter discharge data (section 5.3.1), the implications of melt errors will again be minimal, as comparison of flux hydrographs at the snowpack surface and at depth was only by eye and any small discrepancies caused by error in the melt curve will be insignificant compared to the hydrograph alteration caused by percolation through the snowpack. When percolation velocities are calculated from lysimeter data, the melt curve is converted into a cumulative percentage discharge curve and any error in modelled melt will have little influence on the results of this analysis method. The marked difference between the flux-velocity relationship observed in the field and that which is usually assumed (Figure 5.23 – a key result of lysimeter analysis which corroborates the low snowpack permeability values calculated from dye data) would remain.

Any error in modelled melt will propagate into values of snow permeability calculated from dye tracing data (sections 5.2.5 and 5.2.10). However, the analysis of this data takes into account errors resulting from inaccuracies in flux values used, which occur primarily due to the concentration of percolating meltwater within preferential flow channels and the generation of larger fluxes at depth due to the different percolation rates of small and large fluxes. These errors are discussed fully in section 5.2.5 and Appendix D and are shown to have no important implications for the outcomes of this work. Additional flux errors due to melt modelling will not have any further significant impact on the outcomes of this project.

Appendix C. Quantitative dye experiments carried out

Tables C1 and C2 present chronological lists of all quantitative dye experiments carried out in 2003 and 2004 respectively. The success or otherwise of the experiment is noted for each injection carried out, and the cause of experiment failure suggested (Tables C1 and C2). The primary difficulty in obtaining useful results from dye experiments was positioning the fluorometer in the correct location to detect the dye plume emerging from the basal saturated layer. If the demands of other fieldwork allowed the pit to be observed as the dye emerged, this could be verified as the cause of poor or absent dye returns. Other issues could also complicate the retrieval of useful dye returns as outlined in section 3.6.4.2, resulting in partial or unreliable curves being obtained.

In 2003 46 dye injections were carried out for quantitative detection (Table C1). 26 of these injections produced useful results, corresponding to a success rate of 57%. The success rate for experiments in 2003 was therefore greater than that in 2004 (discussed in the next paragraph); however, fewer dye experiments were carried out in 2003 (due to the early removal of the snowpack in 2003 and a greater focus of quantitative dye work in 2004), work had to be moved between sites due to rapid snowline retreat, and more than two repeated experiments were rarely carried out successfully at the same pit. As a result, work in 2003 provided a less useful data set for considering the evolution of snowpack hydrological behaviour through time. 22 experiments were carried out at U (compared to 15 at L and 9 at M) and the success rate of these was high (73%) – data from U therefore provided the most useful results in 2003.

In 2004 a total of 77 dye injections were carried out for quantitative detection, 40 of which yielded useful results (Table C2). This figure includes the 3 surface injections carried out on 29th May and 8th and 12th June, when dye was seen to emerge above ice layers on the snow pit walls and therefore could not be detected using the fluorometer. These experiments provided useful information about ice layer effect on percolation through the snowpack and failed to be detected by the fluorometer not because of any failings in experimental set-up but rather because of the unsuitability of using this quantitative dye tracing technique early in the melt season. In a further 8 experiments, all injections into the basal saturated layer, dye emerged in the saturated layer but was not properly detected at the fluorometer, and visual observations were instead used to give approximate dye transit times. If these 8 experiments are excluded from the list of useful experiments, and early surface injections

270

for which the quantitative dye tracing technique is unsuitable (those prior to 14th June, when the first successful return from a surface injection was obtained) are excluded from the total count, the overall success rate of the quantitative dye tracing technique was 44%. This value however hides significant variation between the success rates of experiments carried out at L, where 52% of injections yielded useful results, and at M, where only 31% of injections were useful. These poor results at M were due to difficulty in locating the fluorometer to detect emerging dye. The fact that more experiments were carried out at L than at M (48 at L compared to 29 at M) combined with this higher success rate and in particular the repeated success of experiments at Pits A and B which rendered results comparable through time is the reason that work from L in 2004 forms the most useful data set presented in Chapter 5.

Table C1: Chronological list of dye injections carried out for quantitative detection in 2003, noting the date, location and type of each experiment, and whether it yielded useful data. If an experiment did not yield useful data, the cause of this is suggested.

Date	Location	Type of injection	Success?
25/05/2003	L1	Surface	Failed - dye not seen in pit
25/05/2003	L1	Basal	Good
26/05/2003	L1	Basal x 2	Failed - dye not seen in pit or missed fluorometer
29/05/2003	L1	Basal x 2	Failed - dye not seen in pit or missed fluorometer
30/05/2003	L1	Surface	Failed - dye not seen in pit or missed fluorometer
30/05/2003	L1	Basal	Failed - dye not seen in pit or missed fluorometer
02/06/2003	L2	Surface	Failed - dye not seen in pit or missed fluorometer
02/06/2003	L2	Basal	Good
06/06/2003	L3	Surface	Good
06/06/2003	L3	Basal	Good
09/06/2003	L3	Basal	Failed - dye missed fluorometer
10/06/2003	L3	Surface	Good
10/06/2003	L3	Basal	Good
13/06/2003	M3	Surface	Start of curve useful
13/06/2003	M3	Basal	Good
15/06/2003	M1	Basal	Failed - dye not seen in pit or missed fluorometer
16/06/2003	M2	Boreholes x 2 (above and below IL)	Failed - dye missed fluorometer
17/06/2003	M3	Boreholes x 2 (above and below IL)	Failed - dye not seen in pit or missed fluorometer
19/06/2003	M1	Surface	Good
19/06/2003	M1	Basal	Good
20/06/2003	U1	Surface	Failed - poorly defined return curve
20/06/2003	U1	Basal	Good
21/06/2003	U1	Surface	Good
21/06/2003	U1	Surface	Good
22/06/2003	U1	Basal	Good
22/06/2003	U1	Basal	Good
23/06/2003	U1	Surface	Good
23/06/2003	U1	Excavated surface	Good
27/06/2003	U1	Above IL	Failed - dye missed fluorometer
27/06/2003	U1	Below IL	Failed - dye missed fluorometer

28/06/2003	U2	Surface	Good
28/06/2003	U2	Surface	Good
29/06/2003	U3	Surface	Good
29/06/2003	U3	Excavated surface	Failed - poorly defined return curve
30/06/2003	U4	Above IL	Good
30/06/2003	U4	Below IL	Good
05/07/2003	U5	Surface	Good
05/07/2003	U5	Surface	Good
06/07/2003	U5	Surface	Failed - dye missed fluorometer
06/07/2003	U5	Basal	Failed - dye missed fluorometer
10/07/2003	U6	Basal	Good
10/07/2003	U6	Basal	Good

Table C2: Chronological list of dye injections carried out for quantitative detection in 2004, noting the date, location and type of each experiment, and whether it yielded useful data. If an experiment did not yield useful data, the cause of this is suggested.

Date	Location	Type of injection	Success?
28/05/2004	Lysimeter Pit at L	Surface	Failed - dye not seen in pit
29/05/2004	Lysimeter Pit at L	Surface	Dye emerged on ice layers in pit face, but visual observations useful
08/06/2004	Lysimeter Pit at L	Surface	Dye emerged on ice layers in pit face, but visual observations useful
08/06/2004	Lysimeter Pit at L	Basal	Failed - dye not seen in pit or missed fluorometer
09/06/2004	Lysimeter Pit at L	Basal	Failed - dye not seen in pit or missed fluorometer
10/06/2004	Lysimeter Pit at L	Basal	Failed - dye not seen in pit or missed fluorometer
12/06/2004	Wet Pit at L	Surface	Dye emerged on ice layers in pit face, but visual observations useful
12/06/2004	Wet Pit at L	Basal	Dye missed fluorometer but visual observations useful
13/06/2004	Wet Pit at L	Basal	Good
14/06/2004	Pit A at L	Surface	Good
14/06/2004	Pit A at L	Basal	Failed - dye not seen in pit or missed fluorometer
15/06/2004	Pit A at L	Basal x 3	Dye not detected clearly at fluorometer but visual observations useful
16/06/2004	Pit B at L	Surface	Failed - curve disturbed by movement of fluorometer
18/06/2004	Pit A at L	Surface	Good
18/06/2004	Pit A at L	Basal x 4	Dye not detected clearly at fluorometer but visual observations useful
19/06/2004	Pit B at L	Surface	Failed - dye not seen in pit or missed fluorometer
19/06/2004	Pit B at L	Basal x 2	One useful curve
21/06/2004	Pit A at L	Surface	Good
21/06/2004	Pit A at L	Basal	Start of curve useful, but apparent storage of dye
22/06/2004	Pit C at L	Surface	Failed - dye not seen in pit or missed fluorometer
22/06/2004	Pit C at L	Basal	Failed - dye not seen in pit or missed fluorometer
25/06/2004	Pit B at L	Surface	Good
25/06/2004	Pit B at L	Surface	Start of curve useful; otherwise poorly defined
27/06/2004	Pit A at L	Surface	Good
27/06/2004	Pit A at L	Surface	Good
28/06/2004	Pit B at L	Surface	Failed - dye not seen in pit or missed fluorometer

28/06/2004	Pit B at L	Surface	Failed - dye not seen in pit or missed fluorometer
29/06/2004	Pit A at L	Surface	Start of curve useful; otherwise poorly defined
29/06/2004	Pit A at L	Surface	Failed - dye not seen in pit or missed fluorometer
30/06/2004	M1	Surface	Good
30/06/2004	M1	Surface	Failed - dye not seen in pit or missed fluorometer
01/07/2004	Pit B at L	Surface	Good
01/07/2004	Pit B at L	Surface	Good
03/07/2004	Pit A at L	Surface	Good
03/07/2004	Pit A at L	Surface	Failed - dye not seen in pit or missed fluorometer
04/07/2004	Pit B at L	Surface	Good
04/07/2004	Pit B at L	Surface	Good
05/07/2004	Pit A at L	Surface	Failed - dye not seen in pit or missed fluorometer
05/07/2004	Pit A at L	Surface	Failed - dye not seen in pit or missed fluorometer
06/07/2004	Pit B at L	Surface	Good
06/07/2004	Pit B at L	Surface	Good
09/07/2004	Pit B at L	Surface	Start of curve useful; otherwise poorly defined
09/07/2004	Pit B at L	Basal	Failed - dye not seen in pit or missed fluorometer
10/07/2004	Pit A at L	Surface	Good
11/07/2004	M2	Surface	Failed - dye not seen in pit or missed fluorometer
14/07/2004	M1	Surface	Failed - dye not seen in pit or missed fluorometer
14/07/2004	M1	Surface	Failed - dye not seen in pit or missed fluorometer
15/07/2004	M2	Surface	Messy curve but useable
15/07/2004	M2	Surface	Failed - dye not seen in pit or missed fluorometer
17/07/2004	M2	Surface	Failed - dye not seen in pit or missed fluorometer
17/07/2004	M2	Surface	Failed - dye not seen in pit or missed fluorometer
18/07/2004	M3	Surface	Failed - dye not seen in pit or missed fluorometer
18/07/2004	M3	Surface	Failed - dye not seen in pit or missed fluorometer
19/07/2004	M2	Surface	Good
19/07/2004	M2	Basal	Good
21/07/2004	M2	Basal x 3	Curves poorly defined but times derived from two
22/07/2004	M4	Surface	Messy curve but useable
22/07/2004	M4	Basal x 2	Failed - dye not seen in pit or missed fluorometer
25/07/2004	M5	Surface	Failed - dye not seen in pit or missed fluorometer
25/07/2004	M5	Basal x 2	Failed - dye not seen in pit or missed fluorometer
26/07/2004	M5	Surface	Failed - dye not seen in pit or missed fluorometer
26/07/2004	M5	Basal x 2	One useful curve, though poorly defined
27/07/2004	M6	Surface	Failed - dye not seen in pit or missed fluorometer
27/07/2004	M6	Basal x 3	Failed - dye not seen in pit or missed fluorometer

Appendix D. Errors in calculation of net snowpack permeability k_{snow} from dye percolation velocities

The possibility of error in each k_{snow} value due to errors in the value of $dz/dt|_u$ used in its calculation is allowed for by production of upper and lower error bars corresponding to the maximum and minimum percolation velocities derived from assumption of flow in the basal layer taking place at rates of 3 and 25 m hr^{-1} respectively. Two further sources of error in k_{snow} are possible: that resulting from calculation of φ_e from imperfectly-known snow density values, and that due to underestimation of u.

Error due to estimation of φ_e from density data

As density measurements cannot be obtained for the snow through which dye experiments were carried out, and no clear trend in density was observed in measurements taken throughout the field season (Figure 4.18), all calculations of k_{snow} assumed an average snow density of 560 kg m^{-3} (section 4.3.4), from which the corresponding φ_e value of 0.42 was calculated for use in k_{snow} calculation. From Figure 4.18, however, the actual value of snow density might range between 450 and 650 kg m^{-3}, corresponding to variation of φ_e between 0.29 and 0.49. Although it is believed unlikely that net φ_e will in actuality take either of these extreme values, the way in which the estimated value of k_{snow} would vary as φ_e deviates from the assumed 0.42 is considered by reference to Figure B1. Two end cases are shown, for maximum percolation velocity/minimum flux (creating the highest k_{snow} values) and minimum percolation velocity/maximum flux (creating the lowest k_{snow} values). It can be seen that where flux values are low and percolation velocities high, variation in φ_e results in variation in k_{snow} across a large range between 7.4x10^{-10} and 3.5x10^{-9} m^2. Flux values were, however, generally significantly higher than this and percolation velocities lower, such that possible variation will be less (cf. blue line in Figure B1). Error in k_{snow} is therefore greatest for high values, and the lower k_{snow} values generally found here are expected to be reliable in magnitude. A key finding of this study is that k_{snow} values found from dye tracing investigations are very low; error in φ_e will not influence the validity of this outcome.
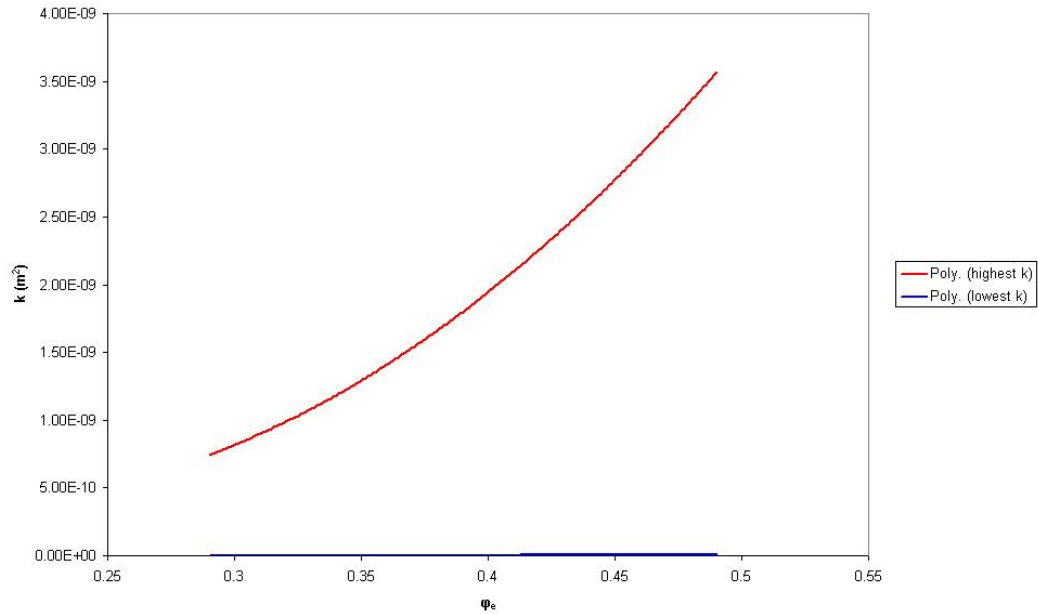
Figure B1: Change in calculated k_{snow} value due to varying φ_e, showing significant variation for large k_{snow} values (red line) but little error for low k_{snow} values (blue line).

Error due to minimal estimation of u

Figure B2 shows the form of the u – k relationship for the two extreme combinations of high φ_e/high percolation velocity and low φ_e/low percolation velocity. Again, for high k_{snow} considerable variation can be caused by error in the driving variable, in this case *u*. Notably, however, the markedly non-linear form of the relationship is such that for larger flux values even this error is reduced. In 2003, total water flux at the time of dye injections was always greater than 0.01 m hr^{-1} (Table 5.1), where the slope of the lines on Figure B2 is gradual and variation in k_{snow} as *u* changes therefore minimal. In 2004, total input water flux at the time of dye injections ranged between 0.0030 and 0.0085 m hr^{-1} (Table 5.5). If *u* was in fact greater than the value used for each calculation of k_{snow}, there will be error in k_{snow}, but real k_{snow} will be *lower* than values presented in section 5.2; research outcomes concerning the low value of net snowpack permeability therefore remain valid. Moreover, for small values of k_{snow} error remains minimal; all but one of the k_{snow} values reported for 2004 were lower than 2.08x10^{-10} m^2. The availability of k_{snow} values calculated independently from lysimeter data (section 5.3) is valuable; as analysis of lysimeter data indicated similarly low net snow permeability (section 5.3.1.1), confidence in the low values of k_{snow} derived from dye tracing experiments is increased.

A further important conclusion based on k_{snow} values was the temporal increase in net snowpack permeability discussed in section 5.2.10. The validity of this outcome was investigated by plotting lines on a graph similar to that in Figure B2 for each 2004 surface dye injection (based on observed dye percolation velocity $dzdt|_u$ and the range of possible *u*

at the time of dye injection). This showed that even if *u* was in fact larger than shown in Table 5.5, the order of k_{snow} values is likely to remain the same, as difference in $dzdt|_u$ outweighs the possible error due to *u* in controlling the value of k_{snow}.
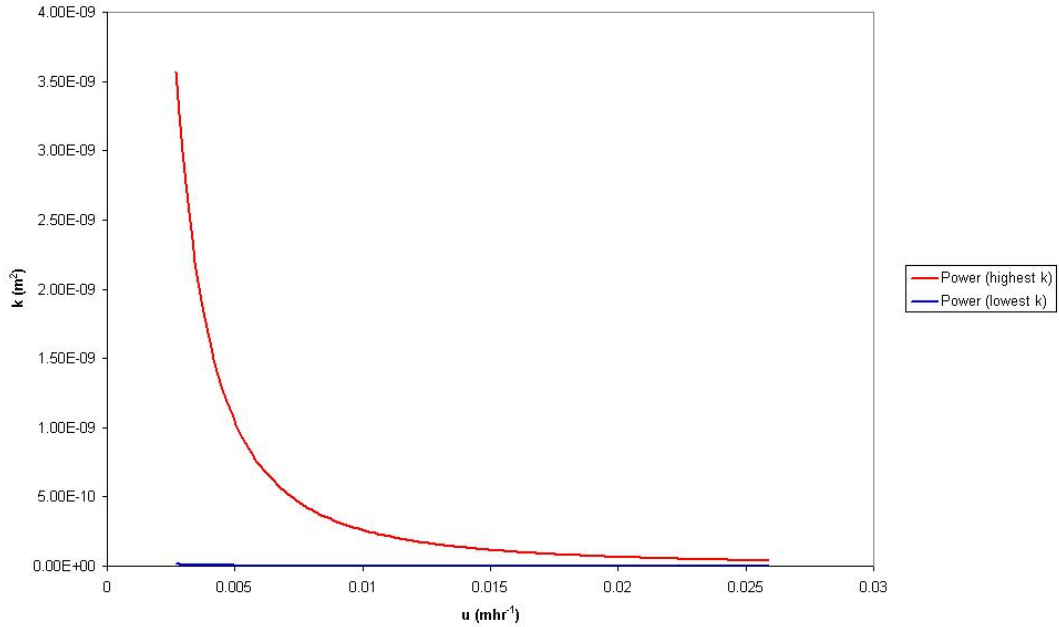

Figure B2: Change in calculated k_{snow} value due to varying *u*, showing significant variation for large k_{snow} values (red line) but little error for low k_{snow} values (blue line).

Appendix E. Errors in calculation of ice surface velocity

The quoted instrumental error in SD (ε_{SD}) for the Wild DI1001 distomat used in 2003 is 5 mm + 5 mm per 1000 m sighted distance:

$$\varepsilon_s = 5 + (0.5 \times 10^{-3})SD \tag{C.1}$$

The quoted error for the Geodimeter Total Station used in 2004 is 2 mm plus 1 mm per 1000 m sighted distance:.

$$\varepsilon_s = 2 + 10^{-3} SD \tag{C.2}$$

The error in the calculated displacement of a stake in the northwards direction relative to the survey station is

$$\varepsilon_{stake\_displ} = \varepsilon_{SD} \frac{1}{\cos\alpha} \tag{C.2}$$

and the error in the calculated displacement of the survey station in the northwards direction relative to the reference prism is

$$\varepsilon_{ss\_displ} = \varepsilon_{SD\_ref} \frac{1}{\sqrt{2}} \tag{C.3}$$

The error in net stake displacement northwards, taking survey station movement into account, is then

$$\varepsilon_{net\_displ} = \sqrt{\varepsilon_{stake\_displ}^2 + \varepsilon_{ss\_displ}^2} \tag{C.4}$$

Finally, the error in calculated stake velocity is

$$\varepsilon_{v\_net} = \frac{\sqrt{\varepsilon_{net\_displ\_1}^2 + \varepsilon_{net\_displ\_2}^2}}{T} \tag{C.5}$$

where $\varepsilon_{net\_displ\_1}$ and $\varepsilon_{net\_displ\_2}$ designate ε_{net_displ} at the start and end of the survey interval respectively.